



Cassini Navigation Performance Assessment

*Duane Roth, Sonia Hernandez,
Sean Wagner*

March 2021

Jet Propulsion Laboratory
California Institute of Technology

DESCANSO

Deep Space Communications and Navigation Systems
Center of Excellence

Design and Performance Summary Series

The Cover

The cover is an artist's conception of Cassini's trajectory, or flight path, during the 22 Grand Finale Orbits at the end of the mission.



DESCANSO Design and Performance Summary Series

Article 17

Cassini Navigation Performance Assessment

*Duane Roth
Sonia Hernandez
Sean Wagner*

*Jet Propulsion Laboratory
California Institute of Technology
Pasadena, California*

**National Aeronautics and
Space Administration
Jet Propulsion Laboratory
California Institute of Technology
Pasadena, California**

March 2021

This research was carried out at the Jet Propulsion Laboratory, California Institute of Technology, under a contract with the National Aeronautics and Space Administration.

Reference herein to any specific commercial product, process, or service by trade name, trademark, manufacturer, or otherwise, does not constitute or imply endorsement by the United States Government or the Jet Propulsion Laboratory, California Institute of Technology.

Copyright 2021 California Institute of Technology. Government sponsorship acknowledged.

DESCANSO DESIGN AND PERFORMANCE SUMMARY SERIES

Issued by the Deep Space Communications and Navigation Systems
Center of Excellence
Jet Propulsion Laboratory
California Institute of Technology

Jon Hamkins, Editor-in-Chief

Published Articles in This Series

Article 1—“Mars Global Surveyor Telecommunications”

Jim Taylor, Kar-Ming Cheung, and Chao-Jen Wong

Article 2—“Deep Space 1 Telecommunications”

Jim Taylor, Michela Muñoz Fernández, Ana I. Bolea Alamañac, and Kar-Ming Cheung

Article 3—“Cassini Orbiter/Huygens Probe Telecommunications”

Jim Taylor, Laura Sakamoto, and Chao-Jen Wong

Article 4—“Voyager Telecommunications”

Roger Ludwig and Jim Taylor

Article 5—“Galileo Telecommunications”

Jim Taylor, Kar-Ming Cheung, and Dongae Seo

Article 6—“Odyssey Telecommunications”

Andre Makovsky, Andrea Barbieri, and Ramona Tung

Article 7—“Deep Space 1 Navigation: Extended Missions”

Brian Kennedy, Shyam Bhaskaran, J. Edmund Riedel, and Mike Wang

Article 8—“Deep Space 1 Navigation: Primary Mission”

Brian Kennedy, J. Edmund Riedel, Shyam Bhaskaran, Shailen Desai, Don Han, Tim McElrath, George Null, Mark Ryne, Steve Synnott, Mike Wang, and Robert Werner

Article 9—“Deep Impact Flyby and Impactor Telecommunications”

Jim Taylor and David Hansen

Article 10—“Mars Exploration Rover Telecommunications”

Jim Taylor, Andre Makovsky, Andrea Barbieri, Ramona Tung, Polly Estabrook, and A. Gail Thomas

Article 11—“ Mars Exploration Rover Navigation”

Louis A. D’Amario

Article 12—“Mars Reconnaissance Orbiter Telecommunications”

Jim Taylor, Dennis K. Lee, and Shervin Shambayati

Article 13—“Dawn Telecommunications”

Jim Taylor

Article 14—“Mars Science Laboratory Telecommunications Systems Design”

Andre Makovsky, Peter Ilott, and Jim Taylor

Article 15—“Phoenix Telecommunications”

Jim Taylor, Stan Butman, Chad Edwards, Peter Ilott, Richard Kornfeld, Dennis Lee, Scott Shaffer, and Gina Signori

Article 16—“Juno Telecommunications”

Ryan Mukai, David Hansen, Anthony Mittskus, Jim Taylor, Monika Danos, and Andrew Kwok
Revision A: Addition of Operations from Early Cruise through First Months of Operation, Five Science Orbits (Sept. 2012–May 2017)

Article 17—“Cassini Navigation Performance Assessment”

Duane Roth, Sonia Hernandez, and Sean Wagner

Foreword

This Design and Performance Summary Series, issued by the Deep Space Communications and Navigation Systems Center of Excellence (DESCANSO), is a companion series to the DESCANSO Monograph Series. Authored by experienced scientists and engineers who participated in and contributed to deep-space missions, each article in this series summarizes the design and performance of major systems, such as communications and navigation, for each mission. In addition, the series illustrates the progression of system design from mission to mission. Lastly, the series collectively provides readers with a broad overview of the mission systems described.

Jon Hamkins

DESCANSO Leader

Blank

Preface

The Cassini mission was designed to conduct science investigations of the planet Saturn and its satellites, rings, and magnetosphere. The Cassini orbiter and attached Huygens probe were launched October 15, 1997, and the first seven years of the mission involved travel from Earth to Saturn. A Titan IVB/Centaur launch system and gravity assists at Venus (twice), Earth, and Jupiter provided the energy required to reach Saturn. Saturn Orbit insertion (SOI) took place July 1, 2004, nineteen days after the first and only targeted encounter of Phoebe, Saturn's largest irregular moon. The next thirteen years spanned prime mission and two extended missions, the Equinox and Solstice Missions, with 127 targeted encounters of Saturn's largest moon Titan and several more of the smaller icy satellites.

All science goals were attained, with Cassini observations leading to many astounding discoveries such as a methane cycle on Titan analogous to Earth's water cycle, an ocean of salty water below Enceladus' frozen crust suggesting the possibility of alien microbial life, and Enceladus' ice geysers as the source of Saturn's E-ring. The European Space Agency's (ESA) Huygens probe, carried to Saturn aboard the Cassini orbiter and successfully landed on Titan's surface, was the first spacecraft to land on a world in the outer solar system. Its suite of instruments characterized Titan's dense atmosphere during descent and surface properties after surviving a soft landing. Navigation of the Cassini spacecraft played an essential role in enabling these discoveries and achieving all science mission goals. Sub-kilometer target misses were routinely achieved in the final years of the mission, not only satisfying tight science pointing and timing requirements, but also ensuring adequate propellant margins through the end of Cassini's second extended mission. With its propellant tanks nearly depleted, the Cassini spacecraft met a fiery demise September 15, 2017, as it was intentionally guided into Saturn's atmosphere deep enough to become captured, thereby satisfying planetary protection requirements.

Blank

Acknowledgments

The material contained within this article was published originally as Volume 4 of the *Cassini Final Mission Report 2018*. It has been reformatted for the DESCANSO Design and Performance Summary Series and is being released as Article 17 in order to make it accessible to the general public.

The following Cassini Navigation Team members are acknowledged for their contribution during intervals within the nearly two decades between launch and end of mission. The achievements described in this report were enabled through their effort and ingenuity.

Vijay Alwar	<i>Optical Navigation Analysis</i>	Ruaraidh Mackenzie	<i>Orbit Determination Analysis</i>
Peter Antreasian	<i>Orbit Determination Analysis</i>	Cameron Meek	<i>Orbit Determination Analysis</i>
Shadan Ardalan	<i>Orbit Determination Analysis</i>	Sumita Nandi	<i>Orbit Determination Analysis</i>
Juan Arrieta-Camacho	<i>Maneuver Analysis</i>	Simon Nolet	<i>Optical Navigation Analysis</i>
Christopher Ballard	<i>Maneuver Analysis</i>	William Owen	<i>Optical Navigation Analysis</i>
Julie Bellerose	<i>Orbit Determination Analysis</i>	Daniel Parcher	<i>Orbit Determination Analysis</i>
Robert Beswick	<i>System Administration</i>	Frederic Pelletier	<i>Orbit Determination Analysis</i>
Dennis Bluhm	<i>Optical Navigation Analysis</i>	Fernando Peralta	<i>Trajectory Analysis</i>
Dylan Boone	<i>Orbit Determination Analysis</i>	Joan Pojman	<i>Trajectory Analysis</i>
John Bordi	<i>Orbit Determination Analysis</i>	Duane Roth	<i>Navigation Office Manager</i>
Brent Buffington	<i>Trajectory Analysis</i>	Ian Roundhill	<i>Orbit Determination Analysis</i>
John Costello	<i>Optical Navigation Analysis</i>	Shawna Santos	<i>Optical Navigation Analysis</i>
Kevin Criddle	<i>Orbit Determination Analysis</i>	Jonathon Smith	<i>Orbit Determination Analysis</i>
Stephen Gillam	<i>Optical Navigation Analysis</i>	Jason Stauch	<i>Orbit Determination Analysis</i>
Emily Gist	<i>Maneuver Analysis</i>	Nathan Strange	<i>Trajectory Analysis</i>
Troy Goodson	<i>Maneuver Analysis</i>	Paul Stumpf	<i>Maneuver Analysis</i>
Donald Gray	<i>Maneuver Analysis</i>	Zahi Tarzi	<i>Orbit Determination Analysis</i>
Mark Guman	<i>Orbit Determination Analysis</i>	Tony Taylor	<i>Orbit Determination Analysis</i>
Yungsun Hahn	<i>Maneuver Analysis</i>	Paul Thompson	<i>Orbit Determination Analysis</i>
Sonia Hernandez	<i>Maneuver Analysis</i>	Powtawche Valerino	<i>Maneuver Analysis</i>
Claude Hildebrand	<i>Optical Navigation Analysis</i>	Mar Vaquero	<i>Maneuver Analysis</i>
Rodica Ionasescu	<i>Orbit Determination Analysis</i>	Andrew Vaughan	<i>Optical Navigation Analysis</i>
Robert Jacobson	<i>Satellite Ephemeris Development</i>	Sean Wagner	<i>Maneuver Analysis</i>
Jeremy Jones	<i>Navigation Office Manager</i>	Mike Wang	<i>Optical Navigation Analysis</i>
Kathleen Kelleher	<i>Optical Navigation Analysis</i>	Mau Wong	<i>Maneuver Analysis</i>
Frank Laipert	<i>Maneuver Analysis</i>		

Blank

Table of Contents

Foreword	vii
Preface	ix
Acknowledgments	xi
1 Introduction	1
1.1 Cassini Navigation Objectives	1
1.2 Cassini Force Models	2
1.3 Tracking Data	4
1.3.1 Doppler and Range	4
1.3.2 VLBI	4
1.3.3 Optical Navigation Images	5
1.4 Trajectory Control	5
1.5 Planetary Protection	7
2 Launch & Interplanetary Cruise	8
2.1 Launch	10
2.1.1 Performance	10
2.2 Venus-1 Flyby	11
2.2.1 Performance	11
2.2.2 Notable Events	12
2.3 Venus-2 Flyby	13
2.3.1 Performance	14
2.3.2 Notable Events	14
2.4 Earth Flyby	15
2.4.1 Performance	16
2.4.2 Notable Events	17
2.5 Jupiter Flyby	17
2.5.1 Performance	18
2.5.2 Notable Events	19
2.6 Saturn Approach	20
2.6.1 Performance	23
2.6.2 Notable Events	26
2.7 Interplanetary Cruise Synopsis	27
3 Saturn Orbit Insertion	29
3.1 Performance	30
3.2 Notable Events	30
4 Tour	31
4.1 Prime Orbital Mission	38
4.1.1 Huygens Probe Relay Redesign	42
4.1.2 Remainder of Prime Mission	46
4.1.3 Performance	47
4.1.4 Notable Events	48
4.2 Equinox Mission	49
4.2.1 Performance	52
4.2.2 Notable Events	53

4.3	Solstice Mission	53
4.3.1	Performance.....	57
4.3.2	Notable Events.....	58
4.4	Tour Synopsis	59
5	In-Flight Adaptations	61
5.1	Trajectory Design Adaptations.....	61
5.1.1	Tethys Close Flyby.....	61
5.1.2	Enceladus Plume Occultation	61
5.2	Orbit Determination Adaptations.....	62
5.2.1	Use of ΔV Telemetry	63
5.2.2	Y-Thruster Calibrations	65
5.3	Optical Navigation Adaptations.....	67
5.4	Maneuver Design Adaptations.....	68
5.4.1	Target Biasing	68
5.4.2	Backup Maneuver Scheduling	71
5.5	Software Adaptations.....	72
6	Conclusion	74
7	References	75
8	Abbreviations and Acronyms	80
Appendix A.	Supplementary Material.....	82
A.1	Targeted Encounter History	82
A.2	Biased Targeted Encounter History	86
A.3	Maneuver History	87
A.4	Orbital Element Change due to Encounter Location on the B-Plane.....	95
A.4.1	Computing the Changes in Orbital Elements	96
A.4.2	Orbital Element Change Plotted on the B-Plane.....	97

List of Figures

Figure 1-1.	Cassini thruster geometry.	3
Figure 1-2.	The Cassini-Huygens spacecraft.	6
Figure 2-1.	The Cassini-Huygens interplanetary trajectory.	8
Figure 2-2.	Venus 1 flyby geometry.....	11
Figure 2-3.	Cassini range anomaly.....	12
Figure 2-4.	Venus 2 flyby geometry.....	13
Figure 2-5.	Earth flyby geometry.	15
Figure 2-6.	Aim-point biasing strategy for Earth (EMO2000 B-plane).	16
Figure 2-7.	Jupiter flyby geometry.	17
Figure 2-8.	Jupiter flyby expected delivery errors and reconstruction in EMO2000 B-plane.....	19
Figure 2-9.	Nominal ascending ring plane crossing (viewed from within ring plane).....	20
Figure 2-10.	Nominal ascending ring plane crossing (viewed from above ring plane).	21
Figure 2-11.	Nominal descending ring plane crossing (viewed from within ring plane).....	21
Figure 2-12.	Nominal descending ring plane crossing (viewed from above ring plane).	22
Figure 2-13.	Saturn B-plane biasing (EMO2000 B-plane).	23
Figure 2-14.	Phoebe B-plane target and solutions.	24

Figure 2-15. Targeted and achieved ascending ring plane crossing.	25
Figure 2-16. Nominal and achieved descending ring plane crossing.	26
Figure 4-1. Prime mission petal plot.	40
Figure 4-2. Prime mission inclination.	40
Figure 4-3. Prime mission periapsis radius.	41
Figure 4-4. Prime mission apoapsis radius.	41
Figure 4-5. Huygens original trajectory (left) and redesigned trajectory (right).	42
Figure 4-6. OPNAV of Huygens Probe taken by Cassini NAC on December 26, 2005.	44
Figure 4-7. Entry angle estimates and uncertainties versus data cut-off.	45
Figure 4-8. Relay pointing errors and uncertainties.	46
Figure 4-9. Equinox Mission petal plot.	49
Figure 4-10. Equinox Mission inclination.	50
Figure 4-11. Equinox Mission periapsis radius.	51
Figure 4-12. Equinox Mission apoapsis radius.	51
Figure 4-13. Solstice Mission petal plot.	54
Figure 4-14. Solstice Mission inclination.	55
Figure 4-15. Solstice Mission periapsis radius.	55
Figure 4-16. Solstice Mission apoapsis radius.	56
Figure 4-17. Accumulated ΔV Cost for Cassini Tour.	60
Figure 5-1. Tethys ground tracks for varying flyby altitudes. Blue: 1000–5000 km, Green: 10,000–20,000 km, Red: 20,000–30,000 km.	62
Figure 5-2. Enceladus plume occultation as viewed from ϵ Orion, before and after reference trajectory update.	62
Figure 5-3. ME maneuver ΔV differences—Navigation reconstruction minus telemetry computations.	64
Figure 5-4. RCS Maneuver ΔV differences—Navigation reconstruction minus telemetry computations.	65
Figure 5-5. Cumulative probability of ME (left) and RCS maneuver errors.	65
Figure 5-6. Thruster mismatch determined from each Y-thruster calibration.	67
Figure 5-7. OTM-409 target time bias versus ΔV cost.	69
Figure 5-8. OTM-460 downstream ΔV cost contours.	70
Figure A-1. Cassini's Orbit During the Titan-107 and Titan-108 Encounters.	95
Figure A-2. Titan-108 (T108) Encounter Orbital Element Change Shown on the B-Plane.	96
Figure A-3. Titan-3 (T3) Encounter Orbital Element Change Shown on the B-Plane.	98
Figure A-4. Enceladus-1 (E1) Encounter Orbital Element Change Shown on the B-Plane.	99
Figure A-5. Titan-4 (T4) Encounter Orbital Element Change Shown on the B-Plane.	99
Figure A-6. Titan-5 (T5) Encounter Orbital Element Change Shown on the B-Plane.	100
Figure A-7. Enceladus-2 (E2) Encounter Orbital Element Change Shown on the B-Plane.	100
Figure A-8. Titan-6 (T6) Encounter Orbital Element Change Shown on the B-Plane.	101
Figure A-9. Titan-7 (T7) Encounter Orbital Element Change Shown on the B-Plane.	101
Figure A-10. Dione-1 (D1) Encounter Orbital Element Change Shown on the B-Plane.	102
Figure A-11. Titan-8 (T8) Encounter Orbital Element Change Shown on the B-Plane.	102
Figure A-12. Rhea-1 (R1) Encounter Orbital Element Change Shown on the B-Plane.	103
Figure A-13. Titan-9 (T9) Encounter Orbital Element Change Shown on the B-Plane.	103

Figure A-14. Titan-10 (T10) Encounter Orbital Element Change Shown on the B-Plane.....	104
Figure A-15. Titan-40 (T40) Encounter Orbital Element Change Shown on the B-Plane.....	104
Figure A-16. Titan-41 (T41) Encounter Orbital Element Change Shown on the B-Plane.....	105
Figure A-17. Enceladus-3 (E3) Encounter Orbital Element Change Shown on the B-Plane....	105
Figure A-18. Titan-42 (T42) Encounter Orbital Element Change Shown on the B-Plane.....	106
Figure A-19. Titan-43 (T43) Encounter Orbital Element Change Shown on the B-Plane.....	106
Figure A-20. Titan-44 (T44) Encounter Orbital Element Change Shown on the B-Plane.....	107
Figure A-21. Titan-45 (T45) Encounter Orbital Element Change Shown on the B-Plane.....	107
Figure A-22. Enceladus-4 (E4) Encounter Orbital Element Change Shown on the B-Plane....	108
Figure A-23. Titan-60 (T60) Encounter Orbital Element Change Shown on the B-Plane.....	108
Figure A-24. Titan-61 (T61) Encounter Orbital Element Change Shown on the B-Plane.....	109
Figure A-25. Titan-62 (T62) Encounter Orbital Element Change Shown on the B-Plane.....	109
Figure A-26. Enceladus-7 (E7) Encounter Orbital Element Change Shown on the B-Plane....	110
Figure A-27. Rhea-2 (R2) Encounter Orbital Element Change Shown on the B-Plane.....	110
Figure A-28. Titan-67 (T67) Encounter Orbital Element Change Shown on the B-Plane.....	111
Figure A-29. Dione-2 (D2) Encounter Orbital Element Change Shown on the B-Plane.....	111
Figure A-30. Enceladus-9 (E9) Encounter Orbital Element Change Shown on the B-Plane....	112
Figure A-31. Enceladus-10 (E10) Encounter Orbital Element Change Shown on the B-Plane.	112
Figure A-32. Titan-68 (T68) Encounter Orbital Element Change Shown on the B-Plane.....	113
Figure A-33. Titan-69 (T69) Encounter Orbital Element Change Shown on the B-Plane.....	113
Figure A-34. Titan-70 (T70) Encounter Orbital Element Change Shown on the B-Plane.....	114
Figure A-35. Titan-82 (T82) Encounter Orbital Element Change Shown on the B-Plane.....	114
Figure A-36. Enceladus-17 (E17) Encounter Orbital Element Change Shown on the B-Plane.	115
Figure A-37. Enceladus-18 (E18) Encounter Orbital Element Change Shown on the B-Plane.	115
Figure A-38. Enceladus-19 (E19) Encounter Orbital Element Change Shown on the B-Plane.	116
Figure A-39. Titan-83 (T83) Encounter Orbital Element Change Shown on the B-Plane.....	116
Figure A-40. Titan-84 (T84) Encounter Orbital Element Change Shown on the B-Plane.....	117
Figure A-41. Titan-85 (T85) Encounter Orbital Element Change Shown on the B-Plane.....	117
Figure A-42. Titan-86 (T86) Encounter Orbital Element Change Shown on the B-Plane.....	118
Figure A-43. Titan-87 (T87) Encounter Orbital Element Change Shown on the B-Plane.....	118
Figure A-44. Titan-88 (T88) Encounter Orbital Element Change Shown on the B-Plane.....	119
Figure A-45. Titan-89 (T89) Encounter Orbital Element Change Shown on the B-Plane.....	119
Figure A-46. Rhea-4 (R4) Encounter Orbital Element Change Shown on the B-Plane.....	120
Figure A-47. Titan-90 (T90) Encounter Orbital Element Change Shown on the B-Plane.....	120
Figure A-48. Titan-110 (T110) Encounter Orbital Element Change Shown on the B-Plane....	121
Figure A-49. Titan-111 (T111) Encounter Orbital Element Change Shown on the B-Plane....	121
Figure A-50. Dione-4 (D4) Encounter Orbital Element Change Shown on the B-Plane.....	122
Figure A-51. Titan-112 (T112) Encounter Orbital Element Change Shown on the B-Plane....	122
Figure A-52. Dione-5 (D5) Encounter Orbital Element Change Shown on the B-Plane.....	123
Figure A-53. Titan-113 (T113) Encounter Orbital Element Change Shown on the B-Plane....	123

Figure A-54. Enceladus-20 (E20) Encounter Orbital Element Change Shown on the B-Plane.	124
Figure A-55. Enceladus-21 (E21) Encounter Orbital Element Change Shown on the B-Plane.	124
Figure A-56. Titan-114 (T114) Encounter Orbital Element Change Shown on the B-Plane.	125
Figure A-57. Enceladus-22 (E22) Encounter Orbital Element Change Shown on the B-Plane.	125
Figure A-58. Titan-115 (T115) Encounter Orbital Element Change Shown on the B-Plane.....	126
Figure A-59. Titan-116 (T116) Encounter Orbital Element Change Shown on the B-Plane.....	126
Figure A-60. Titan-117 (T117) Encounter Orbital Element Change Shown on the B-Plane.....	127
Figure A-61. Titan-118 (T118) Encounter Orbital Element Change Shown on the B-Plane.....	127
Figure A-62. Titan-119 (T119) Encounter Orbital Element Change Shown on the B-Plane.....	128
Figure A-63. Titan-120 (T120) Encounter Orbital Element Change Shown on the B-Plane.....	128
Figure A-64. Titan-121 (T121) Encounter Orbital Element Change Shown on the B-Plane.....	129
Figure A-65. Titan-122 (T122) Encounter Orbital Element Change Shown on the B-Plane.....	129
Figure A-66. Titan-123 (T123) Encounter Orbital Element Change Shown on the B-Plane.....	130
Figure A-67. Titan-124 (T124) Encounter Orbital Element Change Shown on the B-Plane.....	130
Figure A-68. Titan-125 (T125) Encounter Orbital Element Change Shown on the B-Plane.....	131
Figure A-69. Titan-126 (T126) Encounter Orbital Element Change Shown on the B-Plane.....	131

List of Tables

Table 2-1. Interplanetary cruise mission events.	9
Table 2-2. Maneuver execution error model improvement, prelaunch to cruise end.....	28
Table 4-1. Cassini prime mission reference trajectory encounters.....	31
Table 4-2. Cassini Equinox Mission reference trajectory encounters.....	33
Table 4-3. Cassini Solstice Mission reference trajectory encounters.	34
Table 4-4. Reference trajectory updates and motivations.	37
Table 4-5. Maneuver execution error model improvement at prime mission end.....	48
Table 4-6. Maneuver execution error model change at Equinox end.	52
Table 4-7. Loss of signal times and trajectory characteristics.	57
Table 4-8. Maneuver execution error model change at Solstice Mission end.	58
Table A-1. Cassini Targeted Encounter History (Venus-1 to Titan-41).	83
Table A-2. Cassini Targeted Encounter History (Enceladus-3 to Titan-81).....	84
Table A-3. Cassini Targeted Encounter History (Titan-82 to Titan-126).....	85
Table A-4. Biased Targeted Encounter History.	86
Table A-5. Cassini Mission Maneuver History (TCMs 01-22, SOI, OTMs 001-046).....	88
Table A-6. Cassini Mission Maneuver History (OTMs 047-118).....	89
Table A-7. Cassini Mission Maneuver History (OTMs 119-190).....	90
Table A-8. Cassini Mission Maneuver History (OTMs 191-262).....	91
Table A-9. Cassini Mission Maneuver History (OTMs 263-334).....	92
Table A-10. Cassini Mission Maneuver History (OTMs 335-406).....	93
Table A-11. Cassini Mission Maneuver History (OTMs 407-475).....	94

Blank

1 Introduction

The Cassini spacecraft and attached Huygens probe launched October 15, 1997, from Cape Canaveral Air Force Station aboard a Titan IVB/Centaur launch system. JPL assumed navigation responsibilities from the Centaur onboard guidance system approximately forty minutes after lift-off, when the spacecraft and probe were successfully injected into a hyperbolic Earth escape trajectory. The 3.5-billion kilometer, 6.7-year transfer to Saturn included four gravity-assist flybys, two with Venus (1998 and 1999), one with Earth (1999), and one with Jupiter (2000) to gain the energy necessary to reach Saturn. Near the end of interplanetary cruise, Cassini-Huygens achieved its only targeted flyby of Phoebe, an irregular satellite of Saturn. Nineteen days later, on July 1, 2004, Saturn Orbit Insertion (SOI), the largest burn of the mission at 626 meters per second (m/s), was performed to slow the spacecraft so that it would be captured into orbit about Saturn. Both inbound and outbound trajectory legs near SOI passed between Saturn's F-ring and G-ring, with periapsis at an altitude of 0.3 Saturn radii.

Cassini was the first spacecraft to orbit Saturn, and the Huygens probe was the first spacecraft to land on Titan. The orbital tour of Saturn began with a focus on Huygens probe delivery to Titan. The first two targeted Titan encounters set up the trajectory to precisely target the probe to the desired atmospheric entry conditions at the third Titan encounter. After the second encounter, Huygens separated from Cassini and began its ballistic journey to Titan. Cassini then performed a deflection maneuver to avoid impact with the natural satellite. On January 14, 2005, as Huygens plunged into Titan's atmosphere and parachuted to the surface, its science measurements were transmitted to the Cassini orbiter and relayed to Earth.

Cassini continued orbiting Saturn for the remainder of the prime mission and two extended missions. The first extension, called the Equinox Mission, spanned two years from July 2008 to September 2010 as Saturn transitioned from northern winter to spring. Saturn equinox occurred approximately halfway through the Equinox Mission, on August 11, 2009. The second extension, called the Solstice Mission, spanned seven years from the end of the Equinox Mission until Saturn atmospheric entry on September 15, 2017, four months after the northern hemisphere summer solstice. The final 22 orbits of the Solstice Mission passed closer to Saturn than ever before, between the planet's upper atmosphere and its innermost ring. While in orbit about Saturn, the navigation team successfully executed 160 targeted flybys: 127 of Titan, 22 of Enceladus, five of Dione, four of Rhea, and one each of Iapetus and Hyperion.

A broad description of navigation operations and performance follows. Unless otherwise noted, all provided uncertainties and dispersions are one-sigma.

1.1 Cassini Navigation Objectives

The high-level, fundamental objectives for Cassini-Huygens navigation may be summarized as follows:

- Design optimal gravity-assist trajectories that accomplish mission science objectives and minimize spacecraft propellant consumption.
- Determine the trajectories of Cassini and Huygens using radiometric and optical data along with accurate force and measurement models.

- Design propulsive maneuvers to control the flight path of Cassini and Huygens while satisfying mission and spacecraft operational constraints.
- Deliver Cassini and Huygens to their respective targets accurately.

The navigation team achieved these objectives with a consistency and rigor that enabled all science goals to be met or exceeded and translated directly into an extended mission duration of more than double that of prime mission orbital operations.

1.2 Cassini Force Models

Several force models were needed to model the motion of Cassini-Huygens. Gravity, finite burn, impulsive burn, polynomial acceleration, exponential acceleration, solar radiation pressure, and atmospheric drag models were required to obtain the accuracy necessary to meet project requirements.

Gravitational forces predominated. Newtonian point mass gravity models were used for the Sun, planets, Pluto, Saturn's satellites, and Earth's moon. Relativistic gravity corrections were applied for the Sun, Earth, Jupiter, and Saturn. Oblateness was added for several bodies and became active whenever Cassini-Huygens was within the bodies' spheres of influence. Oblateness models were available prelaunch for Earth, Earth's moon, Jupiter, and Saturn. Tracking data obtained during tour operations enabled navigators to improve Saturn's oblateness model and develop new models for Enceladus, Dione, Rhea, and Titan.

Finite burn force models were used for all flight path control maneuvering, regardless of burn duration. The Spacecraft Operations Office (SCO) provided spacecraft mass and thruster force estimates prior to each burn.

Impulsive burn force models were used for spacecraft ΔV activity typically resulting from short-term usage (several minutes) of the Reaction Control System (RCS) thrusters. Managing Reaction Wheel Assembly (RWA) wheel speeds while in RWA mode attitude control was the most common reason for use of this model. Cassini's attitude was primarily controlled via the RWA during tour.

Polynomial acceleration models were used for ΔV activity resulting from long-term usage (several hours) of the RCS thrusters. RCS mode attitude control was the most common reason for use of this model. Cassini's attitude was controlled via the RCS thrusters during all of the early portion of interplanetary cruise and during many targeted flybys in tour when greater control authority was needed to overcome atmospheric drag forces or to perform fast turns. Polynomial accelerations were also used stochastically to absorb low-level errors from other imperfect models such as solar radiation pressure, where surface reflectivity as a function of Sun angle was not well determined.

An exponential acceleration model was used for asymmetric thermal forces resulting from Cassini's radioisotope thermoelectric generators (RTGs). The RTGs are shielded on one side to reflect heat away from the spacecraft. As the heat is reflected in one direction, the spacecraft is accelerated in the opposite direction. Over time, as the radioactive material decays, the force decreases. However, the spacecraft mass decreases more quickly due to propellant usage and release of the Huygens probe, causing the acceleration to increase. The end of mission (EOM) acceleration from this force was more than double the pre-tour value.

Solar radiation pressure forces were more important at the beginning of the mission than the end because of Cassini-Huygens proximity to the Sun. At its closest, Cassini-Huygens was only 0.67 astronomical units (AU) away from the Sun. At its farthest, while in orbit about Saturn, Cassini was ~10 AU from the Sun. Solar radiation pressure imparts direct and indirect forces to the spacecraft. Direct forces are caused by photons pushing the spacecraft away from the Sun. Indirect forces are caused by photons imparting torques to the spacecraft which are then neutralized by thruster firings if in RCS mode or absorbed by reaction wheels if in RWA mode.

Atmospheric drag force models were used when the spacecraft passed close to Titan or Saturn. Drag forces at Titan were generally modeled only when the spacecraft closest approach altitude was 1300 km or less. Above that altitude, drag forces were too small to be measurable. Cassini's closest flyby to Titan was during the T70 flyby, occurring June 21, 2010, and had an altitude of 878 km. Drag forces at Saturn were modeled for the last five Saturn periapses of the Grand Finale, when the altitude from Saturn's 1-bar surface was less than 2000 km.

Impulsive burn forces, polynomial acceleration forces, and solar radiation torque forces all derive from the uncoupled nature of the RCS thrusters. These thrusters always fire in pairs, and are coupled along the spacecraft Y-axis, but not coupled along the Z-axis (Figure 1-1). Thus, Z-thruster firings impart a translational velocity to the spacecraft.

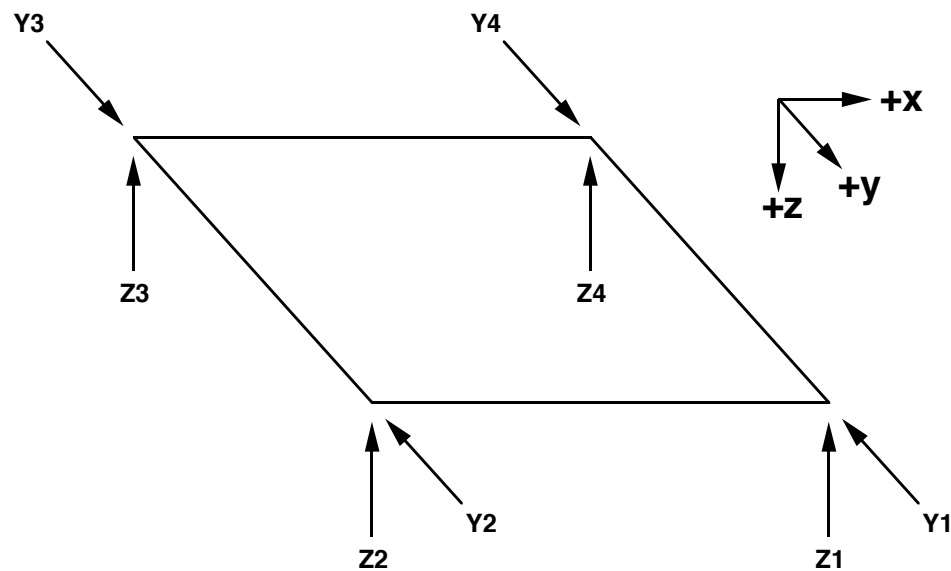


Figure 1-1. Cassini thruster geometry.

Cassini navigators began mission operations using JPL's Double Precision Trajectory/Orbit Determination Program (DPTRAJ/ODP), and Maneuver Operation Program Set (MOPS) FORTRAN based tools. At the end of calendar year 2011, after an extensive 2-year test and checkout period, navigators transitioned to the new C++ based Mission Analysis, Operations, and Navigation Toolkit Environment (MONTE) software set with python layered on top. MONTE was then used through the EOM.

1.3 Tracking Data

Navigators acquired and filtered Doppler and range tracking data, Very Long Baseline Interferometry (VLBI) tracking data, and Optical Navigation (OPNAV) frames during Cassini's operational mission. Doppler and range data were collected and processed throughout the entire operational mission. VLBI data was collected and processed in the few months prior to Huygens probe release to meet atmospheric entry condition requirements. It was also collected roughly biannually afterwards to improve accuracy of the Saturn ephemeris. The acquisition of OPNAV frames began approximately seven months before SOI and extended until about one year before the end of the Solstice Mission.

1.3.1 Doppler and Range

Navigators used X-band tracking data provided by the Deep Space Network (DSN) to estimate the Cassini-Huygens trajectory. During the Grand Finale portion of the mission, some X-band European Space Agency (ESA) tracking data from New Norcia, Australia, and Malargüe, Argentina was also collected and used. Tropospheric and ionospheric calibrations were applied to all DSN radiometric tracking. Additionally, DSN complex interstation clock offsets were applied to DSN 3-way Doppler tracking. Doppler data was generally compressed at 5-minute intervals for interplanetary cruise operations and 1-minute intervals for tour operations. Smaller compression intervals were occasionally used for estimation of parameters with higher frequency signatures, such as gravity field harmonics when tracking was acquired through closest approach of a targeted flyby. Sequential ranging [1] was collected primarily at 5-minute intervals, although there were periods early in interplanetary cruise where up to 35-minute intervals were required due to low signal strength from the Low-Gain Antennas (LGA) while using the High-Gain Antenna (HGA) as a Sun shield.

Weighting algorithms varied during Cassini's operational lifetime. The method ultimately settled upon was a pass by pass weighting strategy where range information within a pass would be effectively collapsed to a single representative point and spacecraft rate information would then be derived primarily from the Doppler data. Range weights were applied on a pass by pass basis according to a representative noise level of 1 m scaled by a factor equal to the square root of the number of points within the pass. Doppler weights were also applied on a pass by pass basis but according to the noise level of the data within each tracking pass scaled by a factor of 3.36 to account for solar plasma effects [2].

1.3.2 VLBI

Near the beginning of tour operations, navigators used VLBI data to examine unexpected results that would affect future Huygens probe operations. Between separation from Cassini and Titan atmospheric entry, Huygens' ballistic trajectory would be gravitationally perturbed by a 124,000 kilometer Iapetus flyby, and an accurate estimate of the perturbation was needed to meet Titan atmospheric entry requirements. Initial Doppler and range tracking data after SOI and a distant 2.5 million kilometer flyby of Iapetus lead to an estimate of Iapetus' mass that varied from its *a priori* value by more than three times its formal uncertainty. Verification was desired, prompting the scheduling of several interferometric measurements using the National Radio Astronomy Observatory's (NRAO) Very Long Baseline Array [3]. Test observations were successfully acquired on June 20 and September 8, 2004. Additional observations were then successfully acquired on October 14, 16 17, 19, and 20, 2004, bracketing a 1.1 million kilometer

distant flyby of Iapetus on October 18, 2004. The observations were nominally weighted at around 0.12 nanosecond, although many alternate weighting strategies were investigated.

VLBI observations were also scheduled approximately biannually while in orbit about Saturn to improve Saturn ephemeris accuracy [4, 5].

1.3.3 Optical Navigation Images

Prior to collecting and filtering Cassini OPNAV images, Saturn-centered satellite ephemeris uncertainties were hundreds of kilometers for most of the icy satellites. Mimas and Phoebe uncertainties were largest at over one thousand kilometers. The first targeted Titan flyby was at an altitude of only 1200 km and, because of its thick atmosphere, safety issues were a concern for altitudes below about 900 km. Yet, Titan ephemeris uncertainties were approximately 150 km. Clearly, OPNAVs were needed to fly the Cassini Mission, and a campaign to reduce satellite ephemeris uncertainties with OPNAVs began in February 2004, five months before SOI.

OPNAV frames of eight of Saturn's icy satellites (Mimas, Enceladus, Tethys, Dione, Rhea, Hyperion, Iapetus, and Phoebe) were collected and used extensively throughout Prime and Equinox Missions. Multiple frames were shuttered almost daily over the first year of orbital operations. Near the end of Equinox Mission, frames were shuttered weekly. During Solstice Mission, when the orbits of Saturn's satellites were well determined, OPNAVs were shuttered at the rate of one frame per transfer between targeted flybys (roughly once per month or longer) to reduce future error growth. The last opnav, an image of Rhea with several stars in the background, was shuttered September 20, 2016 [6].

Stars in OPNAV frames were weighted at 0.1 pixel. Satellites were weighted according to an algorithm that scaled according to the apparent diameter of the satellite: pixel information content was de-weighted as the apparent diameter increased. Apparent diameter scale factors ranged from 1 to 6%, depending on the satellite. A minimum value was root-sum-squared with it to maintain reasonable weights for images of very distant satellites. Minimum values ranged from 0.25 to 0.50 pixel, again depending on the satellite [7].

1.4 Trajectory Control

Trajectory control was required to maintain Cassini-Huygens near the pre-planned trajectory and to meet planetary protection requirements. Deterministic maneuvers were often needed to shape the trajectory while the spacecraft was still distant from the next target and statistical maneuvers were needed to clean up orbit determination (OD) and maneuver execution errors so that misses at the next target would be small. Maneuvers performed during interplanetary cruise were designated as Trajectory Correction Maneuvers (TCMs). During tour, they were designated as Orbit Trim Maneuvers (OTMs).

The maneuver strategy typically required three maneuvers between successive targeted encounters. The first one was soon after the encounter to clean up the dispersions caused by errors in the flyby. The next two maneuvers were targeted to provide an accurate delivery to the next encounter. Additional maneuvers were sometimes added if there were long time intervals between encounters. These extra maneuvers prevented undue buildup in OD error and were sometimes needed to satisfy a flight rule requiring a main engine (ME) flushing maneuver of at least 5 seconds duration within 400-day intervals.

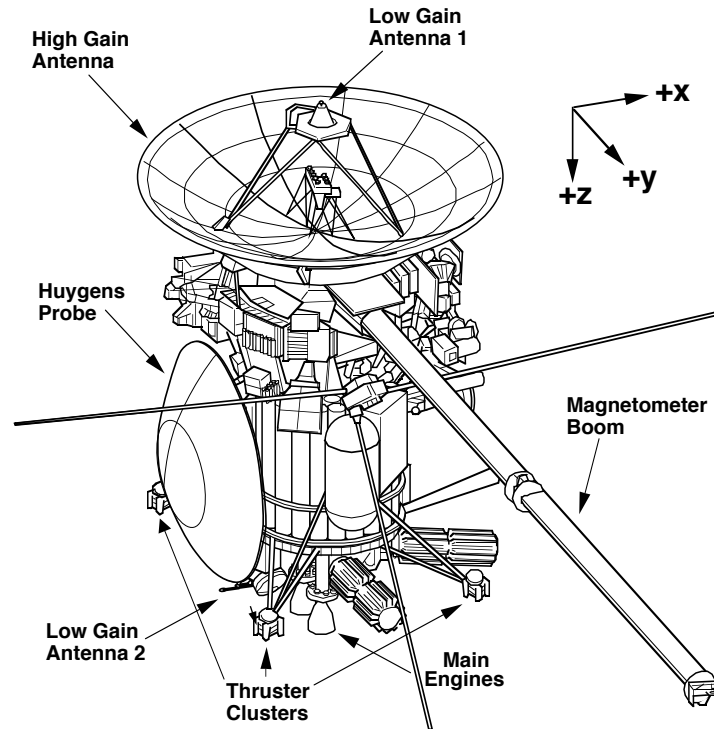


Figure 1-2. The Cassini-Huygens spacecraft.

Cassini used two independent propulsive systems for flight path control (Figure 1-2). The bi-propellant ME system was used for larger maneuvers and consisted of two 445 N gimbaled thrusters, Main Engine A (MEA) and a redundant Main Engine B (MEB). MEB was never used. The $-Z$ -axis facing monopropellant RCS thrusters were used for smaller maneuvers. The RCS consisted of two branches of four coupled $\pm Y$ -facing and four uncoupled $-Z$ -facing 1.0 N thrusters. Branch A thrusters were used through OTM-178 in December 2008. The redundant Branch B thrusters became operational with OTM-183X (March 2009) shortly after the Branch A thrusters were found to be degraded. The crossover boundary in determining which system to use was chosen by considering maneuver accuracy, maneuver duration, and balancing navigation propellant margins between the two systems. Between launch and EOM, the crossover boundary decreased from 0.8 m/s [8] to approximately 0.25 m/s. The final value was chosen to conserve monopropellant and limit RCS thruster throughput while also satisfying a requirement that ME thruster on-times must be at least one second.

Turns to burn attitude were always attained from an initial HGA to Earth or Sun attitude (nearly synonymous with the spacecraft $-Z$ axis to Earth or Sun direction). A roll wind turn of up to 180° about the spacecraft $\pm Z$ axis was performed first. After allowing an appropriate amount of settling time for the Attitude Control Subsystem (ACS), a yaw wind would next be performed about the spacecraft $-Y$ axis. For RCS burns, these two turns were sufficient to achieve the burn attitude. For ME burns, an additional 0.9° turn was needed to account for a misalignment of the MEA. After performing the burn, the spacecraft attitude would unwind in the opposite manner, placing the spacecraft back in the initial Earth or Sun pointed attitude. Turning in this manner ensured protection of sensitive instruments from sunlight and enabled acquisition of tracking data before and after the burn.

Some turns were performed with the RCS and imparted a ΔV to the spacecraft. Reaction wheel speed changes were also often required and imparted additional ΔV to the spacecraft. Commanded ΔV was adjusted accordingly so that the vector sum of commanded and incidental ΔV s equaled the desired ΔV needed to achieve target conditions.

1.5 Planetary Protection

In accordance with references [9], [10], and [11], as well as subsequent verbal communications, NASA designated the Cassini prime mission as Category II. There were no formal implementation requirements for Category II, but the likelihood of accidental impact with a target planet needed to be minimized. The term target planet was interpreted in the broad sense defined in references [9] and [10], namely, the solar system planets (excluding Earth), their satellites (excluding Earth's moon), and such solar system objects as cometary nuclei and asteroids. During prime mission, orbit control was within the predicted normally occurring navigation delivery statistics for all the planetary and satellite encounters as well as for the Huygens probe.

The Cassini Project governed planetary protection requirements for the Earth flyby [12] and [13]. Because the Cassini spacecraft used RTGs to supply electrical power, precautions were taken to ensure that an inadvertent reentry into Earth's atmosphere was not a credible event. The probability of Earth impact by the spacecraft was required to not exceed 10^{-6} taking into account potential spacecraft failures. Efforts taken to achieve this probability are described further in Section 2.4.

With the discovery of a subsurface ocean at Enceladus, NASA planetary protection requirements evolved for Cassini's Equinox and Solstice Missions [14]. The newer requirements stated that the probability that a Category II body would be contaminated during the period of exploration should be no more than 10^{-3} . All of the Saturnian satellites except Enceladus were designated as Category II bodies. Enceladus, now a Category III body with ocean or other liquid water body, required a stricter probability of no more than 10^{-4} .

Planetary protection requirements were met throughout Equinox and Solstice Missions for all but two of Saturn's satellites. With many close flybys of Titan and Enceladus remaining, impact probabilities accumulated with each targeted flyby, eventually exceeding the required limits before mission completion. Because requirements were not met through the entire mission and because spacecraft failure modeling was a significant factor in the accumulation of probabilities, the Cassini Project Office began providing spacecraft health briefings to NASA's planetary protection office six months prior to when allowable probabilities would be exceeded. The spacecraft's health and project's performance to date was assessed and, based on this information, a decision would be made on how to proceed with the remaining mission. Briefings occurred July 7, 2010, October 3, 2012, February 11, 2015, December 2, 2015, and June 6, 2016. At each of these briefings, spacecraft health and project performance were deemed sufficient to re-set impact probabilities to zero, which then defined when the next briefing would occur.

2 Launch & Interplanetary Cruise

Cassini-Huygens' journey from Earth to Saturn began October 15, 1997 on a trajectory that initially took it closer to the Sun for its first gravity assist, a 284 km flyby above Venus' surface that took place six months after launch (April 26, 1998). Fourteen months after this flyby (June 24, 1999), with help from a planned Deep Space Maneuver (DSM) course correction, Cassini-Huygens returned to Venus for a second gravity assist, this time with an altitude of 603 km. Two months later (August 18, 1999), an 1175 km Earth flyby provided the spacecraft with enough energy to reach Jupiter, where it achieved its final interplanetary gravity assist to Saturn from a distant, 9.72 million km flyby (December 30, 2000). The Venus-Venus-Earth-Jupiter Gravity Assist (VVEJGA) trajectory is shown in Figure 2-1, and a list of some key significant events are provided in Table 2-1. Planning for interplanetary cruise is described in the 1996 Cassini Navigation Plan [8] and five subsequent updates [15-19], and one update to maneuver execution dates [20].

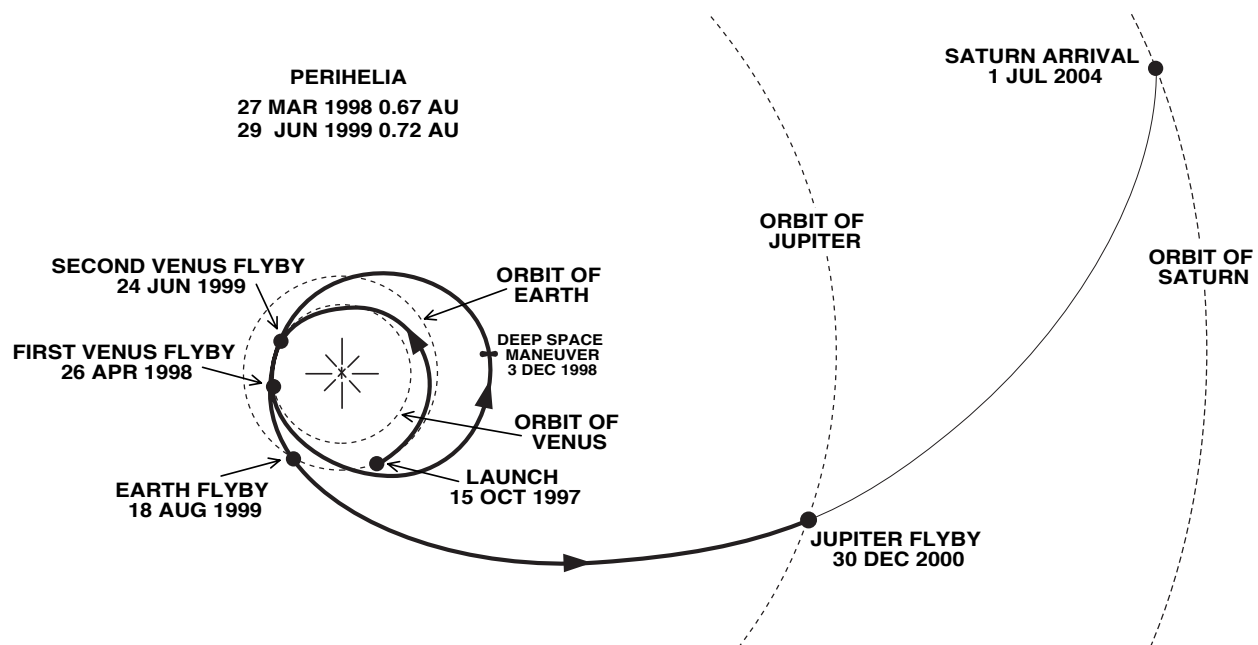


Figure 2-1. The Cassini-Huygens interplanetary trajectory.

In terms of Cassini's high-level operational requirements, interplanetary cruise may be divided into two parts. A Cassini-Sun range of 2.7 AU separates the two parts. While within 2.7 AU from the Sun, ground controllers prevented Cassini-Huygens from overheating by commanding a HGA to Sun attitude. The 4-meter diameter HGA shielded the rest of the spacecraft from sunlight. Two large beamwidth LGAs (LGA-1 and LGA-2) provided communications and tracking data to Earth. LGA-1 was co-located with the HGA, with both directed along the spacecraft -Z axis, whereas LGA-2 was located at the opposite end of the spacecraft and directed along the -X axis. Cassini's HGA provided communications only during two short intervals near solar opposition, from late December 1998 into January 1999 and again in September 1999. Cassini-Huygens crossed the 2.7 AU Sun-range boundary on February 1, 2000 and, in this less intense thermal environment, was allowed to point its HGA away from the Sun and begin using it to provide communications on a regular basis.

Table 2-1. Interplanetary cruise mission events.

Mission Events	Calendar Date	Days from Launch	Comments
Launch	15 Oct 1997	0	$C3 = 16.6 \text{ km}^2/\text{sec}^2$
APHELION	06 Nov 1997	21	Sun range = 1.011 AU
• Conjunction	09 Feb 1998	117	Inferior conjunction
PERIHELION	27 Mar 1998	162	Sun range = 0.6732 AU
Venus flyby	26 Apr 1998	193	Altitude = 284 km; Velocity = 11.8 km/sec
DSM	03 Dec 1998	414	$\Delta V = 450 \text{ m/sec}$
APHELION	07 Dec 1998	418	Sun range = 1.58 AU
HGA	28 Dec 1998	439	25-day instrument checkout period
• Opposition	10 Jan 1999	452	
LGA	21 Jan 1999	462	Thermal constraints restrict HGA usage
Venus flyby	24 Jun 1999	617	Altitude = 603 km; Velocity = 13.6 km/sec
PERIHELION	29 Jun 1999	622	Sun range = 0.7211 AU
• Conjunction	17 Aug 1999	671	Inferior conjunction
Earth flyby	18 Aug 1999	672	Altitude = 1175 km; Velocity = 19.0 km/sec
• •Opposition	13 Sep 1999	698	
Enter Asteroid Belt	11 Dec 1999	787	Sun range = 2.2 AU
HGA	01 Feb 2000	839	HGA is Earth-pointed; use after this date
Exit Asteroid Belt	12 Apr 2000	910	Sun range = 3.3 AU
• Conjunction	13 May 2000	941	Superior Conjunction
• Opposition	28 Nov 2000	1140	Gravitational Wave Opportunity
Jupiter flyby	30 Dec 2000	1172	Altitude = 9722965 km; Velocity = 11.60 km/sec
• Conjunction	07 Jun 2001	1331	Superior Conjunction
• Opposition	16 Dec 2001	1523	Gravitational Wave Experiment—opp \pm 20 days
• Conjunction	21 Jun 2002	1710	Conjunction experiment—conj \pm 15 days
SCIENCE ON	02 Jul 2002	1721	Cruise science begins 2 years before SOI
• Opposition	27 Dec 2002	1899	Gravitational Wave Experiment—opp \pm 20 days
• Conjunction	01 Jul 2003	2085	Conjunction experiment—conj \pm 15 days
• Opposition	04 Jan 2004	2272	Gravitational Wave Experiment—opp \pm 20 days
Phoebe flyby	11 Jun 2004	2430	Altitude = 2,071 km
SOI	01 Jul 2004	2451	$\Delta V = 626 \text{ m/sec}$
• Conjunction	08 Jul 2004	2458	

Tracking via the LGAs while keeping the spacecraft $-Z$ axis Sun-pointed created a minor complexity in scheduling range data. As the active LGA boresight moved angularly from Earth and the spacecraft-to-Earth distance changed, the P_R/N_0 signal strength also changed. To ensure receipt of accurate ranging, range parameters could not remain static. The number of range components, integration time used for the range clock, and integration time used for the ambiguity-

resolving components were computed based on predicted signal strengths and provided to DSN operators. These changes caused intervals between range points to vary between 45 seconds and 35 minutes.

The attitude control mode also differed across the 2.7 AU Sun-range boundary. When the range was less than 2.7 AU, coupled and uncoupled thrusters maintained Cassini's attitude within a pre-commanded angular deadband via RCS mode. When greater, reaction wheels generally maintained Cassini's attitude via RWA mode. In RCS mode, thrusters fired every couple of hours to neutralize angular momentum buildup caused by solar pressure. The navigation team implemented a solar torque model to account for the average acceleration imparted to the spacecraft due to thruster activity, where the modeled acceleration changed with spacecraft attitude and distance from the Sun. In RWA mode, reaction wheels absorbed angular momentum and thrusters fired every few days to manage reaction wheel speeds. The navigation team implemented impulsive maneuver models to account for these less frequent thruster firings.

Navigation activities during launch and interplanetary cruise were well documented in several conference papers [21], [22], [23], [24], and [25].

2.1 Launch

Cassini-Huygens nominal launch period extended from October 6 to November 4, 1997. Launch aboard a Titan IV/Centaur vehicle with Solid Rocket Motor Upgrade (SRMU) strap-on(s) was delayed twice. The first delay, to October 13, resulted when a two-inch tear in Huygens' protective insulation was discovered. An overpowered air conditioner servicing the spacecraft caused the tear. The second delay occurred just minutes before the re-scheduled early morning liftoff on October 13. Launch was scrubbed because of problems with a ground-support computer and upper-level winds blowing at 100 mph or more.

Cassini-Huygens lifted off at the opening of the launch window on October 15 08:43:00.20 Coordinated Universal Time (UTC) with a 93° azimuth from Cape Canaveral Air Force Station. The Multi Mission Navigation Team at JPL produced the first OD estimates using launch orbit updates provided by Lockheed Martin. Their trajectories were used by the DSN to generate antenna pointing and frequency predicts for initial acquisition at Canberra, and the initial passes at Madrid and Goldstone [26]. The Multi Mission Navigation team concluded their support at launch plus 12 hours with a state vector handoff to Cassini navigators, who then continued the navigation effort for the next twenty years.

2.1.1 Performance

The best indicator of hyperbolic injection performance is the magnitude of TCM-1, the cleanup maneuver performed 25 days after launch. TCM-1 required a design magnitude of 2.75 m/s. Because Cassini-Huygens launched at opening of the window and the Venus-1 targets were specified and optimized for a launch that would occur 40 minutes into the window, a deterministic component of 1.4 m/s became necessary. Monte Carlo analysis revealed TCM-1's mean ΔV value to be 3.24 m/s with an uncertainty of 1.45 m/s, and 95% of the samples were 5.88 m/s or smaller [16], [27]. Injection was nominal since the injection cleanup required a ΔV within 0.34 sigma of the predicted mean ΔV .

2.2 Venus-1 Flyby

The Venus-1 flyby provided the first of two Venus gravity assists. Originally designed prelaunch with a flyby altitude of 338 km, navigators opted to cancel TCM-3 and TCM-4 after execution of TCM-2 and redesign the downstream reference trajectory. The redesign resulted in maintaining the 284 km Venus-1 altitude predicted after execution of TCM-2. To avoid a high ΔV penalty from the maneuver cancellations, navigators modestly adjusted the Venus-2, Earth, and Jupiter flybys. Put in perspective, the size of these adjustments was smaller than the variations over the launch space [28]. The Venus-1 flyby imparted a 7.0 kilometers per second (km/s) gravity assist ΔV and 71.3° turn angle to Cassini-Huygens' trajectory (Figure 2-2).

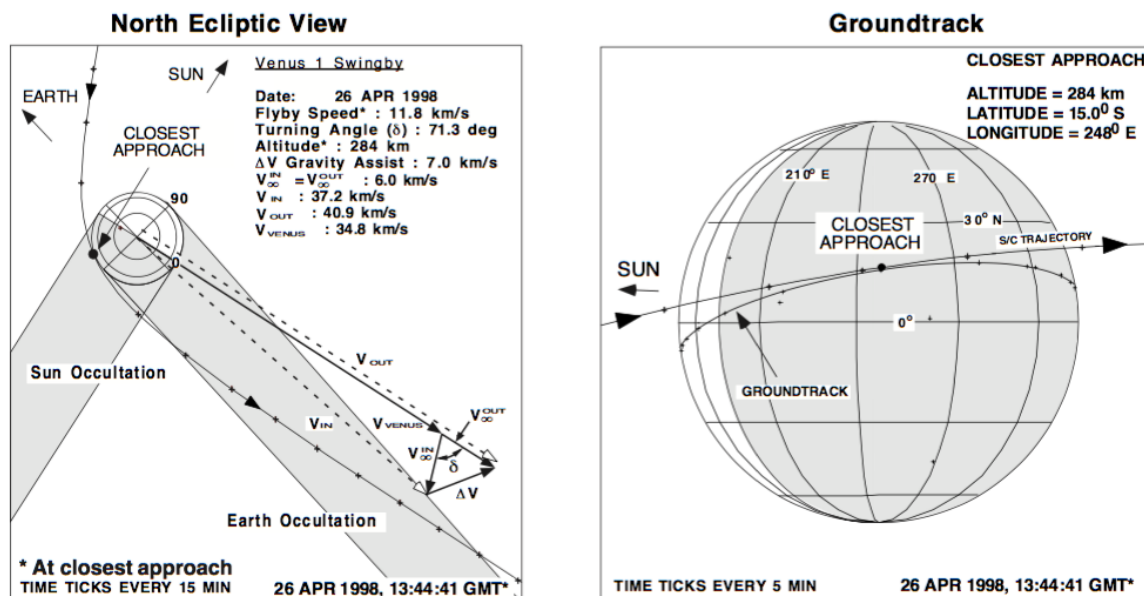


Figure 2-2. Venus 1 flyby geometry.

2.2.1 Performance

Three maneuvers were planned but only two executed between launch and Venus-1. Design magnitudes were within predicted ranges, and both performed maneuvers executed nominally. Both maneuvers were firsts: TCM-1 was the first to be performed with the ME propulsive system, and TCM-2 was the first to be performed with the RCS. TCM-3, the Venus-1 approach maneuver, was canceled with a re-optimized reference trajectory. Performance and other salient characteristics for all maneuvers are tabulated in Appendix A – Supplementary Material, Tables A-5 to A-11 Maneuver History.

With project approval of a reference trajectory update after TCM-2 execution, the prelaunch Venus-1 target was abandoned. ΔV penalties resulting from large target deviations relative to navigation uncertainties were tolerable, so no attempt was made to reduce the Venus-1 flyby differences listed in Appendix A– Supplementary Material, Table A-1 Targeted Encounter History. An OD solution delivered for evaluation of TCM-3, the last control point before Venus-1, predicted differences from the redesigned target to within 1 km in both B·T and B·R and 0.1 seconds in time of closest approach [21], but the benefit of performing the maneuver was outweighed by the benefits of simplifying flight operations and reducing risk by canceling the maneuver.

2.2.2 Notable Events

Some events between launch and Venus-1 having an impact on navigation included deployment of the Radio and Plasma Wave Science (RPWS) instrument on October 26 and, on the same day, a swap from LGA-1 to LGA-2. The RPWS deployment necessitated minor updates to solar pressure and solar torque models, while the LGA swap lead to an update of the transponder delay model. The first of six spacecraft safings occurred March 24 and imparted approximately 5 millimeters per second (mm/s) of unplanned ΔV to Cassini-Huygens. Safing was triggered when an overly sensitive error monitor detected a misalignment between Stellar Reference Units (SRUs).

The Cassini-Huygens Mission demonstrated that it was possible to acquire high quality range tracking data with point-to-point intervals exceeding 30 minutes. Deep Space Station (DSS) 15 and 65 tracks scheduled April 18–21, 1998, successfully acquired range data with P_r/N_0 levels near -10 dB-Hz and intervals of 35 minutes. Acquisition of range data during this portion of the mission was particularly significant to the OD process because the spacecraft geocentric declination was often near zero degrees, where Doppler data's ability to accurately determine declination is very poor [29].

Two tracking anomalies arose shortly after launch, one regarding range data and the other regarding Doppler data, and both were quickly resolved. Range noise was observed to step up in discrete increments over a 10-hour cycle and across different stations from an expected noise level of less than 1 meter peak-to-peak to an unexpected level of 5 meters. The noise then abruptly dropped to less than 1 meter and a new cycle would begin (Figure 2-3). The anomaly occurred when using 24 as the last ranging component and the period of the cycle corresponded to the transit time through component 24's ambiguity modulus. Navigators hypothesized that software was

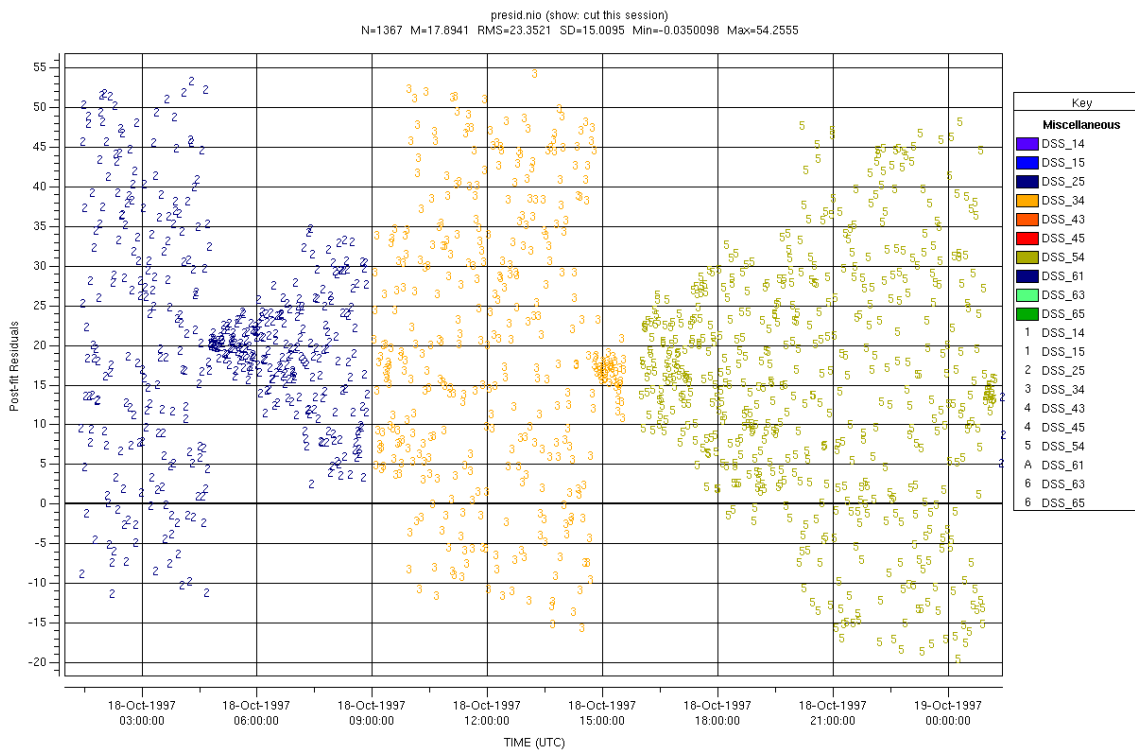


Figure 2-3. Cassini range anomaly.

unable to accommodate the full precision of component 24's ambiguity modulus and truncation of the modulus was creating noise entirely numerical in character [30]. The anomaly was resolved by using 19 as the last ranging component, thereby decreasing the ambiguity modulus by a factor of 25.

The Doppler tracking anomaly was manifested as a banding signature and was caused by jumps in the phase counts. These jumps occurred approximately every half-hour when the Block V Receiver (BVR) processed the next predicts point. The anomaly was traced to BVR software and was initially overcome with a one-line workaround by the station operator. After the Venus-1 flyby, a coding fix was implemented [31].

2.3 Venus-2 Flyby

The Venus-2 flyby provided the second and final Venus gravity assist. It was the only non-targeted flyby during interplanetary cruise. TCM-4 was canceled as a result of the reference trajectory redesign after TCM-2 execution and the four remaining maneuvers between the Venus-1 and Venus-2 flybys targeted Earth's B-plane, not Venus'. The first of these was TCM-5, also called the DSM. With a deterministic ΔV of 450 m/s, the DSM was the largest maneuver to date. Indeed, only one maneuver in the entire mission was larger—SOI. The DSM lowered perihelion so that Cassini would encounter Venus-2 earlier and with a greater flight path angle, imparting a gravity assist ΔV of 6.7 km/s and turn angle of 41.6° to Cassini-Huygens' trajectory (Figure 2-4).

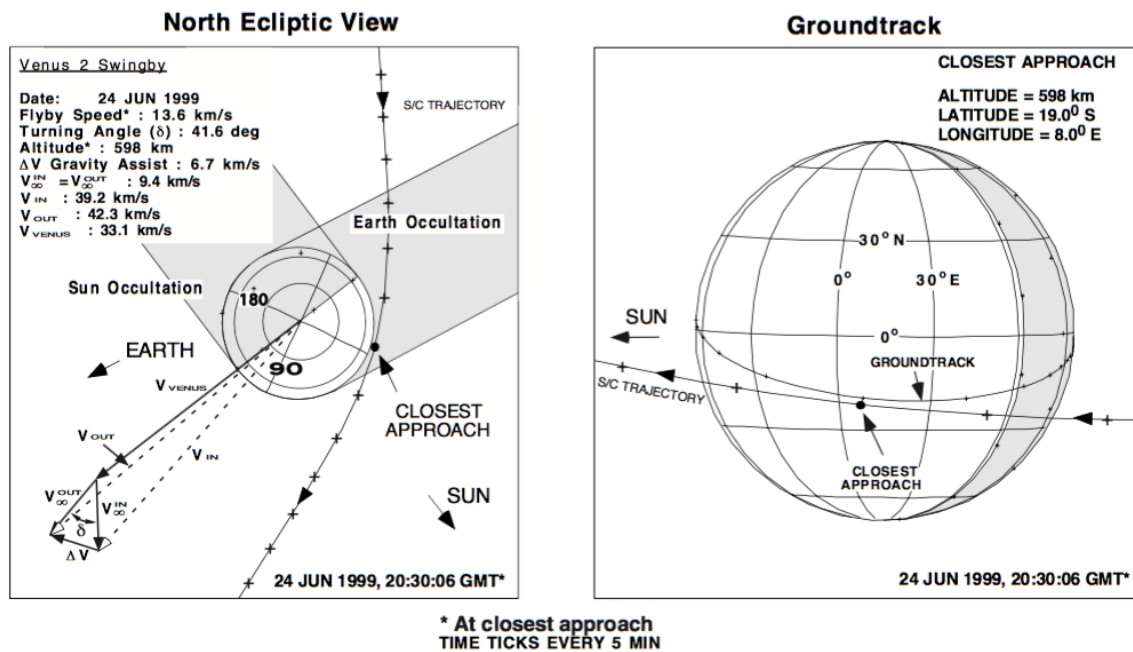


Figure 2-4. Venus 2 flyby geometry.

After execution of the DSM, the best-estimate orbit was used to redesign the reference trajectory. New targets for Earth and Jupiter were devised. While not targeted, the nominal Venus-2 flyby altitude decreased from 607 km to 598 km. The bias removal strategy for the upcoming Earth flyby was held constant. Only the time-of-arrival targets were allowed to change for the biased aim-points, as the probability of Earth impact was independent of target time. Time-of-arrival targets were updated to reduce the ΔV cost of the biasing strategy. As a result of the redesign, the

previously statistical TCM-6 and TCM-7 maneuvers now included deterministic components. TCM-8 remained a statistical maneuver and was ultimately canceled because the small correction it was to make was within the navigation delivery statistics. Expected execution errors from TCM-8 would prevent substantial improvement to the target accuracy. In addition, cancellation translated into a 4 m/s savings for TCM-9 since the target offset already took care of some of the TCM-9 bias removal.

2.3.1 Performance

With the trajectory redesign after TCM-2, four maneuvers were planned between Venus-1 and Venus-2 but only three were executed. TCM-8, a purely statistical maneuver, was not needed and canceled. All performed maneuvers executed nominally. From Appendix A – Supplementary Material, Tables A-5 to A-11 Maneuver History, design magnitudes were within range of the predicted statistics for DSM, but were somewhat lower than predicted statistics for TCM-6 and TCM-7. TCM-6's design magnitude was undoubtedly impacted by instrument check-out activities and the unplanned spacecraft safing, seemingly in a favorable way. TCM-7 owes its small size to the accurate execution of TCM-6.

While Venus-2 was not targeted, OD for the last control point, TCM-8, predicted the time-of-closest approach to within 0.5 seconds and the B-plane to within 10 km from the reconstructed orbit, corresponding to a one-sigma error in both timing and position. Tracking for the TCM-8 OD solution included data obtained until 22 days before Venus-2. Based on the reconstructed trajectory, Cassini-Huygens achieved a flyby altitude of 603 km, five kilometers higher than the value resulting from the trajectory redesign.

Analysis of the DSM execution revealed a ME pointing bias of 0.9° . The DSM's large burn magnitude allowed OD analysts to estimate the DSM pointing error very accurately. It differed significantly from the Attitude and Articulation Control Subsystem (AACS) team's estimate. Whereas AACS data represents the spacecraft system's onboard estimates, navigation data represents what was actually observed from Earth. The discrepancy warranted further investigation. A similar discrepancy was observed in TCM-1, but results were less conclusive: TCM-1's magnitude was much smaller and the navigation team's estimate was therefore much less accurate. Upon revisiting and comparing the TCM-1 discrepancy to that of the DSM, navigators found that the error was similar in size and direction when viewed in the spacecraft-fixed coordinate frame. The navigation team's conclusion of the existence of a pointing bias was supported by a prelaunch analysis that indicated such a bias may exist. To correct the bias, a new rotation of the spacecraft was introduced into the maneuver sequence. The previous sequence—roll wind, yaw wind, maneuver burn, yaw unwind, roll unwind—would now include additional 0.9° wind and unwind turns between the yaw wind/unwind and the maneuver burn. The ΔV imparted by these new turns, 7.6 mm/s initially and 6.1 mm/s once in tour (due to mass property changes associated with probe release, SOI, and one other large burn), would be modeled in future ME burns beginning with TCM-10.

2.3.2 Notable Events

Some events between Venus-1 and Venus-2 having an impact on navigation included a swap from LGA-2 to LGA-1 on June 24, 1998. Analysts updated the transponder delay model accordingly. Solar opposition on January 10, 1999 enabled first use of the HGA. Between December 28, 1998, and January 21, 1999, the HGA could point towards Earth instead of the Sun and continue to

satisfy spacecraft thermal requirements. An instrument check-out period was planned within this 25-day window that would take advantage of the higher data rates made possible with the HGA. Because LGA-1 and the HGA share cabling, an update to the transponder delay was unnecessary. The instrument check-out was interrupted by the second spacecraft safing event on January 12. As part of the safing response, the spacecraft reverted back to LGA-1 and remained on this antenna until spacecraft operators recovered the spacecraft and commanded it back to the HGA on January 15, 1999. This safing event imparted approximately 14 mm/s of unplanned ΔV to Cassini-Huygens. Safing was triggered when an overly sensitive error monitor exceeded its threshold during the slow roll about the spacecraft Z-axis that would keep the $-X$ -axis as close as possible to Sun point while the spacecraft passed through opposition.

2.4 Earth Flyby

The Earth flyby provided a needed gravity assist to boost Cassini-Huygens to Jupiter. With a nominal flyby altitude of 1166 km, the flyby imparted a gravity assist ΔV of 5.5 km/s and a turning angle of 19.7° to Cassini-Huygens' trajectory (Figure 2-5).

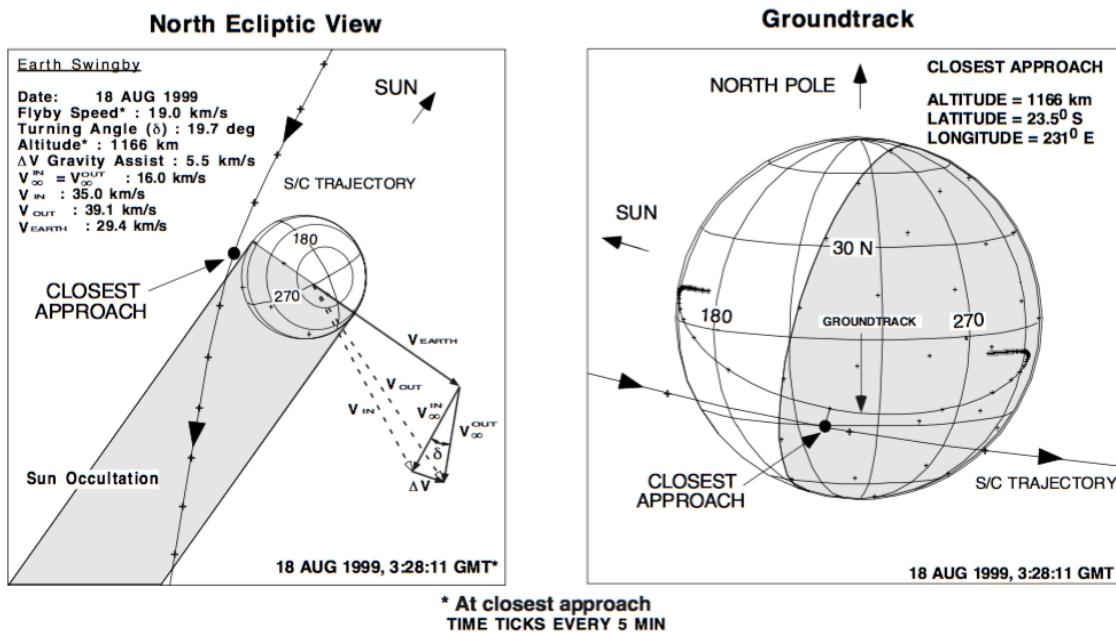


Figure 2-5. Earth flyby geometry.

Four maneuvers, TCM-9, TCM-10, TCM-11, and TCM-12, were planned within the 54 days between Venus-2 and the Earth flyby. Because Cassini used RTGs to supply electrical power, precautions were taken to ensure that an inadvertent reentry into the Earth's atmosphere did not occur. Navigators designed a biased target strategy to satisfy the design requirement that the probability of Earth impact be less than one in a million [12] and [13]. Implementation of the strategy began with the DSM, and targets are shown in Figure 2-6. Aim-points are laid out in the EMO2000 B-plane such that neither the extension of the line connecting TCM-10 and TCM-11 aim-points nor that connecting the TCM-11 and TCM-12 aim-points will cross the Earth disk. Each of the maneuvers has a deterministic component which removes a built-in trajectory bias of the Earth flyby aim-point. Therefore, none of the maneuvers could be canceled. The total deterministic ΔV for this strategy was 101.9 m/s.

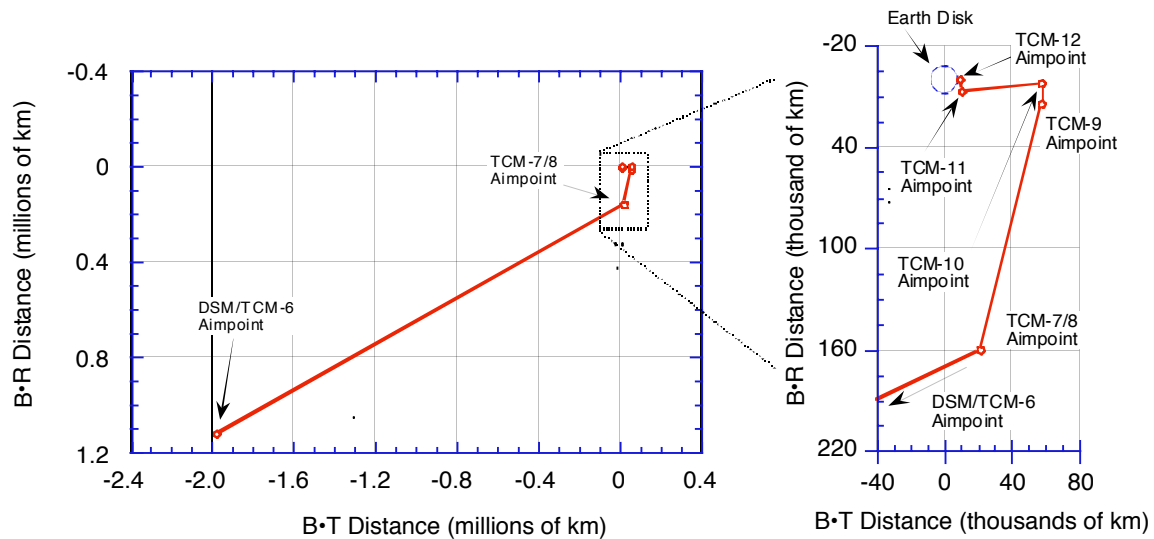


Figure 2-6. Aim-point biasing strategy for Earth (EMO2000 B-plane).

The TCM-12 target time was modified to avoid impacting Earth-orbiting debris. Beginning in 1998 and with more frequency as Cassini approached Earth, data was exchanged with the U.S. Air Force Space Command to determine if any debris hazards warranted concern [32]. Predictions showed one object with a closest approach distance to the spacecraft of 4 km occurring 138 seconds after the spacecraft's perigee. Although the probability of collision was low, the time of perigee was delayed by 14 seconds. That delay increased the closest approach distance with the object from 4 km to about 90 km. Earth Time of Closest Approach listed in Appendix A – Supplementary Material, Table A-1 Targeted Encounter History includes the 14-second timing shift that was implemented.

2.4.1 Performance

All maneuvers between Venus-2 and Earth flyby executed nominally. From Appendix A– Supplementary Material, Tables A-5 to A-11 Maneuver History, design magnitudes were within range of the predicted statistics for TCM-9, TCM-10, and TCM-12, but were somewhat lower than predicted statistics for TCM-11.

Based on the reconstructed trajectory and shown in Appendix A– Supplementary Material, Table A-1 Targeted Encounter History, Cassini-Huygens time of closest approach to Earth was 0.6 seconds later than targeted. The B-plane miss was about 9 km, mostly in B-T, such that the achieved altitude of 1174.9 km was 8.8 km higher than that of the reference trajectory. These differences are much smaller than anticipated [18], owing partly to delaying the TCM-12 final design Data Cut-Off (DCO) by a day.

TCM-9 was the first maneuver to include in its design a ΔV due to deadband tightening. Prior to each cruise maneuver, the attitude control deadband is reduced from 20 to 2 milliradian (mrad), which consistently imparted a ΔV of approximately 3 mm/s to Cassini-Huygens.

TCM-10 was the first maneuver to include in its design a ΔV due to the 0.9° pointing bias wind and unwind turns. During cruise operations, these turns imparted a ΔV of about 7.6 mm/s very near the burn direction. The net effect of including these turns in the design is to reduce the burn

magnitude error by that amount. While the pointing bias was discovered while analyzing TCM-5 data, software modifications and testing were not completed until TCM-10. All later ME maneuvers included these ΔV s in their designs.

2.4.2 Notable Events

The magnetometer boom was deployed two days before closest approach to Earth to collect calibration data during the flyby. Earlier deployment was prohibited because of thermal constraints on the instrument. Besides changing spacecraft mass properties which would affect future maneuver execution errors, the deployment also increased spacecraft torque caused by solar radiation pressure. Navigators modeled the deployment to account for increased ΔV from additional unbalanced thruster firings.

Another event is a discussion of an event that did not happen: an unexplained net velocity gain was not experienced by Cassini-Huygens at Earth closest approach. Prior Earth flybys by the Galileo and Near Earth Rendezvous (NEAR) spacecraft were accompanied with unexplained velocity gains [33]. Galileo experienced a gain of 4.3 mm/s during its first Earth gravity assist in December 1990 and NEAR experienced a gain of 13.0 mm/s during its gravity assist in January 1998. In an ongoing effort to solve this puzzle, some engineers expected Cassini-Huygens to provide another clue. Cassini-Huygens navigators examined Earth flyby tracking data intensively for signs of an unexplained velocity gain, but none were found. Doppler data fit through the flyby did not exhibit any discontinuities greater than its submillimeter per second noise level.

2.5 Jupiter Flyby

The Jupiter flyby provided the final gravity assist to Saturn. Even with a high nominal flyby altitude of 9,722,865 km, the solar system's largest planet imparted a flyby gravity assist ΔV of 2.2 km/s and a turning angle of 12.2° to Cassini-Huygens' trajectory (Figure 2-7).

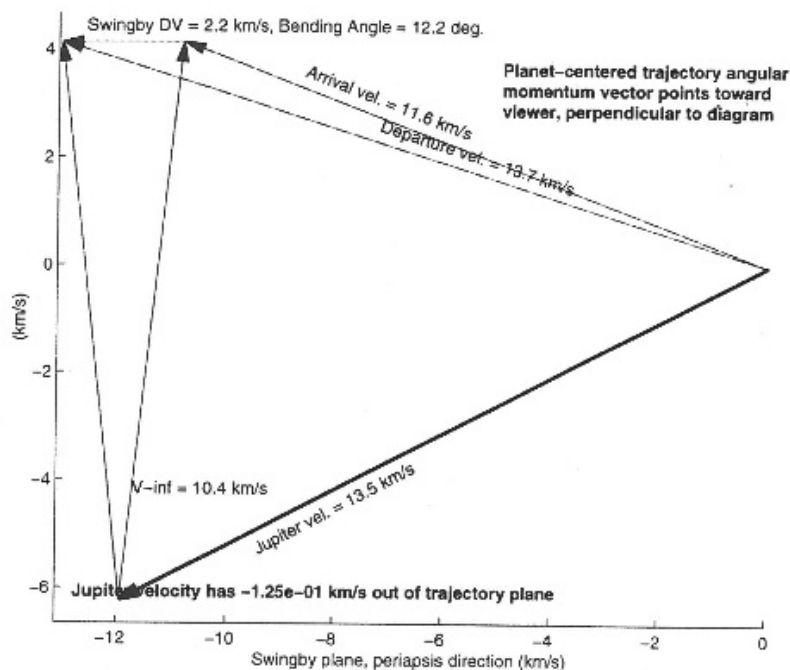


Figure 2-7. Jupiter flyby geometry.

Four maneuvers, TCM-13, TCM-14, TCM-15, and TCM-16, were originally planned in the 16 months between Earth and Jupiter flybys. After execution of TCM-13, the Earth flyby cleanup maneuver, navigators updated the reference trajectory again. With this update, a non-targeted 52,000 km flyby of Saturn's irregular satellite Phoebe was converted into a targeted 2000 km flyby. The update also introduced biases for satisfying the ME-flushing requirement over the next five years leading to SOI. The intent of the flushing requirement was to prevent the precipitation of iron compounds that may go into solution when oxidizer comes into contact with iron alloys in the bipropellant feed system. Precipitated iron compounds can adversely affect engine performance by plugging small orifices. In effect, the wet portion of the ME propellant lines had to be flushed within 400-day intervals. The ME burns of at least five seconds duration would accomplish this.

In the new reference trajectory, TCM-14 was no longer a statistical maneuver. A deterministic component was needed to modify the Jupiter flyby in such a way that the downstream TCM-20 dog-leg maneuver targeting the Phoebe flyby would also align the trajectory with the Saturn ring plane crossing (RPC) aim-point. The deterministic component was also large enough to satisfy the flushing requirement. TCM-15 remained a statistical cleanup maneuver and was canceled after confirming that TCM-14 executed nominally and that the delivery to Jupiter would be reasonably close to the prediction. A decision to cancel TCM-16 was made during development of the new reference trajectory. Considering the superb maneuver execution error performance of the spacecraft, the very distant flyby of Jupiter, and the lack of any requirement for a highly accurate delivery to Jupiter, it was clear that TCM-16 was not necessary.

2.5.1 Performance

TCM-13 and TCM-14 executed nominally. TCM-13, with a design magnitude of 6.7 m/s, was much smaller than the anticipated mean value of 30.5 m/s even when considering the uncertainty of 16.0 m/s. Delaying the TCM-12 DCO by one day clearly paid off in terms of smaller Earth flyby delivery errors for TCM-13 to clean up. TCM-14, with a design magnitude of 0.56 m/s and executed 288 days after TCM-13, re-set the 400-day countdown for ME flushing. The requirement would next be satisfied 259 days later with TCM-17, after the Jupiter flyby.

Based on the reconstructed trajectory and shown in Appendix A – Supplementary Material, Table A-1 Targeted Encounter History, Cassini-Huygens' time of closest approach to Jupiter was 43 seconds later than targeted. The B-plane miss was 160 km in B·R and 114 km in B·T, such that the achieved altitude of 9,722,965 km was 100 km higher than that of the reference trajectory. The target miss was well within expected delivery errors for the last control point, TCM-14. Figure 2-8 shows expected TCM-14 delivery errors about the Jupiter aim-point along with the reconstructed solution, JP83D, in B-plane coordinates.

The maneuver execution error model was updated with in-flight data and used for maneuvers after TCM-13 [34], [23]. While this new model did not improve the accuracy of maneuvers, it did improve the capability to predict maneuver statistics.

The pointing error for TCM-13 was much larger than for the maneuvers immediately preceding it. The cause of the larger error was tracked to a failure to account for the spacecraft center-of-mass shift after deployment of the magnetometer boom. This oversight prevented the ME from being accurately pre-aimed, the goal of which would be to orient the spacecraft such that the initial thrust vector passes through the spacecraft center of mass and towards the desired burn direction. Torques caused by center-of-mass errors must be compensated by the attitude control system as it reorients

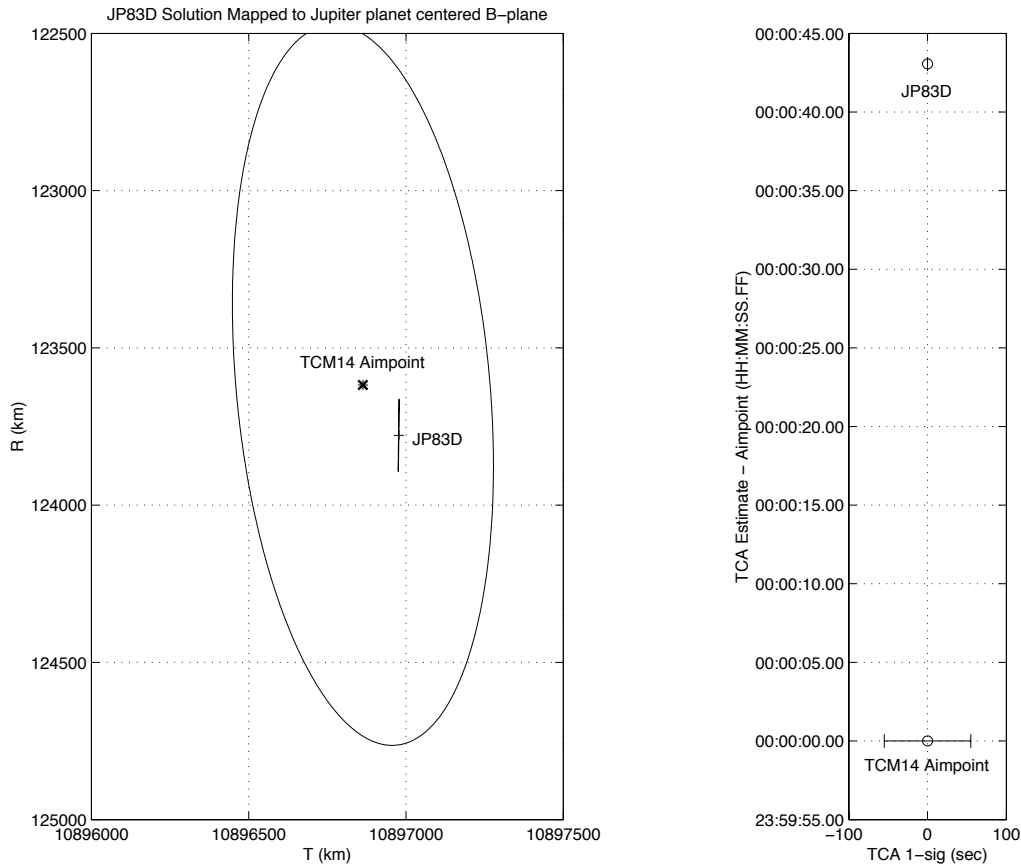


Figure 2-8. Jupiter flyby expected delivery errors and reconstruction in EMO2000 B-plane.

the spacecraft so that the ME thrust vector eventually achieves a steady state direction that matches the desired burn direction. The impact of this oversight was not significant because TCM-13 was much smaller than its pre-execution statistics indicated and because a reference trajectory update between TCM-13 and TCM-14 mitigated potential ΔV costs by re-optimizing downstream targets.

2.5.2 Notable Events

One key event between Earth and Jupiter flybys having an impact on navigation was crossing the 2.7 AU spacecraft-Sun distance boundary on February 1, 2000. On this date, the spacecraft was no longer required to be shaded by the HGA. Default communications were established through the HGA instead of LGA, and signal strength was greatly improved. Range components were selected for a five-minute interval between range measurements and fixed through EOM, requiring no further management. Whereas turns were previously limited to maintaining Sun-point, rolling about the Sun-pointed axis, and turning to maneuver attitudes, restrictions on turns after February 1 were greatly reduced. After checkout of the RWA to ensure proper functioning, attitude control mode transitioned from thrusters to primarily reaction wheels in order to more efficiently accommodate future planned turns. The frequency of thruster firings was reduced from every couple of hours in RCS mode to every few days in RWA mode. To simplify navigation operations and improve navigation accuracies, project schedulers placed RWA management events, or biases, during tracking passes so that ΔV s associated with them could be directly observed.

An unplanned event impacting navigation was an unexpected autonomous swap from RWA to RCS mode that began December 16 and extended until December 22, 2000. This swap imparted roughly 30 mm/s of unmodeled ΔV to Cassini-Huygens' trajectory. It was caused by excessive friction levels within one of the reaction wheels. Prolonged dithering of the wheel at rates very close to zero RPM had led to inadequate lubrication of its ball bearings, with friction levels eventually exceeding fault tolerance limits and triggering the swap. The prescribed corrective action to eliminate future dithering and limit the amount of time spent at low rotation rates resulted in more frequent RWA biases and introduced additional complexities to the maneuver design process.

2.6 Saturn Approach

The last leg of interplanetary cruise spanned the longest interval, from the Jupiter flyby on December 30, 2000, to SOI on July 1, 2004. It includes a 2,000 km targeted encounter of Saturn's largest irregular satellite Phoebe, taking place 19 days before orbit insertion about Saturn. Saturn targeting differed from previous encounter targets. Whereas every prior maneuver had targeted a B-plane, the final approach maneuver to Saturn targeted a specific RPC point free from known or high probability hazards between Saturn's F- and G-rings. Only the ascending node crossing was targeted. The descending node crossing was not targeted as this would have involved an undesirable late update to the SOI maneuver design. The descending node crossing would also nominally pass between the F- and G-rings and was carefully monitored and assessed for safe passage with the design of each maneuver on approach to Saturn. Nominal ascending and descending node crossings relative to three-sigma hazard exclusion zones are shown in Figures 2-9 through 2-12.

Seven of the eight scheduled maneuvers between Jupiter flyby and SOI were performed. TCM-17, TCM-18, and TCM-19 targeted to biased Saturn aim-points in order to satisfy ME flushing requirements. TCM-17 executed 259 days after TCM-14 (the preceding ME maneuver), TCM-18 executed 399 days later, and TCM-19 executed 393 days after TCM-18.

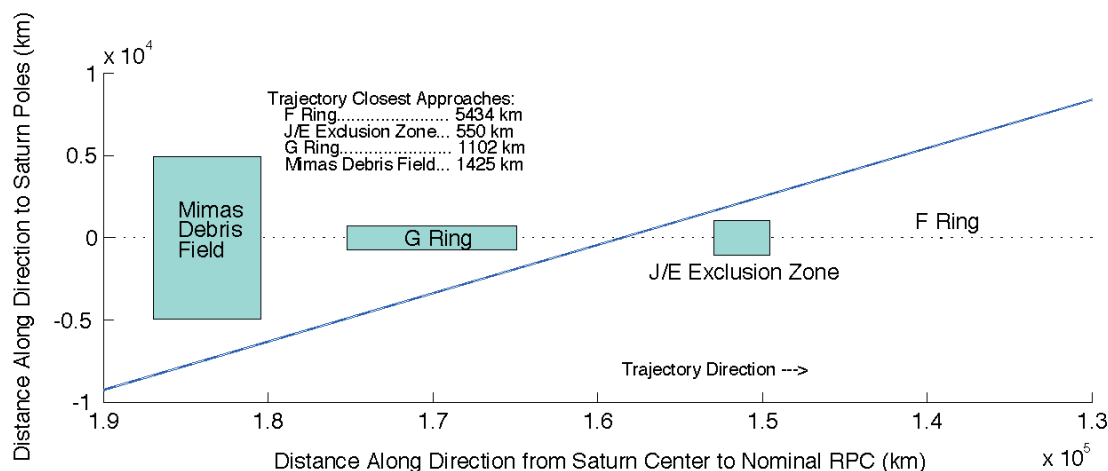


Figure 2-9. Nominal ascending ring plane crossing (viewed from within ring plane).

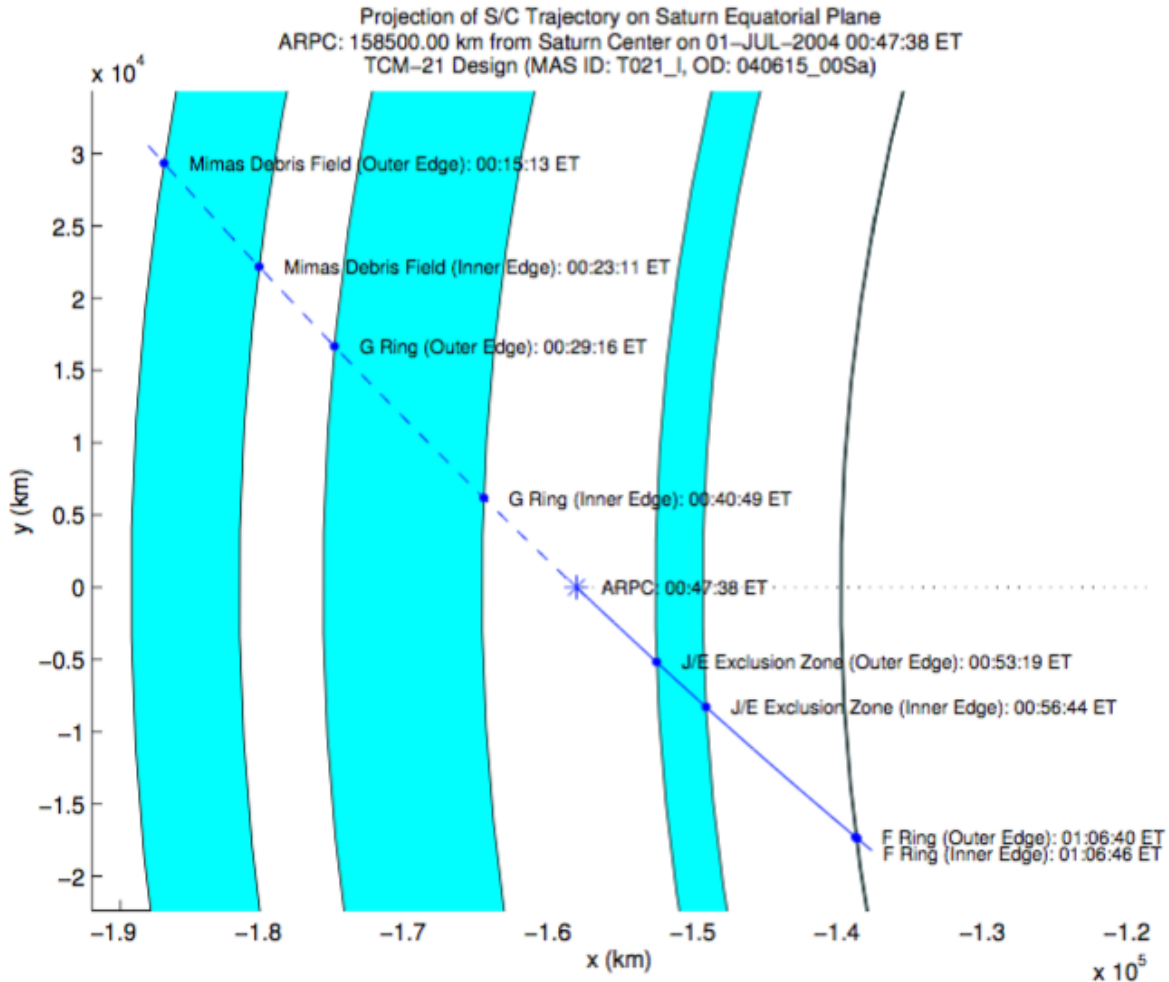


Figure 2-10. Nominal ascending ring plane crossing (viewed from above ring plane).

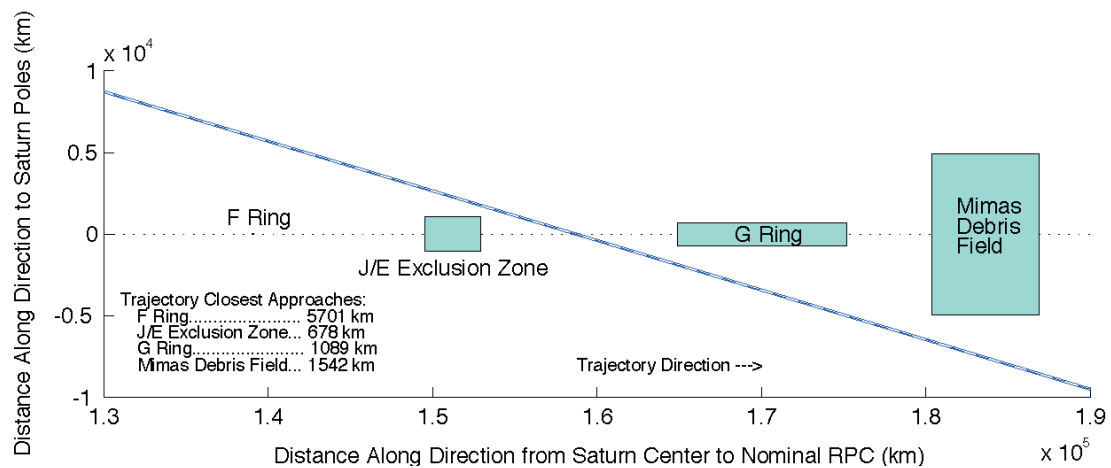


Figure 2-11. Nominal descending ring plane crossing (viewed from within ring plane).

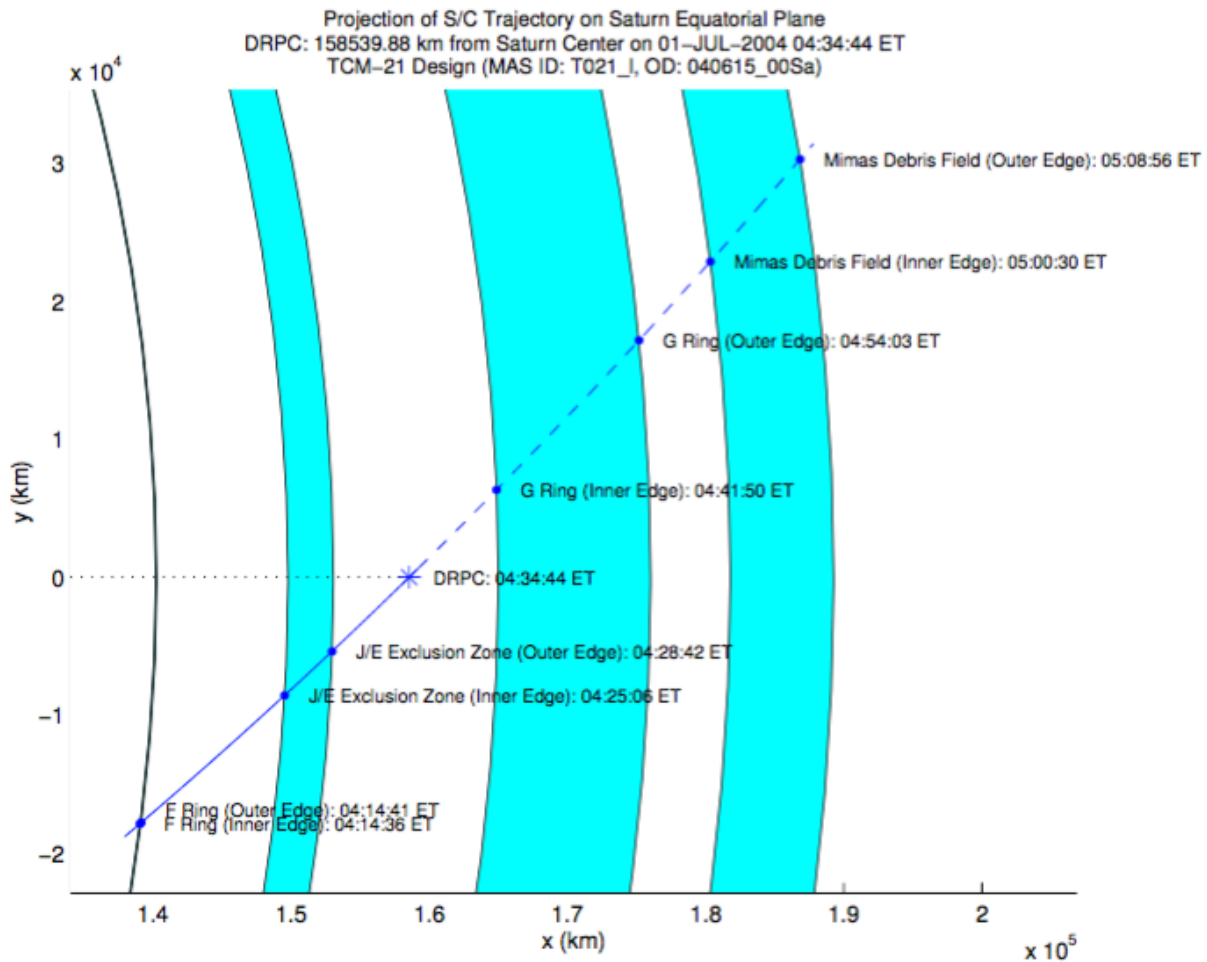


Figure 2-12. Nominal descending ring plane crossing (viewed from above ring plane).

TCM-19a and TCM-19b were introduced as test maneuvers in late 2002. TCM-19a tested a newly developed command sequence for RCS maneuvers, and TCM-19b tested the energy-based termination algorithm and yaw steering that would be used during SOI. Neither maneuver targeted a downstream aim-point—TCM-19 and TCM-20 would absorb most of the downstream ΔV cost required to return to the modified reference trajectory. Magnitudes of both test maneuvers were fixed, 120 mm/s for TCM-19a and 2 m/s for TCM-19b. TCM-19a's burn direction was along the anti-Earth-line direction in order to test with a large turn angle, and TCM-19b's burn direction was chosen to reduce the total ΔV cost and ensure that the pre- and post-TCM-19a trajectory was not on a Saturn impact trajectory.

TCM-20 targeted the Phoebe flyby, executing just fifteen days before the flyby, and TCM-21 executed two days after the flyby, targeting ascending ring-plane conditions at Saturn. TCM-22 was a contingency maneuver requiring execution only in response to an anomaly. It was not needed and canceled.

Figure 2-13 shows how TCM-14 and each of the seven maneuvers between Jupiter flyby and Saturn encounter were biased in the Saturn B-plane. B-plane points plotted in the figure were

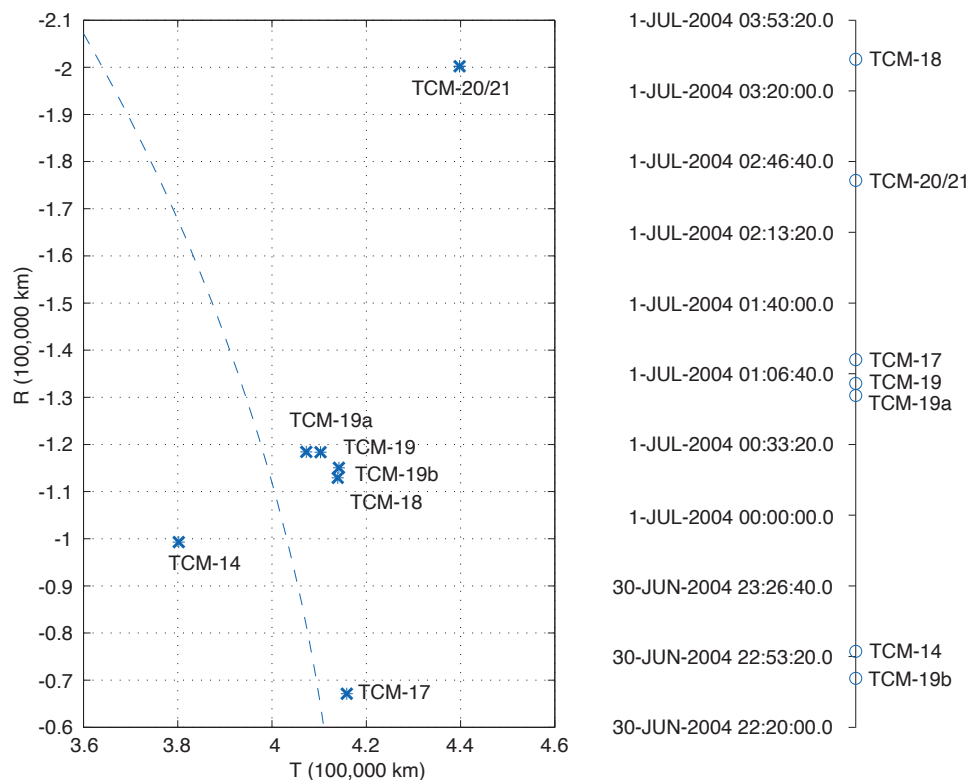


Figure 2-13. Saturn B-plane biasing (EMO2000 B-plane).

derived from a state vector with epoch several hours before Saturn periapsis in order to remove the effect of oblateness on computations.

Navigators began preparing to use OPNAVs more than a year before SOI. OPNAV images would be taken using the Narrow Angle Camera (NAC) of Cassini's Imaging Science Subsystem (ISS). The NAC had a 1024×1024 array of pixels and approximately 6 milliradian field of view—each pixel therefore resolved about 6 microradians (μrad). A geometric calibration of both ISS cameras, narrow and wide angle, was performed in April 2003 [35], and collection of the first set of Saturn satellite images took place in October 2003 at a range of 0.8 AU. A second set of OPNAVs followed in November 2003. These first two sets of images were used to validate commanding procedures and calculate the proper exposure time to be used for imaging each satellite. OPNAV collection and processing began in earnest February 6, 2004, with OPNAV scheduling windows available roughly every three days and several OPNAVs taken within each window. By April, OPNAV windows were available nearly every day.

2.6.1 Performance

All maneuvers between the Jupiter flyby and SOI executed nominally. From Appendix A – Supplementary Material, Tables A-5 to A-11 Maneuver History, design magnitudes were within range of the predicted statistics for TCM-19 and TCM-20, and somewhat lower for TCM-21. Design magnitudes of TCM-19a and TCM-19b were fixed to pre-determined values. Design magnitudes were significantly lower than predicted statistics for TCM-17 and TCM-18. The magnitude of TCM-17, while 3-sigma lower than the predicted mean value, is very close to the

deterministic value. This indicates navigation over-performance at the previously executed maneuver: the combination of OD errors and maneuver execution errors predicted at TCM-14 was overly conservative. It's no longer apparent, sixteen years later, why TCM-18's design magnitude was 3.3 sigma lower than expected, but in an absolute sense, 3.3 sigma is only 34 mm/s and not worrisome.

Based on the reconstructed trajectory and shown in Appendix A – Supplementary Material, Table A-1 Targeted Encounter History, Cassini-Huygens' time of closest approach to Phoebe was 0.2 seconds later than targeted. The B-plane miss was 11 km in B·R and 73 km in B·T, such that the achieved altitude of 2071 km was 71 km higher than that of the reference trajectory. The target miss was well within expected delivery errors for the last control point, TCM-20. Targeted and estimated values are presented in Figure 2-14, where control dispersions resulting from OD uncertainties and TCM-20 execution errors are included with target values. To reduce the effect of control dispersions on science observations, pointing updates based on a late OD estimate were necessary. A live update OD, with DCO five days before Phoebe closest approach, reduced orbit uncertainties considerably.

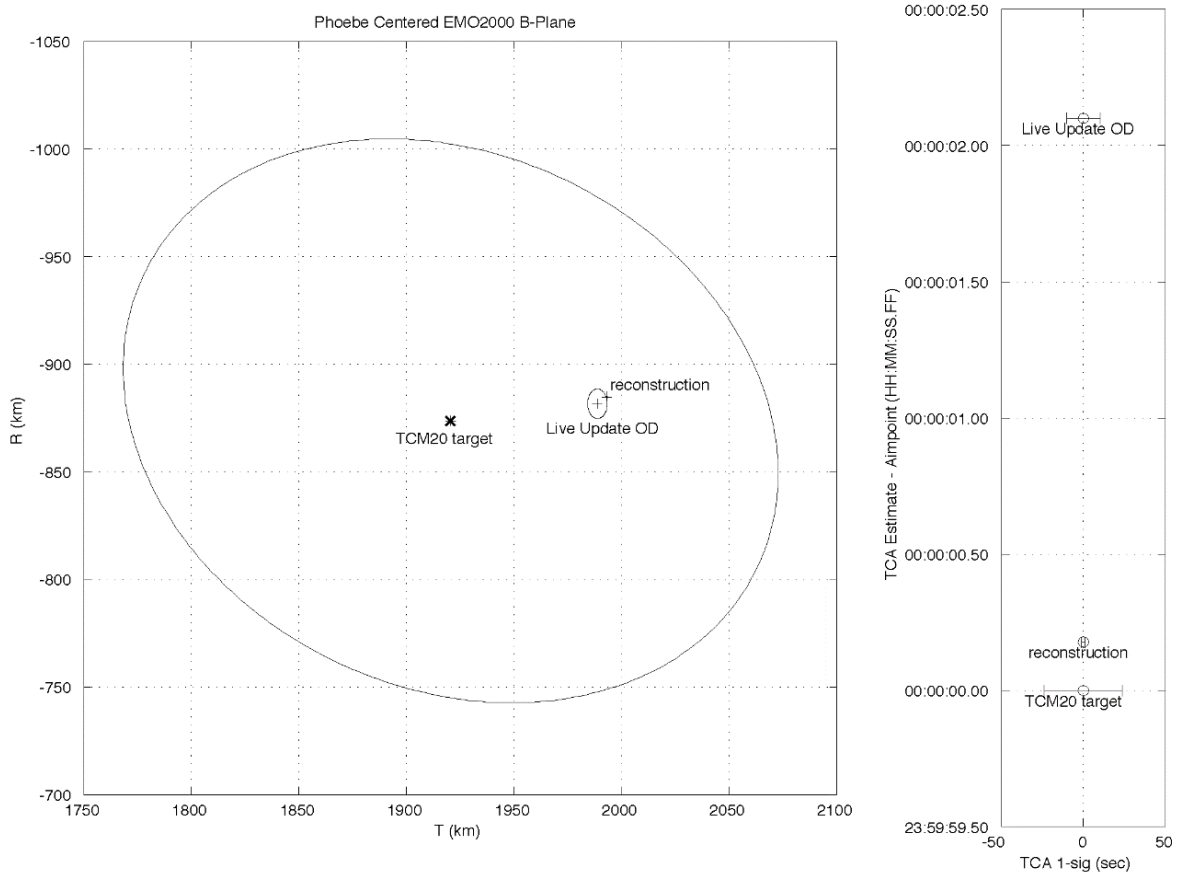


Figure 2-14. Phoebe B-plane target and solutions.

TCM-21 target and control accuracy are compared to the reconstructed ascending RPC in Figure 2-15. Here, the target has been converted from a radius of 158,500 km, Right Ascension (RA) of 157.8° , and declination of 0° to Cartesian coordinates. Figure 2-16 compares the nominal descending RPC with the reconstructed values, where the nominal value is taken from the TCM-21 final design with an updated SOI model that accounts for the intentionally uncorrected 0.9° thrust vector-pointing offset.

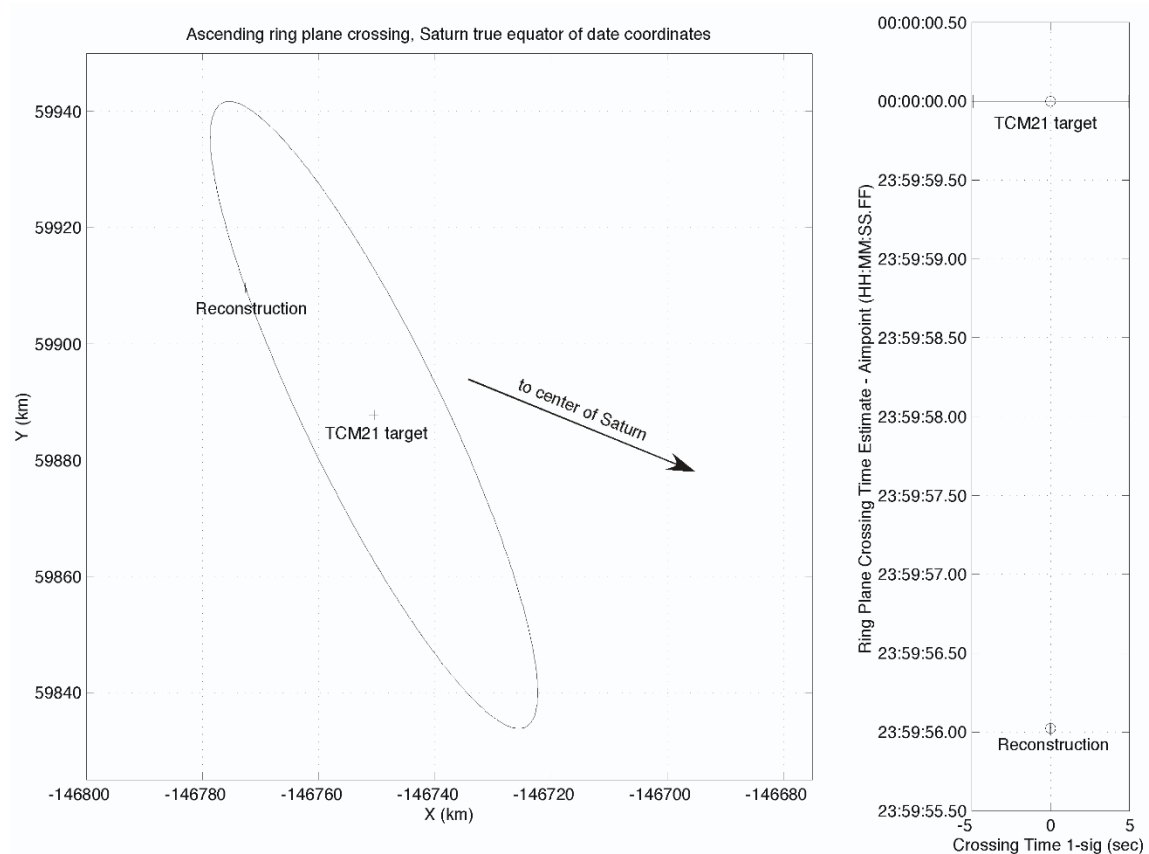


Figure 2-15. Targeted and achieved ascending ring plane crossing.

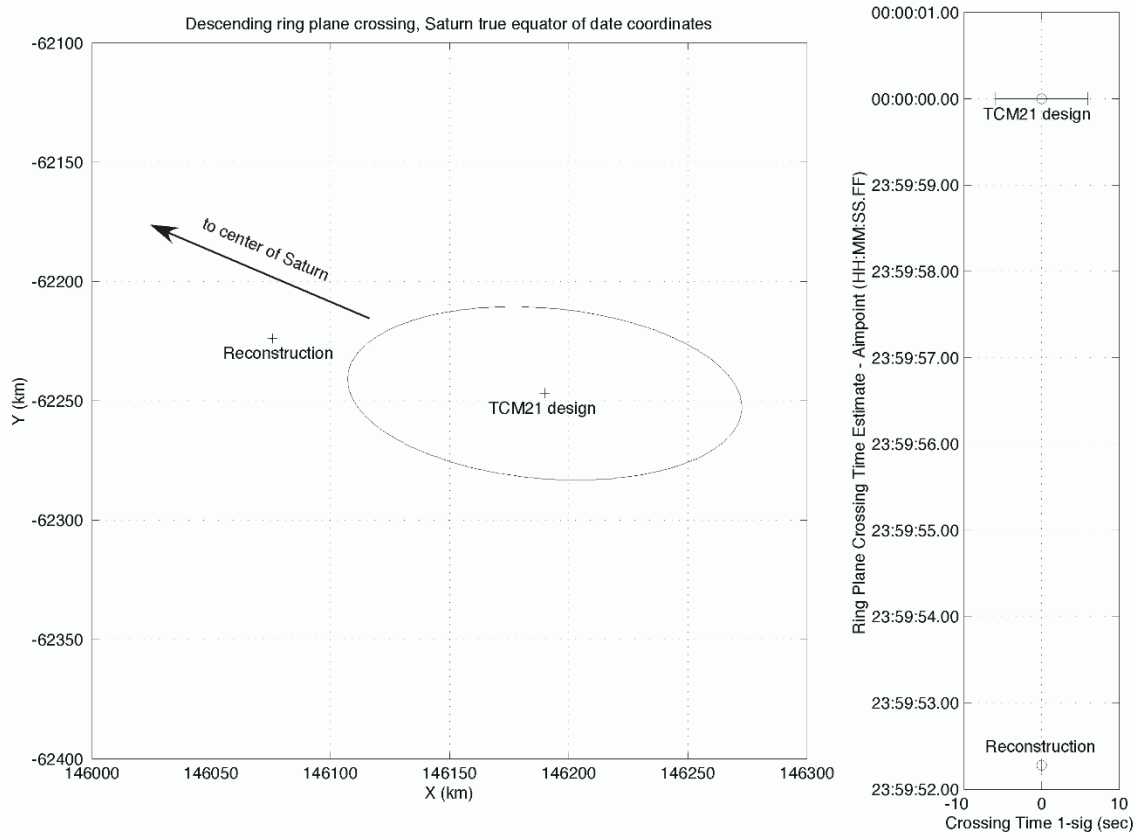


Figure 2-16. Nominal and achieved descending ring plane crossing.

2.6.2 Notable Events

Initial filtering of OPNAVs revealed larger than expected residual noise. Upon investigation, navigators discovered the cause to be small inaccuracies in star directions used during reduction of the images. Star directions were obtained from the Tycho-2 star catalog [36], which is based on observations from the Hipparcos Mission star tracker. Hipparcos' observations were taken over a 3-year baseline through March 1993. Errors in proper motion would have built up significantly in the intervening decade to collection of the Cassini OPNAVs. On March 8, 2004, navigators merged the second U.S. Naval Observatory (USNO) CCD Astrograph Catalog (UCAC2) [37], believed to have more accurate proper motions, with the Tycho-2 catalog. Reduction of OPNAVs would thereafter use positions and proper motions from the UCAC2 catalog unless the star was only available from the Tycho-2 catalog (the UCAC2 catalog contained 48 million stars, while the Tycho-2 catalog had less than a half million stars that were not already in UCAC2). This change significantly reduced OPNAV residual noise. Navigators made one final update to the star catalog on June 2, 2004, when additional parallax information from Hipparcos was added.

Two more spacecraft safing events occurred during this leg of cruise operations. The first, which was the third of the mission, occurred May 10, 2001, when a telemetry mode change was commanded that was not available to the online Command and Data Subsystem (CDS) string. This safing imparted roughly 33 mm/s of unplanned ΔV to Cassini-Huygens. The second, which was the fourth of the mission, occurred almost exactly two years later, on May 12, 2003, when a needed

target vector was not available in the onboard Inertial Vector Table. This safing imparted approximately 18 mm/s of unplanned ΔV to Cassini-Huygens.

Three Gravitational Wave Experiments (GWE) were performed that immensely aided the accurate estimate of Cassini-Huygens' acceleration from asymmetric thermal forces due to RTG radiation. In each of these experiments, the spacecraft remained pointed to Earth in RWA mode for several weeks with no thruster firings. Reaction wheels which had been initialized with near maximum allowable momentum in a direction opposite of that imparted by solar torques enabled the experiments. Only gravitational, direct solar pressure, and RTG forces acted on the spacecraft. The experiments were scheduled around solar oppositions to maximize the quality of continuously collected radiometric tracking data. RTG forces are directed along an axis very close to the spacecraft Z-axis so, with the Z-axis pointed at Earth, the forces are directly observable in Doppler and range data. GWE #1 took place from November 26, 2001, to January 5, 2002, GWE #2 from December 4, 2002, to January 14, 2003, and GWE #3 from November 10, 2003, to November 30, 2003. As the spacecraft steadily moved away from the Sun over the two years spanning the experiments, direct solar pressure forces, inversely proportional to the square of spacecraft-Sun range, are easily distinguished from RTG forces, which decrease much more slowly as the radioisotope, in this case plutonium, decays. The estimate of acceleration due to RTGs obtained from these experiments was the basis for future modeling through the rest of the mission.

An error in DSS 25 station location coordinates was revealed after processing Doppler data from GWE #1. A correction of about 50 cm, mostly in the local vertical direction was required to remove a residual signature in the data. The error was confirmed with subsequent VLBI measurements and an updated set of station locations was released [38].

2.7 Interplanetary Cruise Synopsis

Cassini's seven-year flight from launch to Saturn via a VVEJGA trajectory with biased aim-point strategy for the Earth flyby was conducted with a ΔV cost of 613.5 m/s. Had reference [16] anticipated flushing maneuvers, test maneuvers, and Phoebe targeting costs, cruise deterministic ΔV costs would total 581.9 m/s. The difference between these values, 31.6 m/s, represents the true cost of OD and maneuver execution errors, less than 6% of the deterministic cost.

Of the 24 maneuvers planned, 18 were executed. Fifteen ME maneuvers were executed with a total ΔV of 612.9 m/s and 3 RCS maneuvers were executed with a total ΔV of 0.5 m/s (1.54 kg). Propellant usage for both ME and RCS burns was much lower than predicted. Even prior to including flushing/test maneuvers and Phoebe targeting costs, ME predicted usage, at 719.3 ± 31 m/s, was much higher than the actual ME cost. RCS predicted usage for maneuvers was 7.5 kg, all statistical, with an uncertainty of 1.0 kg. Kilograms are used for RCS propellant predictions instead of meters per second because RCS propellant allocations were assigned in units of kilograms. Besides navigation, allocations were also made for spacecraft attitude control and turns, where units of meters per second are not meaningful.

Navigation's phenomenal performance, even in the presence of unanticipated events (hazard avoidance at Earth flyby and four spacecraft safing events), is attributable to several trajectory re-optimizations, exceptional maneuver performance, and delaying the OD DCO by one day for the Earth approach maneuver. Based on an assessment of the fifteen ME maneuvers performed, navigators updated the maneuver execution error model for future analyses. The updated Gates model is provided in Table 2-2 and was referred to internally as the 2000 model, for the year in

which it was developed. ME proportional magnitude and pointing errors were reduced considerably from the prelaunch model. Magnitude reduced from 0.35% to 0.2% and pointing reduced from 10 mrad to 3.5 mrad. ME fixed errors were unchanged from the prelaunch model. The RCS model was also unchanged, as the set of three maneuvers was insufficient to warrant an update.

Table 2-2. Maneuver execution error model improvement, prelaunch to cruise end.

One Sigma Errors		Main Engine		RCS
		Prelaunch	Cruise End	
Magnitude	Proportional (%)	0.35	0.2	2.0
	Fixed (mm/s)	10.0	10.0	3.5
Pointing (per axis)	Proportional (mrad)	10.0	3.5	12.0
	Fixed (mm/s)	17.5	17.5	3.5

3 Saturn Orbit Insertion

The SOI maneuver, with a ΔV of 626 m/s, was the largest burn of the Cassini-Huygens Mission. As its name suggests, this maneuver transitioned Cassini-Huygens from hyperbolic interplanetary cruise to Saturn captured orbital tour. With the opportunity for capture lasting only a few hours and the prime science mission dependent on a successful outcome, SOI was the most suspenseful maneuver of the mission.

Adding to the suspense, SOI was unlike any other Cassini-Huygens maneuver. Besides being the largest maneuver of the mission, the burn would terminate upon achieving a defined energy level instead of time or commanded ΔV . The thrust direction would be intentionally steered instead of inertially fixed. And because there would be no later chance for capture, a redundant ME would be ready to complete the maneuver if the primary engine was unable to achieve the desired energy level. Burn termination on energy and a non-inertial burn attitude had been accomplished by Cassini-Huygens only once previously, as a test at TCM-19b, a much smaller burn.

The main goal of SOI was to slow Cassini-Huygens into a Saturn-relative elliptical orbit with a period of 116 days. To do so required reducing Cassini-Huygens energy relative to Saturn. The Energy-Cutoff Burn (ECB) algorithm aboard the spacecraft was developed to terminate the burn upon reaching an orbital energy criterion. The algorithm used a prediction of spacecraft velocity as a function of time to generate an approximation of the change in orbital energy imparted while the burn was in progress. This approach made SOI resilient to faults that could interrupt burn execution by switching between ME assemblies. As expressed below, the estimate was based solely on spacecraft velocity, \vec{V} , and acceleration due to the burn, \vec{a} :

$$\Delta E_{target} = \int_{t_0}^{t_f} \vec{V}(\tau) \cdot \vec{a}(\tau) d\tau, \quad (\text{Eq. 1})$$

where t_0 and t_f are the SOI start and stop times, respectively. The algorithm is approximate, assuming two-body conic motion. The most significant approximation, however, is that \vec{V} was modeled by a hyperbolic orbit and computed for a trajectory without SOI. As such, it would incur a burn error of less than 2 m/s for burn interruptions less than 90 minutes, a very small percentage of the total burn magnitude [39]. This approximation allowed \vec{V} to be computed by the onboard Inertial Vector Propagator (IVP), which propagates position and velocity on a conic orbit [40].

A second ME was available to complete SOI in the event of an interruption, and longer interruptions could be tolerated if the burn direction were aligned to best reduce orbital energy. The burn direction that best reduces energy tracks the Saturn-relative anti-velocity direction. It is not inertially fixed. Yaw steering was implemented to address this. With yaw steering, the burn direction during SOI rotated at a constant rate of $0.008^\circ/\text{s}$ —more than 45° during the 96-minute burn. This very slow rate, slightly slower than the hour hand of a typical clock, closely matched the rotation rate of Cassini-Huygens' Saturn-relative velocity. The ΔV cost for an inertially fixed SOI with no interruptions would have been acceptable at about 15 m/s, but if the burn had been interrupted such that the necessary burn duration increased, the cost of an inertially fixed burn direction would have quickly become prohibitively large.

With yaw steering in place, more time would be available to fully complete SOI and ensure capture by Saturn in the event of an interruption. For similar reasons, SOI ΔV was not minimized by placing the midpoint of execution near Saturn periapsis. Rather, SOI started about 25 minutes after

ascending RPC and ended near periapsis, allowing for longer interruptions from burn restarts. This burn placement also satisfied desires of the science team, allowing science observations closer to Saturn and its inner rings than any other time during the prime mission.

3.1 Performance

The best indicator of SOI's performance was that OTM-001 and OTM-001a, clean-up maneuvers scheduled 2 and 16 days after SOI, could both be canceled. If executed, the errors to be corrected would have been a 0.4-day too-short orbital period and a 0.02° too-low inclination. An OTM-001 with magnitude of 2 m/s could have corrected these errors, but the downstream cost of canceling OTM-001 was also 2 m/s. Thus, either way, the ΔV cost was equivalent. After confirming that science instrument pointing would not be adversely affected by the uncorrected trajectory deviations, both clean-up OTMs were canceled.

3.2 Notable Events

SOI executed as Cassini-Huygens headed into solar conjunction. At the time of burn execution, the Sun-Earth-Probe (SEP) angle was only 6.3° . Minimum SEP, at 0.3° , occurred July 8, one week after SOI. While the final design of SOI had been completed months before burn execution and was not affected by solar conjunction, accurate OD for design of OTM-001 became more challenging. Tracking data quality was adequate for the task, however, because requirements on OTM-001 were not very demanding.

Visibility of this critical maneuver was highly desired. Obtaining a signal from the HGA, while possible, was too costly in terms of ΔV because pointing the narrow beamwidth antenna toward Earth would produce a non-optimal burn direction. The ideal burn direction to maintain acceptable ΔV costs would vary HGA pointing between 55° off Earth-point at burn start to 25° at burn termination. Communications were established instead by switching to Cassini-Huygens' wide beamwidth LGA-1 and utilizing the open loop Radio Science Receivers to detect and record the resulting lower strength spacecraft transmission. Acquisition of signal was successful and much of the open-loop data was later formatted as non-coherent Doppler tracking by Radio Science Team (RST) members for use in OD operations.

4 Tour

Tour phase began after capture into orbit about Saturn and includes the prime mission and two extended missions. In total, the tour phase lasted more than 13 years, almost half of one Saturn orbit about the Sun. The prime mission covered the first four years of the tour, starting 18 months after Saturn's northern winter solstice and ending July 2008. The first extended mission, called the Equinox Mission, was two years in duration, and was approximately centered around Saturn's August 11, 2009 northern vernal equinox. The final extended mission, called the Solstice Mission, spanned seven years from September 2010 through Saturn's May 2017 northern summer solstice to EOM in September 2017. The final portion of Solstice Mission, deemed the Grand Finale, consisted of 22 orbits about Saturn, each traversing the region between Saturn and its innermost ring at descending node crossing. Mission boundaries listed here are consistent with NASA funding profiles and differ somewhat from navigation planning documentation, which has Prime and Equinox Missions ending a few months earlier to allow for development of a tie-in from one mission to the next.

The first task in each tour phase was to define a reference trajectory. The Navigation Team worked closely with mission scientists to design a trajectory from which science observations could be conducted to best meet mission objectives. Through an iterative process in which navigators designed and provided candidate trajectories to mission scientists and then used feedback from the scientists to tweak and refine the trajectories, a single, tailored reference trajectory emerged for each phase to meet the investigative demands of twelve science instrument teams and one interdisciplinary science team. The trajectories define a sequence of targeted Titan and icy satellite encounters that comprise each mission tour. The sequence of encounters is provided in Tables 4-1 through 4-3. An encounter is identified by the first letter of the satellite name followed by digits specifying the sequential order for that particular satellite. The first three Titan encounters are identified with letters instead of numbers and the following Titan encounters are sequentially numbered from 3 instead of 4. This scheme results from a redesign of the Huygens probe trajectory, where the original first two Titan flybys (T1, T2) were replaced with three Titan flybys (Ta, Tb, Tc) in the redesign and then synced back to the original trajectory at the original third flyby (T3).

Table 4-1. Cassini prime mission reference trajectory encounters.

Encounter	Satellite	Time (UTC)	In / Out	Altitude (km)	B-plane (deg)	V-Infinity (km/s)	Period (days)	Inc. (deg)	Rev
Ta	Titan	26Oct2004 15:30	I	1200	-39	5.65	47.9	13.8	a
Tb	Titan	13Dec2004 11:38	I	1200	-59	5.64	31.9	5.4	b
Tc	Titan	14Jan2005 11:12	I	60000	180	5.37	31.8	5.3	c
T3	Titan	15Feb05 06:58	I	1577	-30	5.58	20.4	0.4	3
E1	Enceladus	09Mar2005 09:08	I	500	150	6.60	20.5	0.2	4
T4	Titan	31Mar2005 20:05	O	2402	-147	5.61	16.0	7.4	5
T5	Titan	16Apr2005 19:12	O	1025	-76	5.63	18.2	21.6	6
E2	Enceladus	14Jul2005 19:55	I	175	145	8.17	18.3	21.8	11
T6	Titan	22Aug2005 08:54	O	3669	120	5.61	16.0	15.6	13
T7	Titan	07Sep2005 08:12	O	1075	67	5.65	18.4	0.3	14

Table 4-1. Cassini prime mission reference trajectory encounters.

Encounter	Satellite	Time (UTC)	In / Out	Altitude (km)	B-plane (deg)	V-Infinity (km/s)	Period (days)	Inc. (deg)	Rev
H1	Hyperion	26Sep2005 02:25	O	510	124	5.64	18.2	0.3	15
D1	Dione	11Oct2005 17:52	I	500	120	9.10	17.9	0.4	16
T8	Titan	28Oct2005 04:15	I	1353	181	5.54	27.4	0.4	17
R1	Rhea	26Nov2005 22:38	I	500	10	7.29	27.4	0.4	18
T9	Titan	26Dec2005 19:00	O	10409	180	5.49	23.4	0.4	19
T10	Titan	15Jan2006 11:41	I	2043	180	5.48	39.2	0.4	20
T11	Titan	27Feb2006 08:25	O	1813	180	5.51	23.3	0.4	21
T12	Titan	19Mar2006 00:06	I	1951	180	5.47	39.2	0.4	22
T13	Titan	30Apr2006 20:58	O	1855	180	5.49	23.3	0.4	23
T14	Titan	20May2006 12:18	I	1879	180	5.48	39.2	0.4	24
T15	Titan	02Jul2006 09:21	O	1906	180	5.48	23.3	0.4	25
T16	Titan	22Jul2006 00:25	I	950	-92	5.52	24.0	14.9	26
T17	Titan	07Sep2006 20:17	I	1000	-24	5.54	16.0	24.5	28
T18	Titan	23Sep2006 18:59	I	960	-81	5.52	15.9	37.6	29
T19	Titan	09Oct2006 17:30	I	980	-75	5.53	15.9	46.6	30
T20	Titan	25Oct2006 15:58	I	1030	-10	5.54	12.0	54.9	31
T21	Titan	12Dec2006 11:41	I	1000	-123	5.51	15.9	52.8	35
T22	Titan	28Dec2006 10:05	I	1300	-61	5.53	15.9	56.5	36
T23	Titan	13Jan2007 08:39	I	1000	-52	5.53	15.9	59.2	37
T24	Titan	29Jan2007 07:16	I	2631	-69	5.53	18.1	58.8	38
T25	Titan	22Feb2007 03:12	O	1000	-56	5.82	15.9	58.6	39
T26	Titan	10Mar2007 01:49	O	980	-48	5.82	15.9	56.0	40
T27	Titan	26Mar2007 00:23	O	1010	-58	5.82	15.9	52.3	41
T28	Titan	10Apr2007 22:58	O	990	-66	5.82	15.9	46.8	42
T29	Titan	26Apr2007 21:33	O	980	-73	5.81	15.9	39.1	43
T30	Titan	12May2007 20:10	O	960	-79	5.81	15.9	28.2	44
T31	Titan	28May2007 18:52	O	2300	-84	5.81	16.0	18.0	45
T32	Titan	13Jun2007 17:46	O	975	-87	5.81	16.0	2.1	46
T33	Titan	29Jun2007 17:00	O	1932	-9	5.84	22.8	0.4	47
T34	Titan	19Jul2007 01:11	I	1332	-179	5.85	39.7	0.3	48
T35	Titan	31Aug2007 06:33	O	3326	-117	5.82	32.0	6.1	49
I1	Iapetus	10Sep2007 14:16	O	1644	176	2.34	32.0	6.1	49
T36	Titan	02Oct2007 04:43	O	975	120	5.88	23.8	5.0	50
T37	Titan	19Nov2007 00:47	O	1000	158	5.88	16.0	12.0	52
T38	Titan	05Dec2007 00:07	O	1300	96	5.90	16.0	26.0	53
T39	Titan	20Dec2007 22:58	O	970	101	5.91	15.9	37.7	54

Table 4-1. Cassini prime mission reference trajectory encounters.

Encounter	Satellite	Time (UTC)	In / Out	Altitude (km)	B-plane (deg)	V-Infinity (km/s)	Period (days)	Inc. (deg)	Rev
T40	Titan	05Jan2008 21:30	O	1010	166	5.90	12.0	46.6	55
T41	Titan	22Feb2008 17:32	O	1000	140	5.92	10.6	56.1	59
E3	Enceladus	12Mar2008 19:06	I	56	90	14.41	10.6	56.1	61
T42	Titan	25Mar2008 14:28	O	1000	147	5.93	9.6	63.1	62
T43	Titan	12May2008 10:02	O	1000	-161	5.92	8.0	69.3	67
T44	Titan	28May2008 08:25	O	1400	-170	5.91	7.1	74.7	69

In/Out = flyby inbound (I) or outbound (O). B-plane = B-plane angle relative to the satellite's pole (H1 angle is relative to Saturn pole).

Period = spacecraft period after encounter. Inc. = inclination after encounter wrt Saturn's equator. Rev = project rev # of flyby.

Table 4-2. Cassini Equinox Mission reference trajectory encounters.

Encounter	Satellite	Time (UTC)	In / Out	Altitude (km)	B-plane (deg)	V-Infinity (km/s)	Period (days)	Inc. (deg)	Rev
T45	Titan	31Jul2008 02:13	O	1613	127	5.88	7.4	74.5	78
E4	Enceladus	11Aug2008 21:06	I	54	90	17.73	7.4	74.5	80
E5	Enceladus	09Oct2008 19:07	I	28	90	17.7	7.3	74.5	88
E6	Enceladus	31Oct2008 17:15	I	200	90	17.7	7.3	74.5	91
T46	Titan	03Nov2008 17:35	O	1100	7	5.87	7.9	70.6	91
T47	Titan	19Nov2008 15:56	O	1023	151	5.86	8.0	72.3	93
T48	Titan	05Dec2008 14:26	O	960	164	5.86	8.0	73.1	95
T49	Titan	21Dec2008 13:00	O	970	110	5.86	9.4	74.7	97
T50	Titan	07Feb2009 08:51	O	960	60	5.87	11.9	65.3	103
T51	Titan	27Mar2009 04:44	O	960	114	5.86	16.8	63.3	106
T52	Titan	04Apr2009 01:48	I	4150	179	5.53	16.0	61.7	107
T53	Titan	20Apr2009 00:21	I	3600	169	5.54	16.0	61.3	108
T54	Titan	05May2009 22:54	I	3244	158	5.54	15.9	60.6	109
T55	Titan	21May2009 21:27	I	965	147	5.55	16.0	58.7	110
T56	Titan	06Jun2009 20:00	I	965	133	5.55	16.0	55.7	111
T57	Titan	22Jun2009 18:33	I	955	122	5.55	15.9	51.2	112
T58	Titan	08Jul2009 17:04	I	965	113	5.54	15.9	44.5	113
T59	Titan	24Jul2009 15:34	I	955	106	5.54	15.9	34.7	114
T60	Titan	09Aug2009 14:04	I	970	100	5.54	16.0	20.8	115
T61	Titan	25Aug2009 12:52	I	970	161	5.53	24.0	12.1	116
T62	Titan	12Oct2009 08:36	I	1300	61	5.56	19.0	0.5	118
E7	Enceladus	02Nov2009 07:42	O	100	90	7.74	19.0	0.5	119

Table 4-2. Cassini Equinox Mission reference trajectory encounters.

Encounter	Satellite	Time (UTC)	In / Out	Altitude (km)	B-plane (deg)	V-Infinity (km/s)	Period (days)	Inc. (deg)	Rev
E8	Enceladus	21Nov2009 02:10	I	1604	82	7.75	19.0	0.5	120
T63	Titan	12Dec2009 01:03	O	4850	-147	5.47	16.0	4.9	122
T64	Titan	28Dec2009 00:17	O	955	-95	5.49	16.0	21.6	123
T65	Titan	12Jan2010 23:11	O	1073	86	5.50	16.0	5.2	124
T66	Titan	28Jan2010 22:29	O	7490	53	5.53	17.5	0.3	125
R2	Rhea	02Mar2010 17:41	I	100	-99	8.55	17.6	0.4	127
T67	Titan	05Apr2010 15:51	I	7462	180	5.51	20.8	0.4	129
D2	Dione	07Apr2010 05:16	I	504	0	8.36	20.4	0.3	129
E9	Enceladus	28Apr2010 00:10	O	100	90	6.51	20.5	0.3	130
E10	Enceladus	18May2010 06:05	I	439	147	6.52	20.5	0.3	131
T68	Titan	20May2010 03:24	O	1400	131	5.48	16.0	12.1	131
T69	Titan	05Jun2010 02:26	O	2044	-89	5.49	16.0	2.0	132
T70	Titan	21Jun2010 01:28	O	880	-93	5.49	16.0	19.1	133
T71	Titan	07Jul2010 00:23	O	1005	56	5.50	19.9	4.5	134
E11	Enceladus	13Aug2010 22:31	I	2552	90	6.84	20.0	4.6	136
T72	Titan	24Sep2010 18:39	O	8175	15	5.53	23.8	3.0	138

In/Out = flyby inbound (I) or outbound (O). B-plane = B-plane angle relative to the satellite's pole (H1 angle is relative to Saturn pole).

Period = spacecraft period after encounter. Inc. = inclination after encounter wrt Saturn's equator. Rev = project rev # of flyby.

Table 4-3. Cassini Solstice Mission reference trajectory encounters.

Encounter	Satellite	Time (UTC)	In / Out	Altitude (km)	B-plane (deg)	V-Infinity (km/s)	Period (days)	Inc. (deg)	Rev
T73	Titan	11Nov2010 13:37	O	7921	144	5.44	20.6	0.0	140
E12	Enceladus	30Nov2010 11:54	O	50	-119	6.26	20.6	0.1	141
E13	Enceladus	21Dec2010 01:08	O	50	-61	6.22	20.7	0.1	142
R3	Rhea	11Jan2011 04:53	O	75	103	8.02	20.4	0.3	143
T74	Titan	18Feb2011 16:04	I	3651	180	5.49	27.9	0.4	145
T75	Titan	19Apr2011 05:01	O	10053	180	5.42	23.4	0.4	147
T76	Titan	08May2011 22:54	I	1873	180	5.51	39.1	0.4	148
T77	Titan	20Jun2011 18:32	O	1359	180	5.49	21.7	0.4	149
T78	Titan	12Sep2011 02:50	I	5821	0	5.61	17.7	0.3	153
E14	Enceladus	01Oct2011 13:52	I	100	90	7.43	17.8	0.2	154
E15	Enceladus	19Oct2011 09:22	I	1236	14	7.48	17.8	0.2	155
E16	Enceladus	06Nov2011 04:59	I	500	151	7.38	17.9	0.2	156

Table 4-3. Cassini Solstice Mission reference trajectory encounters.

Encounter	Satellite	Time (UTC)	In / Out	Altitude (km)	B-plane (deg)	V-Infinity (km/s)	Period (days)	Inc. (deg)	Rev
D3	Dione	12Dec2011 09:39	O	100	-175	8.70	17.5	0.2	158
T79	Titan	13Dec2011 20:11	O	3586	-8	5.49	23.5	0.9	158
T80	Titan	02Jan2012 15:14	I	29415	120	5.44	24.2	1.6	159
T81	Titan	30Jan2012 13:40	O	31131	120	5.39	23.5	1.4	160
T82	Titan	19Feb2012 08:43	I	3803	-10	5.55	17.9	0.4	161
E17	Enceladus	27Mar2012 18:30	I	75	87	7.48	17.8	0.4	163
E18	Enceladus	14Apr2012 14:02	I	75	93	7.48	17.8	0.4	164
E19	Enceladus	02May2012 09:31	I	75	108	7.51	17.8	0.4	165
T83	Titan	22May2012 01:10	O	955	-107	5.43	16.0	15.8	166
T84	Titan	07Jun2012 00:07	O	959	-40	5.45	23.9	21.1	167
T85	Titan	24Jul2012 20:03	O	1012	-111	5.43	21.2	32.2	169
T86	Titan	26Sep2012 14:36	O	956	-91	5.44	23.9	39.0	172
T87	Titan	13Nov2012 10:22	O	973	-163	5.42	15.9	46.3	174
T88	Titan	29Nov2012 08:57	O	1014	-144	5.42	13.3	53.0	175
T89	Titan	17Feb2013 01:57	O	1978	-149	5.42	12.0	57.1	181
R4	Rhea	09Mar2013 18:17	I	1000	-132	9.27	12.0	57.0	183
T90	Titan	05Apr2013 21:44	O	1400	161	5.42	9.6	61.7	185
T91	Titan	23May2013 17:33	O	970	-90	5.44	12.0	59.4	190
T92	Titan	10Jul2013 13:22	O	964	-93	5.44	16.0	56.7	194
T93	Titan	26Jul2013 11:56	O	1400	-82	5.44	23.9	53.4	195
T94	Titan	12Sep2013 07:44	O	1400	-119	5.43	31.9	51.9	197
T95	Titan	14Oct2013 04:56	O	961	-134	5.43	47.9	49.7	198
T96	Titan	01Dec2013 00:41	I	1400	132	5.44	31.9	51.3	199
T97	Titan	01Jan2014 22:00	I	1400	148	5.43	31.9	50.1	200
T98	Titan	02Feb2014 19:13	I	1236	131	5.43	31.9	48.1	201
T99	Titan	06Mar2014 16:27	I	1500	119	5.43	31.9	45.5	202
T100	Titan	07Apr2014 13:41	I	963	121	5.43	35.8	40.7	203
T101	Titan	17May2014 16:12	O	2994	120	5.36	31.9	44.3	204
T102	Titan	18Jun2014 13:28	O	3659	111	5.36	31.9	46.5	205
T103	Titan	20Jul2014 10:41	O	5103	115	5.36	31.9	48.0	206
T104	Titan	21Aug2014 08:09	O	964	-65	5.39	31.9	44.6	207
T105	Titan	22Sep2014 05:23	O	1400	-72	5.39	31.9	40.3	208
T106	Titan	24Oct2014 02:41	O	1013	-47	5.39	47.8	33.1	209
T107	Titan	10Dec2014 22:27	O	980	-114	5.38	31.9	28.6	210
T108	Titan	11Jan2015 19:49	O	970	-84	5.38	31.9	19.1	211
T109	Titan	12Feb2015 17:08	O	1200	-87	5.38	31.9	8.5	212

Table 4-3. Cassini Solstice Mission reference trajectory encounters.

Encounter	Satellite	Time (UTC)	In / Out	Altitude (km)	B-plane (deg)	V-Infinity (km/s)	Period (days)	Inc. (deg)	Rev
T110	Titan	16Mar2015 14:30	O	2275	-105	5.38	28.0	0.3	213
T111	Titan	07May2015 22:50	I	2721	1	5.38	18.9	0.3	215
D4	Dione	16Jun2015 20:12	O	517	-80	7.31	18.9	0.4	217
T112	Titan	07Jul2015 08:10	O	10953	-1	5.47	21.8	0.5	218
D5	Dione	17Aug2015 18:33	I	479	-96	6.43	21.9	0.4	220
T113	Titan	28Sep2015 21:37	I	1036	1	5.40	13.9	0.6	222
E20	Enceladus	14Oct2015 10:41	I	1846	-78	8.51	13.9	0.6	223
E21	Enceladus	28Oct2015 15:23	O	50	96	8.49	13.9	0.6	224
T114	Titan	13Nov2015 05:47	O	11920	166	5.35	12.7	1.3	225
E22	Enceladus	19Dec2015 17:49	O	5000	-178	4.22	12.9	1.3	228
T115	Titan	16Jan2016 02:20	O	3548	19	5.45	15.9	4.1	230
T116	Titan	01Feb2016 01:00	O	1400	94	5.42	16.0	17.5	231
T117	Titan	16Feb2016 23:50	O	1018	41	5.43	23.9	21.9	232
T118	Titan	04Apr2016 19:43	O	990	72	5.42	31.9	28.8	234
T119	Titan	06May2016 16:55	O	971	100	5.41	31.9	36.0	235
T120	Titan	07Jun2016 14:06	O	975	131	5.40	23.9	43.0	236
T121	Titan	25Jul2016 09:58	O	976	168	5.40	16.0	49.2	238
T122	Titan	10Aug2016 08:31	O	1698	-167	5.40	12.0	53.7	239
T123	Titan	27Sep2016 04:17	O	1774	-153	5.40	9.6	57.9	243
T124	Titan	13Nov2016 23:56	O	1584	-135	5.40	8.0	61.4	248
T125	Titan	29Nov2016 22:15	O	3158	-131	5.39	7.2	63.7	250
T126	Titan	22Apr2017 06:08	O	979	-103	5.40	6.4	62.4	270

In/Out = flyby inbound (I) or outbound (O). B-plane = B-plane angle relative to the satellite's pole (H1 angle is relative to Saturn pole).

Period = spacecraft period after encounter. Inc. = inclination after encounter wrt Saturn's equator. Rev = project rev # of flyby.

Navigators implemented global reference trajectory updates to re-optimize trajectories for ΔV costs as satellite ephemerides changed and accuracies improved via the filtering of orbital tracking data and OPNAVs. Global updates were generally small-scale changes affecting the entire mission. As satellite ephemeris knowledge converged, global updates became less frequent and were absorbed in local updates. Local updates were implemented to enable observations that would advance understanding of new discoveries, improve existing observations, or reduce mission risk. Local updates were large scale changes affecting only a small portion of the mission. The introduction of a new reference trajectory into flight operations was carefully synchronized with the development of command sequences to avoid re-work of observations that had already progressed through the detailed sequence development process. Table 4-4 lists the reference trajectory update names, dates each became operational, command sequences they spanned, and main motivation for each update. Command sequences typically spanned 5-week intervals during Prime and Equinox Missions and 10-week intervals in Solstice Mission.

Table 4-4. Reference trajectory updates and motivations.

Reference Trajectory	Operational Start Date	Command Sequence Span	Trajectory Event Span	Main Motivation for Update
030201	Pre-Tour	S01 – S02	SOI – pre-Ta	Initial tour reference trajectory
040513	30 Jul 2004	S03	SOI – pre-Ta	Re-optimization based on latest ephemeris
040622	12 Sep 2004	S04	SOI – pre-Ta	Constrain 040513 downstream trajectory shifts
041001	18 Oct 2004	S05 – S07	Ta – Tc	Raise rev C Iapetus altitude
041210	22 Jan 2005	S08 – S11	T3 – T5	Raise T5, T7 altitudes to reduce tumble risk
050505	18 Jun 2005	S12	E2 – pre-T6	Lower Tethys, E2, and H1 altitudes
050720	31 Jul 2005	S13 – S19	T6 – T12	Raise T7 altitude to reduce tumble risk
060323	22 Apr 2006	S20 – S29	T13 – T29	Raise Titan flybys, lower E3, add rev 28 occ.
070209	04 May 2007	S30 – S35	T30 – T38	Resolve I1 imaging/occultation science conflict
070918	15 Dec 2007	S36 – S41	T39 – T44	Add Equinox Mission, raise E3
080520	01 Jul 2008	S42 – S45	T45 – T47	Fine tune E5, move 3 maneuvers
080806	26 Nov 2008	S46 – S56	T48 – T65	Add leap second to auxiliary (OPTG) file
090721	23 Jan 2010	S57 – S59	T66 – E9	Add Solstice Mission, lower E10 occultation
091005	17 May 2010	S60 – S71	E10 – T80	Move 5 maneuvers
110818	24 Jan 2012	S72 – S86	T81 – T107	Move 1 maneuver, re-optimization
140114	17 Dec 2014	S87 – S93	T108 – T118	Add rev 233 Enceladus plume occultation
150901	18 Apr 2016	S94 – S101	T119 – EOM	Add Saturn atmosphere model

Flybys of Titan provided the major changes in the orbiter's trajectory necessary to accomplish the tour reference trajectory while the orbiter's propulsion system provided the fine-tuning. Adding some perspective, Cassini-Huygens was launched with a propulsive capability of about 2.4 km/s. Half this amount was used in interplanetary cruise and SOI, and another 0.4 km/s was used to reduce the initial post-SOI orbital period. Prior to the first targeted Titan flyby, the propulsive capability available was reduced to just 0.8 km/s. In contrast, the cumulative ΔV achieved from Titan gravity assists throughout orbital operations was nearly 90 km/s, yielding a propulsive leveraging ratio of more than 100:1. Figures showing period and inclination change contours for several of the targeted flybys demonstrate how the gravity assists could be used to change Cassini-Huygens' orbit and are provided in Appendix A – Supplementary Material, Figures A-1 to A-69.

Maintaining the spacecraft close to the reference trajectory typically involved three OTMs for each transfer from one targeted flyby to the next (Figure 4-1). Generally, a clean-up maneuver three days after a flyby, a trajectory shaping maneuver near apoapsis, and an approach maneuver three days before the next flyby were scheduled. The clean-up maneuver was designed with a chained two-impulse optimization strategy, where the sum of clean-up and shaping maneuvers was minimized together with those maneuvers in several downstream transfers [41]. This strategy achieved a degree of asymptote error control without actively changing downstream flyby aim-

points after each flyby. Shaping maneuvers were always targeted to the next aim-point, making all approach maneuvers statistical.

For ease of recognizing maneuver types, OTM numbers were assigned sequentially in groups of three for each transfer. Shaping maneuver numbers were multiples of three, clean-up maneuvers one less than a multiple of three, and approach maneuvers one more than a multiple of three. Some transfers did not require all three maneuvers. In these instances, maneuver numbers would be skipped. Other transfers required more than three maneuvers to ensure the approach maneuver would remain small. In these instances, the letter “a” would be appended onto an already used number. In one instance, a contingency maneuver was inserted between OTM-183 and OTM-184 and designated as OTM-183X. OTM-183X was the first maneuver to use the B-branch thrusters after transitioning from the degraded A-branch and would ensure a T51 altitude high enough above Titan’s atmosphere to avoid the risk of spacecraft tumbling [42].

Backup maneuver opportunities were scheduled for all tour maneuvers. Initially, backup maneuvers were available to respond only to uplink failures of the prime maneuver or to allow for additional tracking to improve a poorly converged OD solution needed for the maneuver design. After gaining experience and confidence from several flawless maneuver executions, project management began allowing backup maneuvers for additional scenarios. Provided that the backup maneuver was uplinked over the prime maneuver uplink window (so that two uplink windows, prime and backup, were available) and provided that failure to execute the maneuver did not incur a large ΔV penalty, backup maneuvers were allowed if ΔV costs were significantly reduced as compared to the prime maneuver or if wheel speed management was significantly simplified. Maneuvers executed over the backup opportunity are designated in Appendix A – Supplementary Material, Tables A-5 to A-11 Maneuver History with -BU appended to the maneuver name.

Earth-mean-orbital of J2000 B-plane coordinates and time of closest approach were targeted for all controlled flybys. Coupling these targets with the chained two-impulse optimization strategy results in generally larger dispersions from the reference trajectory for locations on the orbit furthest from the target point. Some observations, usually involving occultation of a radio signal or starlight through Enceladus’ plume, required that the spacecraft remain close to the reference trajectory when it was *not* near a targeted flyby. On these occasions, the clean-up maneuver was targeted to the spacecraft reference trajectory position at the time of the following shaping maneuver. A ΔV penalty was incurred in these scenarios because the clean-up maneuver was not optimized to minimize ΔV . Similarly, during the Grand Finale portion of the Solstice Mission, maneuvers were targeted to a reference trajectory position at selected periapses. For Huygens probe relay, a unique targeting strategy for Cassini was implemented. In order for the probe to enter Titan’s atmosphere, both Huygens and Cassini were targeted to a Titan impact trajectory. Probe entry target parameters, determined at the epoch when probe trajectory responsibilities were transferred from Cassini navigators to the ESA, were altitude, B-plane angle, and entry angle. Angle of attack was not targeted, but it was actively monitored with each maneuver design. Upon successful separation of the probe, Cassini performed a deflection maneuver targeting it away from Titan impact where it could receive and relay Huygens’ data to Earth.

4.1 Prime Orbital Mission

Cassini’s prime orbital mission extended from SOI to July 2008. The mission included Huygens probe relay at the third Titan targeted encounter (Tc) and a total of 52 targeted flybys. Of these

flybys, 45 were of Titan, three of Enceladus, and one each of Dione, Rhea, Hyperion, and Iapetus. The Hyperion and Iapetus flybys were the only targeted flybys of these satellites during Cassini's 13-year orbit about Saturn.

The orbital portion of prime mission consists of six different phases defined by different science objectives dominating each phase of the tour design. The first phase, redesigned to recover from an anomaly in Huygens relay link, spans from T_a to T₃, and enables the Huygens probe mission. Probe relay occurs at T_c and the redesigned mission reconnects to the original mission at T₃. The second phase spans from T₃ to T₉ and includes four icy satellite flybys and several radio science occultation of Saturn and its rings. These equatorial occultation pass behind the rings, go through the gap between the rings and Saturn, and then pass behind Saturn. The third phase, from T₉ to T₁₆, quickly rotates the apoapsis of Cassini's orbit into Saturn's magnetotail. At the end of this phase, the Cassini apoapsis is in the anti-Sun direction, and the T₁₆ flyby increases inclination to about 15° so that Cassini passes through Saturn's magnetotail. In the fourth phase, from T₁₆ to T₃₃, Cassini's apoapsis is moved to the other side of Saturn, between Saturn and the Sun, for sunlit full-disc atmospheric observations. After the T₁₆ through T₂₄ flybys raise inclination to the prerequisite 59°, a pi-transfer flips the Titan encounter 180° to the other side of Saturn, and inclination is then lowered back into Titan's plane from T₂₅ to T₃₃. The fifth phase, from T₃₃ to T₃₅, allows Cassini to spend a long time above the daylight side of Saturn and provides the distance needed to observe Saturn's entire disc. The final phase, from T₃₅ to E₄, raises inclination to 75° with periapsis below the illuminated side of the ring plane for close observations of the rings and Saturn's high latitudes. The final two phases have many low altitude Titan flybys which are valuable for Titan science investigations. Petal plots for the orbital portion of prime mission are provided in Figure 4-1. Charts showing inclination, periapsis radius, and apoapsis radius evolution are provided in Figures 4-2 through 4-4, respectively.

Navigators were continuously preparing for the next maneuver with 159 planned during these 51 months, averaging to one maneuver every ten days. The first maneuver performed after SOI was also the largest of the prime mission. The Periapsis Raise Maneuver (PRM), at 393 m/s, raised subsequent Saturn periapsis altitudes from 2.6 Saturn radii to Titan's orbital radius of 20 Saturn radii.

Cassini_Prime_Mission: 01-JUL-2004 00:00:00 to 01-JUL-2008 24:00:00
(Sun on right)

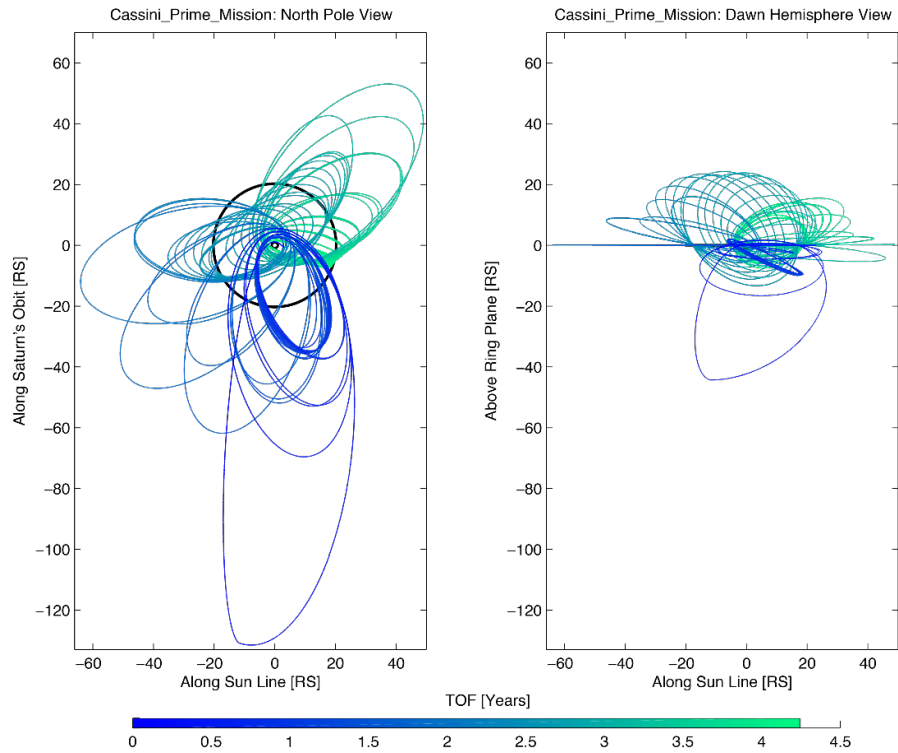


Figure 4-1. Prime mission petal plot.

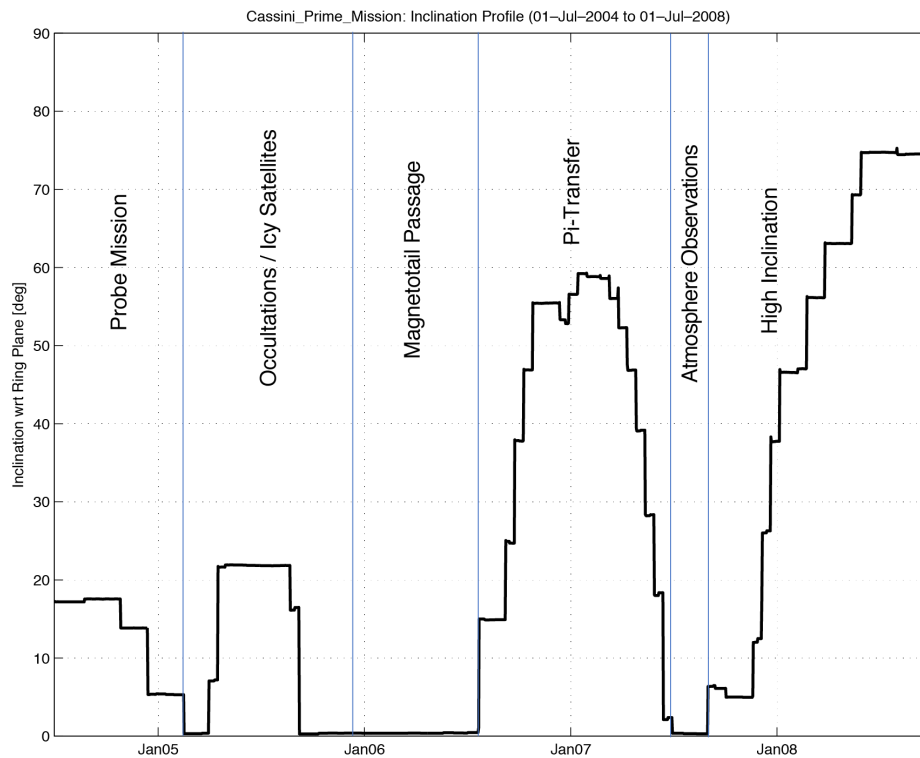


Figure 4-2. Prime mission inclination.

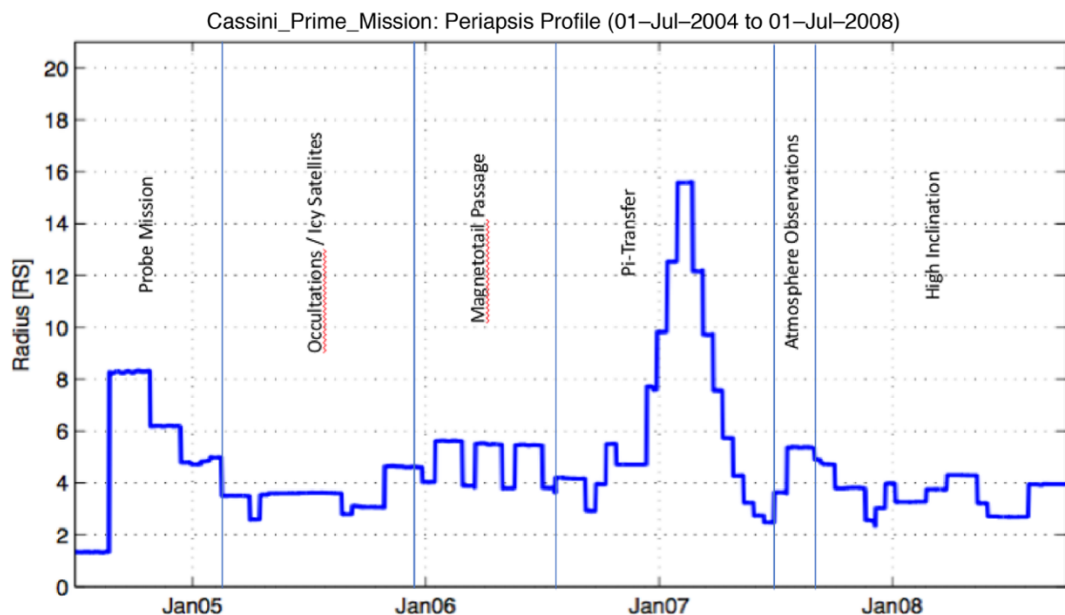


Figure 4-3. Prime mission periapsis radius.

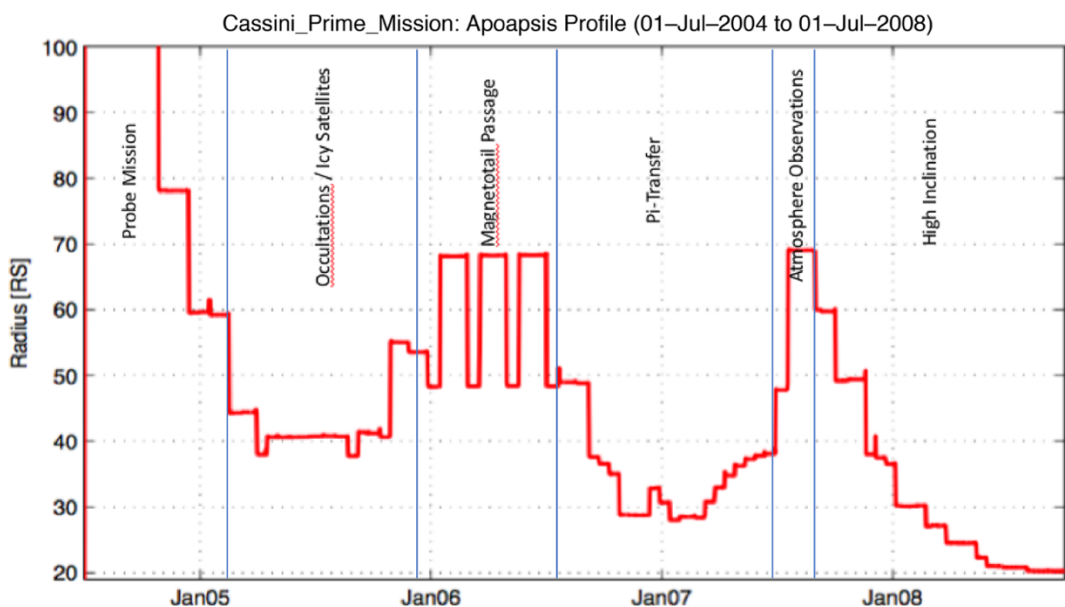


Figure 4-4. Prime mission apoapsis radius.

Eleven reference trajectory updates were implemented during this phase of the mission. While each utilized the latest satellite ephemeris information to globally re-optimize the downstream ephemeris, several also implemented local updates. Rationale for updates included reducing Huygens probe's sensitivity to an Iapetus gravitational perturbation (041001), raising flyby altitudes of selected Titan flybys to reduce atmospheric drag and spacecraft tumbling risks (041210, 050720, and 060323), adding a close 1500 km altitude Tethys flyby—the lowest of the tour (050505) [43], de-conflicting a star occultation observation with remote surface sensing

observations during the only Iapetus targeted flyby of tour (070209) [44], and linking prime mission to Equinox Mission (070918 and 080520).

4.1.1 Huygens Probe Relay Redesign

The beginning of prime mission orbital operations was focused on successfully delivering ESA's Huygens probe to the surface of Titan and relaying Huygens data via the Cassini orbiter to Earth. Huygens landing was both the most distant spacecraft landing and the first successful landing on the moon of another planet. The probe system consisted of two main components: the Huygens probe, which entered Titan's atmosphere after separating from the orbiter, and the probe support equipment, which remained attached to Cassini to establish a communication link to the probe during the probe mission.

The mission was originally designed for landing and relay during the first orbit about Saturn and at the first targeted Titan flyby. However, an end-to-end in-flight test of the probe relay link in February 2000 revealed unexpected behavior of the Huygens receiver onboard the Cassini orbiter. The anomaly was traced to a design flaw of the receiver's bit synchronizer, which had a bandwidth too small to accommodate the Doppler shift of the relay signal [45]. Shortly thereafter, a joint ESA/NASA task force, the Huygens Recovery Task Force (HRTF), was established with a mandate to better understand the anomaly and to develop a plan to recover the Huygens Mission.

Navigators contributed to the recovery by changing Cassini's trajectory to reduce Doppler shift between the orbiter and probe during the data relay period. They reduced the Doppler shift by raising the altitude of the orbiter for the probe delivery encounter from 1200 to 60,000 km so that the radial component of the orbiter's velocity relative to the probe was much smaller. To protect downstream science, navigators isolated these changes to the section of the tour previously dedicated to the probe mission. This required the insertion of an additional orbit and targeted flyby into the tour because a distant flyby at T1 or T2 would not provide sufficient bending to change Cassini's orbit period and re-encounter Titan by T3. By reducing the period of the initial orbit and making the first Titan encounter earlier, the additional orbit and targeted encounter could be added that achieved the necessary orbit period to tie back into the original reference trajectory at T3. T1 and T2 were then replaced by Ta, Tb, and Tc so downstream Titan encounter designations would not need to be incremented. The first three revs of the redesigned trajectory are compared to the original trajectory in Figure 4-5.

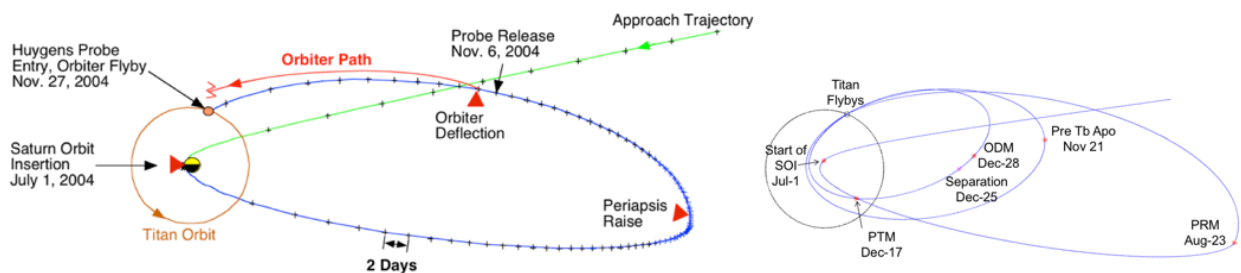


Figure 4-5. Huygens original trajectory (left) and redesigned trajectory (right).

The probe was delivered by targeting both the orbiter and probe to the probe entry conditions and then releasing the probe. Once released, there were no further opportunities to correct the probe's orbit during its 20-day coast to Titan atmospheric entry. After release, the orbiter performed a large

deflection maneuver targeting it away from Titan and onto a trajectory favorable for the relay of data from the probe and resumption of the tour. Clean-up maneuvers were performed for both the Probe Targeting Maneuver (PTM) and Orbit Deflection Maneuver (ODM). These four maneuvers and the separation event, which also imparted a ΔV , were designed, analyzed, and executed during the 32-day interval between Tb and Tc.

The initial redesign included a 64,000 km altitude non-targeted flyby of Iapetus seven days after probe separation. At first, this flyby was considered a fortuitous bonus, especially since closest approach was on the opposite hemisphere from the only targeted future Iapetus flyby. Upon completion of an OD covariance analysis, however, navigators discovered that the perturbation to Huygens' trajectory due to the uncertainty in Iapetus' gravitational force could prevent the probe flight path angle requirement from being met. The final design raised Iapetus' closest approach altitude to 127,000 km by lowering the Tb flyby altitude from 2200 km to 1200 km. This change significantly increased the available margin for error in the Iapetus mass estimate.

Huygens tour redesign used 87 of the 202 m/s ΔV margin available (at the 95% level) from the previously baselined prime mission. Of the extra ΔV spent, 75 m/s was spent on a larger SOI maneuver and PRM to reduce the initial orbit period and move the first Titan flyby 32 days earlier. SOI increases were mitigated by starting the maneuver 9 minutes later, which placed more of the finite burn near periapsis to increase its efficiency. PTM cost increased by nearly an order of magnitude, from 1.4 to 12.5 m/s, mostly because the period of the probe-delivery orbit had changed from 150 days to 32 days. The increased magnitude also necessitated the addition of a PTM clean-up maneuver. By changing the distant flyby from direct to retrograde, ODM cost was *reduced* from 49 to 26 m/s. Had the direct flyby been maintained, ODM would have cost over 100 m/s [46]. The reduced ODM cost was offset by subsequent increased costs of OTM-011 and OTM-012 so that the reference trajectory could be rejoined at T3. Although the redesigned mission increased ΔV costs, delivery statistics were improved as the first two Titan encounters enabled a better estimate of Titan's ephemeris prior to probe release.

4.1.1.1 Huygens Probe Requirements and Performance

The primary concerns in meeting navigation requirements for the probe delivery were robustness and reliability. Robustness was achieved by scheduling maneuvers and separation as early as possible. Unanticipated delays in separation and/or maneuver executions could be accommodated within the same orbit by shifting activities downstream. Reliability was achieved by delaying the OD DCO used for maneuver designs by one day beyond the day for which probe relay accuracy requirements were first met. Separation and all maneuver executions occurred on schedule and all mission requirements were met.

An interface altitude of 1270 km defined a point well outside the atmosphere of Titan where JPL's responsibility for probe orbit propagation ended and ESA's responsibility began. The time at which the nominal probe trajectory crossed the interface altitude was defined as the interface time. Target parameters for PTM and PTM clean-up were determined at the epoch of the interface time, and included altitude, B-plane angle, entry angle, and angle of attack [47]. The required interface time was 09:07 ET on January 14, 2005. At this time and altitude, other requirements were set. The B-plane angle was required to nominally be 167.5° in a coordinate system relative to Titan's equator of date. The entry angle requirement was $-65^\circ \pm 3^\circ$ at the 99% confidence level, in the Titan body-fixed frame. This was referred to as the entry angle corridor. The angle-of-attack,

defined as the angle between the probe's axis of symmetry and the Titan relative velocity of the probe at the interface time, was required to be within 5° (3σ) of the nominal 0° value. Angle-of-attack was computed in the inertial frame, and the assumption was made that the probe's axis of symmetry was aligned with the separation ΔV and the spinning probe's angular momentum vector.

Probe separation took place two days after PTM clean-up, on December 25, 2004. The orbiter with probe still attached turned to orient the probe to the attitude needed to achieve the correct angle-of-attack and then released the probe. To prevent contact between orbiter and the just-released probe, orbiter thrusters were inhibited from firing, and the orbiter was allowed to tumble. When the probe was safely away from the orbiter, the orbiter performed a de-tumble procedure to restore attitude control. PTM and PTM clean-up accounted for the predesigned probe separation ΔV .

Three days after separation, ODM was executed to ensure a successful relay. Both ODM and ODM clean-up were targeted to B-plane coordinates. The B-plane angle was required to be 180° and the flyby altitude was required to be 60,000 km. The Orbiter Delay Time (ODT), the length of time between the interface time and the orbiter's periapsis with Titan, was set to 2.1 hours, making the orbiter flyby closest approach time be 11:13 ET on January 14. Orbiter pointing to the probe was required to be within 6.0 mrad (99% confidence) for three hours beginning from the interface time. This requirement was sub-allocated between AACS and Navigation, with an allocation to Navigation of 3.0 mrad.

ODM was scheduled three days after probe separation to converge OD estimates before introducing more uncertainty via ODM execution errors and to allow time for recovery from potential problems after separation. Images of the probe taken by the orbiter were also successfully obtained and processed during these three days. These OPNAVs were valuable for differentiating estimates of the separation ΔV from the following orbiter de-tumble ΔV and improving knowledge of the probe trajectory. The combination of the separation and de-tumble ΔV s introduced a large uncertainty in the location of the probe relative to the orbiter, which made getting the first image of the probe a challenge. The first set of images was a 5×5 mosaic of wide-angle camera pictures taken 12 hours after separation. The mosaic was taken to increase the odds of successfully capturing the probe in the images. On the following day, December 26, the wide angle camera (WAC) images were processed, and the increased knowledge of the probe position relative to the orbiter allowed the use of the narrow-angle camera to image the probe. Two more WAC images were also taken as a precaution against NAC images missing the probe. The final opnav was taken December 27, using the NAC. In total, four WAC OPNAVs and two NAC OPNAVs were obtained. The first NAC opnav is shown in Figure 4-6.

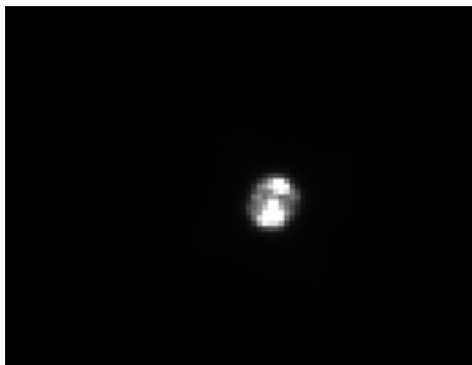


Figure 4-6. OPNAV of Huygens Probe taken by Cassini NAC on December 26, 2005.

Prior to the Tb flyby, a considerable amount of effort was expended to improve the estimate of Iapetus' mass and ensure the probe flight path angle requirement would be met. As late as August 2004, Iapetus' Standard Gravitation Parameter (GM) estimates fluctuated by as much as $16 \text{ km}^3/\text{s}^2$ [48]. An error of this order would have prohibited the requirement from being met. Efforts to improve the estimate focused mainly on a 1.1 million km distant flyby of the satellite that occurred on October 17, 2004. During the flyby, the spacecraft was kept in a quiet mode, with no thrusting or turns. Also, additional tracking was requested and acquired to maximize the amount of Iapetus mass information captured. Ultimately, the value used in operations during this arc was found to be consistent with the later reconstructed value for Iapetus' mass. An Iapetus GM value of $120.55 \pm 0.79 \text{ km}^3/\text{s}^2$ was determined for use with this arc, and the current reconstructed value is $120.5038 \pm 0.0080 \text{ km}^3/\text{s}^2$ [49].

The Huygens probe mission culminated with successful transmission and relay of data for 3 hours, 40 minutes. Transmission began within one minute from main parachute deployment and continued through the 2 hour, 28 minute descent, a soft landing at a speed slightly less than 5 m/s, and an additional 1 hour, 12 minutes from Titan's surface. Communications between probe and orbiter ended when the orbiter passed below the probe's horizon [50].

All Huygens mission requirements on navigation were met within a comfortable margin. Based on the final trajectory reconstruction, the probe interface altitude was achieved 3.29 seconds early with a one-sigma uncertainty of 5.82 seconds. At this time, the probe B-plane angle was 167.5° and the angle-of-attack was 1.4° . The entry angle was estimated to be $-65.4 \pm 0.27^\circ$. The evolution of entry angle estimates from PTM to reconstruction is shown in Figure 4-7. All estimates are within the 3° , 99% confidence level entry angle corridor. Orbiter pointing errors due to differences between the trajectory used to generate the onboard pointing profile and the reconstructed trajectory are shown in Figure 4-8. The onboard pointing profile was based on a trajectory

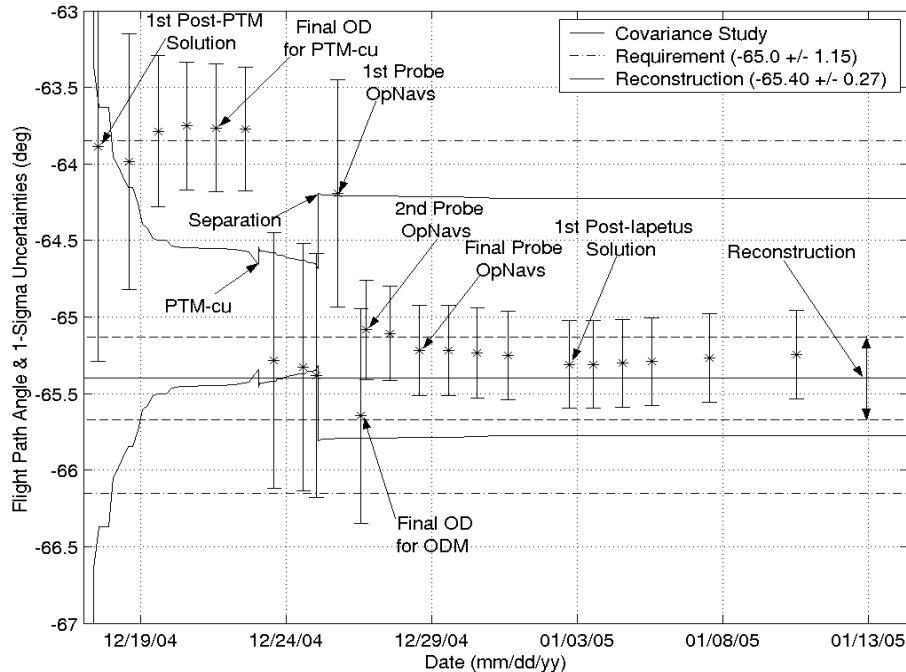


Figure 4-7. Entry angle estimates and uncertainties versus data cut-off.

generated in October 2004 (041015) and the ODM clean-up maneuver was designed to recover this profile. As an aside, an update to the onboard pointing profile would have served the same purpose as the ODM clean-up maneuver. However, the project found that the effort to produce and review for accuracy a pointing update was less desirable than the well understood practice of designing and implementing a maneuver.

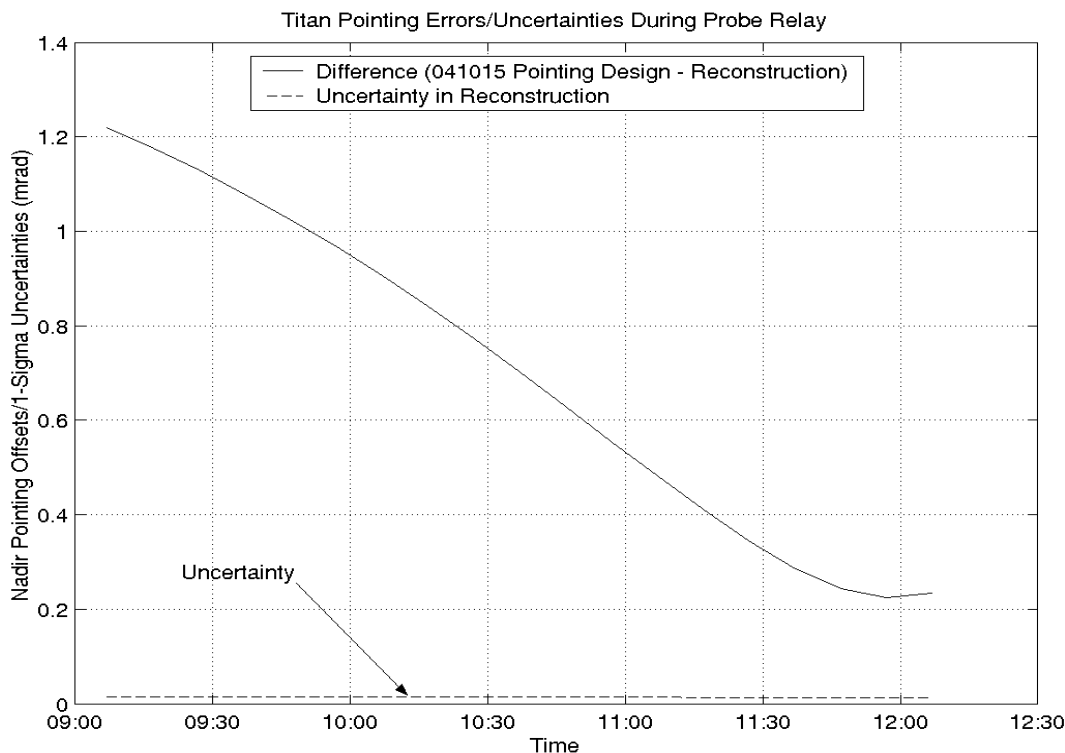


Figure 4-8. Relay pointing errors and uncertainties.

4.1.2 Remainder of Prime Mission

Upon successful completion of the Huygens Mission, navigators turned their attention to the remaining 49 targeted satellite flybys. Each transfer from one target to the next was conducted in three phases. The first phase was a planning update where OD covariance analyses and maneuver Monte Carlo analyses were performed using the latest available information. Current spacecraft state information was extracted from the previous transfer. Simulated tracking data was consistent with the negotiated DSN schedule. Spacecraft attitude and spacecraft small force predicted ΔV s corresponded to activity in command sequences. In contrast to the analysis that went into the Navigation Plan, these analyses were high-fidelity and would influence workforce scheduling and provide a preview of what to expect in operations. Deviations from these expectations in operations were viewed as a possible error indicator and would require explanations to ensure that the operational navigation system was well understood.

The second phase was the operational phase. In keeping with the high-fidelity planning phase, OD initial epochs were usually placed near the apoapsis preceding one targeted encounter and the data arc extended through the next targeted encounter. These arcs were used to design maneuvers and provide trajectory predictions for occasional late sequence updates. As soon as one maneuver was

executed, work would begin on the design of the next maneuver. In this manner, a sense of OD and maneuver design stability could be ascertained and compared against what was expected from the planning phase. An instability, such as solution drift, occurring when the information content of a tracking pass was small could be another error indicator.

The final phase was the reconstruction phase. Upon collection of all tracking data through both encounters in an OD arc, a reconstructed trajectory was generated and provided to science teams for reduction of their observations.

Five arcs in prime mission required special targeting considerations. Three were required for double flybys, where successive close flybys occurred back-to-back with no time to insert a corrective maneuver between them, and two were required for precision occultation targeting to detect or determine the composition and density of particles or gases in Enceladus' plume. Four more double flybys and four more distant occultation would be planned and executed in the extended missions.

Prime mission double flybys occurred in February 2005 with an 1167 km altitude Enceladus flyby occurring 45 hours after the 1577 km nominal altitude T3 flyby, in September 2005 with the 510 km nominal altitude H1 flyby occurring 48 hours after a 1484 km Tethys flyby, and in August 2007 with the 3326 km nominal altitude T35 flyby occurring 29 hours after a 5721 km altitude Rhea flyby. For double flybys, only one satellite can be targeted, but attention must be given to both because a large error in the first flyby would significantly alter the second flyby's geometry, resulting in degraded science observations and increased risk of impact. Prior to a double flyby, an effort is made to ensure the operational trajectory adheres closely to the reference trajectory.

Occultation targeting was performed for two distant Enceladus observations. Enceladus plume occultation took place on September 15, 2006 and October 24, 2007. For the September 15 event, radio signals were passed through the plume on their transit between Cassini and Earth, whereas for the October 24 event the star ξ Orionis was occulted from Cassini by the plume. For both plume occultation, it was necessary to remain near the reference trajectory at the time of the occultation, even though it was not near any targeted flybys. To accomplish this, targeting was not performed with chained optimization between cleanup and shaping maneuvers. Instead, additional ΔV costs were incurred by non-optimally targeting the cleanup maneuver to the position coordinates of the reference trajectory at the time of the apoapsis maneuver (XYZ targeting).

4.1.3 Performance

Performance and other salient characteristics for all prime mission maneuvers, OTM-001 through OTM-159, are tabulated in Appendix A – Supplementary Material, Tables A-5 to A-7 Maneuver History. The average navigation cost per flyby was 0.325 m/s, where navigation cost is defined as the ΔV cost incurred above the deterministic cost needed by the reference trajectory.

Of the 154 planned prime mission maneuvers, 40 were performed on the RCS system with a total ΔV of 4.2 m/s and 72 were performed on the ME with a total ΔV of 790 m/s. At 393 m/s, nearly half of the ME total performed ΔV was expended by the PRM. The remaining 42 planned maneuvers were canceled owing to exceptional OD and maneuver execution performance. Risk reduction also weighed into the decision to cancel many maneuvers. With a propellant rich spacecraft and a flight team adapting to this new rapid pace of maneuvers, project management

was more willing to accept downstream ΔV cost penalties in order to reduce maneuver execution implementation cycles.

Target misses and biases can be seen in Appendix A – Supplementary Material, Tables A-1, A-2, and A-4 Targeted Encounter History. Many of these differences may appear large because approach maneuvers were canceled or targets were intentionally biased for more than half of the flybys.

One year before the end of prime mission, the maneuver execution error model was updated. The number of ME maneuvers available for use in error modeling had increased from 15 to 61 maneuvers. Available RCS maneuvers had increased from three to 26 maneuvers. The resulting execution error model in use at the end of prime mission is provided in Table 4-5. Internally, this model was designated as 2007-02.

Table 4-5. Maneuver execution error model improvement at prime mission end.

One-Sigma Errors		Main Engine		RCS	
		Cruise End	PM End	Cruise End	PM End
Magnitude	Proportional (%)	0.2	0.02	2.0	0.4
	Fixed (mm/s)	10.0	5.0	3.5	1.0
Pointing (per axis)	Proportional (mrad)	3.5	0.6	12.0	9.0
	Fixed (mm/s)	17.5	3.0	3.5	0

The double flybys were all extremely successful. The first double flyby, T3/Enceladus, was the only one to target the first flyby body. The altitude errors for the second flyby body, Enceladus, was 96 km higher than nominal. H1 was targeted in the Tethys/H1 double flyby. The Tethys altitude was 12 km higher and the Hyperion altitude was 22 km lower than nominal. T35 was targeted in the Rhea/T35 double flyby. The Rhea altitude was 4 km higher and the Titan altitude was 2 km lower than nominal [51].

Only one of the two occultations was successful. The first failed because light travel time was not properly accounted for in the reference trajectory design nor was this error caught during an assessment by the science team. Subsequent distant occultations were subject to multiple navigation team independent checks to prevent this mistake from recurring.

4.1.4 Notable Events

The fifth spacecraft safing occurred on September 11, 2007, within one day after the Iapetus targeted flyby, when the Solid-State Power Switch (SSPS) of Traveling Wave Tube Amplifier-B (TWTA-B) line A tripped and shut down the prime TWTA. The spacecraft remained in RCS mode for two days and OTM-128, the Iapetus cleanup maneuver, was executed while the background sequence was deactivated. Upon completion of the burn, the nominal ME command block transitioned the spacecraft back to RWA mode. The spacecraft remained Earth pointed until the background sequence was activated on September 16. This safing imparted approximately 25 mm/s of unplanned ΔV to Cassini.

4.2 Equinox Mission

Cassini's Equinox Mission extended from the end of prime mission until the end of fiscal year 2010. The mission included a total of 38 targeted flybys. Of these, 28 were of Titan, eight of Enceladus, and one each of Rhea and Dione. The second Enceladus flyby of the mission, E5 on October 9, 2008, was also the lowest ever, with a planned altitude of only 25 km. Equinox Mission also includes the lowest Titan flyby ever, T70 on June 21, 2010, with an altitude of only 880 km.

Equinox Mission consisted of five different phases defined by different science objectives dominating each phase of the tour design. The first phase spanned from T44 to T51 and included three Enceladus flybys to further investigate the newly discovered plumes. While maintaining high inclination, orbits also provided favorable geometry for stellar occultation that penetrated the densest parts of the B-ring and in situ measurements of Saturn's auroral region. The second phase spanned from T51 to T52, when an outbound-to-inbound 8-day pi-transfer was implemented to efficiently change the Local Solar Time of the Titan encounters to dusk. The third phase, from T52 to T62, set up the desired inclination profile for rings viewing during the few months around Saturn equinox on August 11, 2009. The fourth phase was dominated by equatorial orbits so that six more icy satellite flybys and two ansa-to-ansa ring occultations could be obtained. The final phase of Equinox Mission consists of a series of successive 16-day transfers designed for Titan gravity measurements, high northern Titan ground tracks, and another ansa-to-ansa occultation. Petal plots for Equinox Mission are provided in Figure 4-9. Charts showing inclination, periapsis radius, and apoapsis radius evolution are provided in Figures 4-10 through 4-12, respectively.

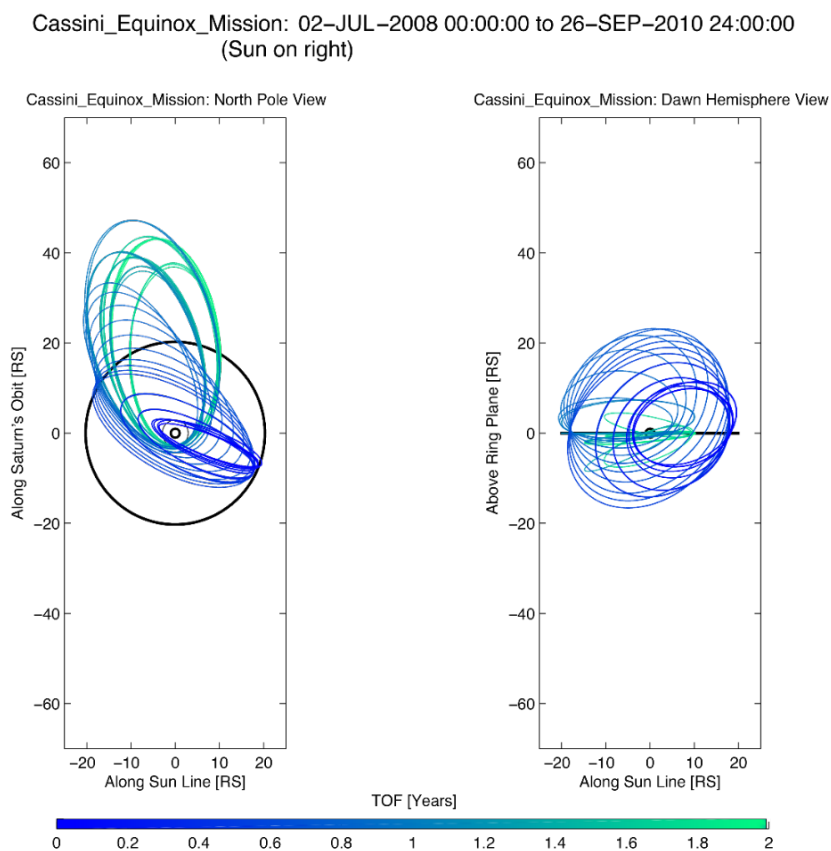


Figure 4-9. Equinox Mission petal plot.

Only two new reference trajectory updates were implemented during Equinox Mission. The first appended Solstice Mission to the end of Equinox Mission and lowered an occultation at E10, and the second changed five maneuver locations to remove conflicts with science observations desired at similar times. A seemingly third update, 080806, was identical to 080520. The objective in producing 080806 was to quickly generate an Orbit Propagation & Timing Geometry (OPTG) ancillary file using an automated procedure. The ancillary file included a newly introduced leap second needed for sequence development. Later leap seconds were included in OPTG files without updating the reference trajectory.

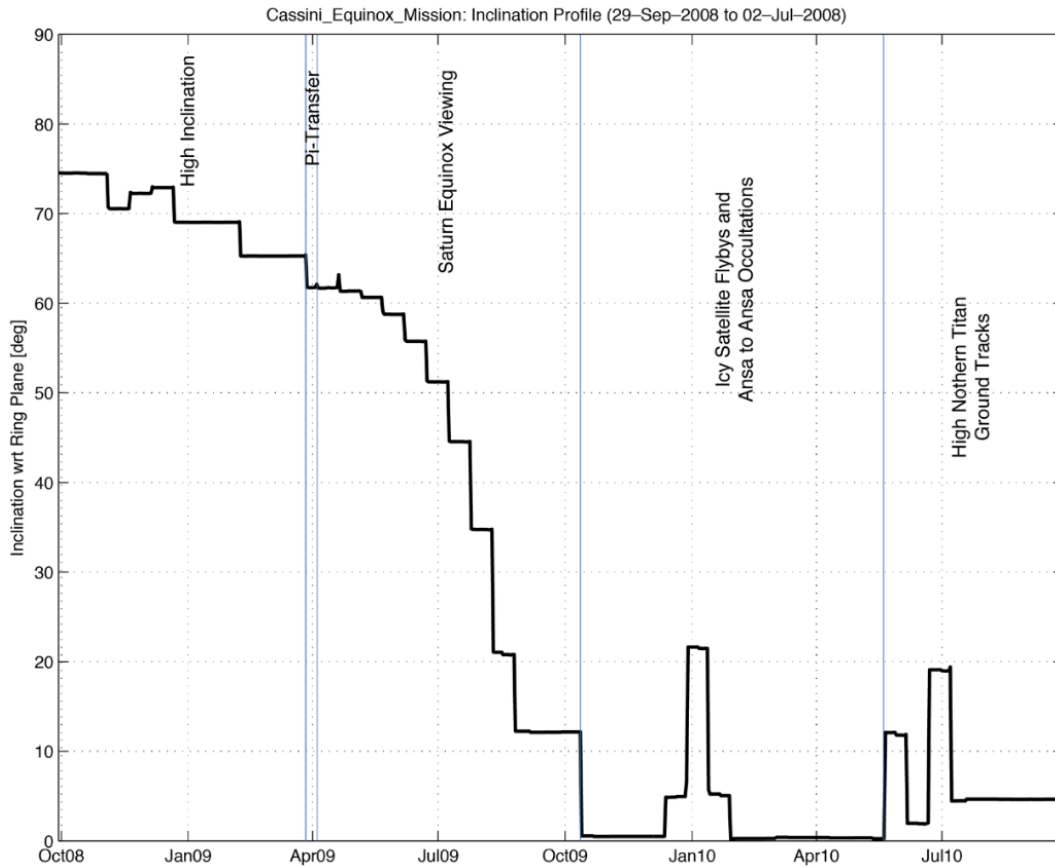


Figure 4-10. Equinox Mission inclination.

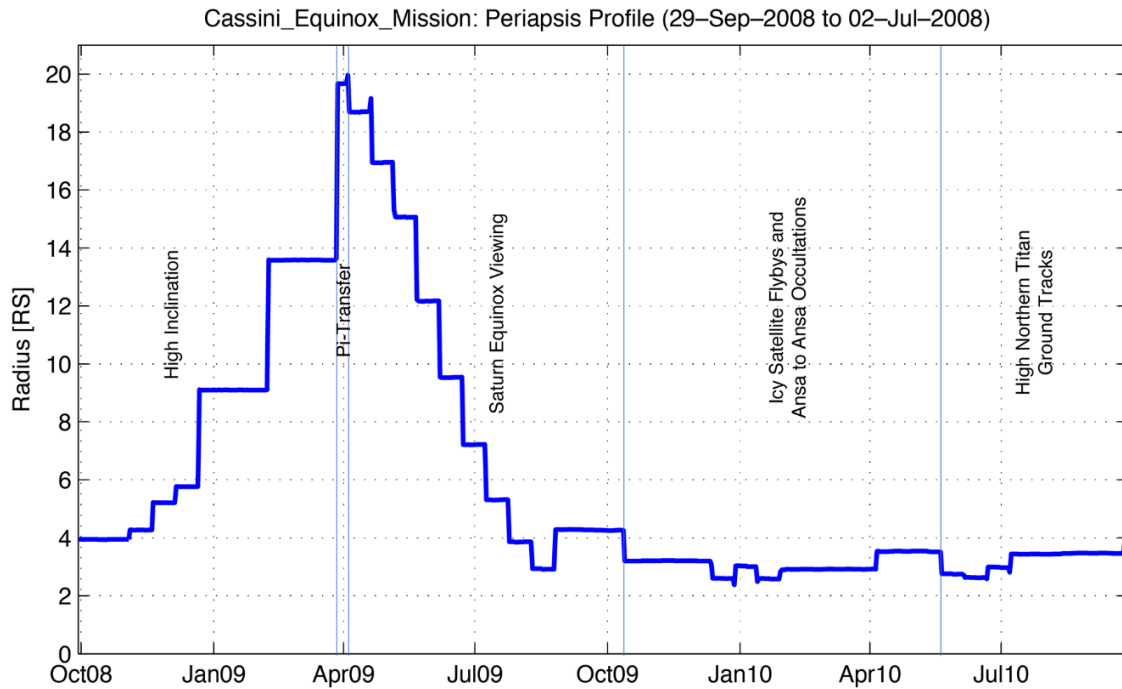


Figure 4-11. Equinox Mission periapsis radius.

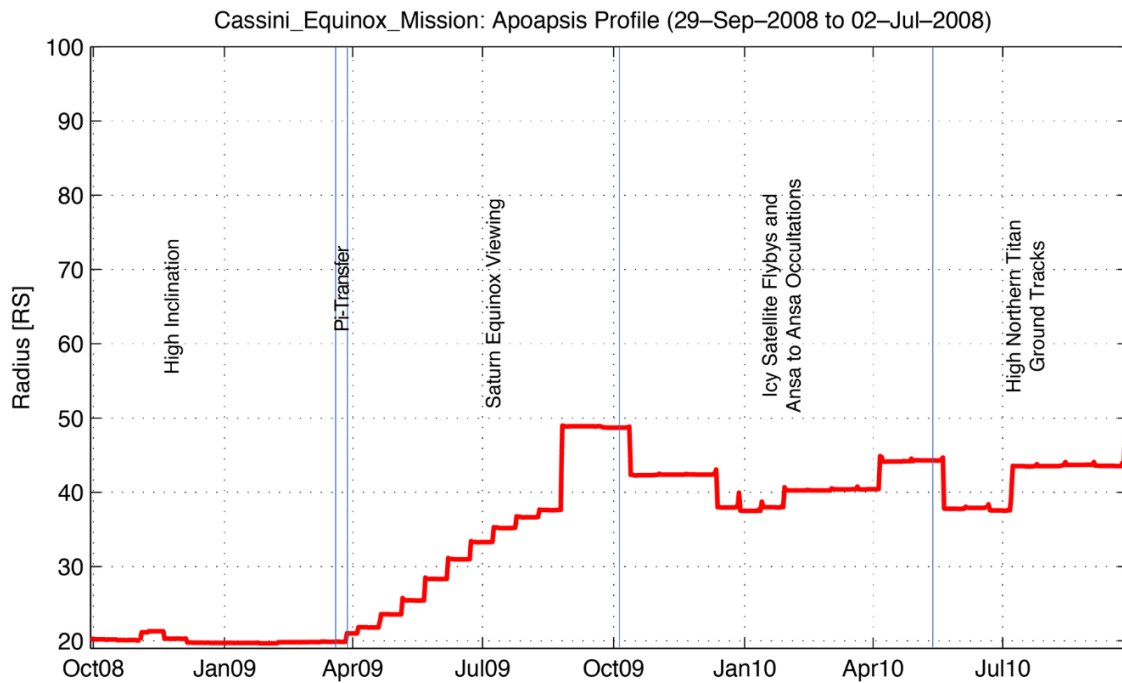


Figure 4-12. Equinox Mission apoapsis radius.

Three arcs in Equinox Mission included double flybys. They occurred in October/November 2008 with the 1100 km nominal altitude T46 flyby occurring 72 hours after the 200 km nominal altitude E6 flyby, in April 2010 with the 504 km nominal altitude D2 flyby occurring 38 hours after the 7462 km nominal T67 flyby, and in May 2010 with the 1400 km nominal altitude T68 flyby occurring 45 hours after the 439 km nominal altitude E10 flyby.

Occultation targeting was performed for two more distant Enceladus observations. Enceladus plume occultations took place on January 26, 2010, and May 18, 2010. Again, XYZ targeting was implemented for both.

4.2.1 Performance

Performance and other salient characteristics for all Equinox Mission maneuvers, OTMs 160 through 262, are tabulated in Appendix A – Supplementary Material, Tables A-7 and A-8 Maneuver History. The average navigation cost per flyby was 0.447 m/s, higher than during prime mission. The increase is attributable to OTM-169, the approach maneuver for the E6/T46 double flyby, which anomalously underperformed. The underperformance resulted in a 10 km target miss at the low altitude (1100 km) T46 flyby and a downstream cost of over 7 m/s.

Maneuvers were scheduled more frequently than during prime mission, with 104 maneuvers planned during the 27 months of Equinox Mission, averaging to one maneuver per week. Once again, navigation performance was exceptional, allowing 34 maneuvers to be canceled. Of the maneuvers executed, 22 were performed using the RCS system with a total ΔV of 1.5 m/s and 48 were performed using the ME with a total ΔV of 197 m/s. The largest maneuver performed was OTM-213, the shaping maneuver prior to T61, with a magnitude of 13 m/s. The remaining 34 planned maneuvers were not needed and canceled.

Target misses and biases can be seen in Appendix A – Supplementary Material, Tables A-2 and A-4 Targeted Encounter History. Many of these differences may again appear large because approach maneuvers were canceled or targets were intentionally biased.

The ME maneuver execution error model was again updated in Equinox Mission as the number of ME maneuvers available for use in error modeling had increased from 61 to 85 maneuvers. The RCS model was not updated because the redundant B-branch was activated shortly after OTM-169 and a characterization of the new thrusters had not yet been completed. The resulting ME execution error model in use at the end of Equinox Mission is provided in Table 4-6. Internally, this model was designated 2008-01.

Table 4-6. Maneuver execution error model change at Equinox end.

One-Sigma Errors		Main Engine	
		PM End	Equinox End
Magnitude	Proportional (%)	0.02	0
	Fixed (mm/s)	5.0	4.5
Pointing (per axis)	Proportional (mrad)	0.6	1.1
	Fixed (mm/s)	3.0	3.0

The double flybys were all extremely successful in spite of the anomalous maneuver performance prior to E6/T46. The second flyby body was targeted in all three double flybys. T46 was targeted in the E6/T46 double flyby. The Enceladus altitude was 29 km lower and the Titan altitude was 5 km higher than in the reference trajectory. The miss distance was much larger for Enceladus than for the nontargeted satellites in the next two double flybys. In the interim between E6/T46 and

T67/D2, navigators discovered that the Enceladus miss distance could have been significantly reduced if XYZ targeting had been implemented. D2 was targeted in the T67/D2 double flyby. The Titan altitude was 0.2 km lower and the Dione altitude was 7 km higher than in the reference trajectory. T68 was targeted in the E10/T68 double flyby. The Enceladus flyby was 0.6 km higher and the Titan flyby was 2 km lower than in the reference trajectory. XYZ targeting was implemented for both T67/D2 and E10/T68 double flybys. Both distant Enceladus plume occultations were successful. In each case, radio signals passing between Earth and Cassini were occulted by the plume.

4.2.2 Notable Events

The most notable unexpected impact to navigation during Equinox Mission was the anomalous RCS OTM-169 approach maneuver on October 29, 2008, preceding the E6/T46 double flyby. Nominally 232 mm/s, the ΔV achieved came up 7 mm/s short and back-to-back gravity assists magnified the trajectory dispersion. The resulting 10 km miss at T46 would incur a hefty downstream ΔV cost of 7 m/s to remain close to the reference trajectory. A-branch thrusters Z3A and Z4A were subsequently determined to be degraded, and approximately five months later, Cassini ground controllers commanded the spacecraft to transition to its redundant B-branch thrusters.

The Cassini project decided to transition to the B-branch thrusters during the week of March 11, 2009—two days after execution of the OTM-183 shaping maneuver and 13 days before OTM-184, the T51 approach maneuver. Nominally, OTM-184 would be the first maneuver to use the redundant set of thrusters. However, OTM-183 dispersions caused Cassini to be placed on a trajectory that would pass too close to Titan's atmosphere. If not corrected, Cassini's attitude control authority could be overcome by atmospheric forces and cause the spacecraft to tumble. This made execution of another maneuver imperative before T51, and there would be little time to troubleshoot potential anomalies associated with first-time use of the B-branch thrusters if OTM-184 was to be relied upon for raising the trajectory above the tumble altitude. This led to the decision to insert a new maneuver, OTM-183X, into the schedule. OTM-183X would be executed on March 18, nine days before the T51 flyby, providing ample recovery time in the event of a failure. Ultimately, OTM-183X executed superbly. Maneuver execution and OD errors were small, allowing OTM-184 to be canceled.

4.3 Solstice Mission

Cassini's Solstice Mission extended from the end of Equinox Mission to Cassini's demise during atmospheric entry at Saturn in September 2017. The mission included a total of 70 targeted flybys. Of these, 54 were of Titan, eleven of Enceladus, three of Dione, and two of Rhea. Nine of the sixteen non-Titan flybys were at altitudes of 100 km or less. The seven-year mission more than doubled the temporal baseline of the combined 6.2-year Prime and Equinox Missions.

Solstice Mission consisted of five different phases predominantly defined at transitions between equatorial and inclined orbital geometries. The first phase was a series of equatorial orbits spanning from T73 to T83. With ring viewing geometry edge-on, these orbits maximized observational coverage of Saturn. Ten icy moon flybys were also achieved (eight of Enceladus, one of Dione, and one of Rhea), four allowing further investigation of the plume around Enceladus' southern pole. The second phase may be divided into three sub-phases, all three providing low solar phase Titan surface coverage. The first sub-phase spanned from T83 to T91 and inclination was increased to a maximum of 61.7°. Most of the Solstice Mission ring and high latitude Saturn atmospheric

occultations occurred in this sub-phase. Inclination was gradually reduced in the second sub-phase (T91–T101) to provide several inclined passages through Saturn’s magnetotail region. In the third sub-phase, from T101 to T110, inclination was initially increased to obtain three polar Titan occultations. The remainder of the flybys decreased inclination to setup the next equatorial phase. The third phase, from T110 to T114, extended the temporal coverage of Saturn observations unobstructed by the rings and includes two more close flybys of both Enceladus and Dione. It also set up the node alignment necessary for the Grand Finale orbits at the end of Solstice Mission. In the fourth phase, inclination was gradually increased while reducing periapsis distance. The final Titan flyby in this phase increased inclination to near critical inclination (the inclination at which apsidal rotation rate due to Saturn’s oblateness becomes zero), enabling the F-ring orbits—twenty low ΔV cost orbits between T125 and T126 with descending node crossing just outside Saturn’s F-ring. The final phase, called the Grand Finale, consisted of 22 orbits each with a 6.5-day period. In this phase, the spacecraft’s descending node was moved to within a 2500 km wide gap between Saturn’s upper atmosphere and innermost ring. A distant non-targeted Titan flyby 22 revs later provided a gravity assist ΔV that then directed Cassini into Saturn’s atmosphere where it became captured, satisfying NASA planetary protection requirements. Petal plots for Solstice Mission are provided in Figure 4-13. Charts showing inclination, periapsis radius, and apoapsis radius evolution are provided in Figures 4-14 through 4-16, respectively.

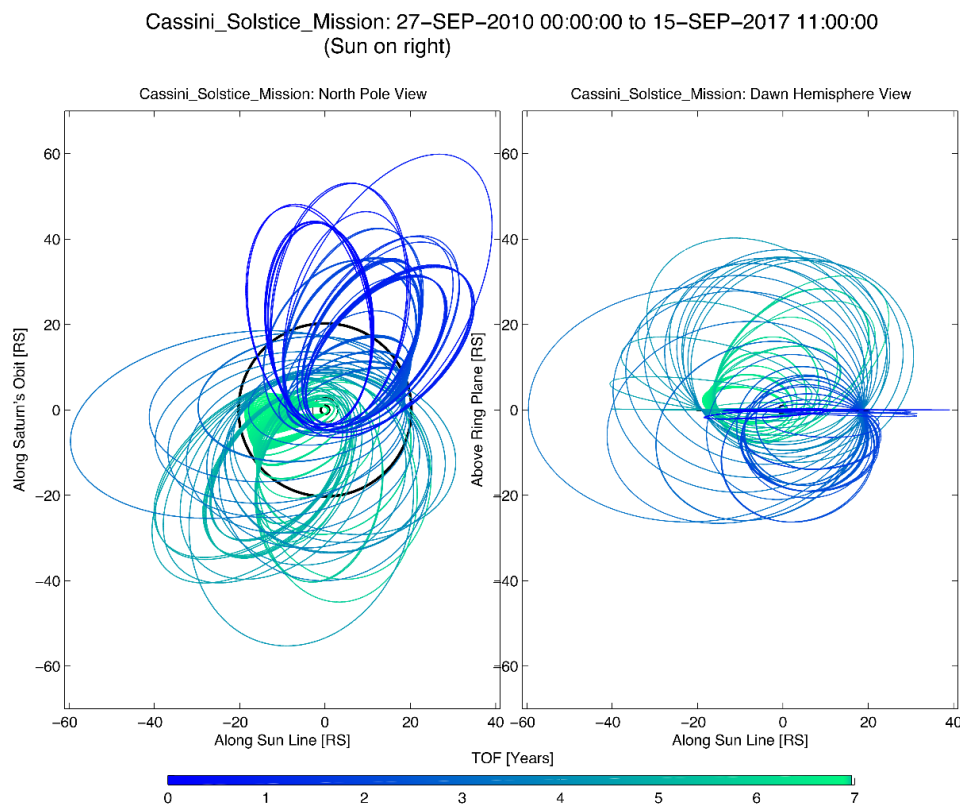


Figure 4-13. Solstice Mission petal plot.

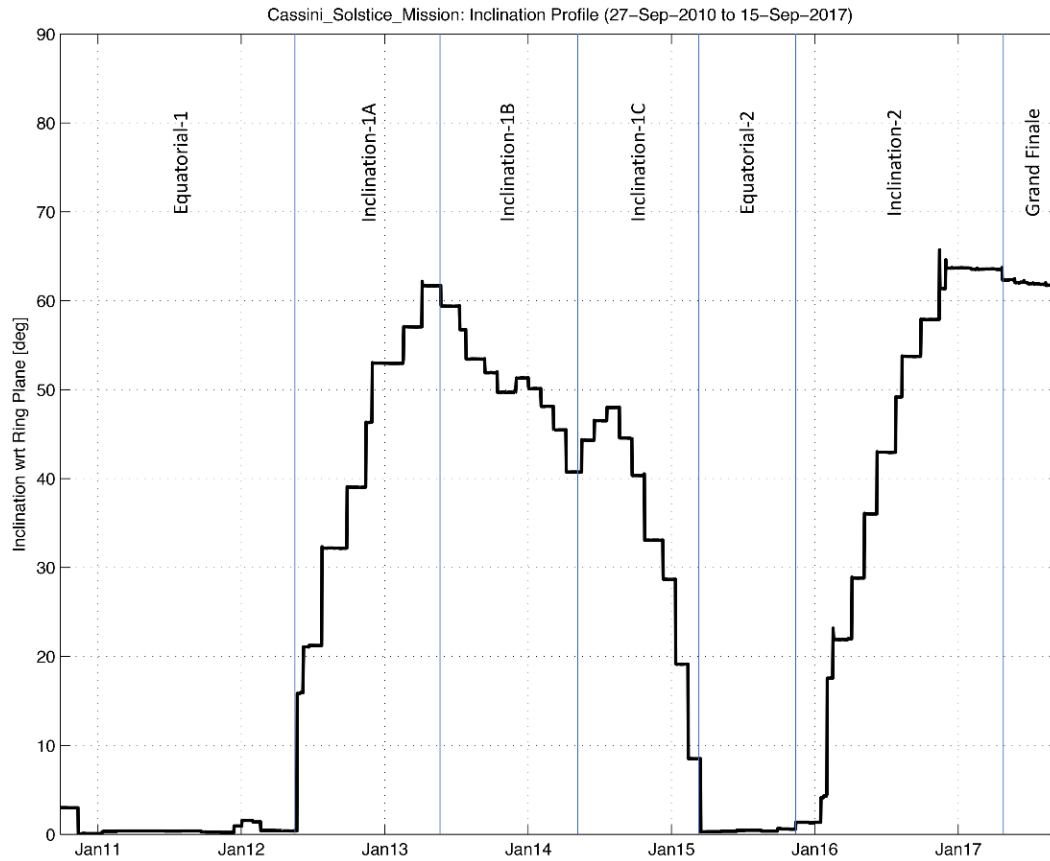


Figure 4-14. Solstice Mission inclination.

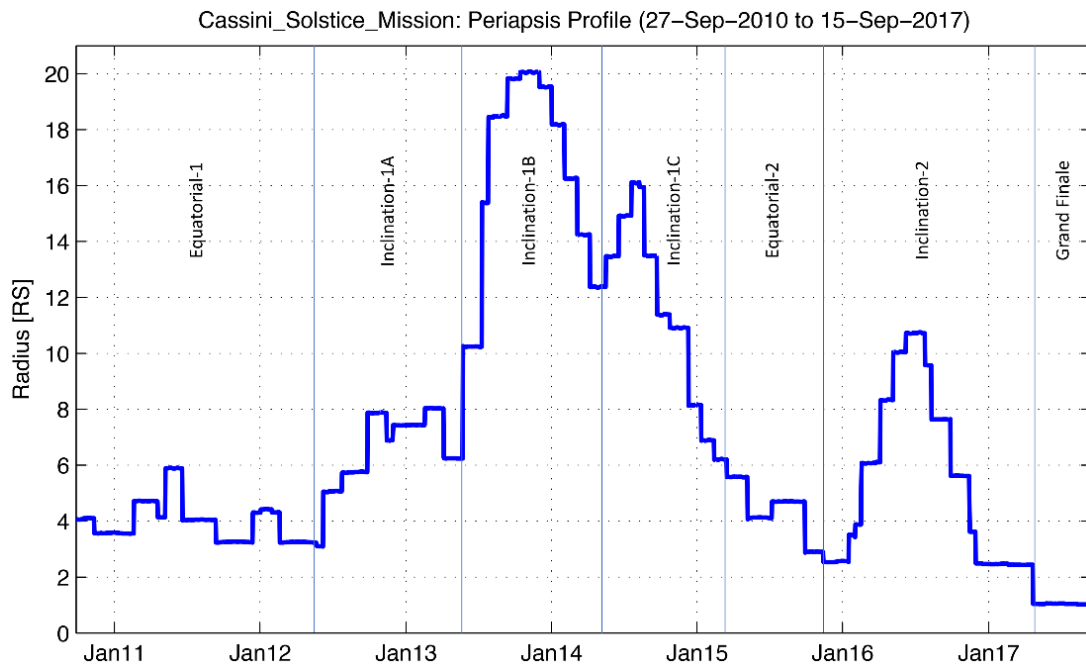


Figure 4-15. Solstice Mission periapsis radius.

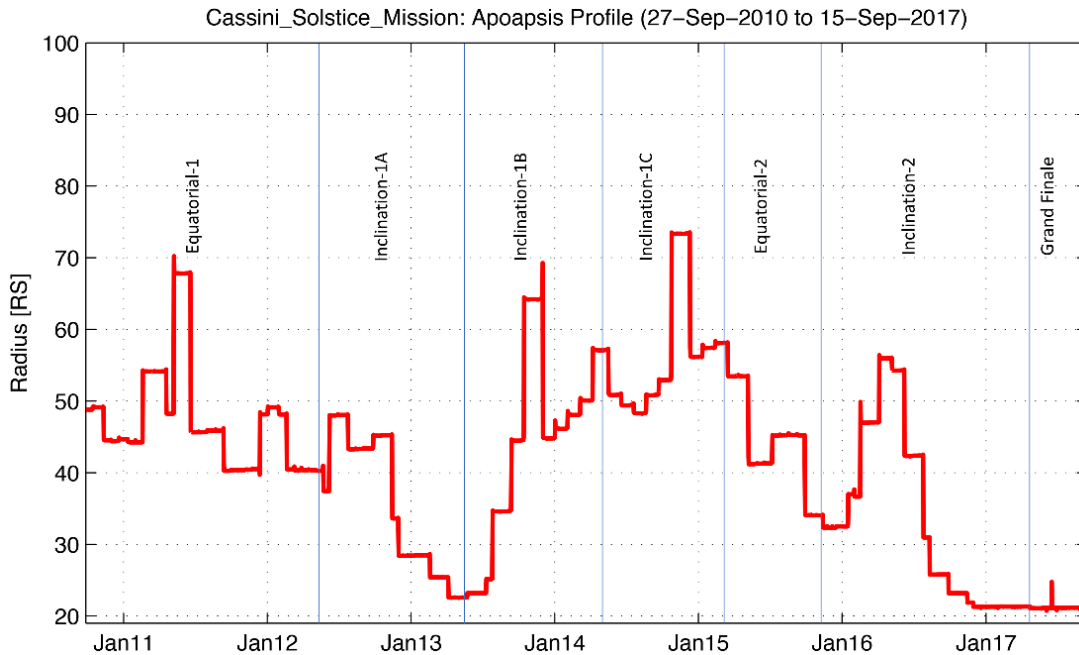


Figure 4-16. Solstice Mission apoapsis radius.

Solstice Mission design constraints included a predicted total ΔV availability of 160 m/s at the 90% confidence level, less than the amount implemented in either of the shorter duration Prime or Equinox Mission orbital operations. Therefore, Solstice Mission maneuvers would generally be less frequent and smaller. In contrast to the previous missions, more monopropellant RCS maneuvers were implemented than bi-propellant ME system maneuvers.

Navigation processes underwent a paradigm shift for Grand Finale operations. Through T126, maneuvers were designed to target satellite flyby conditions. However, with 22 revs until EOM and no future targeted satellite encounters, the control strategy changed. The science team identified segments along the reference trajectory where observations were especially sensitive to pointing and timing errors, and the navigation team's goal was to keep dispersions small along these segments via a minimum number of maneuvers. A prediction of the ΔV to meet this goal was also needed to ensure that available propellant resources were adequate. References [52] and [53] describe the tools developed and analysis conducted to meet this goal.

Three new reference trajectory updates were implemented during Solstice Mission. The first was a global update that also changed a maneuver location in conflict with a science observation. The second included a local update to add a high value Enceladus plume occultation in March 2016. The final update restricted changes to only the Grand Finale portion of the mission by including a Saturn atmospheric density model. This model was necessary for the final five orbits, in which spacecraft drag forces were significant near the periapses.

Only one arc in Solstice Mission included a double flyby. It occurred in December 2011 with the 3586 km nominal altitude T79 flyby occurring 35 hours after the 100 km nominal altitude D3 flyby.

Occultation targeting was performed for two more distant Enceladus observations. Enceladus plume occultations took place on October 19, 2011, and March 11, 2016. Again, XYZ targeting was implemented for both.

The Cassini Mission concluded upon entry into Saturn's atmosphere on September 15, 2017, when the control authority of the spacecraft's thrusters was overcome by drag torques. Telemetry was lost first, then Ka-, X-, and S-band signals in rapid succession as the HGA moved off Earth-point. Loss of signal occurred 729 seconds earlier than predicted based on reference trajectory conditions, primarily because Saturn's atmosphere was five times denser than modeled. Radiometric data acquired during entry was used to reconstruct Saturn's atmospheric density [54]. Entry conditions at loss of signal are provided in Table 4-7. Bold borders surround the observed final times and other times were derived from them. For example, the final telemetry frame was tagged with a Spacecraft Event Time (SCET), and the Earth Received Time (ERT) was computed from it by adding a one-way light time. Altitudes are from a modeled one bar atmosphere radius of 60268 km along Saturn's equator.

Table 4-7. Loss of signal times and trajectory characteristics.

Link	UTC SCET Epoch	UTC ERT Epoch	Altitude (km)	Range (km)	Latitude (deg)	Flight Path Angle (deg)
Telemetry	10:31:51.000	11:55:18.038	1385	61474	9.30	-8.81
Ka-band	10:32:04.770	11:55:31.810	1299	61402	8.92	-8.60
X-band	10:32:07.660	11:55:34.700	1281	61387	8.84	-8.56
S-band	10:32:15.808	11:55:42.850	1231	61346	8.61	-8.44

4.3.1 Performance

Performance and other salient characteristics for all Solstice Mission maneuvers, OTM-263 through OTM-475, are tabulated in Appendix A– Supplementary Material, Tables A-9 to A-11 Maneuver History. The average navigation cost per flyby was 0.132 m/s, significantly lower than both Prime and Equinox Missions. The lower cost reflects better ephemeris modeling, no significant anomalies, and a lower threshold for downstream ΔV costs when considering maneuver cancellations. Maneuver cancellation ΔV cost thresholds were reduced because propellant margins were small, and the risk of introducing an error to the now mature maneuver design and implementation process was considered small.

Solstice Mission plans included 212 maneuvers in seven years, averaging to only one maneuver every 12 days. During flight operations, 53 of these maneuvers were not needed and canceled. Of the maneuvers executed, 112 were performed using the RCS system with a total ΔV of 8 m/s and 47 were performed using the ME with a total ΔV of 112 m/s.

Grand Finale requirements to maintain orbit dispersions within 250 km at periapses 3, 14, and 16 were met. Dispersions from the reference trajectory were only 26 km at periapsis 3, 198 km at periapsis 14, and 7 km at periapsis 16. Three maneuvers were needed to control Grand Finale dispersions, and ΔV s were well predicted. Actual ΔV s for the first two maneuvers were about one sigma lower than the predicted value and the ΔV for the third maneuver was about two sigma

higher than predicted. The ΔV for all three maneuvers combined was about one sigma lower than predicted [55].

Target misses and biases can be seen in Appendix A– Supplementary Material, Tables A-2 to A-4 Targeted Encounter History. As stated previously, many of these differences may appear large because approach maneuvers were canceled or targets were intentionally biased.

The ME maneuver execution error model was again updated in Solstice Mission after the January 2009 fuel side pressurization of the ME system. The new ME model was developed from an analysis of 48 ME maneuvers, beginning from OTM-180. The RCS model was also updated following the March 2009 thruster branch swap. The new RCS model was developed from an analysis of 49 RCS maneuvers, beginning from OTM-183X. The resulting execution error models in use at the end of Solstice Mission are provided in Table 4-8. Internally, this model was designated 2012-1.

Table 4-8. Maneuver execution error model change at Solstice Mission end.

One-Sigma Errors		Main Engine		RCS	
		Equinox End	Solstice End	Equinox End	Solstice End
Magnitude	Proportional (%)	0	0.02	0.4	0.4
	Fixed (mm/s)	4.5	3.5	1.0	0.5
Pointing (per axis)	Proportional (mrad)	1.1	1.0	9.0	4.5
	Fixed (mm/s)	3.0	5.0	0	0

The D3/T79 double-flyby was successful. The second flyby body, T79, was targeted and was 3 km lower than nominal. The Dione altitude was 1 km higher than nominal.

Both distant Enceladus plume occultations were successful. Each was a stellar occultation. Both ϵ and ξ Orionis were occulted in the 2011 observation, and ϵ Orionis was occulted in the 2016 observation.

4.3.2 Notable Events

The sixth and final spacecraft safing occurred on November 2, 2010, six days before the T73 approach maneuver (OTM-265), when a command file sent to the spacecraft was corrupted and caused a Command and Data Subsystem fault. OTM-265 wind and unwind turns were performed in RCS instead of RWA mode because recovery efforts were not complete at the time of the burn. The spacecraft remained at the safing attitude with no sequence executing during the T73 flyby and no science data was taken. OTM-266, the T73 cleanup maneuver, was unneeded and canceled. OTM-267 was executed while the background sequence was deactivated. Upon completion of the burn, the nominal ME command block transitioned the spacecraft back to RWA mode. The spacecraft remained Earth-pointed until the background sequence was activated on November 24, 2010. This safing imparted approximately 35 mm/s of unplanned ΔV to Cassini.

Due to declining support for JPL's legacy navigation software and to ensure Cassini navigators would have the needed skills to work on other missions, the navigation team began using MONTE

operationally at the end of 2011. The python and C++ based MONTE software replaced the legacy software set—the Fortran-based DPRTAJ/ODP and MOPS. OTM-306 was the first maneuver to be based on the new software. The transition was preceded with an extensive two-year development, test, and checkout period in which MONTE was run in parallel with legacy software, ensuring all needed capabilities were available and functioning correctly.

An additional maneuver was inserted to the long transfer between T125 and T126, the F-ring orbits. Originally, only the T125 cleanup maneuver (OTM-467), the shaping maneuver (OTM-468), and the T126 approach maneuver (OTM-469) were scheduled during this nearly five-month transfer. A four-month interval existed between OTM-468 on December 24, 2016, and OTM-469 on April 18, 2017. When OTM-467 was designed, command sequences had not yet been built for the latter portion of the interval and spacecraft attitude and small force prediction files were unavailable. OTM-468a was added and would execute on February 22, 2017, to compensate for the initially unmodeled activity. By doing so, OTM-469 would remain small, and the T126 incoming asymptote would be better aligned with the reference trajectory. Not only would downstream ΔV costs be reduced, but trajectory dispersions between T125 and EOM would be significantly reduced. Dispersions between T125 and the third periapsis after T126 would be reduced by up to 2000 km and dispersions between the third periapsis after T126 and Saturn atmospheric entry would be reduced by over 100 km. The smaller dispersions would alleviate the need for late command sequence updates, and the associated workforce that would be required to build them.

The F-ring orbits offered some of the best opportunities to observe Saturn’s inner satellites. Because of their low masses, the dynamical effects of their gravitational perturbation on Cassini were not normally modeled. A nontargeted 3567 km altitude flyby of Epimetheus on January 30, 2017, however, imparted a noticeable signature into Cassini’s Doppler data. This signature was easily removed once the source was identified by adding a nominal model of Epimetheus’ orbit and mass. Another close flyby, with altitude of 8030 km, occurred three weeks later on February 21. An 8997 km altitude flyby of Janus occurred on April 12, necessitating the modeling of its orbit and mass as well [56].

4.4 Tour Synopsis

The Cassini tour included 160 targeted encounters in 294 revs about Saturn in the 13 years, 2.5 months from SOI to Saturn atmospheric entry. Targeted encounters included 127 of Titan, 22 of Enceladus, five of Dione, four of Rhea, and one each of Hyperion and Iapetus. Huygens probe data during its descent through Titan’s atmosphere and subsequent landing was successfully relayed to Earth via Cassini during the third Titan flyby.

The average navigation cost per flyby for the entire tour was about 0.27 m/s and the total navigation cost was about 43 m/s. Once again, navigation cost is defined as the ΔV usage above the deterministic amount from the reference trajectory. A plot of the accumulated navigation cost is shown in Figure 4-17, starting at E1. Prior to E1, deterministic ΔV usage is high and is not representative of the rest of tour. There were only two exceptions to the excellent maneuver performance during the Saturn tour—OTM-145 and OTM-169. OTM-145 was a ME burn near the end of prime mission. It was the final approach maneuver targeted to the low 1000 km altitude T41 flyby. The use of the ME for the final approach maneuver proved costly as the larger execution errors associated with the burn translated into a nearly 5 km miss at T41 and 3 m/s downstream

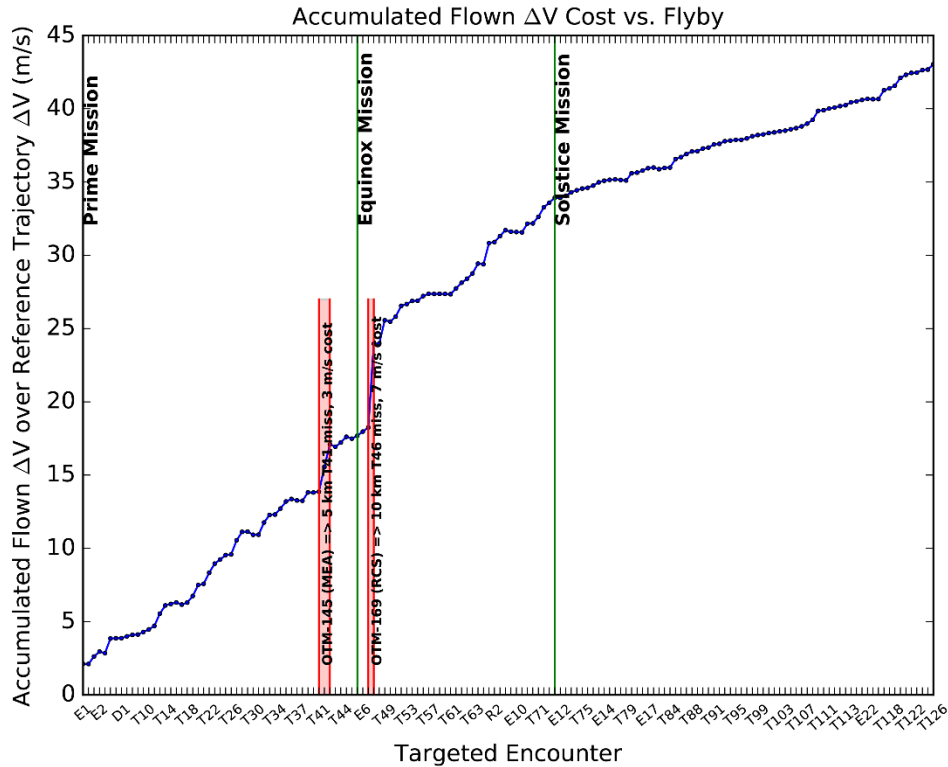


Figure 4-17. Accumulated ΔV Cost for Cassini Tour.

ΔV penalty. OTM-169, the approach maneuver targeting T46, was an RCS maneuver performed near the beginning of Equinox Mission. With a large ΔV of 0.23 m/s, it significantly underperformed and yielded a 10 km miss at T46 and 7 m/s downstream ΔV penalty. The underperformance was due to the degradation of the RCS A-branch thrusters.

Based on maneuver reconstructions, Cassini's 13-year orbital tour was conducted with a ΔV cost of 1113.0 m/s. This value includes PRM but does not include 626.8 m/s from SOL. Cumulative ME ΔV was 1099.4 m/s and RCS maneuver ΔV was 13.6 m/s. Predicted mean ΔV usage was provided in the Navigation Plans for each of the prime and extended missions. Adding the means from each yields a value of 1256 m/s so that actual usage was about 11% lower than predicted. Reasons for actual usage being lower than predicted include use of a conservative maneuver execution error model before being updated with operational data and use of a floor for the minimum OD error at each targeted flyby when performing linearized maneuver analyses.

5 In-Flight Adaptations

In the nearly two decades of Cassini flight, adaptations to navigation processes were applied as characteristics unique to Cassini were identified and spacecraft configuration changes were implemented. Additionally, operational experience was leveraged into more efficient processes, better modeling, and more robust contingency strategies. Trajectory adjustments were implemented to allow further investigation of surprising science discoveries meriting more attention and unique analyses were performed to determine how to best accomplish atypical science observations while maintaining acceptable risk levels.

Now that the mission is over, a description of several operational adaptations and key mission aspects are provided from launch to Saturn atmospheric entry. Future planetary system tour missions in the planning stages may draw upon this material to gain an understanding of the challenges and expectations ahead of them.

5.1 *Trajectory Design Adaptations*

Whereas every reference trajectory update was a trajectory adaptation, some updates deviated from their predecessors more than others. The largest and most consequential deviation was due to the Huygens probe mission redesign, and that was discussed previously in Section 4.1.1. This section will look at two updates benefiting science observations. The first enabled the only close flyby of the satellite Tethys, and the second added an observation that would help unravel the mystery of Enceladus' plumes.

5.1.1 Tethys Close Flyby

The 050505 reference trajectory update lowered a nontargeted 29,800 km altitude Tethys flyby to 1500 km, thereby enabling the only Tethys targeted-quality observations. Whereas the average ΔV cost for targeted icy satellite encounters was 18 m/s in prime mission, only 7.6 m/s of ΔV was ultimately needed to implement these unique observations. Lowering the subsequent Hyperion targeted encounter altitude from 1010 to 510 km and modestly changing its B-plane angle reduced ΔV costs while increasing H1 science resolution and quality. Further ΔV cost reductions were realized by moving a downstream energy correction maneuver, OTM-038, eleven hours closer to Saturn periapsis. At Tethys on September 24, 2005, Cassini flew over Ithaca Chasma and investigated Tethys' subsurface properties. Figure 5-1 shows how the Tethys ground track changed with flyby altitude. Trajectory changes in 050505 were confined from E2 to R1.

5.1.2 Enceladus Plume Occultation

The 140114 reference trajectory update enabled a March 11, 2016 stellar occultation by Enceladus' plume near the satellite's southern pole. This high-priority science investigation complemented previous Enceladus plume occultation observations because it was the first and only to be observed near Enceladus' apoapsis: the five previous observations all occurred when Enceladus was closer to periapsis. The latest observation would help scientists determine if water vapor flow was modulated diurnally, similar to ice particles [57]. The ΔV cost of adding this observation was less than 1 m/s and accepted by the Cassini project, even though this observation was near the EOM and propellant margins were small. Figure 5-2 shows how Cassini's trajectory was changed as viewed from ϵ Orionis, the occulted star. Significant trajectory changes to enable this observation began at T115, three targeted flybys before the occultation. Trajectory changes continued to the

last targeted flyby, T126, but for the additional reason of setting up the correct asymptote to link to the Grand Finale, the final 22 short-period orbits before Saturn atmospheric entry.

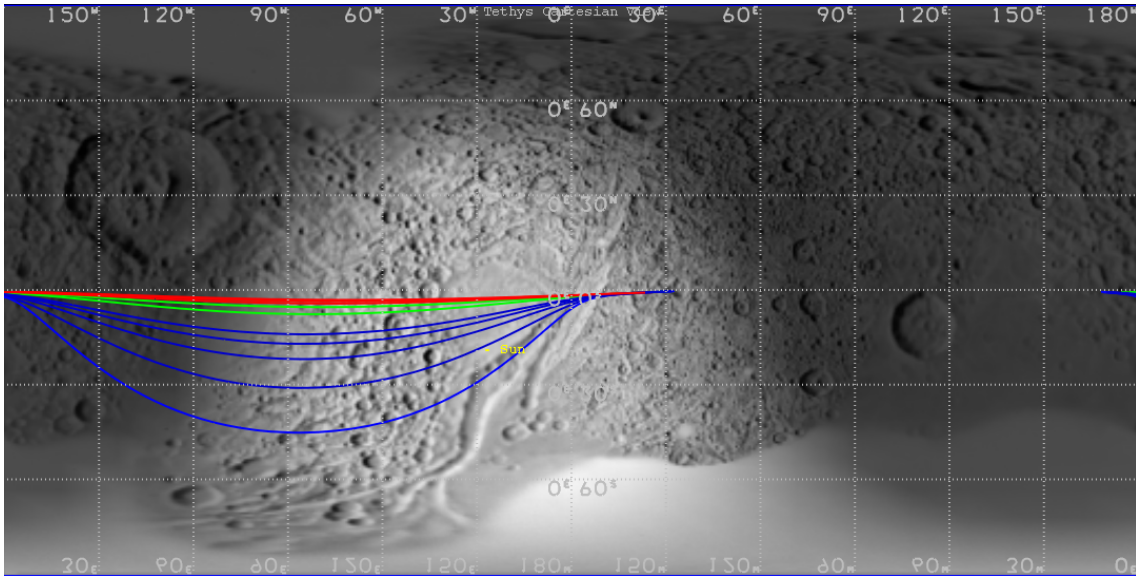


Figure 5-1. Tethys ground tracks for varying flyby altitudes. **Blue:** 1000–5000 km, **Green:** 10,000–20,000 km, **Red:** 20,000–30,000 km.

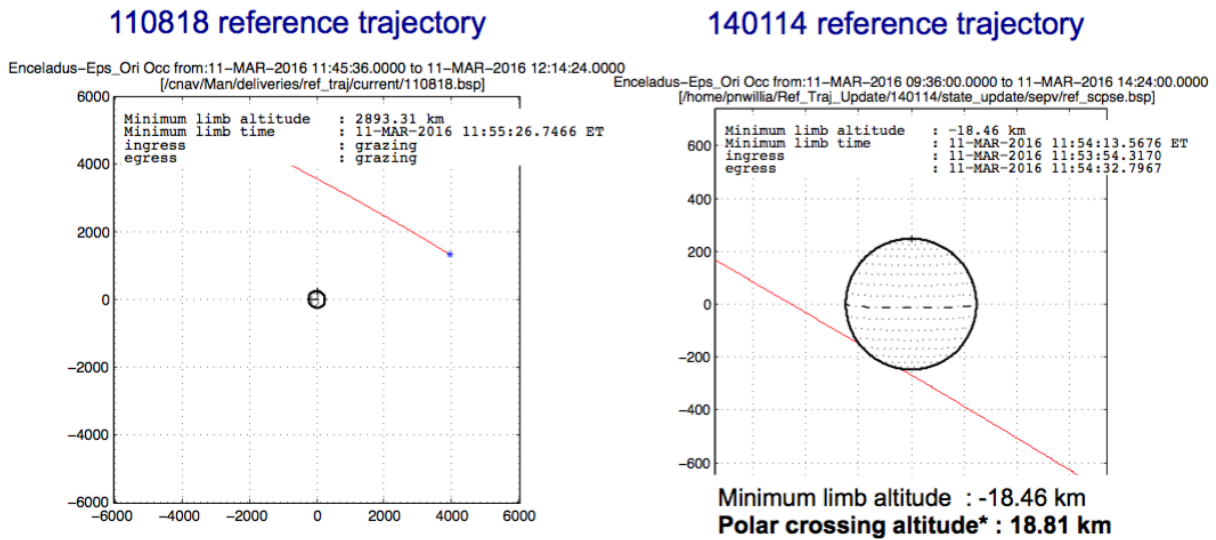


Figure 5-2. Enceladus plume occultation as viewed from ϵ Orion, before and after reference trajectory update.

5.2 Orbit Determination Adaptations

Many of the changes implemented in OD were in response to changes in the spacecraft's operational environment and processes. During the inner cruise, when the spacecraft was close to the Sun, the spacecraft's HGA was used as a solar shade and excursions from a HGA-to-Sun

pointed attitude were small and infrequent. Attitude control was maintained with thrusters. Emphasis was focused on creating adequate non-gravitational force models for solar pressure and asymmetric thermal radiation (induced by the spacecraft's power source). Direct and indirect solar and thermal forces were imparted to the spacecraft, with indirect forces imparted by thruster firings that countered torques from the direct forces. Predictions for ΔV s resulting from engineering maintenance activities were not available, nor were accurate reconstructions from telemetry. In short, there were many nongravitational forces acting on the spacecraft during the inner cruise and, with only two tracking passes scheduled per week on average, it was difficult to accurately resolve them. This was not a cause for concern, however, because trajectory accuracy requirements were generally not as demanding as they were later during Saturn orbital operations.

During outer cruise and orbital operations, nongravitational forces were more accurately resolved. Solar pressure and thermal radiation induced indirect forces disappeared as attitude control defaulted to reaction wheels instead of thrusters. Solar pressure direct forces were reduced by two orders of magnitude as the distance from the Sun increased. Thermal radiation forces were exceptionally well determined during three GWEs conducted near solar oppositions between the Jupiter flyby and Saturn approach. In each of these experiments, the spacecraft remained quiescent and Earth-pointed for several weeks while tracking data was collected continuously. The resulting thermal radiation force estimate was the basis for future thermal force modeling through the end of orbital operations. Modeling of thruster firings also improved when attitude became controlled by the reaction wheels. Thruster activity became more discretized, with thruster firings for momentum management needed every few days. In thruster attitude control mode, thruster firings for deadband limiting occurred every couple of hours.

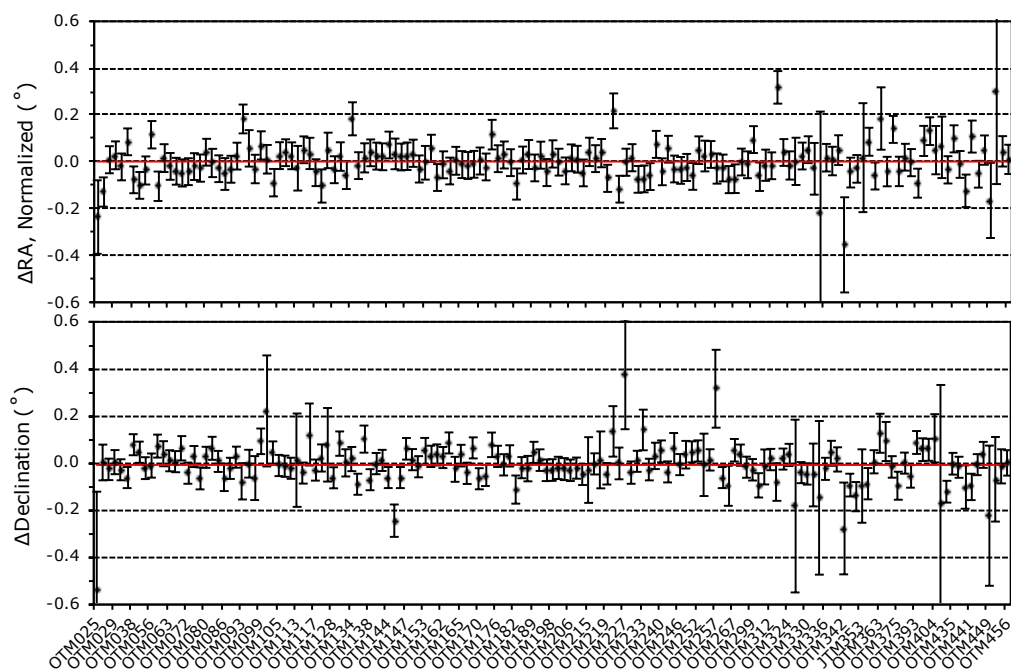
The following subsections discuss two adaptations developed by OD analysts. The first, use of ΔV telemetry, enabled orbit estimates to converge more quickly after maneuver executions. The second, Y-thruster calibrations, was the navigation team's method of monitoring the RCS B-branch thrusters after use of the degraded A-branch was discontinued.

5.2.1 Use of ΔV Telemetry

After successful completion of the Huygens probe mission and at the urging of the navigation team, Cassini spacecraft operators agreed to increase the resolution of telemetered, time-tagged, onboard ΔV computations from spacecraft thrust events. Resolution was increased from 2 to 0.04 mm/s and navigators began including this information in the implementation of dynamical models and in the initialization of filter parameters used in the estimation process.

The primary benefit of telemetry to navigation was rapid convergence of OD after maneuver executions and improved modeling of satellite flybys conducted in thruster mode. Before reaping these benefits, however, its accuracy had to be established. Accuracy estimates were obtained by comparing telemetry computations to navigation team reconstructions of ΔV activity. References [58] and [59] describe the calibration and evaluation process and provide early orbital mission estimates of the accuracy of maneuver pointing angles derived from telemetry. Maneuver pointing accuracies were provided for each of the two Cassini propulsive systems, an ME system for maneuvers larger than 250 mm/s and an RCS for smaller maneuvers. This evaluation was completed near the end of prime mission, when 56 ME samples and 35 RCS were available. By end of orbital operations, the number of ME samples had nearly tripled, to 152 samples, and the number of RCS samples had nearly quintupled, to 169 samples. Figures 5-3 and 5-4 show differences between

navigation reconstructions and telemetry derived computations of maneuver pointing with one-sigma uncertainty bars composed of the root sum square (RSS) of uncertainties from reconstructions and telemetry. Outliers are currently under investigation. Red lines show the mean error. Cumulative distribution functions (CDFs) resulting from all ME samples and all RCS samples are provided in Figure 5-5. Figures 5-3 through 5-5 are updates of the tables in Reference [58].



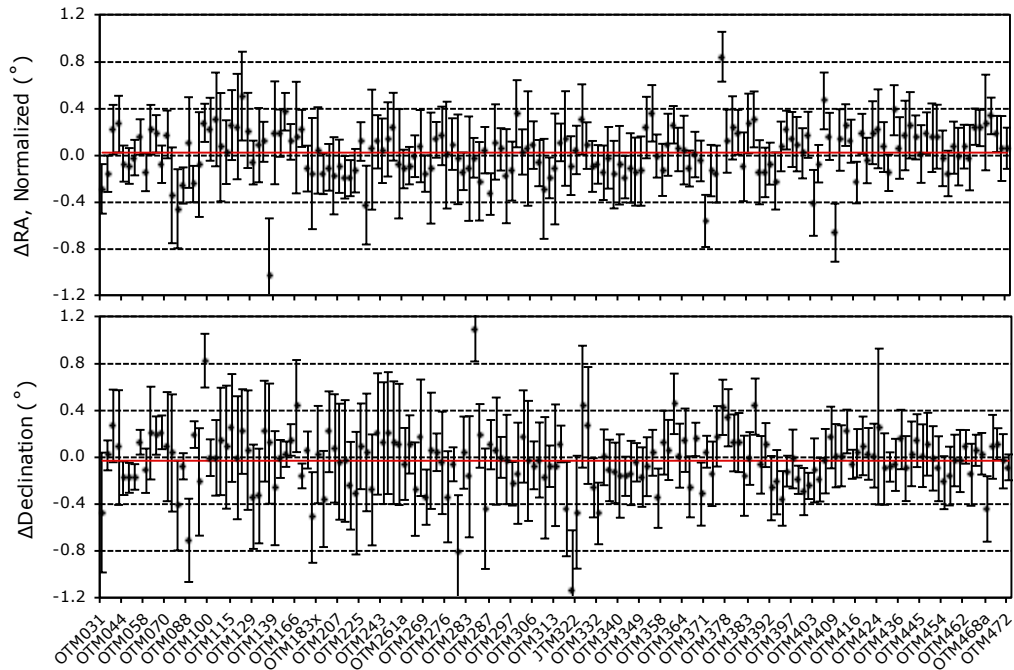


Figure 5-4. RCS Maneuver ΔV differences—Navigation reconstruction minus telemetry computations.

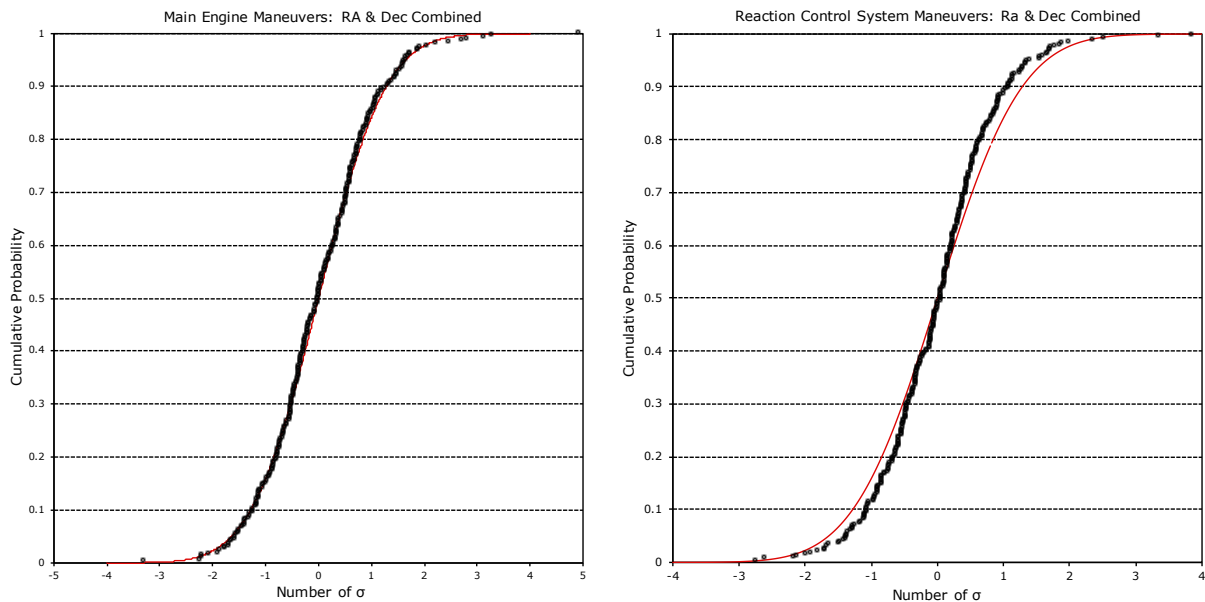


Figure 5-5. Cumulative probability of ME (left) and RCS maneuver errors.

5.2.2 Y-Thruster Calibrations

Navigators noticed after executing OTM-169 (the E6/T46 approach maneuver in October 2008) that the burn magnitude was 2.2 sigma lower than anticipated. Upon further investigation, the project determined that two of eight A-branch RCS thrusters were severely degraded and began making preparations to swap to the redundant B-branch. The leading theory for cause of the

degradation was related to propellant throughput, and an effort was made to more evenly distribute propellant through the B-branch thrusters. The project also began monitoring the thrusters more closely for future signs of degradation. The four uncoupled Z-facing thrusters were used routinely for RCS maneuvers and a degradation in one of them would become apparent as a change in thruster duty cycle. Monitoring the four coupled Y-facing thrusters would require additional attention. As part of the monitoring, the project adopted an annual calibration test of the Y-thrusters. A sign of degradation in the Y-thrusters would appear as less well coupled thrusters.

Cassini's Z-thrusters were used for RCS maneuvers and attitude control about the spacecraft's X- and Y-axes. The Y-thrusters were used for attitude control about the spacecraft's Z-axis. A schematic showing ΔV directions imparted by each thruster and a diagram of the RCS thruster locations on Cassini are shown in Figure 1-1 and Figure 1-2.

Each Y-thruster calibration began with a quiescent spacecraft—HGA pointed at Earth and collecting Doppler tracking data. After at least an hour of coherent Doppler data was acquired, reaction wheels were used to yaw Cassini 90° and align its $-Y$ -axis and Y-thrusters toward the Earth-line. Tracking was interrupted because the HGA was no longer pointed toward Earth. Reaction wheels were then spun up in a manner to change angular momentum only along the spacecraft Z-axis, causing one of the Y-thruster couples (Y2 and Y4, or Y1 and Y3) to begin firing. The calibration was designed to spin up reaction wheels as much as possible without ever exceeding operationally safe limits. This produced the most thruster firings and largest ΔV . Ideally, for perfectly coupled thrusters, no ΔV would be imparted to the spacecraft. When complete, the spacecraft yawed -90° back to Earth point and at least one more hour of coherent Doppler data was acquired. The spacecraft then repeated this process, but reversed the wheel spin up direction, causing the other Y-thruster couple to fire. When complete and the HGA was returned to Earth point, wheel speeds would be the same as at the calibration start, and each set of Y-thruster couple firings was bracketed by coherent Doppler data. This tracking data could then be used to determine the ΔV imparted to Cassini from each couple and hence the mismatch within each couple.

Seven calibrations were performed between the OTM-169 anomaly and Saturn atmospheric entry. One could not be evaluated because a tracking station hardware malfunction prevented acquisition of tracking data. Results from the remaining six [61-65] are shown in Figure 5-6. Thruster mismatch remained below 2.5% for each couple in each test, even when accounting for the one-sigma error bars. An initial upward trend in the Y1/Y3 couple caused some concern, but later reversed itself. Ultimately, no degradation was detected in the Y-thrusters.

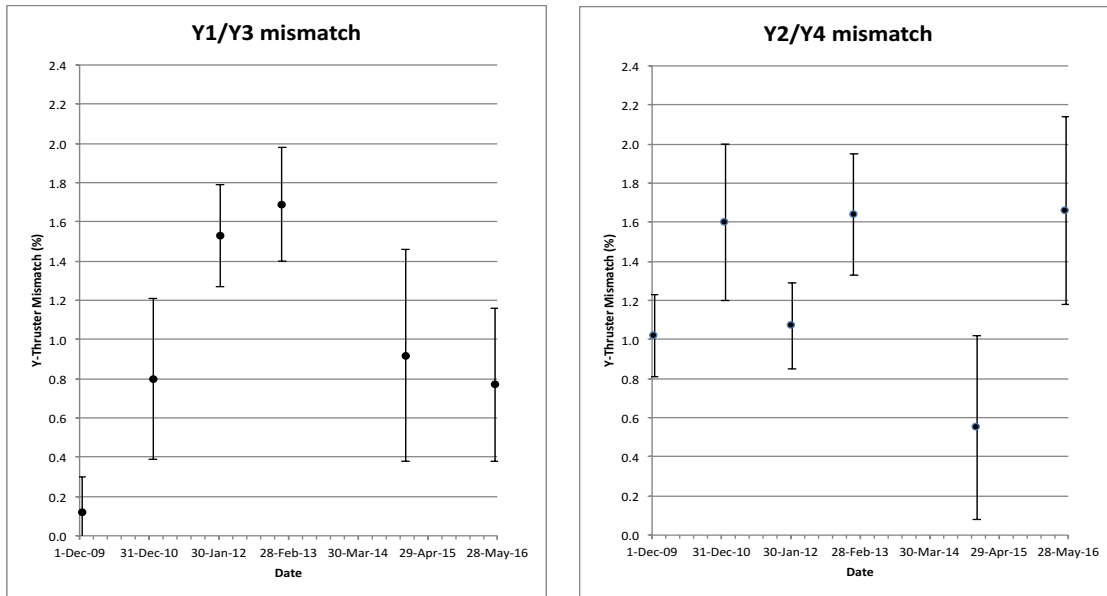


Figure 5-6. Thruster mismatch determined from each Y-thruster calibration.

5.3 Optical Navigation Adaptations

Initially, Cassini was commanded to image multiple satellites immediately before and after most downlink periods. Images were placed in the critical playback partition in Cassini's Solid-State Recorder (SSR) for immediate playback at the start of the next downlink period. During this period of the mission, OPNAVs made significant improvements in the OD process and the latest images were desired to produce the best ephemeris for use in maneuver designs and onboard ephemeris updates. OPNAVs were acquired at the average rate of approximately three images per day through October 2005. From this date through July 2009, nearly halfway through the Equinox extended mission, an average of only four images per week was needed because the satellite ephemeris and Saturnian system parameters (masses, poles, and gravity fields) were markedly improved.

Eventually, ephemeris accuracies obtained through radiometric sensing of the satellite gravitational signature from multiple satellite close flybys surpassed that from OPNAVs. Repeated flybys of Titan, the engine of Cassini's tour, kept Titan's ephemeris in check. Titan OPNAVs, the least accurate because Titan's thick atmosphere prevented its center from being well determined, quickly became unnecessary and were not targeted after April 2006. Hyperion OPNAVs also posed a center-finding challenge because of the satellite's non-spherical shape and chaotic rotation, but they continued to be targeted because of the scarcity of close flybys. Close flybys of the other satellites with significant masses (Mimas, Enceladus, Tethys, Dione, Rhea, and Iapetus) were also less frequent, and OPNAVs of these satellites continued to be necessary, albeit at a low rate, to prevent runoff in the along-track direction due to errors in mean motion. A small number of high value images was carefully selected to accomplish this goal. From July 2009 until September 20, 2016, the date of Cassini's last opnav, OPNAVs were acquired at the rate of 1.1 images per month. Each of the images was selected to reveal position errors in the satellite's along-track direction—the minimum angle between the satellite's Saturn relative velocity and Cassini-satellite line-of-

sight direction was 60° (50° for Iapetus). It was not necessary to place any of these OPNAVs in the SSR's critical playback partition.

5.4 Maneuver Design Adaptations

Pre-Mission statistical maneuver analyses were conducted to determine mean, one-sigma, and 90% or 95% ΔV s for individual maneuvers and the entire mission assuming each prime maneuver was executed. Maneuvers were often canceled in-flight operations however, and sometimes a backup maneuver would be performed instead of a prime maneuver. For these reasons, the statistical analysis for each transfer was updated just prior to entering that transfer based on the latest trajectory information.

During the design of each maneuver in operations, prime, backup, and cancellation opportunities were examined in parallel, with the downstream deterministic cost of each scenario compared. Downstream deterministic costs were determined for maneuvers in three or four additional transfers, by which time the trajectory would normally reconverge to the reference. On rare occasions for backup maneuvers incurring significant ΔV costs, the trajectory might not reconverge in this timeframe, but these high-cost backups were analyzed in previous studies to identify mitigation strategies. Maneuver cancellation scenarios resulting in a trajectory that did not reconverge within this timeframe were not viable cancellation candidates.

5.4.1 Target Biasing

Generally, flyby targets changed only as a result of reference trajectory updates. After nearly three years in orbit, however, the Saturn system was well characterized and OD estimates converged more quickly and accurately. Predicted ΔV s from attitude control activities were improved, thereby improving predictions of Cassini's orbit. Maneuver execution errors were reduced, thereby reducing downstream orbit dispersions. As a result, it occasionally became necessary or advantageous to bias the target.

Target biases were sometimes necessary in order to reduce target errors. As trajectory models improved and maneuver execution errors were reduced, trajectory control improved. Errors remaining after the shaping maneuver were sometimes too small to be corrected with the approach maneuver because the required ΔV was less than the smallest realizable maneuver (15.8 mm/s) allowed by project management. Canceling the maneuver and leaving the target errors uncorrected could have downstream ΔV cost consequences of up to one hundred times larger than the cost of the desired approach maneuver. To avoid large downstream ΔV costs, the two spatial B-plane target components were left unchanged, and the time of closest approach was biased from the reference enough to achieve the minimum allowable maneuver magnitude. By doing so, the desired gravity assist ΔV would be obtained at a slightly earlier or later time with little impact to downstream costs.

An example of implementing a time bias is provided by OTM-409, the T111 approach maneuver. The initial maneuver design had a magnitude of 6 mm/s, much smaller than the minimum allowed value of 15.8 mm/s. It would make a correction of 1.2 km in the B-plane and -0.4 seconds in time of closest approach. The downstream cost of canceling this maneuver was found to be approximately 440 mm/s, seventy times larger than the magnitude of the initial design. A simple linearized analysis was performed to prepare Figure 5-7 from which was concluded that the bias must be either at least 0.62 seconds earlier or 1.11 seconds later than nominal. Usually, the smaller of the two biases was chosen, but reaction wheel speed considerations sometimes made the larger value more desirable. In this case, the target time was biased 0.7 seconds earlier, and the downstream cost was only 40 mm/s, saving 400 mm/s over the cancellation scenario.

Target biases were sometimes advantageous to reduce downstream ΔV costs. The cumulative effect of small modeling errors and canceled maneuvers caused the operational trajectory to deviate from the reference over time. Eventually, the deviations would become large enough that future reference trajectory targets were noticeably non-optimal, increasing ΔV costs. This effect could be corrected by occasionally introducing a small bias to the target's spatial components, B·R and B·T, leveraging the gravity assist to steer the actual trajectory back toward the reference trajectory.

An example of implementing a B-plane bias is provided by OTM-460, the T123 approach maneuver. The initial maneuver design to the flyby target defined in the reference trajectory was 6.8 mm/s, again too small to perform. In this case, however, a time bias was not necessary. A contour plot (Figure 5-8) showing downstream ΔV cost increases as a function of B-plane targets clearly shows that the target from the reference trajectory, the red +, is not optimal. Choosing the optimal B-plane target instead increased the maneuver size to 24.5 mm/s and decreased the downstream cost by 350 mm/s. In this figure, the blue + and ellipse represent the current OD estimate with one-sigma uncertainty. The black + and ellipse represents the optimal target and one-

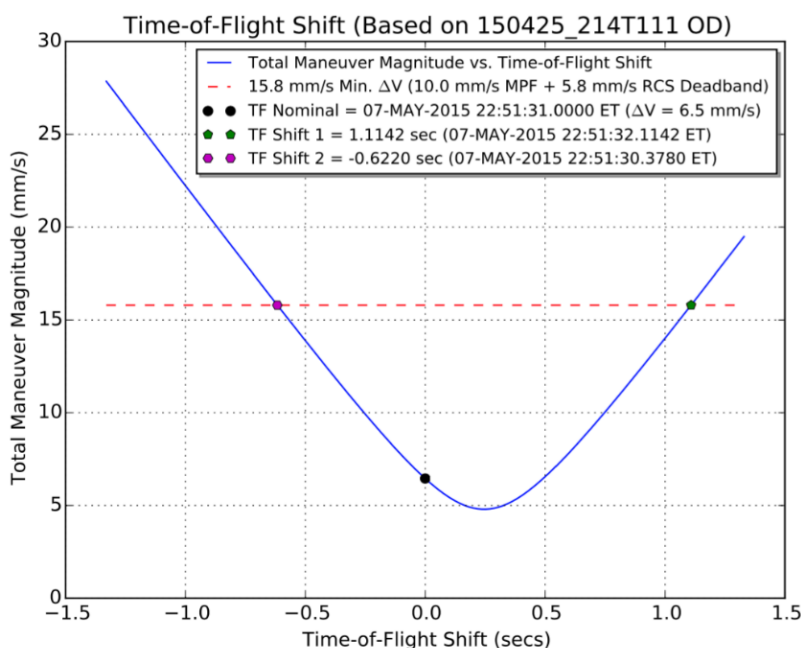


Figure 5-7. OTM-409 target time bias versus ΔV cost.

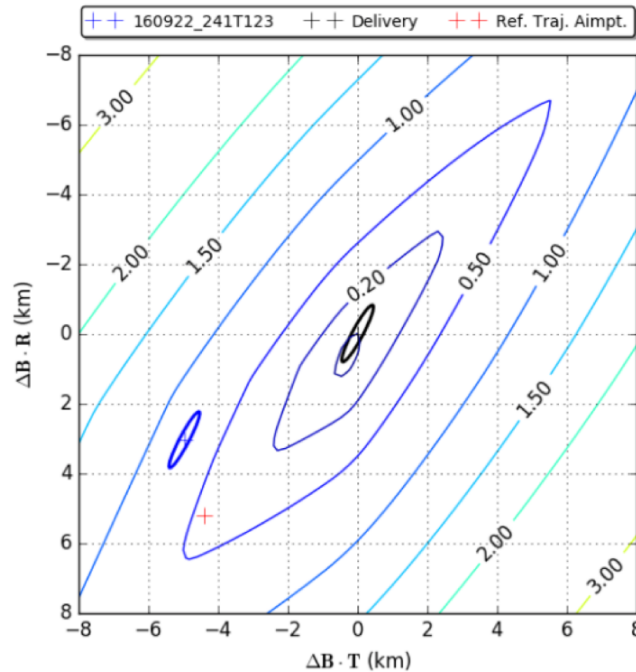


Figure 5-8. OTM-460 downstream ΔV cost contours.

sigma delivery uncertainty. The black + is not centered within the smallest cost contour because the contour plot is based on a linear analysis. If, during the maneuver design process, the contour plots show an advantage by biasing the B-plane target, a second analysis is undertaken to find the true optimal target.

Contour plots were originally developed to determine the likelihood of canceling a maneuver [66], which is another way of introducing a target bias. The cost of canceling a maneuver was deduced by determining which contours are crossed by the OD solution. In Figure 5-8, the orbit estimate error ellipse runs parallel to the cost contours, so the cost of canceling OTM-460 could be confidently determined as 700 mm/s. The shape, size, and orientation of OD error ellipses as a function of DCO were determined by covariance analyses before the start of a particular transfer. Superimposing the ellipse from the final DCO onto the target point provides an early estimate of the range of expected downstream costs if the maneuver were to be performed.

In total, 15 flybys were targeted with time biases. The first time-biased target was implemented with OTM-106 at the T29 flyby. The first of 14 B-plane biases was implemented at the following flyby, T30, with OTM-109 [67]. Before project approval of any target bias, a preliminary trajectory including the bias was provided to science planners. Planners would use it to evaluate the effect of the bias on their observations. Usually, these biases were small enough to have no significant effect on the observations. On rare occasions when a bias did impact observations, however, three options were considered and discussed: remove the bias and pay the resulting ΔV cost, keep the bias and degrade the science, or keep the bias and update the sequence to maintain the full integrity of the observation. Of course, the third option was always preferred if possible after considering workforce and time constraints.

5.4.2 Backup Maneuver Scheduling

Statistical analyses were not generally conducted for backup maneuvers because of the large number of possible permutations and because ΔV costs for backup maneuvers scheduled 24 hours after the prime were generally expected to remain viable. Navigators discovered two scenarios however, that caused backup maneuver costs to grow considerably larger than if the prime maneuver were implemented.

The first backup maneuver scenario leading to large ΔV growth was identified during early operational designs of OTM-159. This maneuver had a large deterministic cost of 12 m/s and would execute less than two hours before periapsis. The backup opportunity, only nine hours after the prime, cost 33 m/s, almost three times more than the prime. Additionally, downstream ΔV costs required to remain near the reference trajectory increased dramatically, such that the total cost became 97 m/s and was prohibitively large. To reduce the risk of needing to perform the backup OTM-159, ground controllers sent maneuver commands to Cassini three days before the planned maneuver execution and confirmed that they were received and registered onboard the spacecraft. Normally, maneuver commands were sent only six hours before maneuver execution so that OD errors were minimized. If a ground antenna was experiencing difficulties and was unable to send commands, commanding would be delayed until the beginning of the next track and the backup maneuver would be implemented. Had the prime OTM-159 maneuver opportunity been missed, navigators had developed backup scenarios that reduced the total cost from 97 m/s to as little as 8 m/s. However, these scenarios significantly altered as many as six of the next seven Titan flybys and removed E6, a 200-km Enceladus flyby, altogether. Science return would be degraded and diminished, and a significant command sequence update effort would be needed to recover the best science observations.

Shortly after the OTM-159 prime maneuver was successfully executed, navigators examined the remaining set of currently existing maneuvers to identify any similar future instances of a large deterministic maneuver near periapsis. Four were found in Equinox Mission: OTM-168, -170, -180, and -183. Two years later, with a reference trajectory for Solstice Mission available, three more were identified: OTM-261, -300, and -312. An analysis of the backup maneuver for each of these maneuvers was conducted. In every case except OTM-168, maneuver commands were sent to the spacecraft early to ensure that the prime maneuver would be executed. Backup maneuver scenarios were investigated and, as with OTM-159, each required significant changes to downstream targets before the backup opportunity became viable. The backup scenario for OTM-168 was not as extreme as the other scenarios, with downstream costs growing to only 4.3 m/s. There were only three tracks between OTM-168 and the preceding OTM-167, so sending maneuver commands early risked basing the maneuver design on a poorly converged orbit estimate. Instead, an additional tracking station was placed on standby, ready to send prime maneuver commands if there were a transmitter problem with the primary station. Also, backup maneuver commanding, if necessary, would be performed at a different DSN complex to mitigate the very unlikely risk that an entire complex was down for the prime maneuver and could not be brought back up in time to send backup maneuver commands.

The second backup maneuver scenario leading to large ΔV growth was identified during early operational designs of OTM-268. In this case, the backup maneuver was nearly singular with central angle travel to the E12 target of 179.3° . Because of the near singularity, ΔV gradients for each of the target parameters became nearly aligned, causing a large ΔV to be needed in one

direction to make a small correction in one of the target parameters. Whereas the cost of prime maneuver was only 65 mm/s and could be accurately performed via the RCS thrusters, the backup maneuver grew nearly an order of magnitude to 580 mm/s and, unless mitigated, would be executed less accurately on the MEA. Making matters worse, the target was a low 50 km altitude flyby of Enceladus. An accurate flyby was especially important because of the high visibility associated with it. To mitigate the backup maneuver cost, one of three targeted parameters, B·R, was allowed to float, or miss the target, by a controlled amount. By allowing B·R to miss the target by -0.5 km, the backup maneuver cost was reduced from 580 mm/s to only 115 mm/s and the -0.5 km float was insignificant compared to the one-sigma 2.7 km OD uncertainty.

Navigators were confident that future n-pi transfers could be dealt with similarly. The experience gained from OTM-268 would allow them to quickly recognize future incidents in-flight operations. For these reasons and because backup maneuvers were rarely needed, a preemptive examination of all maneuvers to identify and flag future n-pi transfers was deemed unnecessary.

5.5 Software Adaptations

As with any other operational project, navigators developed numerous scripts to assist with the more mundane tasks of planning, estimating, and controlling Cassini's trajectory. Two software sets were especially notable however, for their breadth and impact on navigation operations: the Maneuver Automation Software (MAS), and MONTE. The transition to MONTE was discussed previously in Section 4.3.2. A third software tool, MONTE-MOPS, generated a report for each maneuver design. This report was notable for providing information from which key navigation decisions were made.

MAS was developed during cruise operations for use in tour to address the need for a faster maneuver design and implementation process. With only 24 maneuvers scheduled in the nearly seven years of interplanetary cruise, a speedy process was not of critical importance. The typical process starting from the availability of the final OD solution and ending with the availability of ready-for-uplink maneuver commands typically lasted five days. During tour operations, this changed. A typical Titan-to-Titan transfer would require three maneuvers in sixteen days, and the final OD solution required sufficient time to reconverge the orbit after the perturbation from the previous maneuver. The clean-up maneuver would be the most demanding. To keep ΔV costs low, the maneuver was typically scheduled three days after the targeted flyby, and the first two days after were needed to reconverge the orbit estimate. This could leave less than 24 hours for design, implementation, and uplink of the maneuver.

MAS shortened this process from five days to as little as five hours. Files not dependent on the final orbit estimate were prepared in advance. Each subsystem was responsible for configuring their portion of the software within MAS but, once configured, interfaces between each subsystem were automated. MAS would perform all of the necessary checks and provide a report at the end of the process with the result of each check. This report would be reviewed and, as appropriate, approved by all teams before uplink to the spacecraft. Once properly configured, intermediate MAS runs could easily be performed as the day-to-day OD solution changed. These intermediate runs were important for addressing failed checks or other problems and ensured that the final run would successfully complete with a set of commands to execute the desired maneuver.

As the mission progressed, maneuver presentations for project reviews evolved to encompass designs for the prime, backup, cancellation, and alternate maneuvers. MONTE-MOPS was

augmented to automatically assemble a comprehensive presentation package consisting of the prime and backup design history, comparisons of ΔV costs, and trajectory deviation plots. This report generation tool was essential for providing information needed for making informed decisions regarding various maneuver options.

6 Conclusion

The Cassini spacecraft was accurately navigated from launch to EOM, an interval spanning nearly two decades. The navigation team performed splendidly, meeting all their requirements and enabling two successful extended missions. The Cassini Mission ended as the spacecraft entered Saturn's atmosphere and drag torques overcame the control authority of Cassini's attitude control thrusters. In a fitting conclusion, Cassini sent science, telemetry, and coherent tracking data to ground controllers on Earth until the very end—when the HGA could no longer be held on Earth-point.

Knowledge gained of Saturn and its satellites may be used by future projects, and the techniques developed by Cassini navigators will be used by other projects as well.

7 References

- [1] JPL DSN 810-005, “DSN Telecommunications Link Design Handbook,” *Release 42 for DSN Document 810-005*, May 3 2017.
- [2] W. M. Folkner. (1994, March 1) Effect of uncalibrated charged particles on Doppler tracking. *JPL IOM 335.1-94-005*.
- [3] P. G. Antreasian *et al.*, “Cassini Orbit Determination Performance During the First Eight Orbits of the Saturn Satellite Tour,” in *AAS Paper 05-312, Astrodynamics Specialist Conference*, Lake Tahoe, CA, 2005: American Astronautical Society.
- [4] D. L. Jones *et al.*, “Astrometry Of Cassini With The VLBA To Improve The Saturn Ephemeris,” (in English), *Astronomical Journal*, Article vol. 149, no. 1, p. 28, Jan 2015, Art no. 28, doi: <http://dx.doi.org/10.1088/0004-6256/149/1/28>.
- [5] D. Jones, W. Folkner, J. Romney, and E. Fomalont, “A Decade of Astrometric Observations of Cassini: Past Results and Future Prospects,” in *2017 IEEE Aerospace Conference*, Big Sky, MT, 2017: IEEE.
- [6] K. Criddle *et al.*, “Optical Navigation Through Cassini’s Solstice Mission,” in *AAS Paper 17-625, AAS/AIAA Astrodynamics Specialist Conference*, Stevenson, WA, 2017: American Astronomical Society.
- [7] S. D. Gillam *et al.*, “Optical Navigation for the Cassini/Huygens Mission,” in *AAS Paper 07-252, AAS/AIAA Astrodynamics Specialist Conference*, Mackinac Island, MI, 2007: American Astronautical Society.
- [8] JPL D-11621, “Cassini Navigation Plan,” *699-101 Final, JPL D-11621*, May 29 1996.
- [9] NPR 8020.12B. (1995) NPR 8020.12B: Planetary Protection Provisions for Robotic Extraterrestrial Missions (Final Review Draft).
- [10] NPR 8020.12B. (1999, April) NPR 8020.12B: Planetary Protection Provisions for Robotic Extraterrestrial Missions.
- [11] J. D. Rummel, “NASA letter to R. F. Draper identifying Cassini Mission as Category II and specifying basic requirements,” ed, 1990.
- [12] JPL D-10178-3, “Cassini Program Environmental Impact Statement Supporting Study Volume 3: Cassini Earth Swingby Plan,” *699-70-3, JPL D-10178-3*, 11 18 1993.
- [13] JPL D-10178-3, “Cassini Earth Swingby Plan Supplement,” *699-070-3-Sup, JPL D-10178-3*, May 19 1997.
- [14] NPR 8020.12D. (2011, April 20) NPR 8020.12D: Planetary Protection Provisions for Robotic Extraterrestrial Missions.
- [15] Y. Hahn. (1997, May 7) Updates to Nav Plan for 10/6/97 Prime Mission. *JPL IOM 312.H-97-003*.
- [16] T. D. Goodson. (1998, January 15) Navigation Plan Update for October 15, 1997 Prime Mission. *JPL IOM 312.H-97-108-REV.1*.
- [17] R. Ionasescu. (1998, October 2) Navigation Plan Update for October 15, 1997 Prime Mission. *JPL IOM 312.A/024-98*.
- [18] M. D. Guman. (1999, February 12) Navigation Plan Update for October 15, 1997 Prime Mission. *JPL IOM 312.A/003-99*.

- [19] T. D. Goodson. (2000, May 19) Navigation Plan Update #5. *JPL IOM 312.H-00-003*.
- [20] T. D. Goodson. (1998, November 20) Navigation Plan Update to Execution Dates for TCMs 7, 8, 9, and 13. *JPL IOM 312.H-98-014*.
- [21] D. C. Roth, M. D. Guman, R. Ionasescu, and A. H. Taylor, "Cassini Orbit Determination from Launch to the First Venus Flyby," in *AIAA Paper 98-4563, Astrodynamics Specialist Conference*, Boston, MA, 1998: AIAA/AAS Astrodynamics Specialist Conference.
- [22] T. D. Goodson, D. L. Gray, Y. Hahn, and F. Peralta, "Cassini maneuver experience -Launch and early cruise," in *AIAA Guidance, Navigation, and Control Conference and Exhibit*, Boston, MA, Collection of Technical Papers. Pt. 2; UNITED STATES; 10-12 Aug. 1998, 1998, vol. AIAA Paper 1998-4224, VA: American Institute of Aeronautics and Astronautics: Reston, 1998.
- [23] T. D. Goodson, D. L. Gray, Y. Hahn, and F. Peralta, "Cassini maneuver experience: Finishing inner cruise," in *Spaceflight mechanics 2000; Proceedings of the AAS/AIAA Space Flight Mechanics Meeting, Clearwater, FL; 23-26 Jan. 2000*, 2000, vol. 105, no. Pt. 2, San Diego, CA: Univelt Inc, 2000, pp. 1031-1051.
- [24] M. D. Guman, D. C. Roth, R. Ionasescu, T. D. Goodson, A. H. Taylor, and J. B. Jones, "Cassini orbit determination from first Venus flyby to Earth flyby," 2000, vol. 105 II: Univelt Inc, 2000, pp. 1053-1072.
- [25] D. C. Roth, M. D. Guman, and R. Ionasescu, "Cassini orbit reconstruction from earth to jupiter," in *Spaceflight Mechanics 2002*, 2002, vol. 112, no. I, San Antonio, TX, United States: Univelt Inc, 2002, pp. 693-704.
- [26] J. Ellis. (1997, December 12) Cassini Launch Navigation Summary. *JPL IOM 312.C/042-97*.
- [27] JPL D-11621, "Cassini Navigation Plan," *699-101 Update, JPL D-11621*, August 1 2003.
- [28] Y. Hahn. (1998, April 15) Maneuver Analysis for Redesigning the Cassini Post Venus 1 Cruise Trajectory after Skipping TCM 3. *JPL IOM 312.H-98-005*.
- [29] T. H. Taylor, J. K. Campbell, R. A. Jacobson, B. Moultrie, R. A. Nichols, and J. E. Riedel, "Performance of Differenced Range Data Types in Voyager Navigation," in *JPL TDA Progress Report 42-71*, 1982.
- [30] T. Taylor. (1997, October 27) Cassini Ranging Noise. *personal email communication*.
- [31] J. B. Berner. (1998, March 6) Doppler Jumps Explained (and Fixed). *personal email communication*.
- [32] G. D. Lewis. (1999, September 13) Earth Orbiting Debris Collision Avoidance During a Hyperbolic Flyby: The Cassini Experience. *JPL IOM 312.A/034-99*.
- [33] P. G. Antreasian and J. R. Guinn, "Investigations Into the Unexpected Delta-V Increases During the Earth Gravity Assists of Galileo and NEAR," in *AIAA 98-4287, AIAA/AAS Astrodynamics Specialist Conference*, Boston, MA, 1998.
- [34] T. Goodson, B. Buffington, Y. Hahn, N. Strange, S. Wagner, and M. Wong, "Cassini - Huygens maneuver experience: cruise and arrival at Saturn," in *AAS/AIAA Astrodynamics Specialist Conference*, Lake Tahoe, CA, 2004, vol. AAS Paper 05-286, San Diego, CA: American Astronautical Society, 2005, pp. 1-26. [Online]. Available: <http://hdl.handle.net/2014/39621>.

- [35] W. M. Owen. (2003, May 9) Cassini ISS Geometric Calibration of April 2003. *JPL IOM 312.E 2003 001*.
- [36] E. Høg *et al.* (2000) The Tycho-2 Catalogue of the 2.5 million brightest stars. *Astronomy & Astrophysics*.
- [37] N. Zacharias *et al.* (2004) The Second US Naval Observatory CCD Astrograph Catalog (UCAC2). *Astronomical Journal*.
- [38] W. Folkner and C. Jacobs. (2003, April 16) DSN Station Location Update and Plans REVISED.
- [39] T. Goodson, "Evaluation of an energy-cutoff algorithm for the Saturn orbit insertion burn of the Cassini-Huygens Mission," 2004, vol. 119: Univelt Inc. San Diego CA 92198 United States, 2005, pp. 473-489, doi: <http://trs-new.jpl.nasa.gov/dspace/bitstream/2014/38109/1/03-2374.pdf>.
- [40] T. Burk, "Cassini pointing operations flight experience using inertial vector propagation," in *AIAA Guidance, Navigation, and Control Conference 2007*, 2007, vol. 1, Hilton Head, SC, United States: American Institute of Aeronautics and Astronautics Inc. Reston VA 20191-4344 United States, 2007, pp. 417-437.
- [41] D. Roth *et al.*, "Cassini Tour Navigation Strategy," in *AAS Paper 03-546, AAS/AIAA Astrodynamics Specialists Conference*, Big Sky MT, 2003.
- [42] E. M. Gist, C. G. Ballard, Y. Hahn, P. W. Stumpf, S. V. Wagner, and P. N. Williams, "Cassini-huygens maneuver experience: First year of the Equinox Mission," in *2009 AAS/AIAA Astrodynamics Specialist Conference*, Pittsburg, PA, 2009, vol. 135, no. Part 2, San Diego, CA 92198, United States: Univelt Inc, 2009, pp. 787-807.
- [43] B. Buffington, N. Strange, and R. Ionasescu, "Addition of a low altitude Tethys flyby to the nominal Cassini tour," 2005.
- [44] F. Pelletier, B. B. Buffington, N. Strange, and T. Denk, "Re-aiming cassini's iapetus flyby," in *2007 AAS/AIAA Astrodynamics Specialist Conference*, 2007, vol. 129 PART 1, San Diego, CA 92198, United States: Univelt Inc, 2008, pp. 63-76.
- [45] ESA Report HUY-RP-12241, "Huygens Recovery Task Force Final Report," in *ESA Report HUY-RP-12241*, 2001.
- [46] N. J. Strange, T. D. Goodson, and Y. Hahn, "Cassini tour redesign for the Huygens mission," in *AIAA/AAS Astrodynamics Specialist Conference and Exhibit, Monterey, CA; 5-8 Aug. 2002*, 2002, vol. AIAA Paper 2002-4720: Reston VA: American Institute of Aeronautics and Astronautics Inc., 2002.
- [47] T. D. Goodson, Y. Hahn, N. J. Strange, and M. C. Wong, "Maneuver-Targeting Strategies and Results for the Cassini-Huygens Mission," in *3rd International Planetary Probe Workshop*, Anavyssos, Attica, Greece, 2005.
- [48] J. Bordi *et al.*, "Orbit determination results and trajectory reconstruction for the Cassini/Huygens mission," in *3rd International Planetary Probe Workshop; June 27 - July 1, 2005; Attica; Greece*, 2005, Attica Greece, 2005, pp. 1-8. [Online]. Available: <http://hdl.handle.net/2014/38358>. [Online]. Available: <http://hdl.handle.net/2014/38358>
- [49] D. L. Matson, J. C. Castillo-Rogez, G. Schubert, C. Sotin, and W. B. McKinnon, "The Thermal Evolution and Internal Structure of Saturn's Mid-Sized Icy Satellites," in *Saturn*

- from *Cassini-Huygens*, M. K. Dougherty, L. W. Esposito, and S. M. Krimigis Eds. Dordrecht ; New York: Springer, 2009, pp. 577-612.
- [50] J.-P. Lebreton *et al.*, “An overview of the descent and landing of the Huygens probe on Titan,” *Nature*, vol. 438, no. 7069, pp. 758-764, 2005, doi: <http://dx.doi.org/10.1038/nature04347>.
 - [51] S. Wagner and B. Buffington, “The double flybys of the cassini mission: Navigation challenges and lessons learned,” in *13th International Conference on Space Operations, SpaceOps 2014, May 5, 2014 - May 9, 2014, Pasadena, CA*, 2014: American Institute of Aeronautics and Astronautics Inc, 2014, pp. AIAA 2014-1878, doi: <http://dx.doi.org/10.2514/6.2014-1878>.
 - [52] M. Wong, Y. Hahn, D. Roth, and M. Vaquero, “Trajectory Dispersion Control for the Cassini Grand Finale Mission,” in *25th International Symposium on Space Flight Dynamics*, Munich, Germany, 2015.
 - [53] M. Vaquero, Y. Hahn, D. Roth, and M. Wong, “A Linear Analysis for the Flight Path Control of the Cassini Grand Finale Orbits,” in *ISTS-2017-d-010/ISSFD-2017-010, 26th International Symposium of Space Flight Dynamics*, Matsuyama, Japan, 2017.
 - [54] D. Boone, M. Wong, J. Bellerose, and D. Roth, “Preliminary Saturn Atmospheric Density Results from Cassini’s Final Plunge,” in *AAS Paper 18-115, 41st Annual AAS Guidance & Control Conference*, Breckinridge, CO, 2018.
 - [55] M. Vaquero *et al.*, “Flying Cassini Through the Grand Finale Orbits: Prediction vs. Reality,” in *Paper 18-151*, Breckinridge, CO, 2018.
 - [56] J. Bellerose, D. Roth, D. Boone, Z. Tarzi, R. Ionasescu, and K. Criddle, “Cassini Orbit Determination Operations Through the Final Titan Flybys and the Mission Grand Finale (February 2016 - September 2017),” in *AAS Paper 18-152*, Breckinridge, CO, 2018.
 - [57] C. J. Hansen *et al.*, “Investigation of diurnal variability of water vapor in Enceladus’ plume by the Cassini ultraviolet imaging spectrograph,” *Geophysical Research Letters*, vol. 44, no. 2, pp. 672-677, 2017, doi: <http://dx.doi.org/10.1002/2016GL071853>.
 - [58] D. C. Roth *et al.*, “Navigational Use of Cassini DeltaV Telemetry,” in AIAA Guidance, Navigation and Control Conference and Exhibit, AIAA Atmospheric Flight Mechanics Conference and Exhibit, AIAA Modeling and Simulation Technologies Conference and Exhibit, AIAA/AAS Astrodynamics Specialist Conference and Exhibit, and the 26th AIAA Applied Aerodynamics Conference; Honolulu, HI; USA; 18-21 Aug. 2008, 2008, vol. AIAA Paper 2008-6746, AIAA/AAS Astrodynamics Specialist Conference and Exhibit, and the 26th AIAA Applied Aerodynamics Conference: American Institute of Aeronautics and Astronautics 1801 Alexander Bell Drive Suite 500 Reston VA 20191-4344 USA URL: <http://www.aiaa.org>, 2008.
 - [59] S. M. Ardalan *et al.*, “Integration of spacecraft telemetry into navigation operations for the cassini-huygens mission,” in *SpaceOps 2008 Conference, May 12, 2008 - May 16, 2008, Heidelberg, Germany*, 2008: American Institute of Aeronautics and Astronautics Inc, 2008.
 - [60] J. Bellerose, D. Roth, K. Criddle, D. Boone, R. Ionasescu, and Z. Tarzi, “The Cassini Mission: Reconstructing Thirteen Years of the Most Complex Gravity-Assist Trajectory Flown to Date,” *SpaceOps 2018 Conference, AIAA 2018-xxx*, Marseille, France, 2018.

- [61] D. Roth and B. Buffington. (2011, May 24) January 2011 Y-thruster calibration results and comparison to the previous event.
- [62] D. Roth. (2012, March 7) February 2012 Y-thruster calibrations results and comparison to the previous calibrations.
- [63] D. Roth and R. Ionasescu. (2013, March 5) January 2013 Y-thruster calibration results and comparison to the previous calibrations.
- [64] D. Roth. (2015, May 9) December 2014 Y-thruster calibration results and comparison to the previous calibrations.
- [65] D. Roth. (2016, August 31) May 2016 Y-thruster calibration and comparison to the previous calibrations.
- [66] P. W. Stumpf, E. M. Gist, T. D. Goodson, Y. Hahn, S. V. Wagner, and P. N. Williams, “Flyby Error Analysis Based on Contour Plots for Cassini Tour,” (in English), *J.Spacecraft Rockets*, vol. 46, no. 5, pp. 1016-1022, Sep-Oct 2009, doi: <http://dx.doi.org/10.2514/1.42143>.
- [67] P. N. Williams, E. M. Gist, T. D. Goodson, Y. Hahn, P. W. Stumpf, and S. V. Wagner, “Cassini-huygens maneuver experience: Third year of saturn tour,” in *2007 AAS/AIAA Astrodynamics Specialist Conference*, 2007, vol. 129 PART 1, San Diego, CA 92198, United States: Univelt Inc, 2008, pp. 41-62.

8 Abbreviations and Acronyms

AACS	Attitude and Articulation Control Subsystem
ACS	Attitude Control Subsystem
AU	astronomical unit
BVR	Block V Receiver
CDF	Cumulative distribution function
CDS	Command and Data Subsystem
DCO	Data Cut-Off
DPTRAJ	Double Precision Trajectory
DSM	Deep Space Maneuver
DSN	Deep Space Network
DSS	Deep Space Station
ECB	Energy-Cutoff Burn
EOM	end of mission
ERT	Earth Received Time
ESA	European Space Agency
GM	Gravitation Parameter
GWE	Gravitational Wave Experiments
HGA	High-Gain Antenna
IVP	Inertial Vector Propagator
JPL	Jet Propulsion Laboratory
LGA	Low-Gain Antenna
MAS	Maneuver Automation Software
ME	main engine
MEA	Main Engine A
MEB	Main Engine B
MONTE	Mission Analysis, Operations, and Navigation Toolkit Environment
MOPS	Maneuver Operation Program Set
NAC	Narrow Angle Camera
NEAR	Near Earth Rendezvous
NRAO	National Radio Astronomy Observatory
OD	orbit determination
ODM	Orbit Deflection Maneuver
ODP	Orbit Determination Program
ODT	Orbiter Delay Time
OPNAV	Optical Navigation
OPTG	Orbit Propagation & Timing Geometry

OTM	Orbit Trim Maneuver
PRM	Periapsis Raise Maneuver
PTM	Probe Targeting Maneuver
RA	Right Ascension
RCS	Reaction Control System
RPC	ring plane crossing
RPWS	Radio and Plasma Wave Science
RTG	radioisotope thermoelectric generator
RWA	Reaction Wheel Assembly
SCET	Spacecraft Event Time
SCO	Spacecraft Operations Office
SEP	Sun-Earth-Probe
SOI	Saturn Orbit Insertion
SRMU	Solid Rocket Motor Upgrade
SRU	Stellar Reference Unit
SSR	Solid-State Recorder
TCM	Trajectory Correction Maneuver
USNO	U.S. Naval Observatory
UTC	Coordinated Universal Time
VLBI	Very Long Baseline Interferometry
VVEJGA	Venus-Venus-Earth-Jupiter Gravity Assist
WAC	wide angle camera

Appendix A. Supplementary Material

A.1 Targeted Encounter History

Information on the 156 targeted satellite encounters during the Saturn tour are provided in Tables A-1 to A-3. The three encounter conditions that were targeted via maneuvers are shown in the tables: the spatial B-plane components $B \cdot R$ and $B \cdot T$ and the time of closest approach (TCA). The differences between the target conditions and what was actually achieved are also given in the tables. Finally, the last control point is reported which is the final maneuver performed prior to an encounter. Not included in Tables A-1 to A-3 are the four non-targeted encounters (Enceladus-6, Titan-67, Enceladus-10, and Dione-3) which were part of four distinct double flybys (see Table A-2). These non-targeted flybys are listed in Tables A-4 and A-5.

Table A-1. Cassini Targeted Encounter History (Venus-1 to Titan-41).

Encounter	Encounter Target Conditions (Earth Mean Orbital Plane & Equinox of J2000.0)			Reconstructed Differences from Encounter Target Conditions			Last Control Point to Target Encounter
	B·R	B·T	Time of Closest	$\Delta B \cdot R$	$\Delta B \cdot T$	ΔTCA	
	(km)	(km)	Approach (UTC)	(km)	(km)	(sec)	
Venus-1	−1910.71	12301.85	26-Apr-1998 13:44:46	−3.39	−67.07	−4.44	TCM-02
Venus-2	3295.91	−9064.32	24-Jun-1999 20:29:57	11.38	−0.56	−2.51	TCM-07
(non-targeted)	(Venus-2 flyby conditions for Earth flyby target)						↳ Earth
Earth	164.00	8960.00	18-Aug-1999 03:28:25	3.07	8.91	0.61	TCM-12
Jupiter	123623.00	10897196.00	30-Dec-2000 10:03:39	159.93	113.97	42.87	TCM-14
Phoebe	−873.69	1920.63	11-Jun-2004 19:33:37	−11.01	72.73	0.18	TCM-20
Titan-a	−1901.48	3571.38	26-Oct-2004 15:30:09	−5.51	−32.09	−4.05	OTM-004
Titan-b	−2882.59	2840.58	13-Dec-2004 11:38:13	−5.45	−17.00	2.54	OTM-006
Titan-c	−17828.17	−60304.98	14-Jan-2005 11:11:56	−33.06	6.41	2.97	OTM-010a
Titan-3	−1046.33	4305.10	15-Feb-2005 06:57:53	−3.98	1.52	0.32	OTM-013
Enceladus-1	27.92	−746.96	09-Mar-2005 09:08:01	−1.55	−1.84	1.54	OTM-015
Titan-4	−4595.27	−2546.90	31-Mar-2005 20:05:16	−5.55	6.07	0.15	OTM-018
Titan-5	−2882.09	2586.39	16-Apr-2005 19:11:46	−3.94	−0.79	0.13	OTM-022
Enceladus-2	−32.00	−421.19	14-Jul-2005 19:55:22	4.60	1.72	−0.67	OTM-025
Titan-6	3493.62	−5507.97	22-Aug-2005 08:53:37	4.43	12.84	0.89	OTM-027
Titan-7	3907.82	−328.74	07-Sep-2005 08:11:58	−0.15	−4E−03	−0.02	OTM-031
Hyperion-1	300.47	−565.10	26-Sep-2005 02:24:46	1.11	26.23	2.92	OTM-033
Dione-1	607.78	−869.53	11-Oct-2005 17:52:02	6.07	5.58	−1.47	OTM-035
Titan-8	−1368.20	−3981.87	28-Oct-2005 04:15:25	−0.60	0.07	−0.43	OTM-039
Rhea-1	685.91	1065.16	26-Nov-2005 22:37:39	−2.91	4.34	−0.41	OTM-043
Titan-9	−6012.93	−11838.63	26-Dec-2005 18:59:30	−12.85	4.00	−3.94	OTM-044
Titan-10	−991.65	−4806.87	15-Jan-2006 11:41:27	1.16	0.10	−0.10	OTM-047
Titan-11	−1841.04	−4297.24	27-Feb-2006 08:25:19	1.31	0.68	0.60	OTM-051
Titan-12	220.65	−4811.44	19-Mar-2006 00:05:57	0.29	1.67	−0.39	OTM-053
Titan-13	−1102.88	−4587.75	30-Apr-2006 20:58:14	−1.81	−0.79	−0.14	OTM-058
Titan-14	1280.80	−4567.23	20-May-2006 12:18:11	0.02	−0.40	0.09	OTM-061
Titan-15	70.12	−4769.87	02-Jul-2006 09:20:47	−0.37	−0.14	0.06	OTM-064
Titan-16	−3414.47	−1685.98	22-Jul-2006 00:25:26	0.09	0.06	−0.03	OTM-065
Titan-17	−2945.89	2488.76	07-Sep-2006 20:16:51	0.78	0.13	−0.01	OTM-070
Titan-18	−3682.40	−1008.54	23-Sep-2006 18:58:49	−0.32	2.09	−0.51	OTM-072
Titan-19	−3759.34	−771.28	09-Oct-2006 17:30:07	0.34	0.05	0.02	OTM-076
Titan-20	−2451.47	3016.10	25-Oct-2006 15:58:07	0.33	−0.54	−1E−02	OTM-079
Titan-21	−1948.11	−3331.58	12-Dec-2006 11:41:31	0.21	9E−03	−0.02	OTM-081 BU
Titan-22	−4144.64	−339.48	28-Dec-2006 10:05:22	2.94	4.14	−0.33	OTM-084
Titan-23	−3857.46	−38.22	13-Jan-2007 08:38:31	−0.16	0.48	−0.05	OTM-088
Titan-24	−5044.38	−2173.01	29-Jan-2007 07:15:55	0.19	0.09	0.03	OTM-091
Titan-25	−3479.86	−1602.96	22-Feb-2007 03:12:24	−0.28	−0.11	0.01	OTM-094
Titan-26	−3802.40	−256.77	10-Mar-2007 01:49:00	−0.42	−1.28	0.04	OTM-096
Titan-27	−3805.96	−519.09	26-Mar-2007 00:23:27	0.11	−0.04	0.11	OTM-100
Titan-28	−3748.33	−742.98	10-Apr-2007 22:58:00	−0.73	−0.56	−0.16	OTM-103
Titan-29	−3690.23	−953.12	26-Apr-2007 21:32:58	−0.78	−0.18	−0.08	OTM-106
Titan-30	−3610.97	−1155.26	12-May-2007 20:09:58	0.97	−0.42	−0.03	OTM-109
Titan-31	−4805.08	−1806.43	28-May-2007 18:51:55	1.53	−1.18	0.21	OTM-111
Titan-32	−3478.12	−1520.70	13-Jun-2007 17:46:11	−0.06	−0.18	1E−02	OTM-115
Titan-33	−2655.50	3954.85	29-Jun-2007 16:59:46	0.06	0.28	−4E−03	OTM-118
Titan-34	530.95	−4127.55	19-Jul-2007 01:11:20	−0.28	0.21	−0.21	OTM-121
Titan-35	−4075.95	−4619.26	31-Aug-2007 06:32:34	−1.69	4.51	1.80	OTM-123 BU
Iapetus-1	799.05	−2245.86	10-Sep-2007 14:15:40	−0.14	−7.38	8.43	OTM-125
Titan-36	3744.17	−652.74	02-Oct-2007 04:42:43	−2.14	−0.82	0.06	OTM-130
Titan-37	2533.97	−2866.69	19-Nov-2007 00:47:25	−0.39	0.45	0.01	OTM-133
Titan-38	4040.65	827.48	05-Dec-2007 00:06:50	−1.90	1.00	−0.09	OTM-136
Titan-39	3756.11	531.16	20-Dec-2007 22:57:55	−0.45	−0.32	−0.05	OTM-139
Titan-40	2162.62	−3166.55	05-Jan-2008 21:30:20	−2.97	−6.94	−0.37	OTM-141
Titan-41	3207.07	−2080.45	22-Feb-2008 17:32:07	−2.70	−3.80	−0.08	OTM-145

Table A-2. Cassini Targeted Encounter History (Enceladus-3 to Titan-81).

Encounter	Encounter Target Conditions (Earth Mean Orbital Plane & Equinox of J2000.0)			Reconstructed Differences from Encounter Target Conditions			Last Control Point to Target Encounter
	B·R	B·T	Time of Closest	$\Delta B \cdot R$	$\Delta B \cdot T$	ΔTCA	
	(km)	(km)	Approach (UTC)	(km)	(km)	(sec)	
Enceladus-3	88.66	290.09	12-Mar-2008 19:06:12	0.64	-2.37	0.02	OTM-147
Titan-42	2806.42	-2594.81	25-Mar-2008 14:27:48	-1.81	-0.94	-5E-04	OTM-150
Titan-43	-631.49	-3770.16	12-May-2008 10:01:58	-1.96	-1.05	-0.04	OTM-153
Titan-44	-615.54	-4178.73	28-May-2008 08:24:32	-0.44	0.14	0.03	OTM-156
Titan-45	3246.44	-3029.17	31-Jul-2008 02:13:11	0.61	3E-03	0.03	OTM-160
Enceladus-4	73.39	291.73	11-Aug-2008 21:06:19	-0.58	-0.48	-0.11	OTM-162
Enceladus-5	68.19	267.25	09-Oct-2008 19:06:40	0.04	-0.42	0.02	OTM-166
Titan-46	1319.98	3698.55	03-Nov-2008 17:35:23	-5.92	7.63	-0.13	OTM-169
Titan-47	1533.12	-3531.74	19-Nov-2008 15:56:28	0.03	-0.69	-0.11	OTM-171
Titan-48	86.16	-3786.58	05-Dec-2008 14:25:45	0.15	-0.53	5E-03	OTM-175
Titan-49	2737.62	-2631.62	21-Dec-2008 12:59:52	0.32	-0.30	0.02	OTM-178
Titan-50	3778.47	-253.61	07-Feb-2009 08:50:52	6.25	-6.55	0.81	OTM-180
Titan-51	1621.74	-3422.68	27-Mar-2009 04:43:37	1.74	-2.08	0.28	OTM-183x
Titan-52	6416.68	-2827.31	04-Apr-2009 01:47:48	-2.12	3.82	-0.47	OTM-186
Titan-53	6194.01	-1837.93	20-Apr-2009 00:20:46	-1.86	-1.49	0.04	OTM-189
Titan-54	6010.05	-1071.48	05-May-2009 22:54:16	-2.23	-0.21	-0.14	OTM-192
Titan-55	3811.44	-266.33	21-May-2009 21:26:42	0.53	-0.68	0.08	OTM-196
Titan-56	3818.68	123.32	06-Jun-2009 20:00:01	2.58	-0.42	0.11	OTM-198
Titan-57	3785.36	439.49	22-Jun-2009 18:32:36	-0.04	-0.31	0.01	OTM-201
Titan-58	3751.96	722.81	08-Jul-2009 17:04:04	0.93	-1.40	0.25	OTM-204
Titan-59	3682.34	981.64	24-Jul-2009 15:34:04	1.44	-1.17	0.14	OTM-207
Titan-60	3613.32	1257.75	09-Aug-2009 14:03:54	1.07	-0.04	0.10	OTM-210
Titan-61	2803.51	-2593.11	25-Aug-2009 12:51:39	0.04	2.10	-0.41	OTM-213
Titan-62	2318.47	3448.40	12-Oct-2009 08:36:25	0.52	-1.02	0.19	OTM-217
Enceladus-7	308.30	160.15	02-Nov-2009 07:41:59	1.10	-2.36	-0.14	OTM-220
Enceladus-8	1606.22	920.72	21-Nov-2009 02:09:51	16.48	-42.67	6.62	OTM-221
Titan-63	-2214.92	-7395.04	12-Dec-2009 01:03:15	4.86	1.15	-0.27	OTM-225
Titan-64	-3521.26	-1470.24	28-Dec-2009 00:16:60	3.51	1.20	-0.37	OTM-228
Titan-65	3602.39	1579.09	12-Jan-2010 23:10:36	1.92	-1.33	-0.09	OTM-232
Titan-66	5914.63	8499.34	28-Jan-2010 22:28:49	0.73	-5.30	0.69	OTM-234
Rhea-2	-700.55	-509.28	02-Mar-2010 17:40:36	-3.12	3.36	-0.08	OTM-237
Dione-2	-468.37	952.08	07-Apr-2010 05:16:11	-0.62	6.98	0.01	OTM-241
Enceladus-9	307.00	162.74	28-Apr-2010 00:10:17	1.10	0.98	0.03	OTM-243
Titan-68	3960.88	-1577.78	20-May-2010 03:24:20	-2.40	0.36	0.28	OTM-246
Titan-69	-4632.25	-1620.97	05-Jun-2010 02:26:27	1.35	1.06	-4E-03	OTM-250
Titan-70	-3410.81	-1536.77	21-Jun-2010 01:27:43	1.73	0.88	-0.06	OTM-253
Titan-71	2172.40	3196.98	07-Jul-2010 00:22:45	-1.86	-0.33	0.06	OTM-256
Enceladus-11	2602.38	1030.82	13-Aug-2010 22:30:59	-9.34	35.94	-7.23	OTM-258
Titan-72	-842.63	11007.01	24-Sep-2010 18:38:41	-0.62	2.76	0.07	OTM-261a
Titan-73	8687.39	-6411.68	11-Nov-2010 13:37:01	1.14	-2.27	2E-03	OTM-265
Enceladus-12	-164.28	-248.01	30-Nov-2010 11:53:59	-0.77	3.18	0.60	OTM-268
Enceladus-13	-297.40	7.00	21-Dec-2010 01:08:27	-0.47	0.91	0.25	OTM-270
Rhea-3	821.35	153.37	11-Jan-2011 04:53:25	0.41	-0.62	5E-03	OTM-274
Titan-74	2957.82	-5806.42	18-Feb-2011 16:04:11	-2.12	-1.51	0.23	OTM-276
Titan-75	5014.68	-11917.22	19-Apr-2011 05:00:39	-0.27	-0.21	-0.04	OTM-280
Titan-76	2128.65	-4228.96	08-May-2011 22:53:44	-0.34	0.39	-0.11	OTM-283
Titan-77	1922.11	-3758.27	20-Jun-2011 18:32:00	-0.08	-0.18	-0.02	OTM-286
Titan-78	-2948.62	8160.97	12-Sep-2011 02:50:06	1.34	0.44	-0.05	OTM-288
Enceladus-14	306.59	163.44	01-Oct-2011 13:52:26	-0.74	1.16	-0.10	OTM-292
Enceladus-15	-365.69	1437.71	19-Oct-2011 09:22:12	0.18	-0.39	-0.04	OTM-294
Enceladus-16	629.00	-403.75	06-Nov-2011 04:58:53	0.57	-0.69	0.15	OTM-297
Titan-79	-3654.83	5316.20	13-Dec-2011 20:11:24	-6.11	-7.63	-0.81	OTM-301
Titan-80	32261.86	-2880.49	02-Jan-2012 15:13:38	0.34	-0.13	0.08	OTM-304
Titan-81	33951.59	-2051.12	30-Jan-2012 13:39:48	-0.43	2.19	0.08	OTM-306

Table A-3. Cassini Targeted Encounter History (Titan-82 to Titan-126).

Encounter	Encounter Target Conditions (Earth Mean Orbital Plane & Equinox of J2000.0)			Reconstructed Differences from Encounter Target Conditions			Last Control Point to Target Encounter
	B·R	B·T	Time of Closest	$\Delta B \cdot R$	$\Delta B \cdot T$	ΔTCA	
	(km)	(km)	Approach (UTC)	(km)	(km)	(sec)	
Titan-82	-3758.26	5502.71	19-Feb-2012 08:43:17	0.88	0.26	-0.03	OTM-310 BU
Enceladus-17	279.90	160.06	27-Mar-2012 18:30:09	-0.44	1.14	-0.10	OTM-313
Enceladus-18	293.38	133.22	14-Apr-2012 14:01:38	0.20	0.33	-8E-03	OTM-316
Enceladus-19	318.82	48.13	02-May-2012 09:31:29	-0.46	-0.20	-8E-03	OTM-319
Titan-83	-2894.99	-2495.50	22-May-2012 01:10:11	1.07	1.17	-0.06	OTM-322 BU
Titan-84	-3496.63	1548.74	07-Jun-2012 00:07:21	0.76	1.87	-0.17	OTM-325
Titan-85	-2687.57	-2797.75	24-Jul-2012 20:03:08	-0.61	0.42	-0.05	OTM-328
Titan-86	-3341.26	-1857.32	26-Sep-2012 14:35:39	-0.06	-0.18	0.03	OTM-331
Titan-87	1038.03	-3698.26	13-Nov-2012 10:22:09	1.40	-0.24	-0.01	OTM-334
Titan-88	-74.22	-3881.46	29-Nov-2012 08:56:60	-0.28	-0.60	0.11	OTM-337
Titan-89	479.35	-4824.93	17-Feb-2013 01:56:36	0.70	0.14	-3E-03	OTM-340
Rhea-4	-1537.16	-868.99	09-Mar-2013 18:17:28	-3.00	6.88	-0.68	OTM-342
Titan-90	3534.49	-2394.42	05-Apr-2013 21:43:32	0.01	0.06	-0.03	OTM-346
Titan-91	-3211.28	-2098.69	23-May-2013 17:32:56	0.13	0.05	-0.03	OTM-349
Titan-92	-2897.67	-2505.31	10-Jul-2013 13:21:48	0.34	0.40	-0.07	OTM-352
Titan-93	-3529.87	-2398.45	26-Jul-2013 11:56:23	0.39	0.38	0.04	OTM-355
Titan-94	-739.84	-4200.28	12-Sep-2013 07:43:57	-0.11	-0.08	0.02	OTM-358
Titan-95	219.27	-3821.68	14-Oct-2013 04:56:28	0.11	0.17	-0.04	OTM-361
Titan-96	4198.46	-767.96	01-Dec-2013 00:41:20	0.06	-7E-03	0.01	OTM-364
Titan-97	3250.83	-2766.13	01-Jan-2014 21:59:42	-0.17	-0.12	0.03	OTM-367
Titan-98	3409.29	-2283.90	02-Feb-2014 19:12:39	0.13	0.42	-0.04	OTM-370
Titan-99	3841.06	-2081.48	06-Mar-2014 16:26:48	-0.18	0.15	0.01	OTM-373
Titan-100	3207.94	-2093.17	07-Apr-2014 13:41:15	0.23	-0.35	-0.02	OTM-376
Titan-101	2129.40	-5471.13	17-May-2014 16:12:16	0.06	0.04	-7E-03	OTM-379
Titan-102	2802.59	-5907.25	18-Jun-2014 13:28:26	-0.30	-0.12	-0.04	OTM-382
Titan-103	2270.82	-7654.82	20-Jul-2014 10:40:59	0.15	-0.05	7E-04	OTM-385
Titan-104	-741.35	3763.50	21-Aug-2014 08:09:10	-0.03	0.07	-5E-03	OTM-388
Titan-105	-2012.39	3770.93	22-Sep-2014 05:23:20	-0.19	-0.07	-0.05	OTM-391
Titan-106	-649.36	3829.79	24-Oct-2014 02:40:31	8E-03	0.07	3E-03	OTM-394
Titan-107	-3823.78	473.77	10-Dec-2014 22:26:35	-0.23	0.07	0.02	OTM-397
Titan-108	-3194.43	2135.11	11-Jan-2015 19:48:35	-0.11	-0.18	2E-03	OTM-400 BU
Titan-109	-3620.19	1866.37	12-Feb-2015 17:08:04	-0.44	-1.69	0.06	OTM-403
Titan-110	-5102.76	700.16	16-Mar-2015 14:29:48	0.04	0.05	0.04	OTM-406
Titan-111	2700.26	4903.33	07-May-2015 22:50:23	0.46	0.31	-0.09	OTM-409
Dione-4	-872.81	632.83	16-Jun-2015 20:11:52	-0.92	-0.90	-0.12	OTM-411
Titan-112	3539.80	13363.96	07-Jul-2015 08:09:51	-0.25	-0.59	5E-03	OTM-414
Dione-5	-1009.06	256.69	17-Aug-2015 18:33:26	0.21	-0.63	0.06	OTM-417
Titan-113	1841.27	3445.51	28-Sep-2015 21:37:13	-0.15	-0.06	-0.04	OTM-421
Enceladus-20	-1895.43	888.65	14-Oct-2015 10:41:30	-0.09	-1.67	0.24	OTM-424
Enceladus-21	262.88	-139.07	28-Oct-2015 15:22:43	-0.36	-0.80	-0.22	OTM-426
Titan-114	2663.63	-14568.62	13-Nov-2015 05:46:32	-0.37	-2.28	-0.13	OTM-429
Enceladus-22	4902.46	-1871.06	19-Dec-2015 17:49:17	2.80	3.97	0.35	OTM-431
Titan-115	2525.74	5900.66	16-Jan-2016 02:20:25	0.36	-0.43	0.04	OTM-436
Titan-116	4250.71	-405.23	01-Feb-2016 01:00:06	-1.89	1.46	-0.11	OTM-439 BU
Titan-117	2644.39	2846.56	16-Feb-2016 23:49:42	-0.35	-0.12	-0.02	OTM-442
Titan-118	3613.45	1353.72	04-Apr-2016 19:42:43	-0.25	0.34	-0.04	OTM-445
Titan-119	3827.05	-324.53	06-May-2016 16:54:37	-2.11	1.30	-0.30	OTM-448 BU
Titan-120	3123.37	-2243.40	07-Jun-2016 14:06:17	-0.10	1.10	-0.07	OTM-450
Titan-121	582.50	-3802.45	25-Jul-2016 09:58:23	-0.53	0.59	-0.18	OTM-454
Titan-122	-2438.43	-3865.92	10-Aug-2016 08:30:53	-1.19	0.19	-0.15	OTM-456
Titan-123	-3694.08	-2821.74	27-Sep-2016 04:16:59	-0.03	-0.15	0.03	OTM-460
Titan-124	-4258.56	-1316.21	13-Nov-2016 23:55:56	-0.06	-0.38	-0.02	OTM-463
Titan-125	-5865.94	-1414.75	29-Nov-2016 22:14:32	-0.32	0.13	-0.03	OTM-464
Titan-126	-3720.74	992.62	22-Apr-2017 06:08:08	0.28	0.21	0.01	OTM-469

A.2 Biased Targeted Encounter History

Tables A-1 to A-3 list the actual encounter conditions that were targeted. In most cases, these target conditions were defined by the reference trajectory. One or more of these target conditions for 29 targeted encounters were modified, usually to save downstream ΔV or to make a necessary maneuver large enough to be implementable (see Table A-4). The three encounter target conditions from the reference trajectory are shown in Table A-4: the spatial B-plane components B·R and B·T and the time of closest approach (TCA). The differences between the reference trajectory target conditions and the modified target conditions, referred to as flyby biases, are also given in the table. Finally, the last control point for each encounter is reported. The last control point is the final maneuver performed prior to an encounter to achieve the modified flyby aimpoint.

Table A-4. Biased Targeted Encounter History.

Encounter	Reference Trajectory Target Conditions (Earth Mean Orbital Plane & Equinox of J2000.0)			Flyby Biases from Reference Trajectory Target Conditions			Last Control Point to Target Encounter
	B·R (km)	B·T (km)	Time of Closest Approach (UTC)	$\Delta B \cdot R$ (km)	$\Delta B \cdot T$ (km)	ΔTCA (sec)	
Titan-29	−3690.23	−953.12	26-Apr-2007 21:32:59			0.10	OTM-106
Titan-30	−3609.69	−1159.26	12-May-2007 20:09:59	−1.30	4.00		OTM-109
Titan-32	−3487.51	−1524.80	13-Jun-2007 17:46:12	9.40	4.10		OTM-115
Titan-34	530.95	−4127.55	19-Jul-2007 01:11:21			0.39	OTM-121
Enceladus-5	68.19	267.25	09-Oct-2008 19:06:40			0.02	OTM-166
Titan-61	2801.51	−2607.11	25-Aug-2009 12:51:39	2.00	14.00		OTM-213
Titan-73	8682.89	−6413.18	11-Nov-2010 13:37:01	4.50	1.50		OTM-265
Enceladus-13	−297.40	7.00	21-Dec-2010 01:08:26			0.70	OTM-270
Rhea-3	826.35	158.37	11-Jan-2011 04:53:25	−5.00	−5.00		OTM-274
Titan-75	5026.68	−11912.22	19-Apr-2011 05:00:39	−12.00	−5.00		OTM-280
Titan-76	2128.65	−4228.96	08-May-2011 22:53:45			−0.40	OTM-283
Titan-77	1922.11	−3758.27	20-Jun-2011 18:32:01			−0.40	OTM-286
Titan-80	32167.96	−2828.99	02-Jan-2012 15:13:38	93.90	−51.50		OTM-304
Enceladus-17	279.90	160.06	27-Mar-2012 18:30:09			0.30	OTM-313
Enceladus-18	295.18	129.72	14-Apr-2012 14:01:38	−1.80	3.50		OTM-316
Titan-90	3534.49	−2394.42	05-Apr-2013 21:43:32			−0.30	OTM-346
Titan-91	−3211.28	−2098.69	23-May-2013 17:32:56			−0.20	OTM-349
Titan-94	−741.84	−4203.28	12-Sep-2013 07:43:57	2.00	3.00		OTM-358
Titan-96	4198.46	−767.96	01-Dec-2013 00:41:20			−0.25	OTM-364
Titan-101	2128.65	−5473.63	17-May-2014 16:12:16	0.75	2.50		OTM-379
Titan-105	−2011.39	3769.93	22-Sep-2014 05:23:20	−1.00	1.00		OTM-391
Titan-107	−3823.78	473.77	10-Dec-2014 22:26:35			0.40	OTM-397
Titan-110	−5102.76	700.16	16-Mar-2015 14:29:49			−0.70	OTM-406
Titan-111	2700.26	4903.33	07-May-2015 22:50:24			−0.70	OTM-409
Titan-114	2663.63	−14563.62	13-Nov-2015 05:46:32		−5.00		OTM-429
Titan-116	4250.71	−405.23	01-Feb-2016 01:00:06			−0.20	OTM-439 BU
Titan-123	−3688.88	−2826.14	27-Sep-2016 04:16:59	−5.20	4.40		OTM-460
Titan-124	−4257.76	−1316.21	13-Nov-2016 23:55:56	−0.80		−0.20	OTM-463
Titan-126	−3719.84	992.12	22-Apr-2017 06:08:08	−0.90	0.50		OTM-469

A.3 Maneuver History

Of the 492 maneuvers designed during Cassini’s nearly twenty-year history, 360 were executed: 183 with the main engine (MEA) and 177 with the RCS thrusters. Tables A-5 to A-11 provide ΔV magnitudes for maneuvers performed or cancelled during interplanetary cruise (TCMs) and the Saturn tour (OTMs), grouped by each targeted encounter. In the tables, an orbit location description for each maneuver is given (e.g., number of days to next encounter), as well as the maneuver time in UTC SCET, the reference trajectory deterministic ΔV magnitude if non-zero, and the predicted ΔV statistics (mean, 1-sigma, and ΔV_{95}) which account for both maneuver and OD statistical variations. For performed maneuvers, the design and reconstructed ΔV magnitudes are also supplied, including the burn types (MEA or RCS). For maneuvers not performed, the status “cancelled” or “contingency” is instead given. Finally, the predicted ΔV magnitude error for an executed maneuver is computed by taking the absolute difference between the reconstructed and predicted ΔV mean magnitudes and dividing that quantity by the predicted ΔV 1-sigma value. This error shows how well the reconstructed ΔV s matched the predicted ΔV s.

Table A-5. Cassini Mission Maneuver History (TCMs 01-22, SOI, OTMs 001-046).

Maneuver	Orbit Location	Maneuver Time (UTC SCET)	Ref. Traj. Det. ΔV (m/s)	Predicted ΔV Statistics			Design ΔV (m/s)	Recon. ΔV (m/s)	Predicted ΔV Error (σ)*	Burn Type
				Mean (m/s)	1- σ (m/s)	ΔV 95 (m/s)				
TCM-01	Launch+25d	09-Nov-1997 20:00:00		3.24	—	5.88	2.7461	2.7770	—	MEA
TCM-02	Venus-1-60d	25-Feb-1998 20:00:00		0.35	—	0.89	0.1851	0.1788	—	RCS
TCM-03	Venus-1-18d	08-Apr-1998 20:00:00		0.06	—	0.13	CANCELLED			
TCM-04	Venus-1+18d	14-May-1998 20:00:00		0.47	—	1.25	CANCELLED			
TCM-05	DSM Venus-2-203d	03-Dec-1998 06:00:00	449.97	450.02	1.52	452.56	449.9739	450.2368	0.1426	MEA
TCM-06	Venus-2-140d	04-Feb-1999 20:00:00		11.67	0.04	11.74	11.5510	11.5516	2.9606	MEA
TCM-07	Venus-2-37d	18-May-1999 17:00:00	0.24	0.54	0.27	1.08	0.2386	0.2249	1.1669	RCS
TCM-08	Venus-2-14d	10-Jun-1999 18:00:00		0.05	0.03	0.10	CANCELLED			
TCM-09	Venus-2+12d	06-Jul-1999 17:00:00	47.33	52.01	11.82	75.44	43.5440	43.4996	0.7200	MEA
TCM-10	Earth-29d	19-Jul-1999 16:00:00		5.04	0.29	5.55	5.1328	5.1309	0.1755	MEA
TCM-11	Earth-15d	02-Aug-1999 21:30:00	36.89	36.89	0.15	37.12	36.3092	36.2876	4.0159	MEA
TCM-12	Earth-6d	11-Aug-1999 15:30:00	12.38	12.39	0.56	13.33	12.2564	12.2471	0.2552	MEA
TCM-13	Earth+14d	31-Aug-1999 16:00:00		30.48	15.96	61.1	6.7104	6.6835	1.4910	MEA
TCM-14	Jupiter-199d	14-Jun-2000 17:00:00	0.5457	0.58	0.012	0.60	0.5546	0.5386	3.4500	MEA
TCM-15	Jupiter-80d	11-Oct-2000 00:00:00		0.11	0.048	0.20	CANCELLED			
TCM-16	Jupiter-23d	07-Dec-2000 00:00:00		—	—	—	CANCELLED			
TCM-17	Jupiter+60d	28-Feb-2001 17:29:50	0.5000	0.84	—	1.03	0.5123	0.5286	—	MEA
TCM-18	SOI-819d	03-Apr-2002 18:00:00		0.8665	0.0105	0.8836	0.9007	0.8968	2.8857	MEA
TCM-19	SOI-426d	01-May-2003 20:00:00	1.3661	1.4633	0.3440	2.0842	1.5983	1.5965	0.3874	MEA
TCM-19a	SOI-294d	10-Sep-2003 20:00:00	0.1200	0.1200	0.0043	0.1269	0.1200	0.1230	0.6852	RCS
TCM-19b	SOI-273d	02-Oct-2003 04:00:00	2.0000	2.0002	0.0107	2.0180	2.0000	2.0217	2.0083	MEA
TCM-20	Phoebe-15d	27-May-2004 22:26:00	35.8893	34.6420	1.5769	37.2655	34.7319	34.7098	0.0430	MEA
TCM-21	SOI-14d	16-Jun-2004 21:07:00		7.2223	1.9876	10.5601	3.7048	3.6968	1.7739	MEA
TCM-22	SOI-9d	21-Jun-2004 20:52:00		—	—	—	CONTINGENCY			
Saturn Orbit Insertion (SOI)		01-Jul-2004 01:12:08	626.3533	630.551	1.2527	632.610	625.6161	626.7153	2.9943	MEA
OTM-001	SOI+2d	03-Jul-2004 20:06:00		5.3442	3.9293	10.7605	CANCELLED			
OTM-001a	SOI+17d	17-Jul-2004 19:21:00		—	—	—	CONTINGENCY			
OTM-002	PRM Ta-63d	23-Aug-2004 15:53:00	391.7300	391.752	1.0049	393.067	392.9517	393.0521	1.2937	MEA
OTM-003	LCU Ta-48d	07-Sep-2004 16:30:00		2.5162	1.2351	4.2081	0.5065	0.5123	1.6224	MEA
OTM-004	LCU Ta-3d	23-Oct-2004 06:16:00		1.0749	0.7526	2.1404	0.3723	0.3831	0.9191	RCS
OTM-005	Ta+3d	29-Oct-2004 06:15:00		0.8347	0.6283	1.7297	0.6546	0.6464	0.2998	MEA
OTM-006	Tb-22d	21-Nov-2004 05:00:00	2.8701	0.3476	0.1912	0.6107	0.4196	0.4201	0.3792	MEA
OTM-007	Tb-3d	10-Dec-2004 03:06:00		0.1237	0.1012	0.2389	CANCELLED			
OTM-008	PTM Tb+4d	17-Dec-2004 01:22:00	11.8810	11.9308	0.0742	12.0270	11.9375	11.9286	0.0291	MEA
OTM-009	LCU Tc-22d	23-Dec-2004 00:52:00		0.1114	0.0738	0.2179	0.0176	0.0207	1.2307	RCS
OTM-010	ODM Tc-17d	28-Dec-2004 00:37:00	23.7333	23.7348	0.0842	23.8432	23.7852	23.7934	0.6958	MEA
OTM-010a	LCU Tc-10d	03-Jan-2005 23:38:00		0.1960	0.0906	0.3163	0.1347	0.1388	0.6314	RCS
OTM-011	Tc+2d	16-Jan-2005 09:20:00	21.8099	21.1993	0.0438	21.2552	21.6231	21.6330	9.9037	MEA
OTM-012	T3-18d	28-Jan-2005 07:08:00	19.0388	19.2940	0.1054	19.4324	18.7016	18.7096	5.5435	MEA
OTM-013	T3-3d	12-Feb-2005 06:07:00		0.8276	0.5356	1.5989	0.2058	0.2076	1.1577	RCS
OTM-014	T3+2d	18-Feb-2005 06:00:00	0.0019	0.5348	0.4371	1.1326	0.7224	0.7163	0.4153	MEA
OTM-015	E1-7d	02-Mar-2005 04:50:00	5.2426	2.8104	1.8330	5.4026	6.2586	6.2623	1.8831	MEA
OTM-016	E1-3d	06-Mar-2005 04:35:00		0.0661	0.0339	0.1111	CANCELLED			
OTM-017	E1+3d	12-Mar-2005 03:20:00	0.3580	0.6495	0.5385	1.4047	0.4514	0.4492	0.3719	MEA
OTM-018	T4-12d	19-Mar-2005 18:19:00	1.7164	1.7110	0.1395	1.8886	1.6234	1.6200	0.6519	MEA
OTM-019	T4-4d	28-Mar-2005 02:00:00		0.1106	0.0766	0.2172	CANCELLED			
OTM-020	T4+3d	04-Apr-2005 02:22:00	0.0022	1.2010	0.9797	2.5628	0.9270	0.9188	0.2881	MEA
OTM-021	T5-7d	10-Apr-2005 02:00:00	6.3311	6.3599	0.8114	7.4419	5.8704	5.8630	0.6124	MEA
OTM-022	T5-3d	14-Apr-2005 02:40:00		0.1178	0.0728	0.2202	0.0641	0.0648	0.7278	RCS
OTM-023	T5+3d	20-Apr-2005 00:59:00	0.0039	0.7285	1.1361	2.2604	CANCELLED			
OTM-024	E2-77d	29-Apr-2005 00:58:00	20.6159	20.5461	0.9494	21.7775	20.5692	20.5872	0.0433	MEA
OTM-025	E2-6d	08-Jul-2005 20:37:00		1.4341	1.0735	2.9465	0.3724	0.3659	0.9950	MEA
OTM-026	E2+20d	03-Aug-2005 11:50:00	2.6640	2.8739	1.2623	4.5399	2.6281	2.6217	0.1998	MEA
OTM-027	T6-12d	10-Aug-2005 13:21:00	2.4819	2.6390	0.2114	2.9034	2.4180	2.4164	1.0529	MEA
OTM-028	T6-4d	18-Aug-2005 11:00:00		0.1092	0.0755	0.2165	CANCELLED			
OTM-029	T6+3d	25-Aug-2005 17:08:00	0.0017	1.6626	1.2865	3.5140	1.4593	1.4528	0.1631	MEA
OTM-030	T7-8d	30-Aug-2005 18:43:00	14.8721	14.6058	0.2012	14.8309	14.3505	14.3566	1.2383	MEA
OTM-031	T7-4d	03-Sep-2005 17:30:00		0.1686	0.1000	0.3056	0.0631	0.0646	1.0404	RCS
OTM-032	T7+3d	10-Sep-2005 17:09:00	0.0070	2.5801	1.8609	5.0942	CANCELLED			
OTM-033	H1-6d	19-Sep-2005 16:40:00	27.9048	27.8225	0.6463	28.6794	27.9099	27.9299	0.1662	MEA
OTM-034	H1-3d	23-Sep-2005 07:45:00		0.4073	0.2282	0.7175	CANCELLED			
OTM-035	H1+3d	28-Sep-2005 16:11:00	0.0141	1.7096	1.2517	3.4878	0.2948	0.2963	1.1291	RCS
OTM-036	D1-10d	01-Oct-2005 14:26:00	0.2793	0.1656	0.1983	0.4337	CANCELLED			
OTM-037	D1-3d	08-Oct-2005 09:30:00		0.1685	0.1182	0.3376	CANCELLED			
OTM-038	D1+1d	12-Oct-2005 05:57:00	14.7892	14.8740	0.1207	15.0001	14.8287	14.8318	0.3499	MEA
OTM-039	T8-7d	21-Oct-2005 14:58:00	0.0098	0.7125	0.5315	1.4706	0.0905	0.0914	1.1687	RCS
OTM-040	T8-3d	25-Oct-2005 07:14:00		0.0613	0.0302	0.1026	CANCELLED			
OTM-041	T8+3d	31-Oct-2005 13:59:00	12.4227	12.5945	0.8505	13.7449	12.4159	12.4228	0.2019	MEA
OTM-042	R1-13d	13-Nov-2005 14:02:00	2.0851	2.2595	0.7842	3.2736	2.1282	2.1262	0.1700	MEA
OTM-043	R1-3d	23-Nov-2005 13:03:00		0.1552	0.0980	0.2948	0.0603	0.0604	0.9679	RCS
OTM-044	R1+1d	28-Nov-2005 04:15:00	0.2002	0.5260	0.3411	0.9889	0.2375	0.2409	0.8358	RCS
OTM-045	T9-15d	11-Dec-2005 11:35:00	0.0156	0.2253	0.1460	0.4295	CANCELLED			
OTM-046	T9-3d	23-Dec-2005 12:25:00		0.0785	0.0720	0.1508	CANCELLED			

* Predicted ΔV Magnitude Error = $|\text{Reconstructed } \Delta V - \text{Predicted } \Delta V \text{ Mean}| / \text{Predicted } \Delta V \text{ 1-}\sigma$

Table A-6. Cassini Mission Maneuver History (OTMs 047-118).

Maneuver	Orbit Location	Maneuver Time (UTC SCET)	Ref. Traj. Det. ΔV (m/s)	Predicted ΔV Statistics			Design ΔV (m/s)	Recon. ΔV (m/s)	Predicted ΔV Error (σ)*	Burn Type
				Mean (m/s)	1- σ (m/s)	ΔV_{95} (m/s)				
OTM-047	T9+3d	30-Dec-2005 02:47:00	0.0088	0.2600	0.1583	0.4515	0.1828	0.1816	0.4955	RCS
OTM-049	T10-3d	12-Jan-2006 09:23:00		0.2400	0.1696	0.4809	CANCELLED			
OTM-050	T10+3d	18-Jan-2006 08:37:00	0.0025	0.9155	0.6950	1.8597	CANCELLED			
OTM-051	T11-25d	02-Feb-2006 07:53:00	0.0027	0.3337	0.2272	0.6419	0.1862	0.1852	0.6538	RCS
OTM-052	T11-3d	24-Feb-2006 06:26:00		0.3404	0.3275	0.7597	CANCELLED			
OTM-053	T11+3d	02-Mar-2006 05:51:00	0.0164	0.7715	0.4684	1.4373	0.2649	0.2634	1.0847	RCS
OTM-055	T12-3d	16-Mar-2006 04:50:00		0.1024	0.0684	0.1963	CANCELLED			
OTM-056	T12+3d	22-Mar-2006 04:19:00	0.0004	0.6675	0.5162	1.3941	0.4671	0.4706	0.3813	MEA
OTM-057	T13-25d	06-Apr-2006 03:32:00	0.0820	0.3141	0.2136	0.6170	0.3704	0.3673	0.2494	MEA
OTM-058	T13-4d	27-Apr-2006 01:59:00		0.0750	0.0539	0.1519	0.0755	0.0786	0.0666	RCS
OTM-059	T13+3d	04-May-2006 01:28:00	0.0720	0.8795	0.5783	1.7038	0.5051	0.5101	0.6387	MEA
OTM-061	T14-2d	18-May-2006 00:41:00		0.3848	0.2847	0.7893	0.1184	0.1221	0.9227	RCS
OTM-062	T14+3d	23-May-2006 16:41:00	0.0091	0.4365	0.3413	0.9222	CANCELLED			
OTM-063	T15-24d	07-Jun-2006 23:24:00	1.8751	1.9802	0.2832	2.3872	1.9225	1.9160	0.2268	MEA
OTM-064	T15-3d	28-Jun-2006 22:07:00		0.1083	0.0762	0.2155	0.0679	0.0694	0.5104	RCS
OTM-065	T15+3d	05-Jul-2006 21:36:00	0.0323	0.9906	0.6045	1.8254	0.1374	0.1378	1.4108	RCS
OTM-067	T16-3d	18-Jul-2006 20:51:00		0.0785	0.0553	0.1540	CANCELLED			
OTM-068	T16+3d	24-Jul-2006 20:30:00	0.2028	0.2975	0.2812	0.7074	CANCELLED			
OTM-069	T17-37d	01-Aug-2006 20:05:00	5.5891	5.3797	0.1098	5.4778	5.4239	5.4198	0.3643	MEA
OTM-070	T17-3d	04-Sep-2006 18:21:00		0.1849	0.1338	0.3700	0.2277	0.2275	0.3182	RCS
OTM-071	T17+3d	10-Sep-2006 18:00:00	6.1694	7.0629	1.4369	8.9644	6.5742	6.5809	0.3354	MEA
OTM-072	T18-9d	14-Sep-2006 10:07:00	8.4368	8.4580	0.9822	9.7571	8.1681	8.1626	0.3008	MEA
OTM-073	T18-3d	20-Sep-2006 16:32:00		0.0557	0.0285	0.0946	CANCELLED			
OTM-074	T18+3d	26-Sep-2006 17:30:00	0.0029	0.2039	0.2751	0.5877	CANCELLED			
OTM-075	T19-8d	01-Oct-2006 09:08:00	6.0638	5.9564	0.1013	6.0551	6.4796	6.4738	5.1091	MEA
OTM-076	T19-3d	06-Oct-2006 16:24:00		0.0396	0.0212	0.0688	0.0400	0.0410	0.0645	RCS
OTM-077	T19+3d	12-Oct-2006 16:10:00	0.0056	0.4079	0.3143	0.8528	CANCELLED			
OTM-078	T20-8d	17-Oct-2006 15:40:00	0.1550	0.2751	0.1647	0.5017	0.8596	0.8475	3.4762	MEA
OTM-079	T20-3d	22-Oct-2006 15:26:00		0.0265	0.0155	0.0488	0.0620	0.0637	2.4000	RCS
OTM-080	T20+15d	09-Nov-2006 14:28:00	3.6686	3.8007	0.1582	3.9958	3.6712	3.6633	0.8690	MEA
OTM-081 BU	T21-15d	27-Nov-2006 13:15:00	0.0668	0.6353	0.4804	1.2982	0.2198	0.2203	0.8638	RCS
OTM-082	T21-3d	09-Dec-2006 12:32:00		0.0310	0.0186	0.0574	CANCELLED			
OTM-083	T21+3d	15-Dec-2006 12:03:00	0.0798	0.8263	0.2114	1.0938	0.8025	0.7914	0.1649	MEA
OTM-084	T22-8d	20-Dec-2006 11:48:00	6.8259	6.9592	0.0209	6.9867	6.8740	6.8667	4.4199	MEA
OTM-085	T22-3d	25-Dec-2006 11:34:00		0.0412	0.0226	0.0719	CANCELLED			
OTM-086	T22+3d	31-Dec-2006 11:05:00	0.0049	0.3060	0.2974	0.6376	0.4920	0.4952	0.6364	MEA
OTM-087	T23-8d	05-Jan-2007 10:50:00	1.5583	1.5434	0.1786	1.7471	1.6573	1.6491	0.5915	MEA
OTM-088	T23-3d	10-Jan-2007 10:20:00		0.0344	0.0211	0.0640	0.0417	0.0419	0.3568	RCS
OTM-089	T23+3d	16-Jan-2007 02:36:00	0.0152	0.2471	0.2153	0.5129	0.2135	0.2131	0.1577	RCS
OTM-090	T24-8d	21-Jan-2007 09:36:00	2.3266	2.3341	0.0856	2.4408	2.3942	2.3947	0.7079	MEA
OTM-091	T24-3d	26-Jan-2007 09:21:00		0.0381	0.0240	0.0713	0.0153	0.0150	0.9630	RCS
OTM-092	T24+3d	01-Feb-2007 08:52:00	0.0087	0.2277	0.2464	0.5968	CANCELLED			
OTM-093	T25-15d	07-Feb-2007 08:37:00	0.0082	0.3588	0.2927	0.7922	0.2822	0.2781	0.2756	MEA
OTM-094	T25-3d	19-Feb-2007 07:37:00		0.1118	0.0828	0.2256	0.0415	0.0414	0.8500	RCS
OTM-095	T25+3d	25-Feb-2007 07:22:00	0.0046	0.2430	0.2227	0.5428	CANCELLED			
OTM-096	T26-8d	02-Mar-2007 06:51:00	0.6141	0.6401	0.1050	0.7648	0.6651	0.6645	0.2322	MEA
OTM-097	T26-3d	06-Mar-2007 23:06:00		0.0513	0.0332	0.0986	CANCELLED			
OTM-098	T26+3d	13-Mar-2007 06:06:00	0.0029	0.5698	0.4563	1.1795	1.0765	1.0747	1.1066	MEA
OTM-099	T27-8d	18-Mar-2007 05:50:00	1.7898	1.7261	0.0725	1.8023	1.6188	1.6117	1.5784	MEA
OTM-100	T27-3d	22-Mar-2007 20:30:00		0.0691	0.0358	0.1184	0.0687	0.0695	0.0120	RCS
OTM-101	T27+3d	28-Mar-2007 20:49:00	0.0045	0.7093	0.5285	1.4254	0.5307	0.5404	0.3195	MEA
OTM-102	T28-8d	03-Apr-2007 04:34:00	2.6932	2.6916	0.1104	2.8328	2.7017	2.6939	0.0202	MEA
OTM-103	T28-3d	07-Apr-2007 20:48:00		0.0514	0.0258	0.0874	0.0375	0.0378	0.5256	RCS
OTM-104	T28+3d	14-Apr-2007 03:47:00	0.0033	0.7459	0.5919	1.5570	CANCELLED			
OTM-105	T29-8d	19-Apr-2007 03:32:00	3.5297	3.5359	0.1814	3.7439	3.5401	3.5325	0.0190	MEA
OTM-106	T29-3d	24-Apr-2007 03:16:00		0.0488	0.0265	0.0846	0.0157	0.0171	1.1976	RCS
OTM-107	T29+3d	30-Apr-2007 02:45:00	0.0031	0.7691	0.6347	1.6799	CANCELLED			
OTM-108	T30-8d	04-May-2007 19:00:00	5.8206	5.9090	0.2697	6.2078	5.5859	5.5829	1.2092	MEA
OTM-109	T30-4d	09-May-2007 02:14:00		0.0278	0.0157	0.0500	0.0244	0.0253	0.1581	RCS
OTM-110	T30+3d	16-May-2007 01:43:00	0.0053	1.4684	1.1014	3.0320	CANCELLED			
OTM-111	T31-8d	21-May-2007 01:27:00	5.5236	5.6983	0.3819	6.1590	5.5348	5.5339	0.4305	MEA
OTM-112	T31-3d	26-May-2007 01:12:00		0.0375	0.0224	0.0693	CANCELLED			
OTM-113	T31+3d	01-Jun-2007 00:41:00	0.0059	0.8573	0.6687	1.7769	0.6999	0.6985	0.2375	MEA
OTM-114	T32-8d	05-Jun-2007 16:55:00	12.1308	12.3466	0.3045	12.7373	12.2371	12.2366	0.3613	MEA
OTM-115	T32-3d	11-Jun-2007 00:10:00		0.0609	0.0397	0.1152	0.0372	0.0364	0.6175	RCS
OTM-116	T32+3d	16-Jun-2007 23:39:00	0.0069	1.3291	0.9919	2.7329	0.7542	0.7461	0.5877	MEA
OTM-117	T33-8d	21-Jun-2007 23:23:00	8.2086	8.4181	0.3446	8.8850	7.9682	7.9703	1.2995	MEA
OTM-118	T33-3d	26-Jun-2007 23:08:00		0.0462	0.0297	0.0876	0.0134	0.0132	1.1123	RCS

* Predicted ΔV Magnitude Error = $|\text{Reconstructed } \Delta V - \text{Predicted } \Delta V \text{ Mean}| / \text{Predicted } \Delta V \text{ 1-}\sigma$

Table A-7. Cassini Mission Maneuver History (OTMs 119-190).

Maneuver	Orbit Location	Maneuver Time (UTC SCET)	Ref. Traj. Det. ΔV (m/s)	Predicted ΔV Statistics			Design ΔV (m/s)	Recon. ΔV (m/s)	Predicted ΔV Error (σ)*	Burn Type
				Mean (m/s)	1- σ (m/s)	ΔV_{95} (m/s)				
OTM-119	T33+3d	03-Jul-2007 22:37:00	0.0086	0.9388	0.6457	1.8382	0.0229	0.0243	1.4164	RCS
OTM-121	T34-3d	15-Jul-2007 22:06:00		0.0253	0.0118	0.0417	0.0135	0.0137	0.9824	RCS
OTM-122	T34+3d	21-Jul-2007 21:36:00	0.0074	1.0373	0.7444	2.0952	CANCELLED			
OTM-123 BU	T35-24d	06-Aug-2007 20:35:00	0.0054	0.3790	0.2381	0.7093	0.4306	0.4268	0.2009	MEA
OTM-124	T35-3d	27-Aug-2007 19:20:00		0.0899	0.0656	0.1814	CANCELLED			
OTM-125	T35+2d	02-Sep-2007 11:35:00	0.0015	0.4800	0.3008	0.8799	0.4869	0.4879	0.0262	MEA
OTM-127	I1-2d	08-Sep-2007 18:50:00		0.0747	0.0402	0.1288	CANCELLED			
OTM-128	I1+3d	13-Sep-2007 18:20:00	13.4294	10.1319	1.1694	11.4840	13.4823	13.4700	2.8546	MEA
OTM-129	T36-14d	17-Sep-2007 18:21:00	0.0008	2.9947	0.9771	4.3472	0.1028	0.1029	2.9595	RCS
OTM-130	T36-3d	28-Sep-2007 17:36:00		0.0526	0.0334	0.0999	0.0235	0.0242	0.8488	RCS
OTM-131	T36+3d	05-Oct-2007 17:22:00	1.3849	1.6261	0.2635	1.9638	1.3310	1.3270	1.1350	MEA
OTM-132	T37-17d	01-Nov-2007 15:40:00	1.0836	1.0622	0.1570	1.2663	0.9819	0.9770	0.5430	MEA
OTM-133	T37-3d	15-Nov-2007 14:56:00		0.0644	0.0463	0.1310	0.0668	0.0675	0.0668	RCS
OTM-134	T37+3d	22-Nov-2007 06:57:00	1.3156	1.1724	0.7445	2.1623	1.1717	1.1727	0.0004	MEA
OTM-135	T38-8d	27-Nov-2007 06:43:00	15.6608	15.8417	0.1390	16.0261	15.7637	15.7621	0.5722	MEA
OTM-136	T38-2d	02-Dec-2007 13:44:00		0.0834	0.0545	0.1615	0.0184	0.0195	1.1730	RCS
OTM-137	T38+3d	08-Dec-2007 06:00:00	0.0009	0.8972	0.7201	1.9063	0.6799	0.6809	0.3004	MEA
OTM-138	T39-8d	13-Dec-2007 07:10:00	9.7604	9.5774	0.1568	9.7519	9.6426	9.6361	0.3744	MEA
OTM-139	T39-3d	18-Dec-2007 05:16:00		0.0493	0.0315	0.0929	0.0136	0.0137	1.1320	RCS
OTM-140	T39+3d	24-Dec-2007 05:02:00	0.0093	0.8670	0.8073	2.0073	CANCELLED			
OTM-141	T40-7d	29-Dec-2007 12:02:00	2.0416	1.9196	0.2377	2.1846	2.0524	2.0464	0.5334	MEA
OTM-142	T40-3d	03-Jan-2008 04:18:00		0.0285	0.0157	0.0496	CANCELLED			
OTM-143	T40+10d	16-Jan-2008 04:15:00	2.8842	2.8885	0.2001	3.1500	2.8807	2.8786	0.0493	MEA
OTM-144	T41-17d	06-Feb-2008 02:06:00	37.6436	37.6146	0.3428	38.0850	37.3966	37.4063	0.6078	MEA
OTM-145	T41-3d	19-Feb-2008 08:36:00		0.2389	0.1777	0.4877	0.2986	0.2911	0.2938	MEA
OTM-146	T41+8d	01-Mar-2008 22:56:00	6.4197	6.6024	0.3033	7.0450	7.0276	7.0206	1.3788	MEA
OTM-147	E3-5d	07-Mar-2008 07:21:00	0.0239	0.6298	0.5214	1.3030	1.1210	1.1204	0.9411	MEA
OTM-148	E3-3d	10-Mar-2008 07:06:00		0.0483	0.0289	0.0887	CANCELLED			
OTM-149	E3+1d	13-Mar-2008 23:21:00	1.2406	2.8401	0.1117	2.9901	2.7599	2.7529	0.7809	MEA
OTM-150	T42-7d	18-Mar-2008 06:35:00	0.0327	0.1036	0.0610	0.1868	0.0540	0.0552	0.7925	RCS
OTM-151	T42-3d	22-Mar-2008 22:50:00		0.0113	0.0064	0.0194	CANCELLED			
OTM-152	T42+16d	11-Apr-2008 01:04:00	3.9968	3.3867	0.3952	3.8127	3.3287	3.3273	0.1504	MEA
OTM-153	T43-16d	26-Apr-2008 03:47:00	0.0093	1.3034	1.6215	3.8146	0.5122	0.5153	0.4860	MEA
OTM-154	T43-3d	09-May-2008 03:00:00		0.0320	0.0240	0.0654	CANCELLED			
OTM-155	T43+5d	17-May-2008 01:20:00	1.0659	1.0188	0.2971	1.3288	1.1762	1.1728	0.5183	MEA
OTM-156	T44-6d	22-May-2008 02:13:00	0.0079	0.8754	0.8210	2.0338	0.1963	0.1958	0.8278	RCS
OTM-157	T44-3d	25-May-2008 01:58:00		0.0137	0.0080	0.0246	CANCELLED			
OTM-158	T44+4d	01-Jun-2008 00:27:00	0.1384	0.3657	0.4224	0.9771	CANCELLED			
OTM-159	T45-38d	23-Jun-2008 06:24:00	11.8213	12.1195	0.2330	12.4107	12.1850	12.1793	0.2565	MEA
OTM-160	T45-3d	27-Jul-2008 14:36:00		0.3170	0.2404	0.6651	0.1730	0.1695	0.6138	RCS
OTM-162	T45+4d	03-Aug-2008 22:15:00	2.6671	2.8240	0.4376	3.3869	2.5405	2.5391	0.6513	MEA
OTM-163	E4-3d	08-Aug-2008 21:20:00		0.1352	0.0876	0.2570	CANCELLED			
OTM-164	E4+11d	23-Aug-2008 02:49:00	14.3484	14.2134	1.3128	15.8442	13.5277	13.5181	0.5296	MEA
OTM-164a	E5-19d	20-Sep-2008 18:49:00		1.0859	0.8704	2.3353	0.8933	0.8813	0.2351	MEA
OTM-165	E5-7d	02-Oct-2008 10:19:00	3.8059	3.6096	0.2155	3.8902	3.9372	3.9348	1.5086	MEA
OTM-166	E5-3d	06-Oct-2008 18:05:00		0.2041	0.1317	0.3873	0.0145	0.0149	1.4365	RCS
OTM-167	E5+3d	12-Oct-2008 23:51:00	3.1194	3.3132	0.2025	3.6032	3.3396	3.3367	0.1158	MEA
OTM-168	T46-17d	17-Oct-2008 09:10:00	7.1441	7.1885	0.1008	7.3159	6.9929	6.9881	1.9885	MEA
OTM-169	T46-5d	29-Oct-2008 16:37:00		0.1333	0.0978	0.2726	0.2320	0.2248	0.9352	RCS
OTM-170	T46+5d	08-Nov-2008 22:23:00	8.3960	8.3729	0.2881	8.7467	9.1002	9.0973	2.5140	MEA
OTM-171	T47-7d	12-Nov-2008 22:09:00	0.1366	1.3547	1.1086	2.8075	5.1554	5.1495	3.4230	MEA
OTM-172	T47-3d	16-Nov-2008 08:09:00		0.0191	0.0107	0.0334	CANCELLED			
OTM-173	T47+4d	23-Nov-2008 21:25:00	0.7270	0.9705	0.1967	1.2665	0.7870	0.7789	0.9740	MEA
OTM-174	T48-8d	27-Nov-2008 21:10:00	0.1111	0.9125	0.7356	1.9345	CANCELLED			
OTM-175	T48-4d	01-Dec-2008 20:56:00		0.0154	0.0096	0.0286	0.0684	0.0677	5.4553	RCS
OTM-176	T48+4d	09-Dec-2008 20:27:00	2.9374	3.2866	0.2924	3.7072	3.0383	3.0339	0.8642	MEA
OTM-177	T49-8d	13-Dec-2008 20:13:00	0.1538	1.6131	0.7100	2.5490	1.6275	1.6197	0.0092	MEA
OTM-178	T49-4d	17-Dec-2008 19:58:00		0.0252	0.0133	0.0432	0.0264	0.0265	0.0999	RCS
OTM-179	T49+3d	24-Dec-2008 19:44:00	0.0291	0.4446	0.3331	0.9203	CANCELLED			
OTM-180	T50-14d	24-Jan-2009 03:48:00	4.7331	5.0872	0.4471	5.6936	4.6727	4.6699	0.9332	MEA
OTM-181	T50-3d	04-Feb-2009 10:34:00		0.0611	0.0449	0.1249	CANCELLED			
OTM-182	T50+3d	10-Feb-2009 10:04:00	0.0171	0.4586	0.3431	0.9337	0.3704	0.3637	0.2767	MEA
OTM-183	T51-18d	09-Mar-2009 08:20:00	5.0493	5.2923	0.4477	5.9061	5.0259	5.0226	0.6025	MEA
OTM-183x	T51-9d	18-Mar-2009 00:05:00		—	—	—	0.0203	0.0218		RCS
OTM-184	T51-3d	24-Mar-2009 07:20:00		0.0838	0.0622	0.1720	CANCELLED			
OTM-186	T51+2d	29-Mar-2009 13:05:00	0.0159	1.3039	0.8333	2.4488	0.7528	0.7482	0.6668	MEA
OTM-186a	T52-3d	01-Apr-2009 06:35:00		—	—	—	CONTINGENCY			
OTM-188	T52+3d	07-Apr-2009 06:19:00	0.0234	0.2401	0.2404	0.5748	CANCELLED			
OTM-189	T53-8d	12-Apr-2009 12:04:00	6.9771	6.9657	0.1123	7.0842	7.1281	7.1237	1.4070	MEA
OTM-190	T53-3d	17-Apr-2009 05:33:00		0.0380	0.0241	0.0715	CANCELLED			

* Predicted ΔV Magnitude Error = $| \text{Reconstructed } \Delta V - \text{Predicted } \Delta V \text{ Mean} | / \text{Predicted } \Delta V \text{ 1-}\sigma$

Table A-8. Cassini Mission Maneuver History (OTMs 191-262).

Maneuver	Orbit Location	Maneuver Time (UTC SCET)	Ref. Traj. Det. ΔV (m/s)	Predicted ΔV Statistics			Design ΔV (m/s)	Recon. ΔV (m/s)	Predicted ΔV Error (σ)*	Burn Type
				Mean (m/s)	1- σ (m/s)	ΔV 95 (m/s)				
OTM-191	T53+3d	23-Apr-2009 05:03:00	0.0042	0.0543	0.0657	0.1520	CANCELLED			
OTM-192	T54-7d	28-Apr-2009 11:02:00	2.2665	2.2623	0.0590	2.3493	2.4913	2.4860	3.7890	MEA
OTM-193	T54-3d	02-May-2009 21:02:00		0.0290	0.0164	0.0514	CANCELLED			
OTM-194	T54+3d	09-May-2009 04:01:00	0.0004	0.1290	0.1309	0.3158	CANCELLED			
OTM-195	T55-7d	14-May-2009 10:00:00	2.2524	2.2513	0.0800	2.3428	2.2289	2.2224	0.3615	MEA
OTM-196	T55-3d	18-May-2009 19:45:00		0.0273	0.0155	0.0486	0.0469	0.0444	1.1064	RCS
OTM-197	T55+3d	25-May-2009 02:59:00	0.0134	0.2691	0.2244	0.5889	CANCELLED			
OTM-198	T56-7d	30-May-2009 08:58:00	1.1321	1.1127	0.2332	1.3877	1.4689	1.4630	1.5022	MEA
OTM-199	T56-3d	03-Jun-2009 18:42:00		0.0249	0.0132	0.0431	CANCELLED			
OTM-200	T56+3d	10-Jun-2009 08:12:00	2.0051	1.9233	0.3199	2.2592	2.1457	2.1396	0.6762	MEA
OTM-201	T57-8d	15-Jun-2009 01:26:00	0.0074	0.1787	0.2461	0.5412	0.0299	0.0296	0.6055	RCS
OTM-202	T57-3d	19-Jun-2009 17:40:00		0.0212	0.0120	0.0370	CANCELLED			
OTM-203	T57+4d	26-Jun-2009 07:09:00	2.4433	2.3813	0.3319	2.7064	2.4248	2.4245	0.1301	MEA
OTM-204	T58-8d	01-Jul-2009 00:24:00	0.0097	0.1803	0.2975	0.6037	0.0159	0.0162	0.5518	RCS
OTM-205	T58-3d	05-Jul-2009 16:38:00		0.0224	0.0118	0.0383	CANCELLED			
OTM-206	T58+4d	12-Jul-2009 16:22:00	3.5290	3.4757	0.2834	3.7018	3.5179	3.5129	0.1314	MEA
OTM-207	T59-7d	17-Jul-2009 15:52:00	0.0065	0.1540	0.3064	0.5462	0.0324	0.0318	0.3988	RCS
OTM-208	T59-3d	21-Jul-2009 15:36:00		0.0195	0.0099	0.0330	CANCELLED			
OTM-209	T59+4d	28-Jul-2009 15:21:00	6.3182	5.0880	0.8192	6.3229	6.2957	6.2945	1.4727	MEA
OTM-210	T60-8d	01-Aug-2009 22:35:00	0.0058	1.5256	0.9135	2.7067	0.0224	0.0226	1.6453	RCS
OTM-211	T60-3d	06-Aug-2009 22:05:00		0.0287	0.0148	0.0485	CANCELLED			
OTM-212	T60+4d	13-Aug-2009 21:49:00	0.0065	1.1670	1.7522	3.8969	CANCELLED			
OTM-213	T61-9d	16-Aug-2009 14:04:00	13.0166	12.0797	1.5720	13.1180	13.0040	13.0018	0.5866	MEA
OTM-214	T61-3d	22-Aug-2009 03:34:00		0.0628	0.0357	0.1117	CANCELLED			
OTM-215	T61+4d	29-Aug-2009 13:19:00	0.0071	0.6914	0.6495	1.6314	0.5136	0.5149	0.2718	MEA
OTM-216	T62-37d	05-Sep-2009 02:48:00	4.7319	4.6122	0.2189	4.7798	4.4801	4.4757	0.6233	MEA
OTM-217	T62-3d	09-Oct-2009 11:04:00		0.1113	0.0771	0.2180	0.1505	0.1457	0.4462	RCS
OTM-218	T62+4d	16-Oct-2009 00:34:00	0.0034	0.2744	0.3970	0.8026	0.8515	0.8441	1.4349	MEA
OTM-219	E7-12d	21-Oct-2009 00:04:00	4.6851	4.8967	0.5125	5.5251	4.1688	4.1621	1.4334	MEA
OTM-220	E7-3d	29-Oct-2009 23:35:00		0.0575	0.0339	0.1044	0.0677	0.0669	0.2788	RCS
OTM-221	E7+3d	05-Nov-2009 09:20:00	0.0178	0.4290	0.3373	0.9062	0.3120	0.3026	0.3749	MEA
OTM-222	E8-9d	12-Nov-2009 09:06:00	0.0072	0.5580	0.5972	1.4284	CANCELLED			
OTM-223	E8-3d	17-Nov-2009 22:37:00		0.0277	0.0144	0.0473	CANCELLED			
OTM-224	E8+2d	22-Nov-2009 22:22:00	2.3821	2.2322	0.1365	2.4074	2.5564	2.5532	2.3517	MEA
OTM-225	T63-8d	04-Dec-2009 07:39:00	0.0146	0.9435	0.6464	1.8610	0.2016	0.1991	1.1516	RCS
OTM-226	T63-3d	08-Dec-2009 21:24:00		0.0208	0.0110	0.0358	CANCELLED			
OTM-227	T63+3d	15-Dec-2009 06:55:00	0.0035	0.3152	0.2753	0.7033	0.7187	0.7161	1.4561	MEA
OTM-228	T64-8d	20-Dec-2009 06:41:00	2.2642	2.1736	0.0639	2.2380	2.2312	2.2249	0.8033	MEA
OTM-229	T64-3d	24-Dec-2009 20:26:00		0.0220	0.0132	0.0405	CANCELLED			
OTM-230	T64+3d	31-Dec-2009 05:57:00	0.0054	0.3799	0.3723	0.9041	CANCELLED			
OTM-231	T65-8d	05-Jan-2010 05:43:00	8.1293	7.9962	0.0699	8.0675	8.0498	8.0536	0.8198	MEA
OTM-232	T65-3d	09-Jan-2010 19:29:00		0.0354	0.0223	0.0667	0.0359	0.0354	0.0011	RCS
OTM-233	T65+3d	16-Jan-2010 04:59:00	0.0013	1.8565	0.6907	2.8113	2.2699	2.2660	0.5929	MEA
OTM-234	T66-8d	21-Jan-2010 04:45:00	6.8959	6.2331	0.1721	6.4550	6.0720	6.0749	0.9190	MEA
OTM-235	T66-3d	25-Jan-2010 18:16:00		0.0297	0.0188	0.0562	CANCELLED			
OTM-236	T66+3d	01-Feb-2010 04:01:00	6.1061	6.1083	0.0394	6.1601	6.2029	6.1970	2.2534	MEA
OTM-237	R2-7d	23-Feb-2010 16:33:00	0.0364	0.0548	0.0234	0.0864	0.0150	0.0160	1.6627	RCS
OTM-238	R2-3d	27-Feb-2010 16:19:00		0.0208	0.0099	0.0342	CANCELLED			
OTM-239	R2+8d	11-Mar-2010 01:34:00	1.0870	1.2410	0.3444	1.7046	CANCELLED			
OTM-240	D2-12d	26-Mar-2010 14:19:00	1.5435	1.7258	0.4377	2.3343	3.0017	3.0023	2.9163	MEA
OTM-241	D2-5d	02-Apr-2010 13:49:00		0.0326	0.0155	0.0534	0.0342	0.0339	0.0821	RCS
OTM-242	D2+4d	10-Apr-2010 23:19:00	9.0915	9.1070	0.0445	9.1661	9.0417	9.0441	1.4139	MEA
OTM-243	E9-9d	18-Apr-2010 12:33:00	0.0985	0.0360	0.0242	0.0706	0.0447	0.0449	0.3670	RCS
OTM-244	E9-3d	24-Apr-2010 22:18:00		0.0324	0.0203	0.0605	CANCELLED			
OTM-245	E9+2d	29-Apr-2010 11:47:00	5.8063	5.8005	0.1148	5.9463	5.7144	5.7158	0.7381	MEA
OTM-246	T68-9d	11-May-2010 11:01:00	8.8145	8.8330	0.0642	8.9181	8.8841	8.8811	0.7493	MEA
OTM-247	T68-4d	16-May-2010 04:31:00		0.0719	0.0373	0.1228	CANCELLED			
OTM-248	T68+3d	23-May-2010 10:15:00	0.0039	1.0274	0.7994	2.1514	0.8523	0.8450	0.2281	MEA
OTM-249	T69-8d	28-May-2010 09:44:00	11.0492	10.7615	0.2178	11.0096	10.7673	10.7657	0.0195	MEA
OTM-250	T69-3d	01-Jun-2010 19:44:00		0.0449	0.0287	0.0852	0.0368	0.0365	0.2927	RCS
OTM-251	T69+3d	08-Jun-2010 02:43:00	0.0057	0.7103	0.5119	1.4260	CANCELLED			
OTM-252	T70-8d	13-Jun-2010 08:42:00	1.2442	1.0855	0.1204	1.2209	1.2393	1.2420	1.2994	MEA
OTM-253	T70-3d	18-Jun-2010 02:11:00		0.0259	0.0160	0.0484	0.0249	0.0252	0.0440	RCS
OTM-254	T70+3d	24-Jun-2010 07:56:00	0.0073	0.7322	0.5324	1.4629	0.8744	0.8701	0.2591	MEA
OTM-255	T71-7d	30-Jun-2010 07:40:00	6.6961	6.5050	0.1481	6.6672	6.2579	6.2555	1.6852	MEA
OTM-256	T71-3d	04-Jul-2010 01:09:00		0.0329	0.0199	0.0607	0.0218	0.0228	0.5044	RCS
OTM-257	T71+3d	10-Jul-2010 06:53:00	0.0100	0.5803	0.4300	1.1782	0.8380	0.8319	0.5853	MEA
OTM-258	E11-27d	18-Jul-2010 06:37:00	6.9309	6.8227	0.0922	6.9233	6.7704	6.7651	0.6251	MEA
OTM-259	E11-3d	10-Aug-2010 22:35:00		0.0833	0.0569	0.1628	CANCELLED			
OTM-260	E11+3d	17-Aug-2010 04:49:00	0.0039	0.0749	0.0637	0.1639	CANCELLED			
OTM-261	T72-22d	03-Sep-2010 03:33:00	2.2994	2.3337	0.0701	2.4259	2.4395	2.4376	1.4828	MEA
OTM-261a	T72-9d	16-Sep-2010 02:47:00		0.0869	0.0649	0.1778	0.1763	0.1748	1.3540	RCS
OTM-262	T72-3d	21-Sep-2010 12:47:00		0.0171	0.0090	0.0291	CANCELLED			

* Predicted ΔV Magnitude Error = $|\text{Reconstructed } \Delta V - \text{Predicted } \Delta V \text{ Mean}| / \text{Predicted } \Delta V \text{ 1-}\sigma$

Table A-9. Cassini Mission Maneuver History (OTMs 263-334).

Maneuver	Orbit Location	Maneuver Time (UTC SCET)	Ref. Traj. Det. ΔV (m/s)	Predicted ΔV Statistics			Design ΔV (m/s)	Recon. ΔV (m/s)	Predicted ΔV Error (σ)*	Burn Type
				Mean (m/s)	1- σ (m/s)	ΔV 95 (m/s)				
OTM-263	T72+3d	28-Sep-2010 02:02:00	0.0019	0.0868	0.0709	0.1854	CANCELLED			
OTM-264	T73-28d	15-Oct-2010 01:02:00	0.0022	0.0412	0.0302	0.0818	0.1818	0.1773	4.5027	RCS
OTM-265	T73-3d	08-Nov-2010 09:49:00		0.1312	0.0977	0.2670	0.1721	0.1669	0.3653	RCS
OTM-266	T73+3d	14-Nov-2010 23:19:00	0.0016	0.4514	0.3922	0.9946	CANCELLED			
OTM-267	E12-9d	21-Nov-2010 23:05:00	2.3169	1.9803	0.3177	2.2758	2.2497	2.2488	0.8451	MEA
OTM-268	E12-3d	27-Nov-2010 16:20:00		0.0573	0.0333	0.1026	0.0647	0.0651	0.2350	RCS
OTM-269 BU	E12+1d	01-Dec-2010 22:21:00	0.0007	0.0702	0.0518	0.1411	0.1626	0.1618	1.7685	RCS
OTM-270	E13-12d	08-Dec-2010 22:07:00	0.0361	0.0882	0.0433	0.1483	0.0158	0.0164	1.6581	RCS
OTM-271	E13-3d	17-Dec-2010 21:23:00		0.0226	0.0118	0.0386	CANCELLED			
OTM-272	E13+3d	24-Dec-2010 07:09:00	0.0023	0.1051	0.0835	0.2212	CANCELLED			
OTM-273	R3-10d	01-Jan-2011 06:40:00	0.0033	0.1883	0.2357	0.5290	0.2098	0.2076	0.0820	RCS
OTM-274	R3-3d	08-Jan-2011 06:26:00		0.0175	0.0108	0.0307	0.0344	0.0343	1.5596	RCS
OTM-275	R3+3d	14-Jan-2011 13:27:00	2.6392	2.5621	0.1505	2.6657	2.7661	2.7625	1.3318	MEA
OTM-276	T74-17d	01-Feb-2011 04:44:00	0.0076	0.4548	0.6738	1.4428	0.0202	0.0214	0.6432	RCS
OTM-277	T74-3d	15-Feb-2011 17:46:00		0.0701	0.0547	0.1423	CANCELLED			
OTM-278	T74+3d	22-Feb-2011 03:31:00	0.0005	0.2632	0.1787	0.5165	CANCELLED			
OTM-279	T75-48d	02-Mar-2011 10:17:00	0.0024	0.1408	0.0799	0.2497	0.1004	0.1002	0.5080	RCS
OTM-280	T75-3d	15-Apr-2011 23:48:00		0.1035	0.0777	0.2138	0.0201	0.0217	1.0536	RCS
OTM-281	T75+3d	22-Apr-2011 06:48:00	0.0016	0.2416	0.1598	0.4670	0.0425	0.0419	1.2497	RCS
OTM-282	T76-10d	29-Apr-2011 06:18:00	0.0019	0.0409	0.0353	0.0921	CANCELLED			
OTM-283	T76-3d	05-May-2011 22:17:00		0.0173	0.0113	0.0333	0.0141	0.0147	0.2344	RCS
OTM-284	T76+3d	12-May-2011 05:32:00	0.0119	0.7218	0.5695	1.5241	0.1211	0.1197	1.0571	RCS
OTM-285	T77-28d	24-May-2011 04:46:00	0.0084	0.3533	0.2592	0.7223	0.0365	0.0366	1.2221	RCS
OTM-286	T77-3d	17-Jun-2011 02:57:00		0.0523	0.0458	0.1157	0.0149	0.0155	0.8046	RCS
OTM-287	T77+3d	24-Jun-2011 08:42:00	0.0057	0.9228	0.6387	1.8304	0.1456	0.1446	1.2183	RCS
OTM-288	T78-20d	22-Aug-2011 15:04:00	0.0112	0.1373	0.1028	0.2803	0.0925	0.0922	0.4385	RCS
OTM-288a	T78-10d	01-Sep-2011 22:03:00		0.0149	0.0117	0.0303	CANCELLED			
OTM-289	T78-3d	09-Sep-2011 03:48:00		0.0183	0.0093	0.0308	CANCELLED			
OTM-290	T78+3d	15-Sep-2011 13:47:00	0.0125	0.0024	0.0112	0.0027	CANCELLED			
OTM-291	E14-11d	20-Sep-2011 03:17:00	4.9645	4.9364	0.0855	5.0430	5.0542	5.0538	1.3728	MEA
OTM-292	E14-3d	28-Sep-2011 13:02:00		0.0547	0.0373	0.1075	0.0330	0.0329	0.5860	RCS
OTM-294	E14+4d	05-Oct-2011 02:17:00	0.0135	0.1419	0.1014	0.2862	0.0746	0.0747	0.6629	RCS
OTM-295	E15-9d	10-Oct-2011 02:01:00		0.0071	0.0041	0.0120	CANCELLED			
OTM-296	E15+3d	21-Oct-2011 01:31:00	0.0110	0.0074	0.0057	0.0151	CANCELLED			
OTM-297	E16-9d	28-Oct-2011 11:17:00	0.0057	0.0117	0.0045	0.0177	0.0459	0.0463	7.6648	RCS
OTM-298	E16-3d	03-Nov-2011 00:47:00		0.0149	0.0073	0.0248	CANCELLED			
OTM-299	E16+3d	09-Nov-2011 00:17:00	2.1920	2.2513	0.0905	2.3689	2.0879	2.0864	1.8223	MEA
OTM-300	T79-20d	24-Nov-2011 05:18:00	2.9481	3.0955	0.1788	3.3125	2.9755	2.9756	0.6711	MEA
OTM-300a	T79-12d	01-Dec-2011 23:04:00		0.0461	0.0330	0.0920	0.0207	0.0218	0.7358	RCS
OTM-301	T79-4d	09-Dec-2011 08:49:00		0.0176	0.0090	0.0300	0.0177	0.0190	0.1581	RCS
OTM-303	T79+4d	17-Dec-2011 08:20:00	0.0318	1.7635	1.2778	3.5254	0.5127	0.5071	0.9832	MEA
OTM-304	T80-11d	22-Dec-2011 21:51:00		0.0122	0.0066	0.0214	0.0164	0.0168	0.6987	RCS
OTM-306	T81-14d	16-Jan-2012 06:39:00	0.0056	0.1183	0.0662	0.2400	0.0492	0.0501	1.0283	RCS
OTM-308	T81+4d	03-Feb-2012 05:27:00	0.0086	0.1135	0.0641	0.2320	0.1359	0.1363	0.3563	RCS
OTM-309	T82-9d	10-Feb-2012 12:28:00	0.0081	0.0086	0.0052	0.0165	CANCELLED			
OTM-310 BU	T82-2d	17-Feb-2012 04:29:00		0.0171	0.0098	0.0360	0.0197	0.0205	0.3392	RCS
OTM-311	T82+4d	23-Feb-2012 04:14:00	0.0259	0.1464	0.1576	0.4662	CANCELLED			
OTM-312	E17-18d	10-Mar-2012 03:01:00	3.4998	3.6176	0.1230	3.8760	3.5749	3.5646	0.4306	MEA
OTM-312a	E17-12d	16-Mar-2012 02:46:00		0.0373	0.0275	0.0907	0.1047	0.1040	2.4233	RCS
OTM-313	E17-3d	24-Mar-2012 16:02:00		0.0128	0.0083	0.0289	0.0163	0.0173	0.5385	RCS
OTM-314	E17+4d	31-Mar-2012 01:32:00	0.0621	0.1562	0.1189	0.3759	0.1445	0.1427	0.1135	RCS
OTM-315	E18-9d	05-Apr-2012 08:47:00	0.0633	0.0415	0.0324	0.1039	CANCELLED			
OTM-316	E18-3d	11-Apr-2012 14:48:00		0.0161	0.0084	0.0318	0.0314	0.0318	1.8796	RCS
OTM-317	E18+3d	18-Apr-2012 00:18:00	0.2735	0.2889	0.1644	0.5688	CANCELLED			
OTM-318	E19-8d	24-Apr-2012 07:33:00	0.1178	0.1192	0.0640	0.2327	0.2458	0.2404	1.8942	MEA
OTM-319	E19-3d	29-Apr-2012 07:17:00		0.0117	0.0059	0.0227	0.0350	0.0349	3.8987	RCS
OTM-320	E19+4d	06-May-2012 06:47:00	0.0004	0.1125	0.0919	0.2921	CANCELLED			
OTM-321	T83-8d	14-May-2012 06:01:00	8.2659	8.2267	0.0453	8.2847	8.2722	8.2669	0.8883	MEA
OTM-322 BU	T83-2d	19-May-2012 22:16:00		0.0433	0.0271	0.0962	0.0822	0.0823	1.4379	RCS
OTM-323	T83+3d	25-May-2012 05:16:00	0.0116	0.2629	0.2472	0.7602	CANCELLED			
OTM-324	T84-8d	30-May-2012 05:00:00	3.7088	3.6413	0.0718	3.7229	3.7142	3.7127	0.9940	MEA
OTM-325	T84-3d	03-Jun-2012 21:15:00		0.0243	0.0137	0.0501	0.0375	0.0371	0.9337	RCS
OTM-326	T84+3d	10-Jun-2012 10:29:00	0.0055	0.7638	0.5715	1.8815	0.4216	0.4115	0.6165	MEA
OTM-327	T85-34d	21-Jun-2012 03:28:00	10.1176	9.9983	0.0943	10.1117	10.1186	10.1191	1.2815	MEA
OTM-328	T85-4d	21-Jul-2012 07:38:00		0.1915	0.1382	0.4598	0.1721	0.1719	0.1423	RCS
OTM-329	T85+3d	28-Jul-2012 07:08:00	0.0141	0.9241	0.7150	2.3238	CANCELLED			
OTM-330	T86-50d	07-Aug-2012 06:36:00	4.2676	4.1417	0.1719	4.3132	4.3525	4.3565	1.2493	MEA
OTM-331	T86-3d	23-Sep-2012 13:47:00		0.2115	0.1548	0.5154	0.0612	0.0607	0.9736	RCS
OTM-332	T86+4d	30-Sep-2012 03:16:00	0.0076	1.2076	0.8000	2.7117	0.1901	0.1895	1.2726	RCS
OTM-333	T87-35d	09-Oct-2012 13:01:00	0.7989	0.6101	0.1674	0.8412	0.7608	0.7636	0.9170	MEA
OTM-334	T87-4d	09-Nov-2012 18:46:00		0.0862	0.0587	0.2041	0.0600	0.0600	0.4467	RCS

* Predicted ΔV Magnitude Error = $| \text{Reconstructed } \Delta V - \text{Predicted } \Delta V \text{ Mean} | / \text{Predicted } \Delta V \text{ 1-}\sigma$

Table A-10. Cassini Mission Maneuver History (OTMs 335-406).

Maneuver	Orbit Location	Maneuver Time (UTC SCET)	Ref. Traj. Det. ΔV (m/s)	Predicted ΔV Statistics			Design ΔV (m/s)	Recon. ΔV (m/s)	Predicted ΔV Error (σ)*	Burn Type
				Mean (m/s)	1- σ (m/s)	ΔV 95 (m/s)				
OTM-335	T87+4d	17-Nov-2012 00:31:00	0.0129	0.9364	0.7688	2.3754	0.2548	0.2529	0.8891	MEA
OTM-336	T88-7d	22-Nov-2012 00:16:00	5.0468	4.9256	0.1860	5.1376	4.9593	4.9606	0.1882	MEA
OTM-337	T88-3d	26-Nov-2012 00:01:00		0.0411	0.0216	0.0805	0.0219	0.0214	0.9123	RCS
OTM-338	T88+4d	02-Dec-2012 23:32:00	0.0342	0.5138	0.4082	1.3094	0.0276	0.0286	1.1887	RCS
OTM-339	T89-17d	30-Jan-2013 20:09:00	1.6593	1.7294	0.1056	1.9266	1.6575	1.6540	0.7131	MEA
OTM-340	T89-4d	13-Feb-2013 05:26:00		0.0517	0.0371	0.1233	0.0323	0.0314	0.5471	RCS
OTM-341	T89+7d	24-Feb-2013 12:12:00	1.4481	1.4870	0.2270	1.8571	1.4498	1.4474	0.1742	MEA
OTM-342	R4-8d	02-Mar-2013 04:28:00	0.0768	0.8385	0.5704	1.9353	0.2644	0.2612	1.0121	MEA
OTM-343	R4-3d	06-Mar-2013 17:58:00		0.0331	0.0176	0.0659	CANCELLED			
OTM-344	R4+3d	12-Mar-2013 03:44:00	0.0507	0.2017	0.1666	0.5167	CANCELLED			
OTM-345	T90-20d	17-Mar-2013 03:30:00	0.0885	0.1367	0.2122	0.5908	0.1859	0.1858	0.2317	RCS
OTM-346	T90-4d	01-Apr-2013 16:16:00		0.0164	0.0117	0.0369	0.0166	0.0167	0.0307	RCS
OTM-347	T90+3d	09-Apr-2013 01:46:00	0.0083	0.4235	0.3253	1.0371	0.1228	0.1223	0.9260	RCS
OTM-348	T91-23d	30-Apr-2013 08:02:00	0.4132	0.4360	0.1587	0.7020	0.4945	0.4954	0.3742	MEA
OTM-349	T91-4d	19-May-2013 12:46:00		0.0388	0.0266	0.0925	0.0169	0.0170	0.8187	RCS
OTM-350	T91+4d	27-May-2013 06:01:00	0.0715	0.8378	0.6628	2.1582	0.0511	0.0507	1.1876	RCS
OTM-351	T92-29d	11-Jun-2013 21:14:00	0.8144	0.7704	0.2520	1.0871	0.8201	0.8187	0.1916	MEA
OTM-352	T92-3d	07-Jul-2013 09:26:00		0.1080	0.0778	0.2597	0.0576	0.0583	0.6384	RCS
OTM-353 BU	T92+5d	15-Jul-2013 02:40:00		0.7685	0.6174	1.9634	0.2530	0.2491	0.8414	MEA
OTM-354	T93-7d	19-Jul-2013 02:25:00	2.3708	2.2672	0.2057	2.4759	2.2655	2.2688	0.0082	MEA
OTM-355	T93-3d	23-Jul-2013 08:24:00		0.0323	0.0191	0.0699	0.0721	0.0713	2.0410	RCS
OTM-356	T93+4d	30-Jul-2013 07:53:00	0.0016	0.5874	0.4769	1.5035	CANCELLED			
OTM-357	T94-36d	07-Aug-2013 07:22:00	3.6085	3.5526	0.1489	3.7275	3.6145	3.6196	0.4495	MEA
OTM-358	T94-3d	09-Sep-2013 05:18:00		0.1287	0.0940	0.3087	0.0346	0.0341	1.0071	RCS
OTM-359	T94+4d	16-Sep-2013 04:47:00	0.0054	0.2465	0.1960	0.6282	0.0331	0.0320	1.0946	RCS
OTM-360	T95-14d	30-Sep-2013 04:01:00	0.0684	0.0839	0.0412	0.1546	0.0714	0.0706	0.3213	RCS
OTM-361	T95-3d	11-Oct-2013 03:15:00		0.0197	0.0119	0.0430	0.0185	0.0197	0.0038	RCS
OTM-362	T95+3d	17-Oct-2013 13:15:00	0.0079	0.2687	0.2118	0.6793	CANCELLED			
OTM-363	T96-29d	02-Nov-2013 12:15:00	0.3702	0.3659	0.0486	0.4345	0.3642	0.3654	0.0086	MEA
OTM-364	T96-3d	28-Nov-2013 00:45:00		0.1354	0.1055	0.3457	0.0140	0.0137	1.1529	RCS
OTM-365	T96+4d	04-Dec-2013 18:00:00	0.0376	0.4375	0.3414	1.0824	CANCELLED			
OTM-366	T97-15d	17-Dec-2013 23:32:00	0.3618	0.3239	0.1144	0.5000	0.3859	0.3793	0.4846	MEA
OTM-367	T97-3d	29-Dec-2013 22:48:00		0.0435	0.0358	0.1179	0.1154	0.1157	2.0161	RCS
OTM-368	T97+4d	05-Jan-2014 16:03:00	0.0004	0.4286	0.3506	1.1266	0.1033	0.1027	0.9295	RCS
OTM-369	T98-8d	25-Jan-2014 14:51:00	0.0038	0.0829	0.0716	0.2290	CANCELLED			
OTM-370	T98-3d	30-Jan-2014 20:51:00		0.0191	0.0091	0.0358	0.0558	0.0541	3.8299	RCS
OTM-371	T98+3d	05-Feb-2014 14:07:00	0.0056	0.1109	0.1027	0.3126	0.0891	0.0904	0.1992	RCS
OTM-372	T99-17d	17-Feb-2014 13:24:00	1.7128	1.7743	0.0844	1.9769	1.6829	1.6806	1.1096	MEA
OTM-373	T99-3d	03-Mar-2014 18:56:00		0.0662	0.0456	0.1570	0.0242	0.0243	0.9175	RCS
OTM-374	T99+4d	10-Mar-2014 12:12:00	0.0022	0.1185	0.1079	0.3325	CANCELLED			
OTM-375	T100-18d	20-Mar-2014 11:28:00	0.5513	0.5583	0.0834	0.7150	0.5420	0.5451	0.1580	MEA
OTM-376	T100-3d	04-Apr-2014 10:29:00		0.0661	0.0459	0.1542	0.0549	0.0541	0.2605	RCS
OTM-377	T100+4d	11-Apr-2014 10:00:00	0.0006	0.0796	0.0724	0.2275	0.0373	0.0359	0.6032	RCS
OTM-378	T101-23d	24-Apr-2014 09:01:00	0.0012	0.2579	0.2470	0.7744	0.0362	0.0356	0.8999	RCS
OTM-379	T101-3d	14-May-2014 07:46:00		0.0679	0.0615	0.1918	0.0228	0.0214	0.7564	RCS
OTM-380	T101+4d	21-May-2014 07:16:00	0.0006	0.1449	0.1228	0.3667	0.0200	0.0204	1.0140	RCS
OTM-381	T102-15d	03-Jun-2014 06:15:00	0.0026	0.0089	0.0061	0.0201	CANCELLED			
OTM-382	T102-3d	15-Jun-2014 11:44:00		0.0110	0.0069	0.0243	0.0272	0.0282	2.4990	RCS
OTM-383	T102+4d	22-Jun-2014 04:59:00	0.0022	0.0575	0.0436	0.1418	0.0459	0.0452	0.2830	RCS
OTM-384	T103-15d	05-Jul-2014 03:58:00	0.0052	0.0071	0.0039	0.0144	CANCELLED			
OTM-385	T103-3d	17-Jul-2014 09:40:00		0.0113	0.0072	0.0253	0.0322	0.0323	2.9380	RCS
OTM-386	T103+4d	24-Jul-2014 02:40:00	0.0023	0.0545	0.0426	0.1369	CANCELLED			
OTM-387	T104-12d	09-Aug-2014 08:08:00	12.4462	12.4432	0.0102	12.4585	12.4598	12.4660	2.2244	MEA
OTM-388	T104-3d	18-Aug-2014 07:37:00		0.0945	0.0633	0.2186	0.0324	0.0324	0.9820	RCS
OTM-389	T104+4d	25-Aug-2014 07:06:00	0.0013	0.1973	0.1615	0.4974	CANCELLED			
OTM-390	T105-15d	07-Sep-2014 06:19:00	1.2539	1.2445	0.0215	1.2721	1.2659	1.2616	0.7943	MEA
OTM-391	T105-3d	19-Sep-2014 05:33:00		0.0731	0.0488	0.1710	0.0837	0.0855	0.2545	RCS
OTM-392	T105+4d	26-Sep-2014 05:02:00	0.0006	0.1999	0.1663	0.5188	0.0664	0.0665	0.8020	RCS
OTM-393	T106-15d	09-Oct-2014 04:16:00	1.0847	1.0672	0.0298	1.1204	1.0647	1.0613	0.1971	MEA
OTM-394	T106-3d	21-Oct-2014 03:30:00		0.0796	0.0497	0.1737	0.0357	0.0357	0.8851	RCS
OTM-395	T106+4d	27-Oct-2014 20:44:00	0.0026	0.2527	0.1686	0.5784	0.0623	0.0631	1.1248	RCS
OTM-396	T107-19d	22-Nov-2014 01:44:00	0.1730	0.1764	0.0339	0.2316	0.1975	0.1962	0.5854	RCS
OTM-397	T107-3d	07-Dec-2014 18:30:00		0.0719	0.0456	0.1600	0.0371	0.0366	0.7735	RCS
OTM-398	T107+3d	14-Dec-2014 00:15:00	0.0010	0.1591	0.1038	0.3548	0.1612	0.1606	0.0148	RCS
OTM-399	T108-13d	29-Dec-2014 23:31:00	0.9941	0.9914	0.0331	1.0367	0.9683	0.9646	0.8094	MEA
OTM-400 BU	T108-2d	09-Jan-2015 22:47:00		0.1676	0.1029	0.3668	0.0555	0.0562	1.0821	RCS
OTM-401	T108+3d	14-Jan-2015 22:32:00	0.0015	0.3746	0.3415	0.9452	0.2289	0.2294	0.4250	RCS
OTM-402	T109-12d	31-Jan-2015 21:34:00	1.2720	1.2815	0.0647	1.3731	1.2677	1.2727	0.1355	MEA
OTM-403	T109-3d	09-Feb-2015 21:06:00		0.0648	0.0348	0.1291	0.0293	0.0297	1.0093	RCS
OTM-404	T109+3d	15-Feb-2015 20:36:00	0.0019	0.4308	0.3096	1.0342	0.4971	0.4954	0.2089	MEA
OTM-405	T110-12d	04-Mar-2015 19:39:00	0.0038	0.0470	0.0262	0.0950	0.0996	0.0999	2.0198	RCS
OTM-406	T110-3d	13-Mar-2015 19:10:00		0.0126	0.0067	0.0249	0.0228	0.0224	1.4770	RCS

* Predicted ΔV Magnitude Error = $|\text{Reconstructed } \Delta V - \text{Predicted } \Delta V \text{ Mean}| / \text{Predicted } \Delta V \text{ 1-}\sigma$

Table A-11. Cassini Mission Maneuver History (OTMs 407-475).

Maneuver	Orbit Location	Maneuver Time (UTC SCET)	Ref. Traj. Det. ΔV (m/s)	Predicted ΔV Statistics			Design ΔV (m/s)	Recon. ΔV (m/s)	Predicted ΔV Error (σ)*	Burn Type
				Mean (m/s)	1-σ (m/s)	ΔV95 (m/s)				
OTM-407	T110+3d	19-Mar-2015 18:41:00	0.0094	0.1984	0.1441	0.4841	CANCELLED			
OTM-408	T111-17d	20-Apr-2015 16:29:00	0.0086	0.0085	0.0063	0.0206	0.0470	0.0461	5.9417	RCS
OTM-409	T111-3d	04-May-2015 15:30:00		0.0113	0.0068	0.0247	0.0181	0.0186	1.0716	RCS
OTM-410	T111+4d	11-May-2015 15:00:00	0.0004	0.0799	0.0558	0.1874	0.0610	0.0615	0.3302	RCS
OTM-411	D4-8d	08-Jun-2015 13:00:00	0.0051	0.0691	0.0372	0.1396	0.0599	0.0604	0.2322	RCS
OTM-412	D4-3d	13-Jun-2015 12:45:00		0.0059	0.0029	0.0113	CANCELLED			
OTM-413	D4+4d	20-Jun-2015 12:14:00	0.0008	0.0555	0.0438	0.1397	CANCELLED			
OTM-414	T112-11d	26-Jun-2015 11:44:00	0.0050	0.0360	0.0230	0.0800	0.0704	0.0707	1.5106	RCS
OTM-415	T112-3d	04-Jul-2015 11:13:00		0.0114	0.0073	0.0257	CANCELLED			
OTM-416	T112+3d	10-Jul-2015 10:58:00	0.0093	0.1116	0.0743	0.2616	0.0960	0.0963	0.2057	RCS
OTM-417	D5-8d	09-Aug-2015 08:54:00	0.0094	0.0233	0.0165	0.0561	0.0181	0.0179	0.3274	RCS
OTM-418	D5-3d	14-Aug-2015 08:23:00		0.0053	0.0026	0.0101	CANCELLED			
OTM-419	D5+4d	21-Aug-2015 08:07:00	0.0023	0.0459	0.0264	0.0964	0.0581	0.0572	0.4278	RCS
OTM-420	T113-21d	08-Sep-2015 06:50:00	0.0112	0.0265	0.0138	0.0525	CANCELLED			
OTM-421	T113-4d	25-Sep-2015 05:48:00		0.0578	0.0424	0.1393	0.0222	0.0216	0.8551	RCS
OTM-422	T113+3d	02-Oct-2015 05:17:00	0.0062	0.3868	0.3296	1.0745	0.2521	0.2464	0.4260	MEA
OTM-423	E20-8d	06-Oct-2015 05:02:00	2.6956	2.6676	0.2733	3.0719	2.6256	2.6234	0.1617	MEA
OTM-424	E20-3d	11-Oct-2015 04:46:00		0.0278	0.0170	0.0605	0.0345	0.0344	0.3864	RCS
OTM-426	E21-8d	20-Oct-2015 04:15:00	0.0145	0.1809	0.1126	0.3967	0.0704	0.0712	0.9747	RCS
OTM-427	E21-3d	25-Oct-2015 04:00:00		0.0098	0.0071	0.0231	CANCELLED			
OTM-428	E21+1d	29-Oct-2015 03:45:00	0.0013	0.0638	0.0488	0.1569	CANCELLED			
OTM-429	T114-8d	05-Nov-2015 03:29:00	0.0087	0.2509	0.1586	0.5623	0.1108	0.1095	0.8917	RCS
OTM-430	T114-3d	10-Nov-2015 02:59:00		0.0112	0.0094	0.0317	CANCELLED			
OTM-431	T114+3d	16-Nov-2015 02:29:00	0.0059	0.1445	0.1345	0.4263	0.1036	0.1028	0.3102	RCS
OTM-432	E22-24d	26-Nov-2015 02:13:00	0.0225	0.0428	0.0368	0.1161	CANCELLED			
OTM-433	E22-4d	16-Dec-2015 00:44:00		0.0323	0.0232	0.0777	CANCELLED			
OTM-434	E22+3d	23-Dec-2015 00:29:00	0.0205	0.0202	0.0304	0.0855	CANCELLED			
OTM-435	T115-17d	30-Dec-2015 00:00:00	3.0237	2.9813	0.0520	3.0275	2.9863	2.9846	0.0625	MEA
OTM-436	T115-3d	12-Jan-2016 23:16:00		0.0538	0.0394	0.1306	0.0362	0.0367	0.4351	RCS
OTM-437	T115+3d	18-Jan-2016 23:01:00	0.0040	0.1292	0.1155	0.3488	CANCELLED			
OTM-438	T116-8d	23-Jan-2016 22:47:00	6.8455	6.8149	0.0324	6.8474	6.8471	6.8441	0.9010	MEA
OTM-439 BU	T116-2d	29-Jan-2016 22:17:00		0.0353	0.0232	0.0799	0.0158	0.0161	0.8267	RCS
OTM-440	T116+3d	03-Feb-2016 22:03:00	0.0089	0.5441	0.4391	1.3952	0.5826	0.5774	0.0759	MEA
OTM-441	T117-8d	08-Feb-2016 21:49:00	0.7285	0.6072	0.1259	0.7320	0.7469	0.7450	1.0950	MEA
OTM-442	T117-3d	13-Feb-2016 21:34:00		0.0239	0.0147	0.0523	0.0153	0.0154	0.5784	RCS
OTM-443 BU	T117+4d	20-Feb-2016 21:05:00		0.2355	0.1766	0.5738	0.0688	0.0682	0.9476	RCS
OTM-444	T118-10d	25-Mar-2016 18:55:00	7.9489	7.9294	0.0289	7.9600	7.9518	7.9563	0.9311	MEA
OTM-445	T118-3d	01-Apr-2016 18:26:00		0.0619	0.0389	0.1385	0.0625	0.0627	0.0222	RCS
OTM-446	T118+3d	07-Apr-2016 18:11:00	0.0035	0.4185	0.3121	1.0117	0.1668	0.1673	0.8049	RCS
OTM-447	T119-14d	22-Apr-2016 17:13:00	1.7545	1.7352	0.0280	1.7716	1.7674	1.7617	0.9440	MEA
OTM-448 BU	T119-2d	04-May-2016 16:29:00		0.1039	0.0553	0.2064	0.0172	0.0170	1.5707	RCS
OTM-449	T119+3d	09-May-2016 15:59:00	0.0006	0.2311	0.1786	0.5627	0.5512	0.5513	1.7925	MEA
OTM-450	T120-16d	22-May-2016 15:00:00	0.0480	0.0468	0.0177	0.0781	0.0261	0.0268	1.1269	RCS
OTM-451	T120-3d	04-Jun-2016 14:15:00		0.0342	0.0216	0.0759	CANCELLED			
OTM-452	T120+4d	11-Jun-2016 13:45:00	0.0013	0.2759	0.1750	0.6021	0.2542	0.2465	0.1680	MEA
OTM-453	T121-8d	17-Jul-2016 11:13:00	2.1061	2.0457	0.0532	2.1230	2.0250	2.0207	0.4698	MEA
OTM-454	T121-3d	22-Jul-2016 10:42:00		0.0485	0.0255	0.0950	0.0501	0.0499	0.0567	RCS
OTM-455	T121+3d	28-Jul-2016 10:27:00	0.0090	0.4093	0.3482	1.0754	0.1839	0.1849	0.6445	RCS
OTM-456	T122-8d	02-Aug-2016 10:11:00	0.8417	0.8016	0.1222	0.9676	0.7940	0.7934	0.0676	MEA
OTM-457	T122-3d	07-Aug-2016 09:40:00		0.0488	0.0255	0.0965	CANCELLED			
OTM-458	T122+4d	14-Aug-2016 09:10:00	0.0079	0.2849	0.2510	0.8146	CANCELLED			
OTM-459 BU	T123-38d	20-Aug-2016 08:54:00	0.0504	0.0983	0.0797	0.2607	0.0554	0.0556	0.5359	RCS
OTM-460	T123-4d	23-Sep-2016 06:34:00		0.0840	0.0669	0.2053	0.0245	0.0241	0.8951	RCS
OTM-461	T123+3d	30-Sep-2016 06:03:00	0.0138	0.1352	0.1744	0.5095	CANCELLED			
OTM-462	T124-40d	05-Oct-2016 05:48:00	0.0066	0.0787	0.0668	0.2032	0.1710	0.1718	1.3932	RCS
OTM-463	T124-4d	10-Nov-2016 03:29:00		0.0503	0.0380	0.1245	0.0184	0.0195	0.8107	RCS
OTM-464	T124+3d	17-Nov-2016 03:14:00	0.0086	0.0327	0.0304	0.0716	0.1427	0.1420	3.5988	RCS
OTM-465	T125-8d	22-Nov-2016 02:59:00	0.0962	0.3845	0.2430	0.8645	CANCELLED			
OTM-466	T125-2d	27-Nov-2016 16:15:00		0.0133	0.0097	0.0334	CANCELLED			
OTM-467	T125+5d	04-Dec-2016 11:58:00	1.0431	0.9886	0.0467	1.0785	0.9935	0.9900	0.0293	MEA
OTM-468	T126-119d	24-Dec-2016 00:58:00	0.0704	0.2784	0.3401	1.0368	0.2265	0.2249	0.1575	RCS
OTM-468a	T126-59d	22-Feb-2017 15:49:00		0.0285	0.0152	0.0571	0.1962	0.1990	11.1945	RCS
OTM-469	T126-3d	18-Apr-2017 18:12:00		0.0876	0.0621	0.2086	0.0595	0.0578	0.4803	RCS
OTM-470	T126+2d	24-Apr-2017 17:52:00		0.5143	0.2693	0.8874	0.1556	0.1550	1.3343	RCS
OTM-471	Per3+1d	10-May-2017 16:58:00		0.1302	0.0957	0.2691	0.0201	0.0207	1.1434	RCS
OTM-472	Per13+3d	15-Jul-2017 12:21:00		0.0395	0.0322	0.0837	0.1447	0.1429	3.2132	RCS
OTM-473	Per16+16d	17-Aug-2017 09:55:00		—	—	—	CONTINGENCY			
OTM-474	Per19+10d	30-Aug-2017 09:01:00		—	—	—	CONTINGENCY			
OTM-475	Per21+3d	05-Sep-2017 08:38:00		—	—	—	CONTINGENCY			

* Predicted ΔV Magnitude Error = $|\text{Reconstructed } \Delta V - \text{Predicted } \Delta V \text{ Mean}| / \text{Predicted } \Delta V \text{ 1-}\sigma$

A.4 Orbital Element Change due to Encounter Location on the B-Plane

During preliminary mission design, a useful tool is to plot the orbital element change due to a flyby in the B-plane of the encounter. The incoming asymptote v_∞ determines the orbital elements before the encounter. However, depending on where the v_∞ pierces the B-plane, different outgoing orbital elements can be achieved. In this section, a variety of figures showing the changes in both period and inclination for each of the encounters during the mission are shown, giving an insight as to why the encounters during the tour were designed at specific B-plane locations.

As an example, take the Titan-108 encounter, which occurred on 11-Jan-2015. The trajectory before the flyby was on a 2:1 resonance with Titan, as can be seen in Figure A-1, where the path of Cassini is plotted beginning at the previous Titan flyby (Titan-107). For the 2:1 resonance to be maintained after the Titan-108 encounter, the period before and after the flyby must remain constant; however, other orbital elements can increase or decrease in value. Both the period and inclination change are plotted in the B-plane of the encounter in Figure A-2, where the red circle represents Titan and the black square is the encounter location. The orbital period with respect to Saturn is approximately 32 days after the encounter occurs (top-left), and the change in the period is negligible (bottom-left); the orbital inclination is 19.12° with respect to Saturn's equator (top-right), with a reduction in inclination of 9.54° (bottom-right). Depending on where on the B-plane the encounter might have occurred, different outgoing orbital elements would have been achieved, which are represented by the contour lines in Figure A-2 for all the possible B-plane encounter positions around Titan. There is a clear asymptote in the period change plot where the encounter had to occur for the period to be kept constant (0.00 dark blue line).

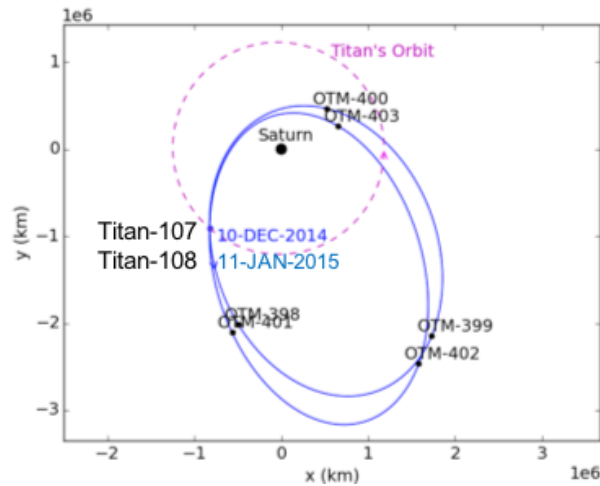


Figure A-1. Cassini's Orbit During the Titan-107 and Titan-108 Encounters.

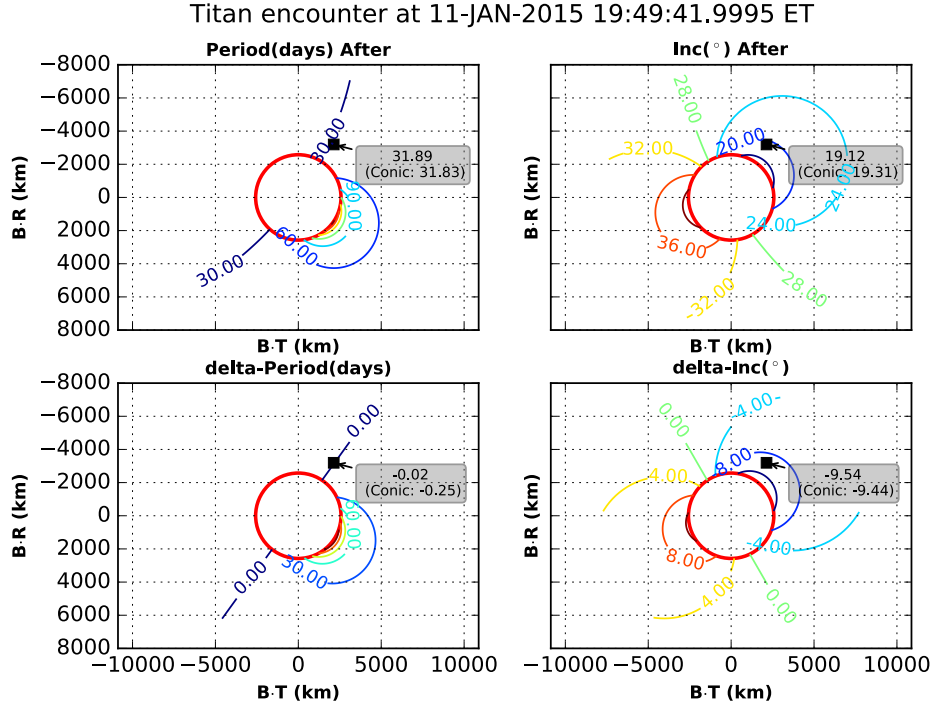


Figure A-2. Titan-108 (T108) Encounter Orbital Element Change Shown on the B-Plane.

A.4.1 Computing the Changes in Orbital Elements

The steps necessary to compute the changes in the orbital elements due to a flyby, assuming two-body equations of motion, are as follows:

1. The B-plane is defined as a plane which is normal to the incoming asymptote of the hyperbolic orbit (v_∞) and contains the target body's center of mass. The B-vector is the vector from the target body's center of mass to the point where the v_∞ vector intersects the B-plane. Three orthogonal unit vectors are defined with the origin at the target body to describe the B-plane: \hat{S} , \hat{T} , and \hat{R} . The \hat{S} vector is parallel to the v_∞ vector, \hat{T} is parallel to a convenient reference frame (usually chosen as the ecliptic, in the direction defined by crossing \hat{S} into the pole vector), and \hat{R} completes the orthogonal triad. Defining $\hat{k} = [0, 0, 1]$:

$$\hat{S} = \hat{v}_\infty$$

$$\hat{T} = \hat{S} \times \hat{k}$$

$$\hat{R} = \hat{S} \times \hat{T}$$

The B-vector is $\vec{B} = \frac{1}{v_\infty} (\hat{S} \times \vec{h})$, where \vec{h} is the angular momentum vector at the time of the encounter. The location of the flyby on the B-plane is computed with the components of the B-vector onto the \hat{T} and \hat{R} axis, i.e. $\vec{B} \cdot \hat{T}$ and $\vec{B} \cdot \hat{R}$.

2. The v_∞ vector after the flyby is

$$\vec{v}_\infty^+ = v_\infty (\cos(\delta) \hat{S} - \sin(\delta) \hat{b}_f)$$

where the turning angle δ is computed via

$$\frac{1}{e_{hyp}} = \sin\left(\frac{\delta}{2}\right)$$

and e_{hyp} is the eccentricity with respect to the flyby body, and is computed as

$$e_{hyp} = \sqrt{1 + v_{\infty}^4 \left(\frac{B}{\mu_{fb}}\right)^2}$$

where $B = \|\vec{B}\|$ and μ_{fb} is the gravitational parameter of the flyby body. The vector \hat{b}_J is

$$\hat{b}_J = R_{J2TRS} \hat{b}_{TRS}$$

where

$$R_{J2TRS} = [\hat{T}, \hat{R}, \hat{S}]_{3 \times 3}$$

and

$$\hat{b}_{TRS} = [\cos(\theta), \sin(\theta), 0]^T, \text{ with } \theta = \tan^{-1}\left(\frac{\vec{B} \cdot \hat{R}}{\vec{B} \cdot \hat{T}}\right)$$

3. The hyperbolic velocity vector before and after the flyby are now known from steps 1 and 2. Therefore, the orbital elements before and after the flyby can be computed using two-body equations of motion.

A.4.2 Orbital Element Change Plotted on the B-Plane

Figures of orbital element change plotted on the B-plane of each encounter during the Prime, Equinox, and Solstice mission follows.

1. Prime Mission: SOI to July 2008

The first three Titan flybys (Ta, Tb, and Tc) are not shown here. The first numbered Titan flyby (T3) is shown in Figure A-3, followed by the subsequent flybys up to T10, including two Enceladus, one Dione, and one Rhea targeted flybys (see Figure A-1 to Figure A-14). Notice how the smaller satellite flybys occur close to Saturn's equator, and Titan is used as a leverage to obtain the necessary orbits at zero inclination. The targeted flybys from T11 up to T39 are not shown. Figure A-15 to Figure A-22 show the orbital element change on the B-plane for the targeted flybys T40 through T45, including two Enceladus flybys (E3 and E4). These Titan flybys (T40 – T45) are designed to increase inclination and reduce the period of the Saturn centered orbit.

2. Equinox Mission: August 2008 to September 2010

Figure A-23 to Figure A-26 show the B-plane plots for the targeted encounters T60, T61, T62, and E7. The second targeted Rhea flyby of the mission (R2) is shown in Figure A-27. The next four Titan flybys (T67, T68, T69, and T70), the second targeted Dione flyby (D2), and the

Enceladus flybys E9 and E10 are shown in Figure A-28 to Figure A-34. Notice how the Titan flybys are designed to place Cassini on a near equatorial orbit, in order to target encounters of the smaller bodies Enceladus, Dione, and Rhea.

3. Solstice Mission: September 2010 to September 2017

The Solstice mission spanned three inclined phases and two equatorial phases. The First Inclined and First Equatorial phase flybys are not shown. The encountered flybys from T82 through T90 are shown in Figure A-35 to Figure A-47, which forms part of the Second Inclined phase (In-2) of the mission. The figures shown for this part of the mission include flybys of Enceladus (E17 through E19) and Rhea (R4). The Second Equatorial phase (Eq-2) includes flybys from T110 through T114, including two Dione (D4 and D5) and two Enceladus flybys (E20 and E21), and are shown in Figure A-48 to Figure A-56. Note from these figures how the Titan flybys are designed to maintain inclination near zero degrees in order to allow multiple flybys of the smaller satellites of Saturn. The final phase of the mission is the Third Inclined phase (In-3), from T114 through T126, and all these encounters are shown in the B-plane plots in Figure A-56 to A-69. Note how all these Titan flybys were designed to increase inclination and reduce orbital period with the final goal of reaching the Proximal Orbits with 6.5 day period and 62.5° inclination.

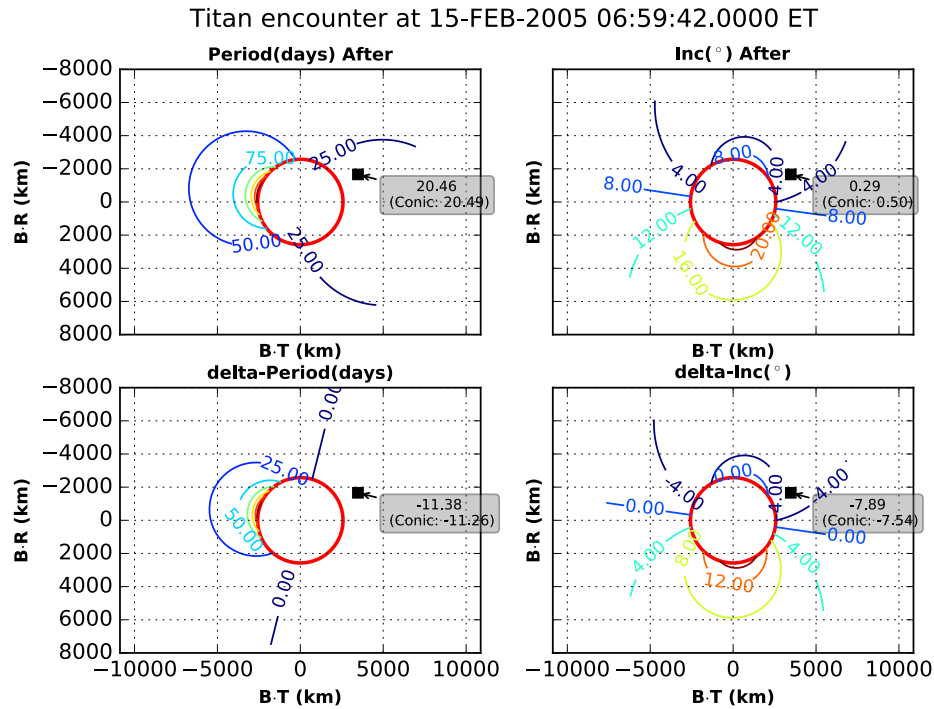


Figure A-3. Titan-3 (T3) Encounter Orbital Element Change Shown on the B-Plane.

Enceladus encounter at 09-MAR-2005 09:07:45.0000 ET

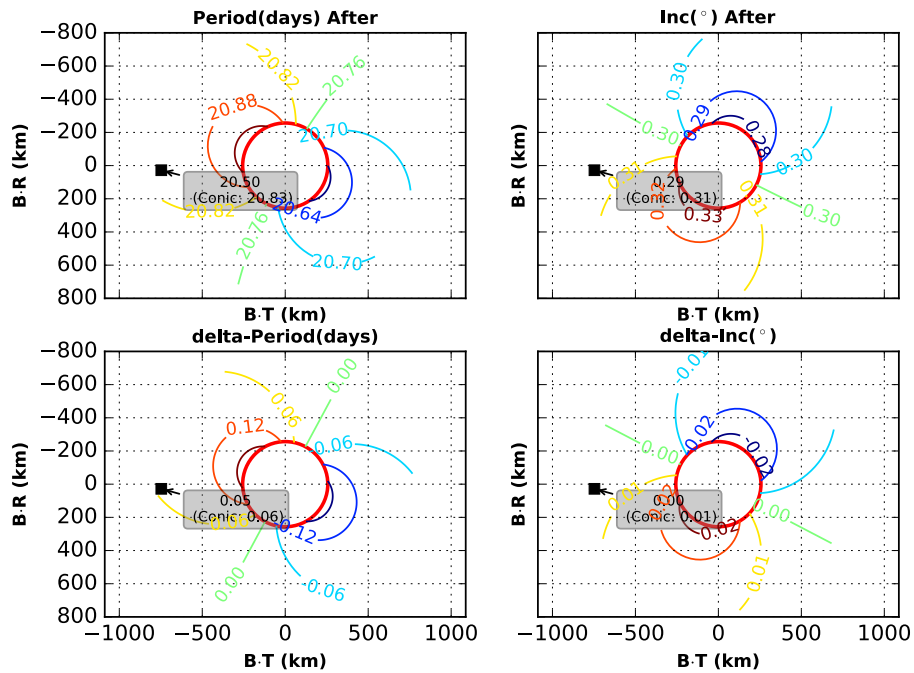


Figure A-4. Enceladus-1 (E1) Encounter Orbital Element Change Shown on the B-Plane.

Titan encounter at 31-MAR-2005 20:08:22.0000 ET

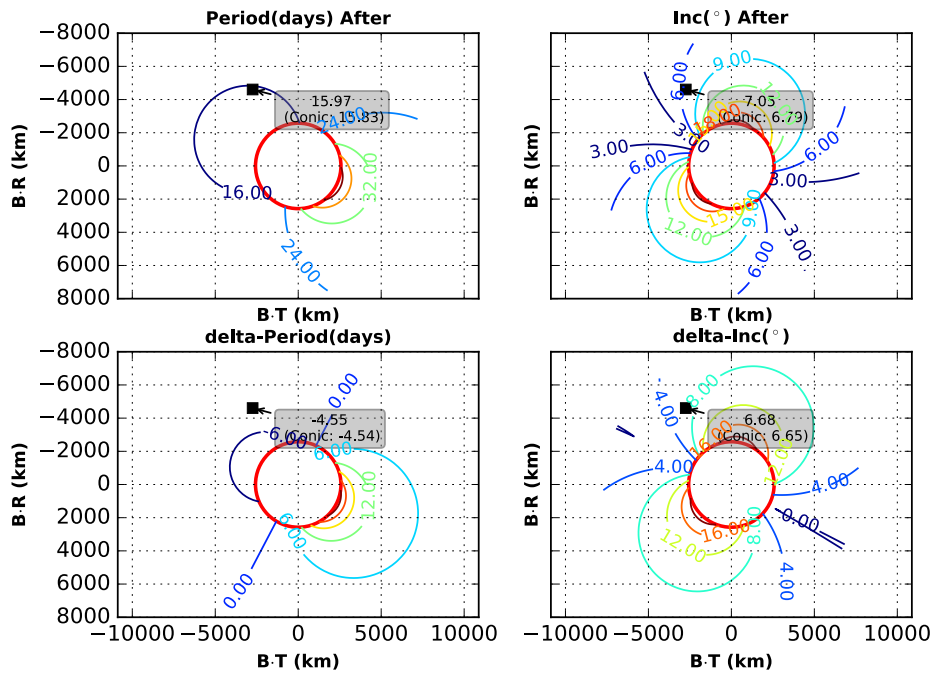


Figure A-5. Titan-4 (T4) Encounter Orbital Element Change Shown on the B-Plane.

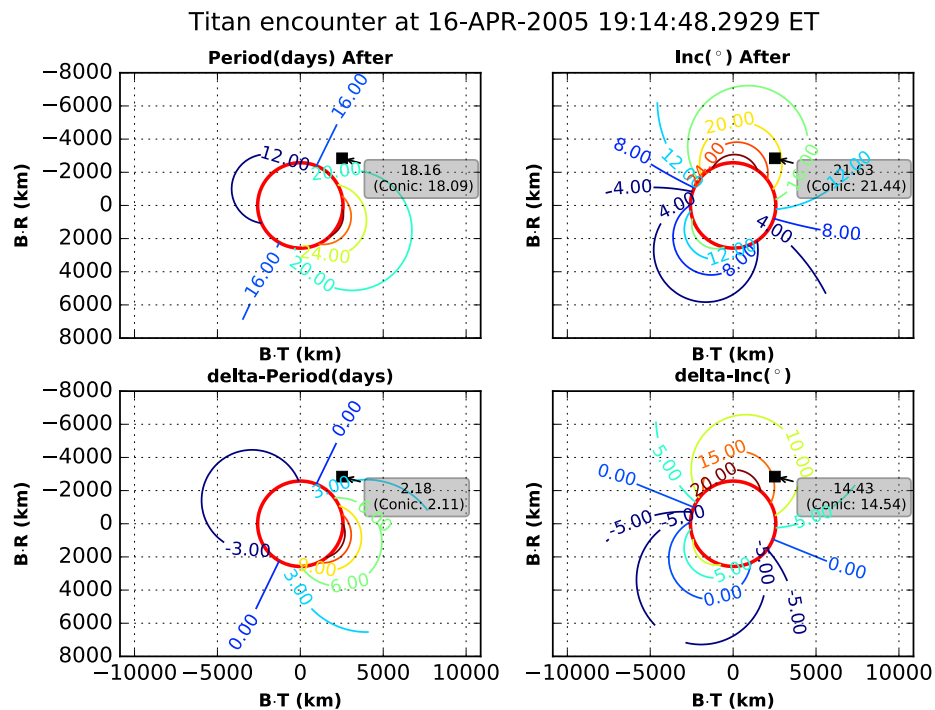


Figure A-6. Titan-5 (T5) Encounter Orbital Element Change Shown on the B-Plane.

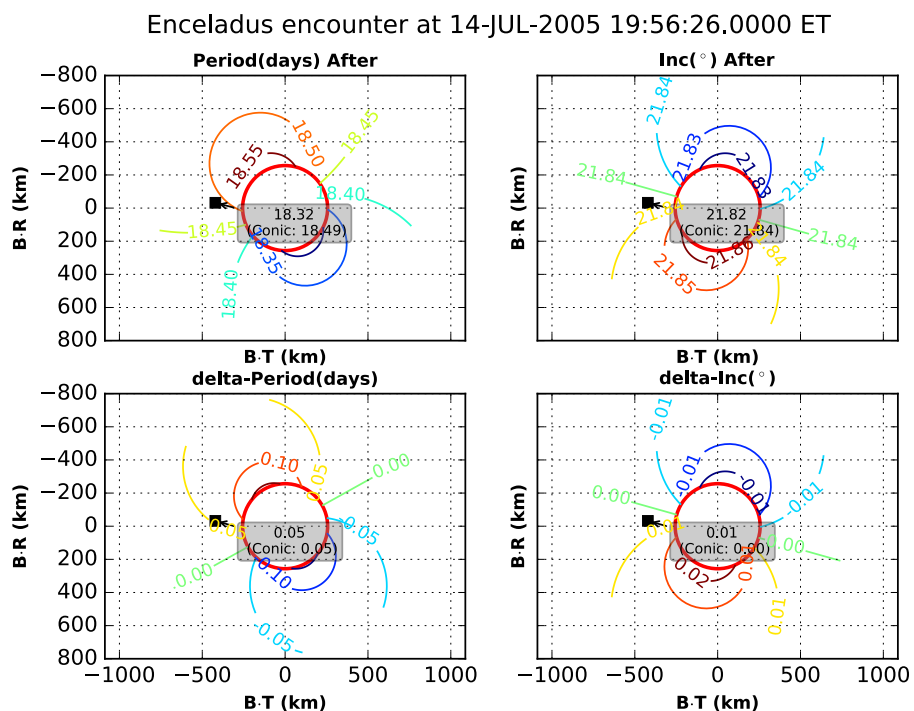


Figure A-7. Enceladus-2 (E2) Encounter Orbital Element Change Shown on the B-Plane.

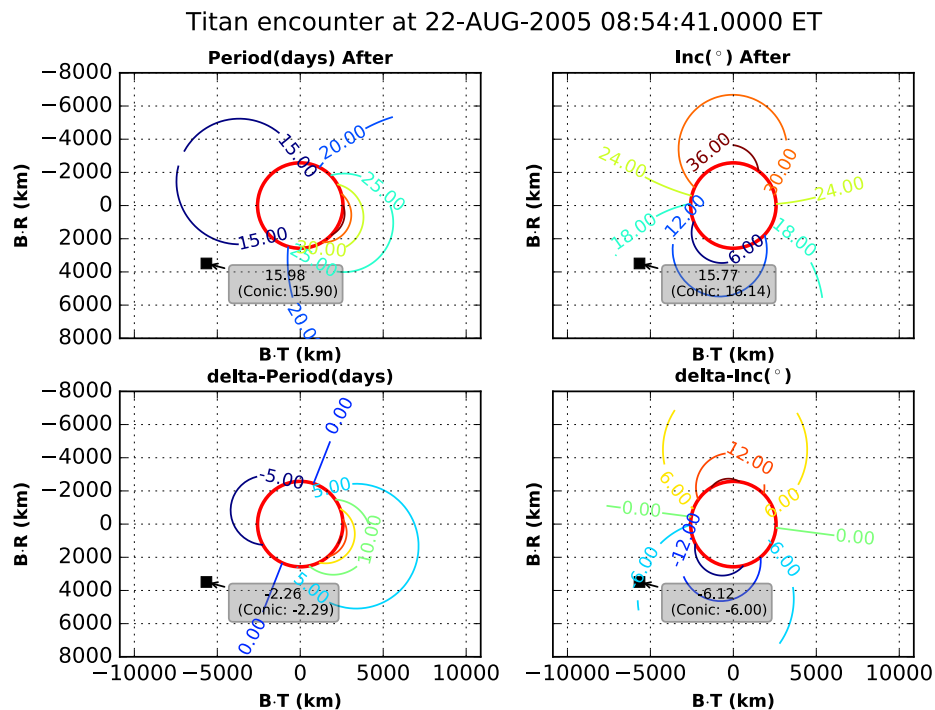
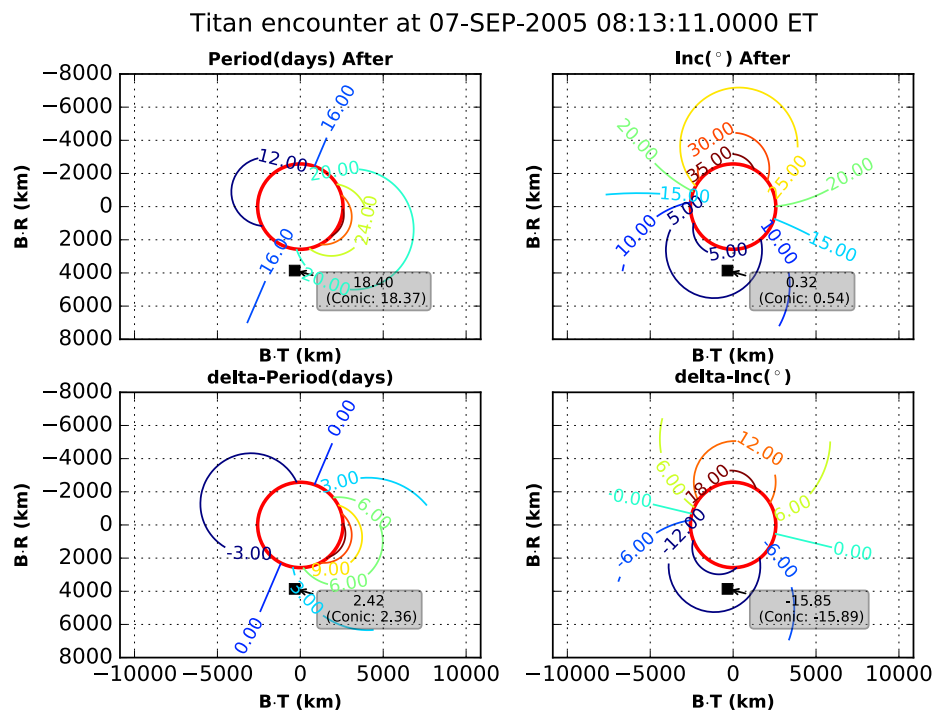


Figure A-8. Titan-6 (T6) Encounter Orbital Element Change Shown on the B-Plane.



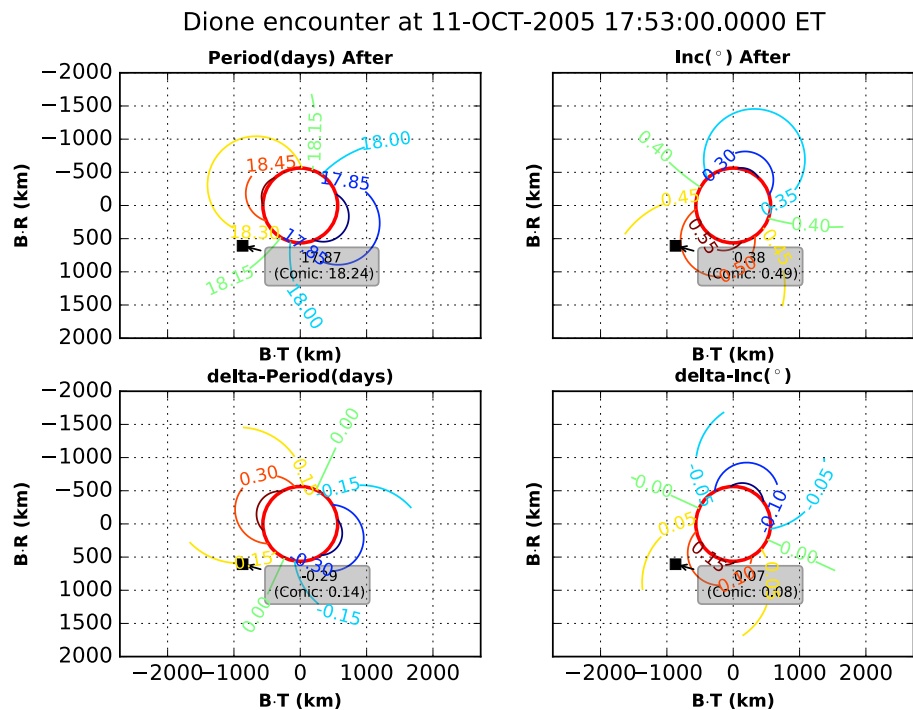


Figure A-10. Dione-1 (D1) Encounter Orbital Element Change Shown on the B-Plane.

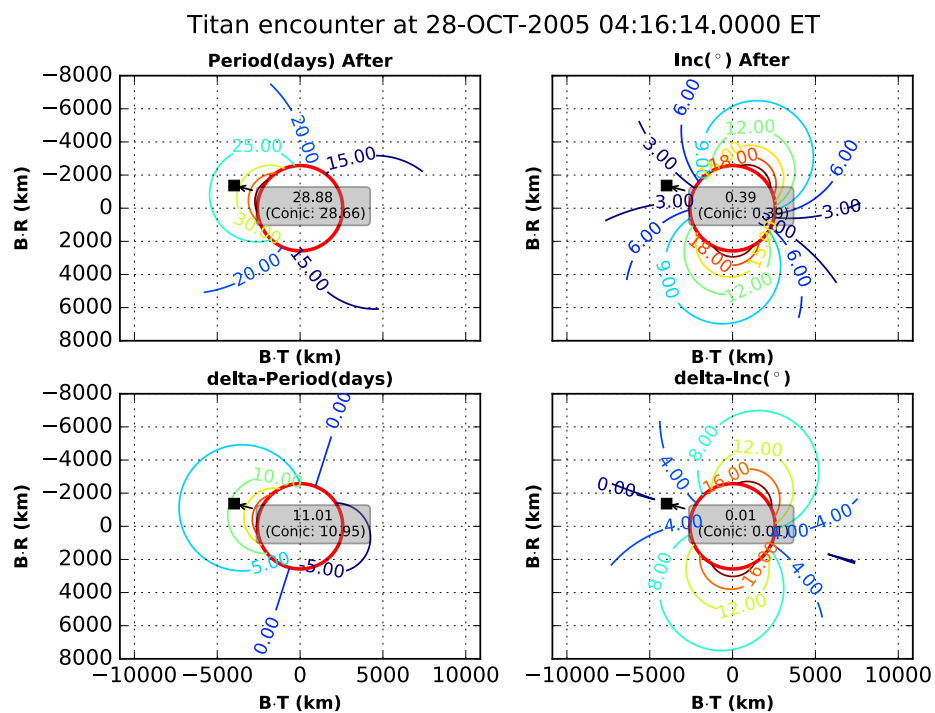


Figure A-11. Titan-8 (T8) Encounter Orbital Element Change Shown on the B-Plane.

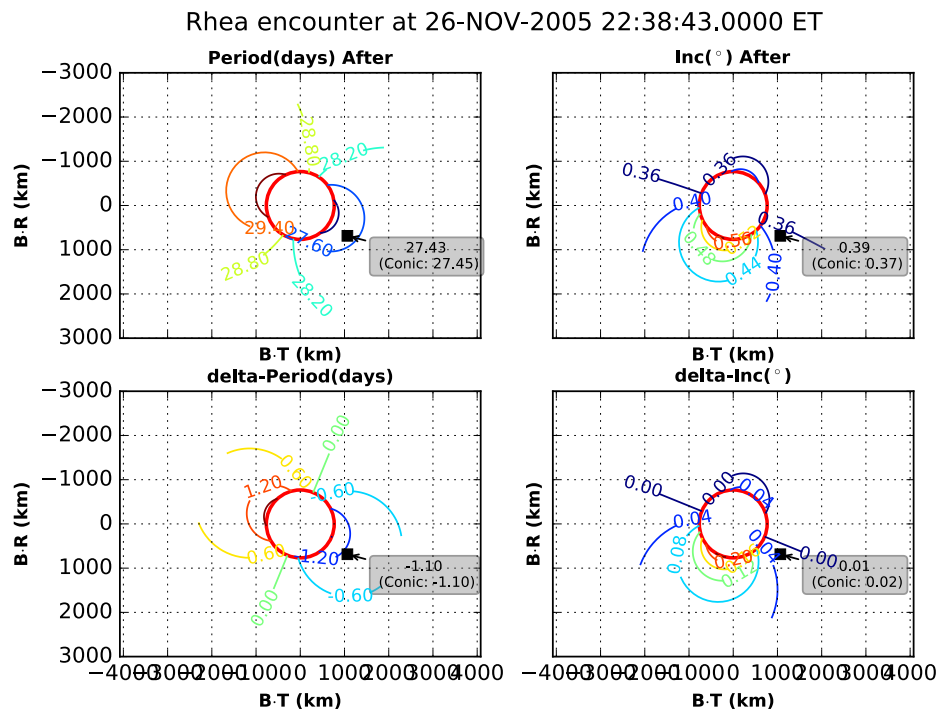


Figure A-12. Rhea-1 (R1) Encounter Orbital Element Change Shown on the B-Plane.

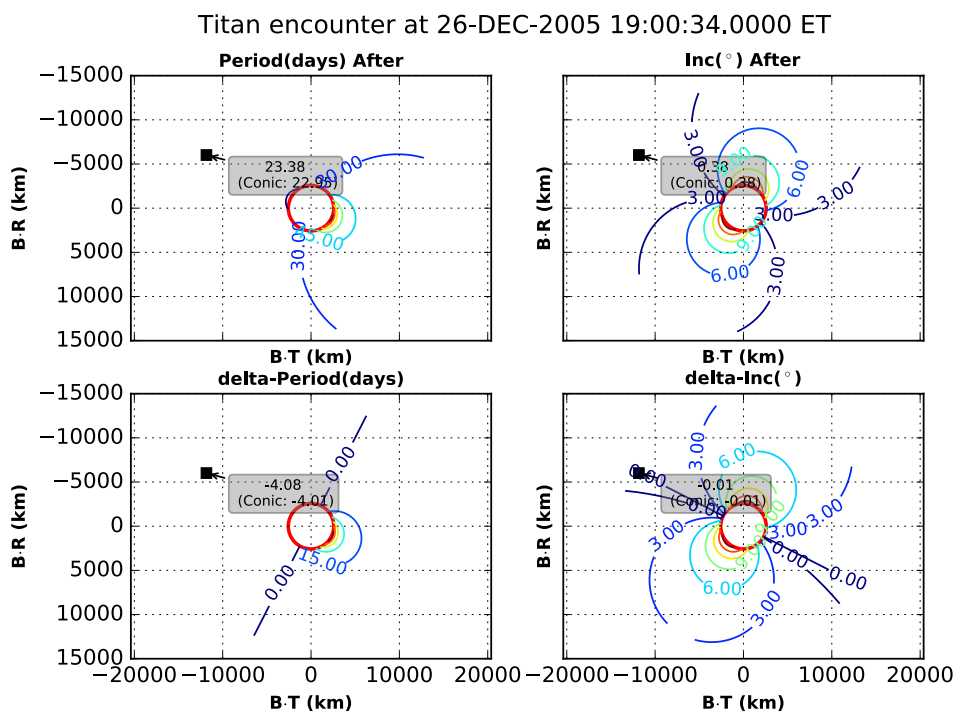


Figure A-13. Titan-9 (T9) Encounter Orbital Element Change Shown on the B-Plane.

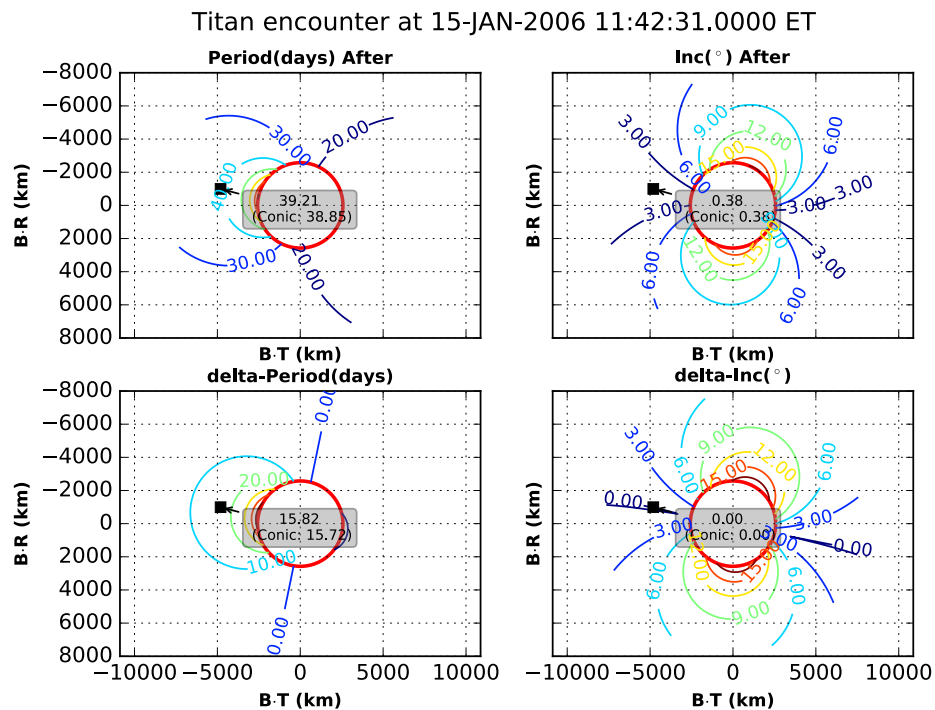


Figure A-14. Titan-10 (T10) Encounter Orbital Element Change Shown on the B-Plane.

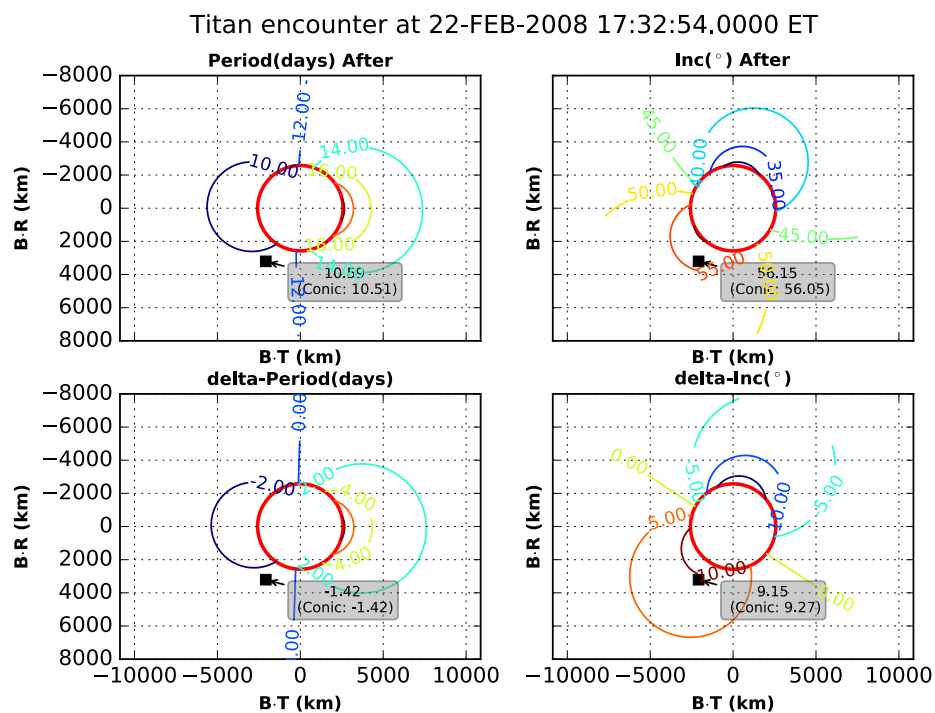


Figure A-15. Titan-40 (T40) Encounter Orbital Element Change Shown on the B-Plane.

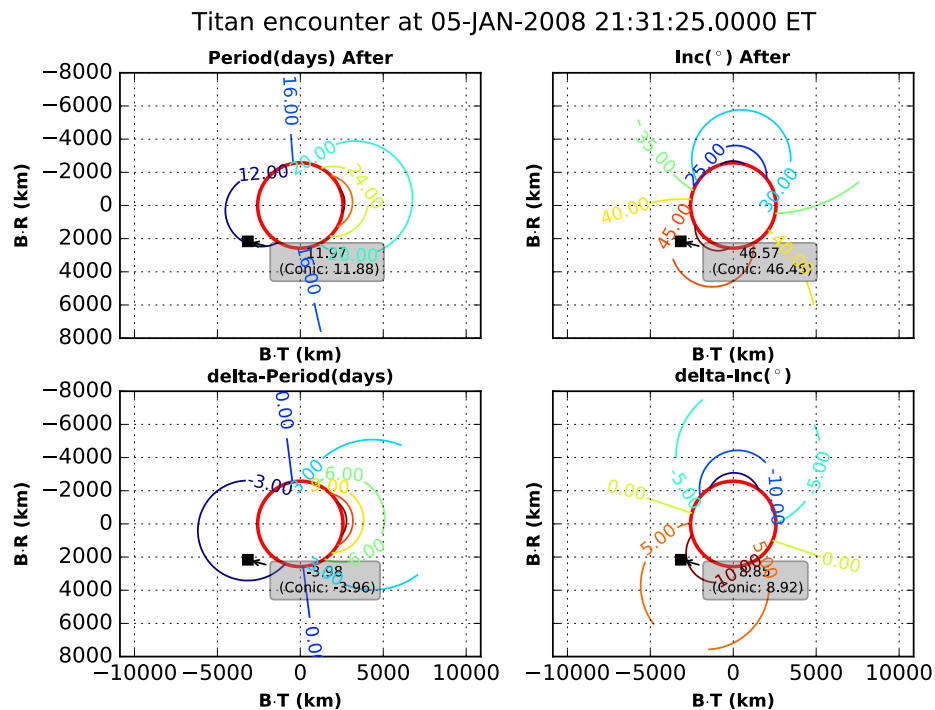


Figure A-16. Titan-41 (T41) Encounter Orbital Element Change Shown on the B-Plane.

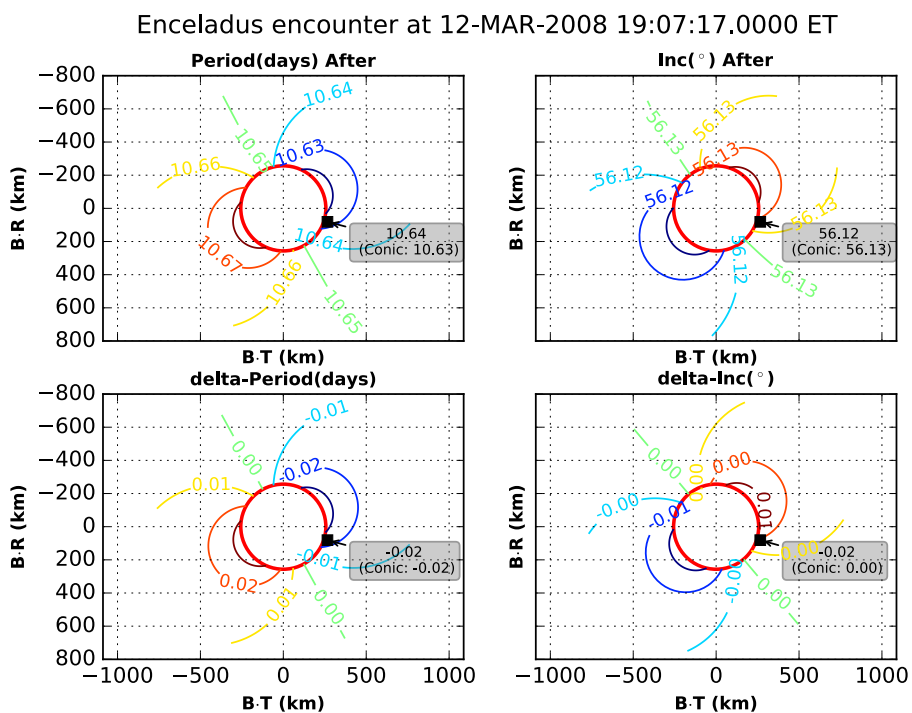


Figure A-17. Enceladus-3 (E3) Encounter Orbital Element Change Shown on the B-Plane.

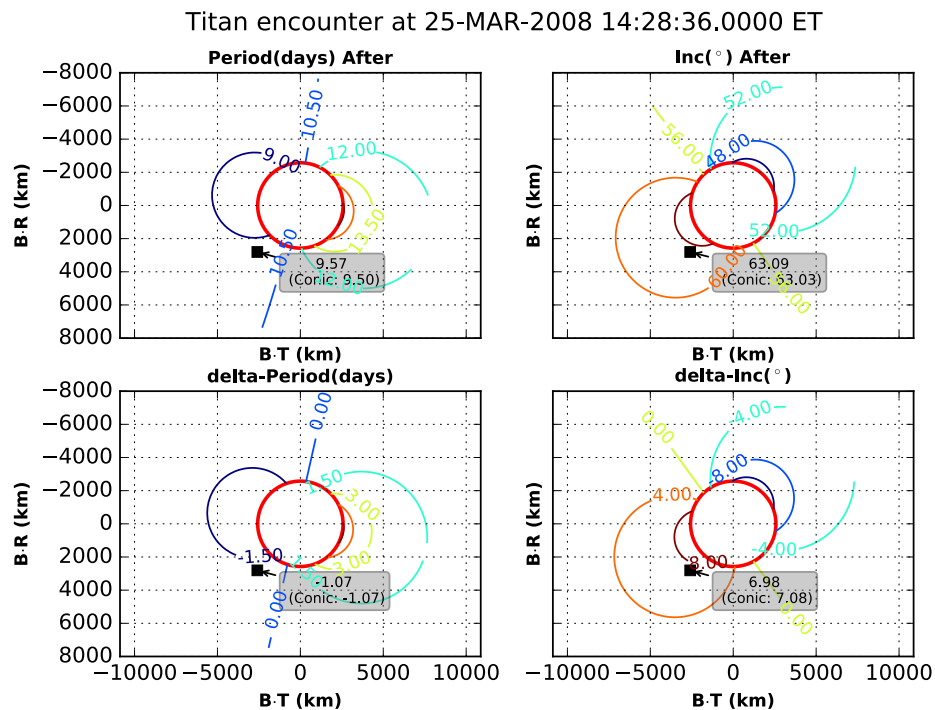


Figure A-18. Titan-42 (T42) Encounter Orbital Element Change Shown on the B-Plane.

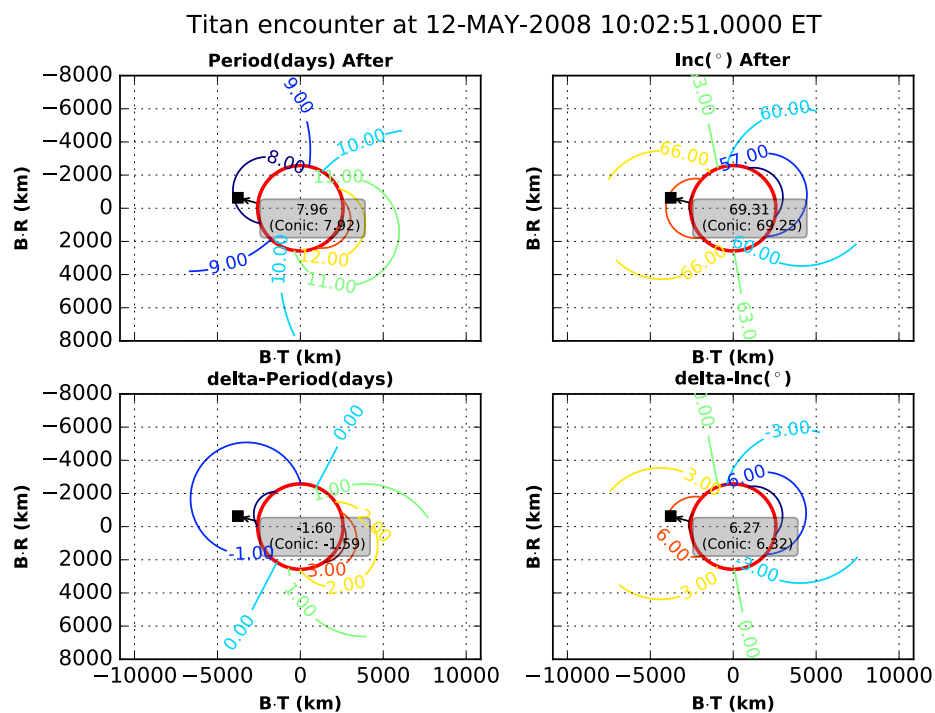


Figure A-19. Titan-43 (T43) Encounter Orbital Element Change Shown on the B-Plane.

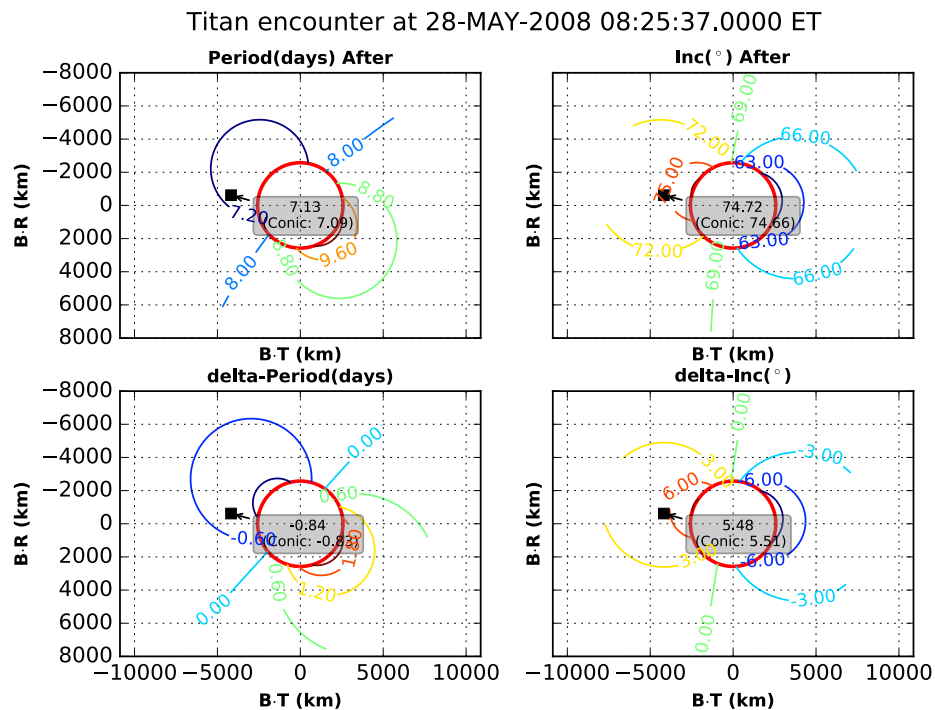


Figure A-20. Titan-44 (T44) Encounter Orbital Element Change Shown on the B-Plane.

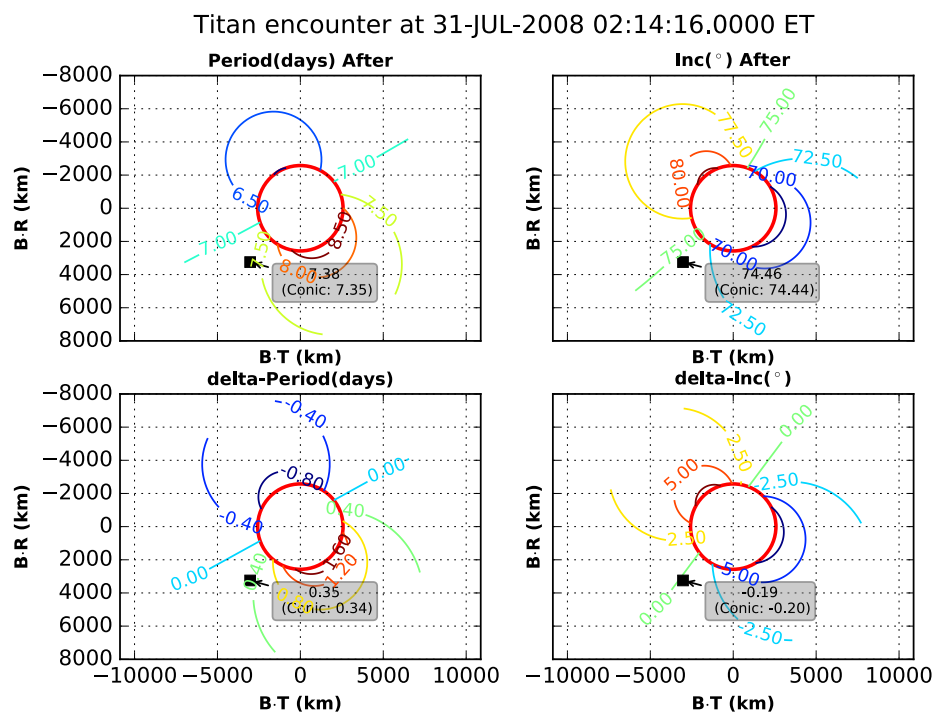


Figure A-21. Titan-45 (T45) Encounter Orbital Element Change Shown on the B-Plane.

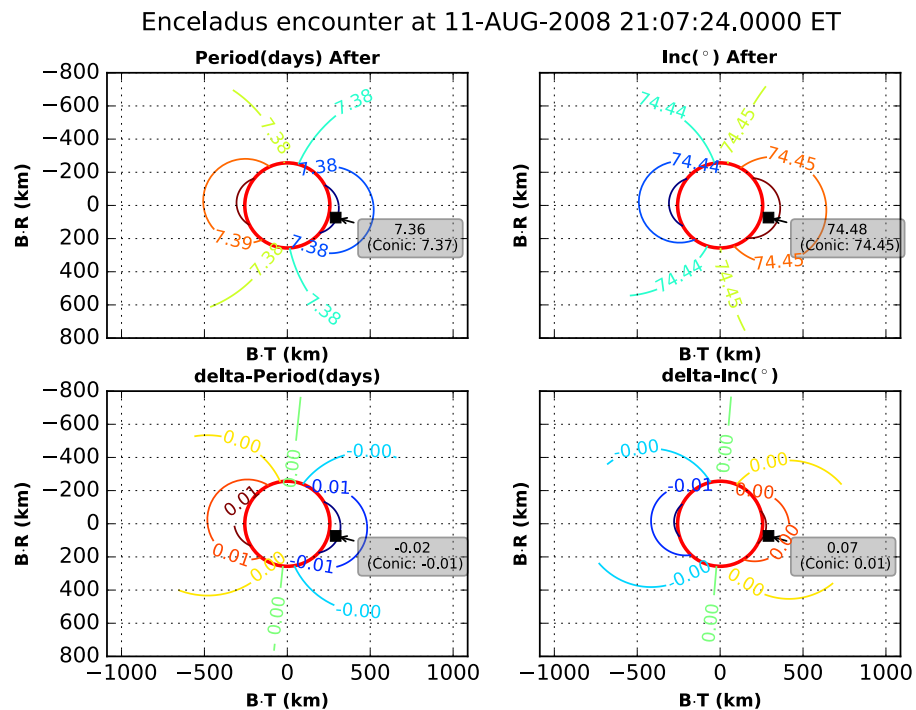


Figure A-22. Enceladus-4 (E4) Encounter Orbital Element Change Shown on the B-Plane.

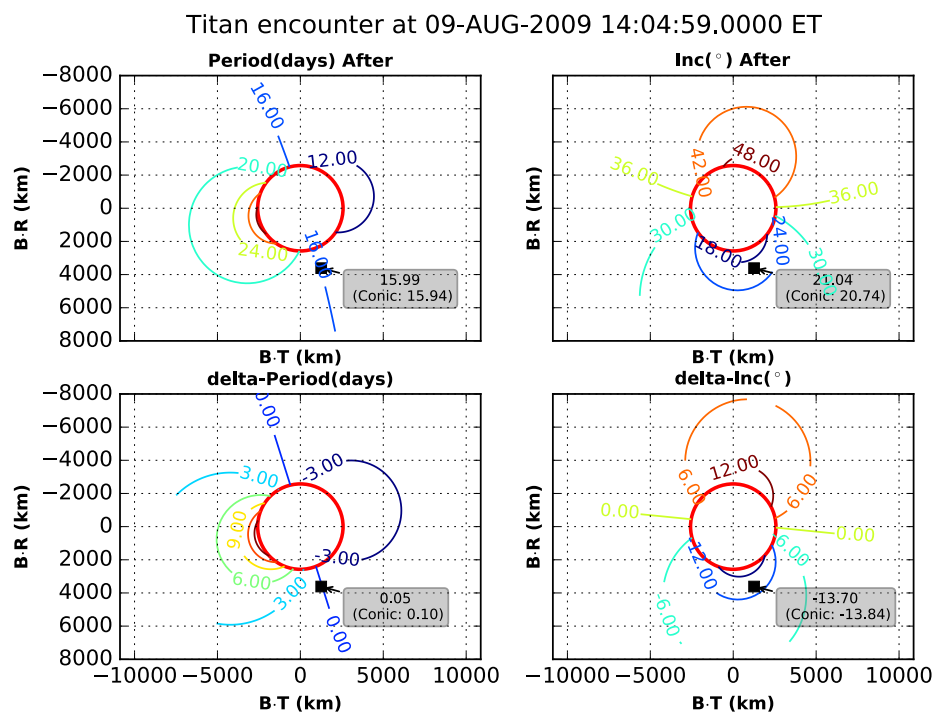


Figure A-23. Titan-60 (T60) Encounter Orbital Element Change Shown on the B-Plane.

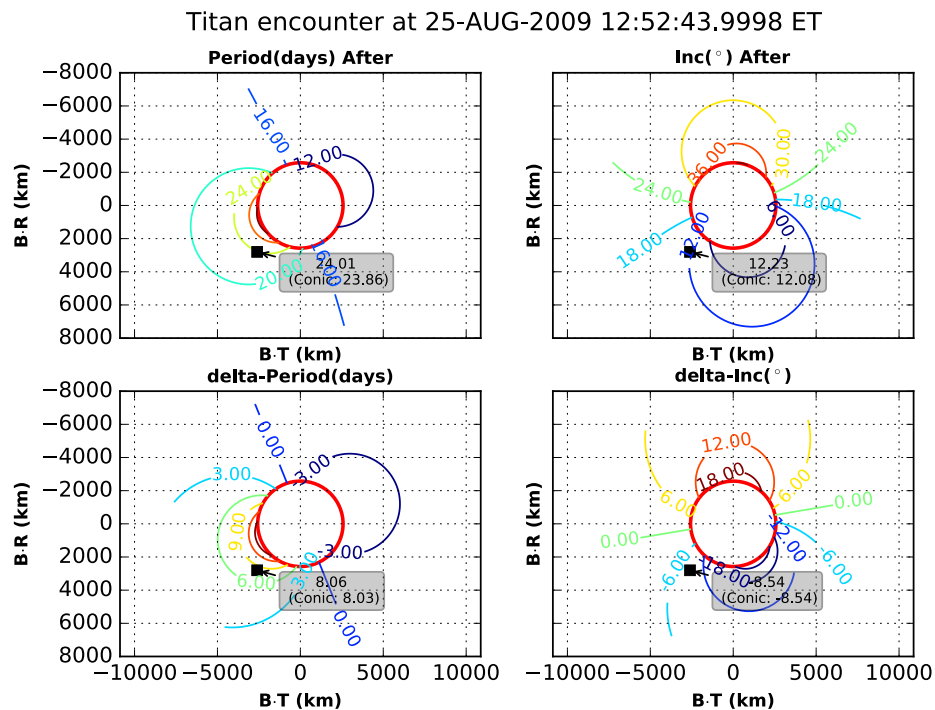


Figure A-24. Titan-61 (T61) Encounter Orbital Element Change Shown on the B-Plane.

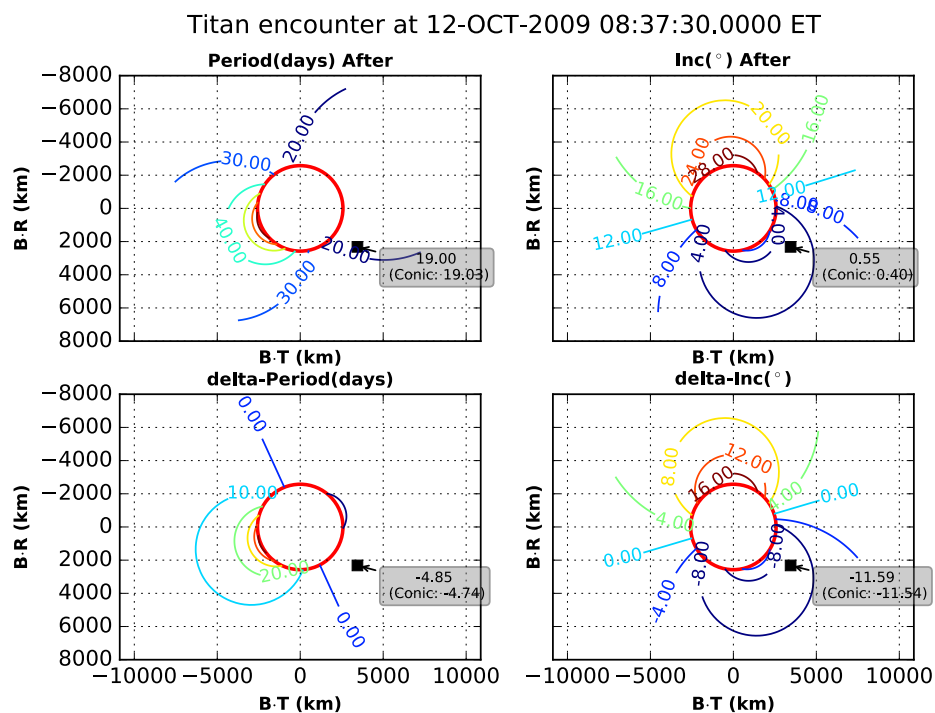


Figure A-25. Titan-62 (T62) Encounter Orbital Element Change Shown on the B-Plane.

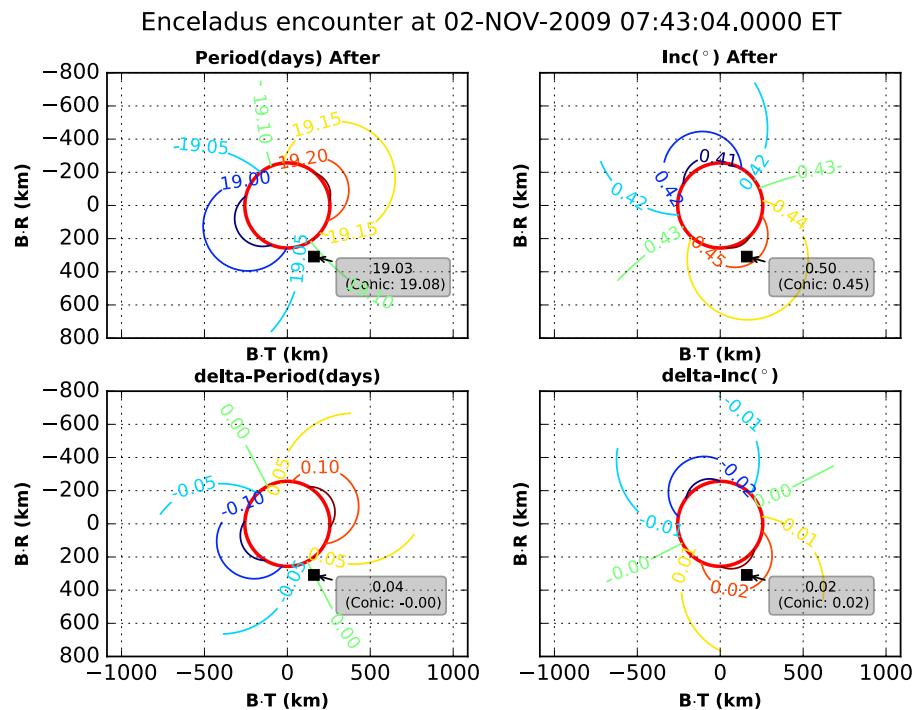


Figure A-26. Enceladus-7 (E7) Encounter Orbital Element Change Shown on the B-Plane.

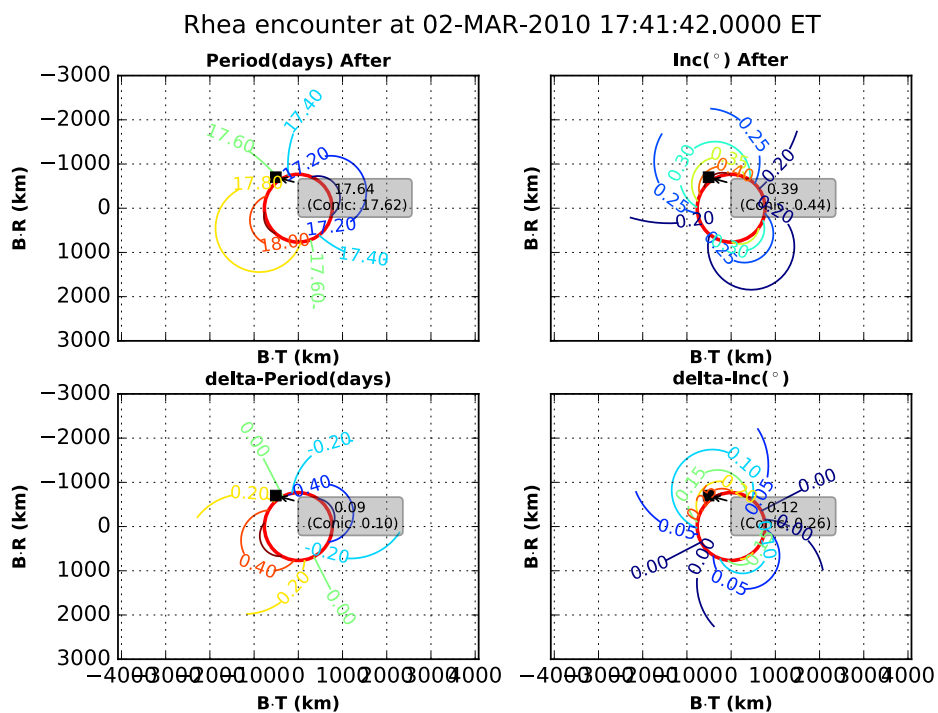


Figure A-27. Rhea-2 (R2) Encounter Orbital Element Change Shown on the B-Plane.

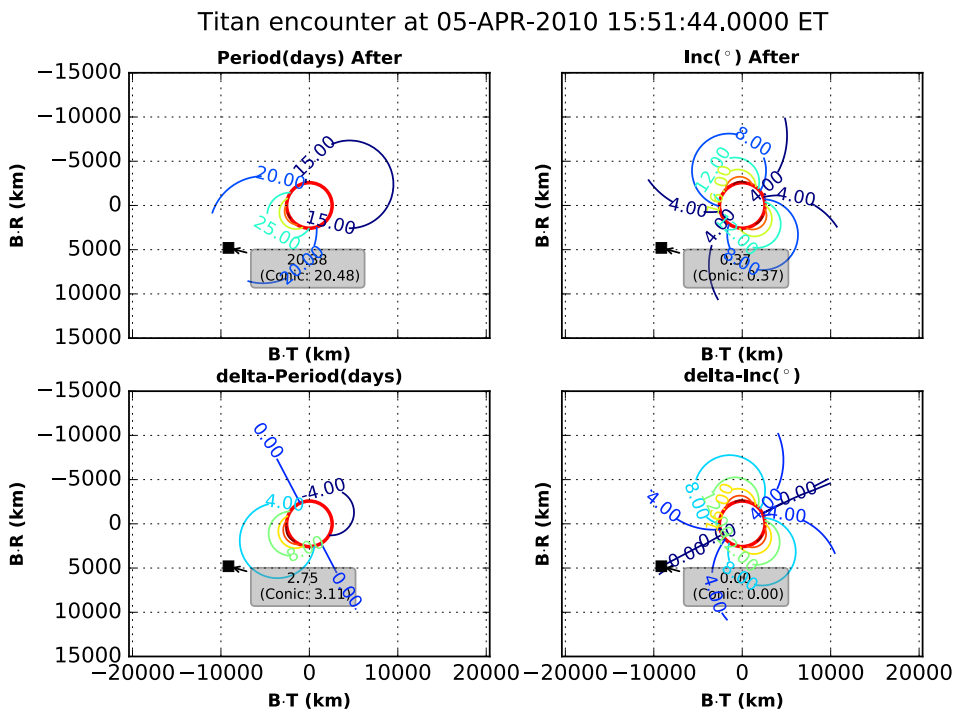


Figure A-28. Titan-67 (T67) Encounter Orbital Element Change Shown on the B-Plane.

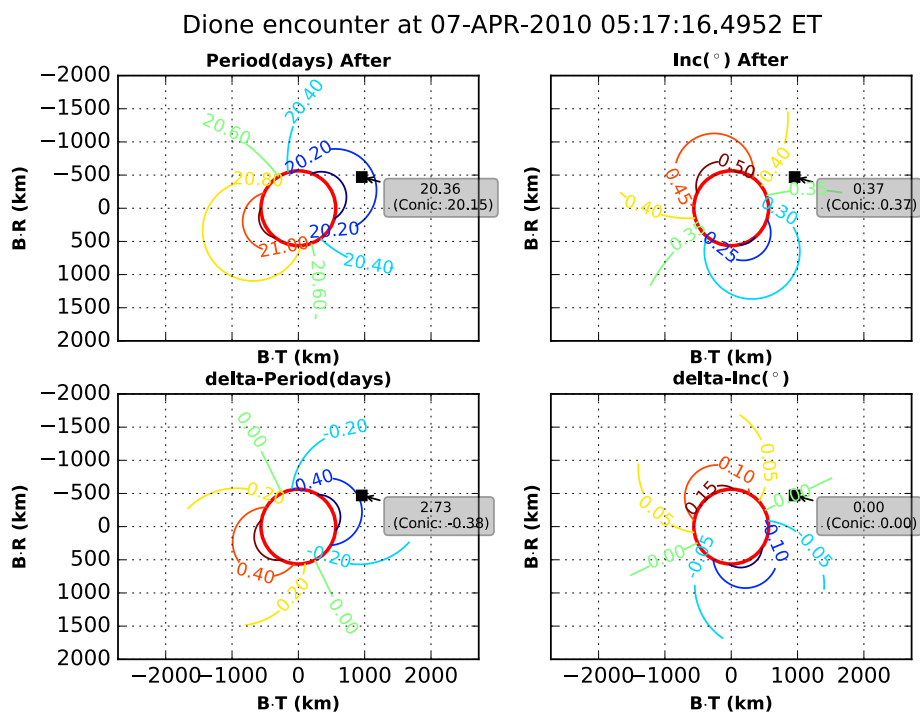


Figure A-29. Dione-2 (D2) Encounter Orbital Element Change Shown on the B-Plane.

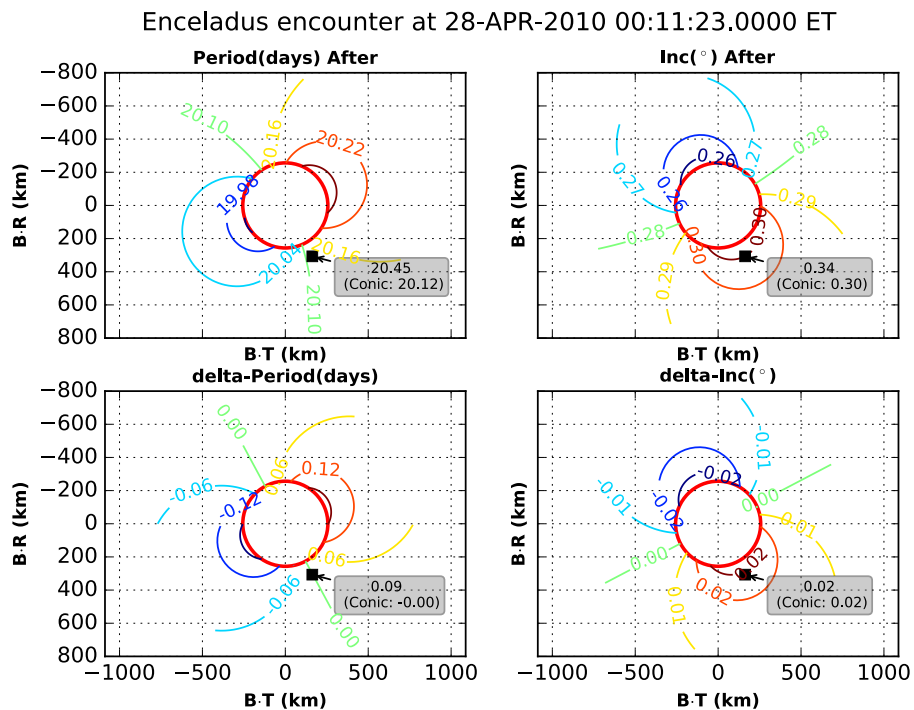


Figure A-30. Enceladus-9 (E9) Encounter Orbital Element Change Shown on the B-Plane.

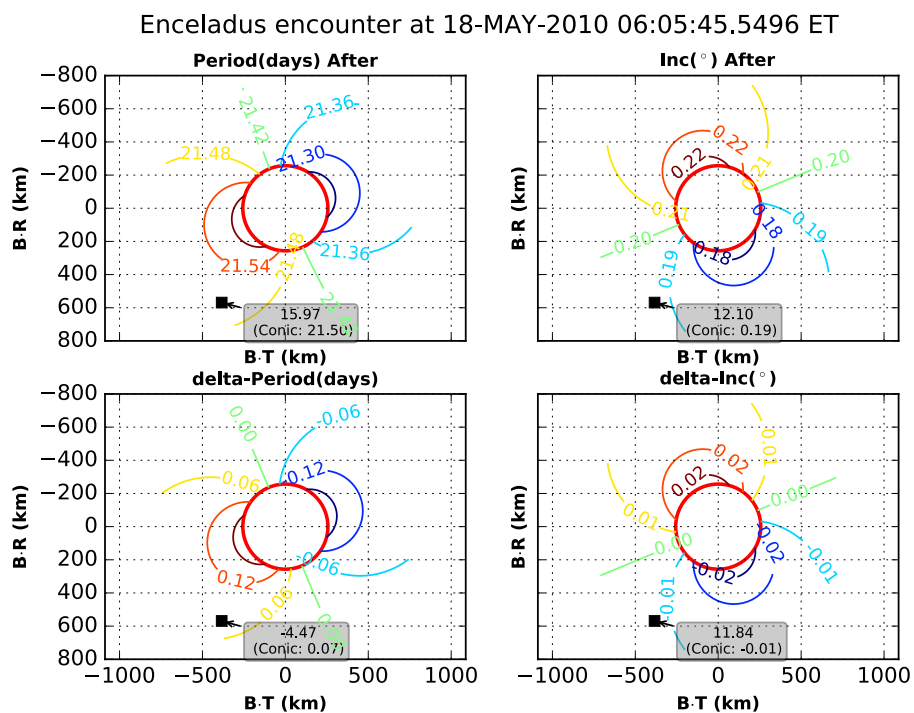


Figure A-31. Enceladus-10 (E10) Encounter Orbital Element Change Shown on the B-Plane.

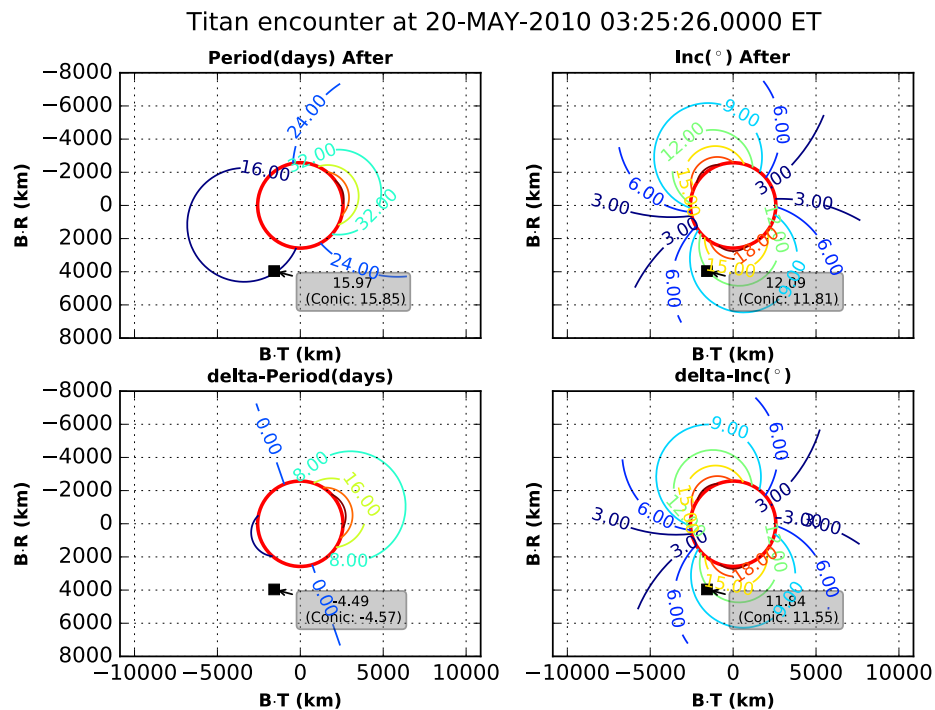


Figure A-32. Titan-68 (T68) Encounter Orbital Element Change Shown on the B-Plane.

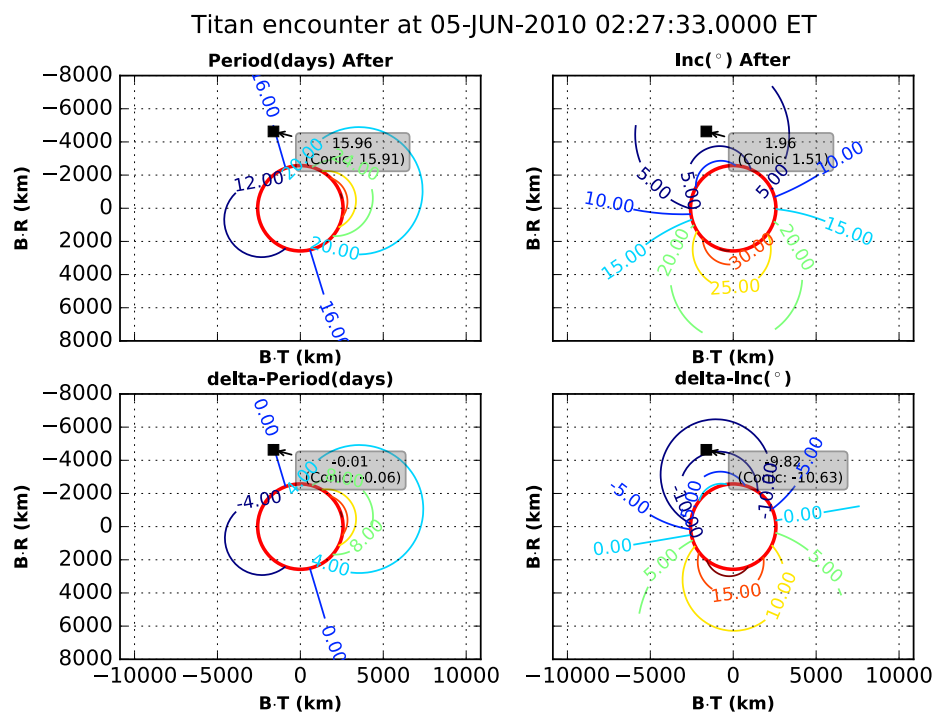


Figure A-33. Titan-69 (T69) Encounter Orbital Element Change Shown on the B-Plane.

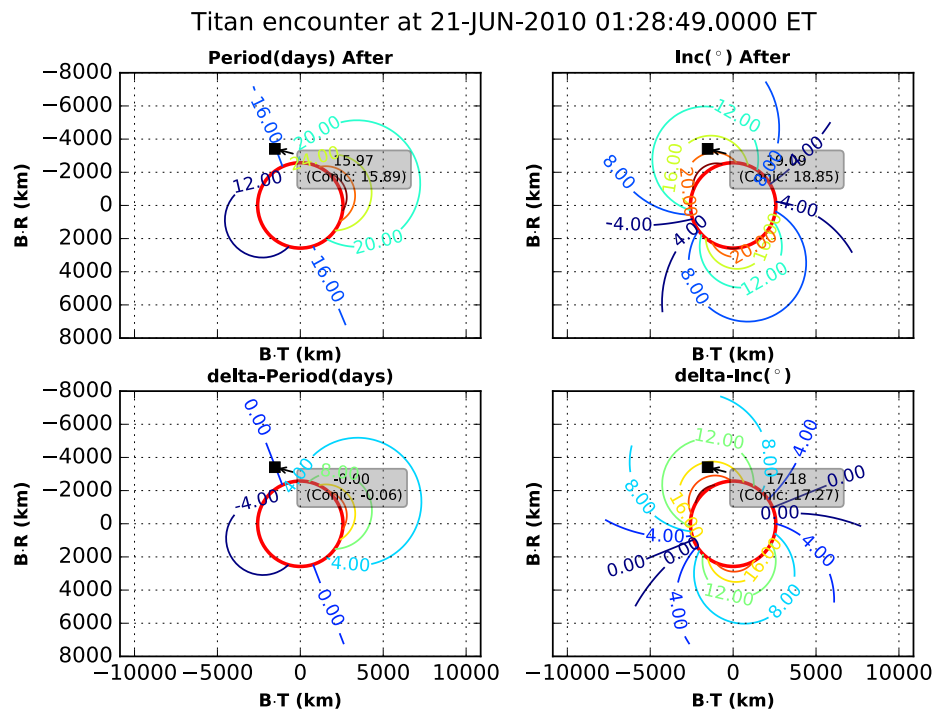


Figure A-34. Titan-70 (T70) Encounter Orbital Element Change Shown on the B-Plane.

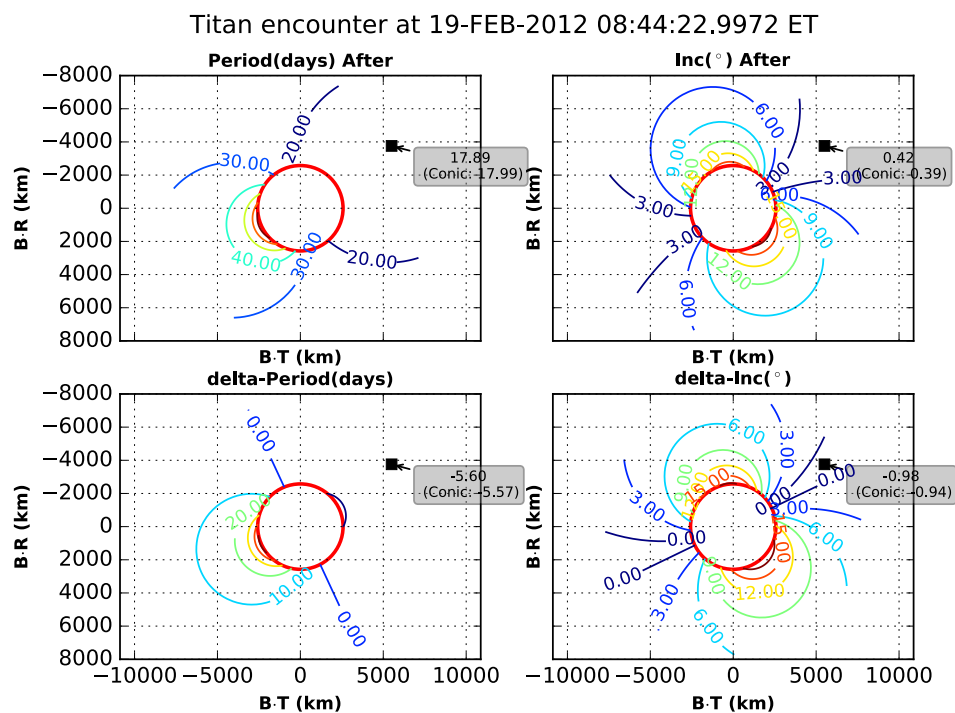


Figure A-35. Titan-82 (T82) Encounter Orbital Element Change Shown on the B-Plane.

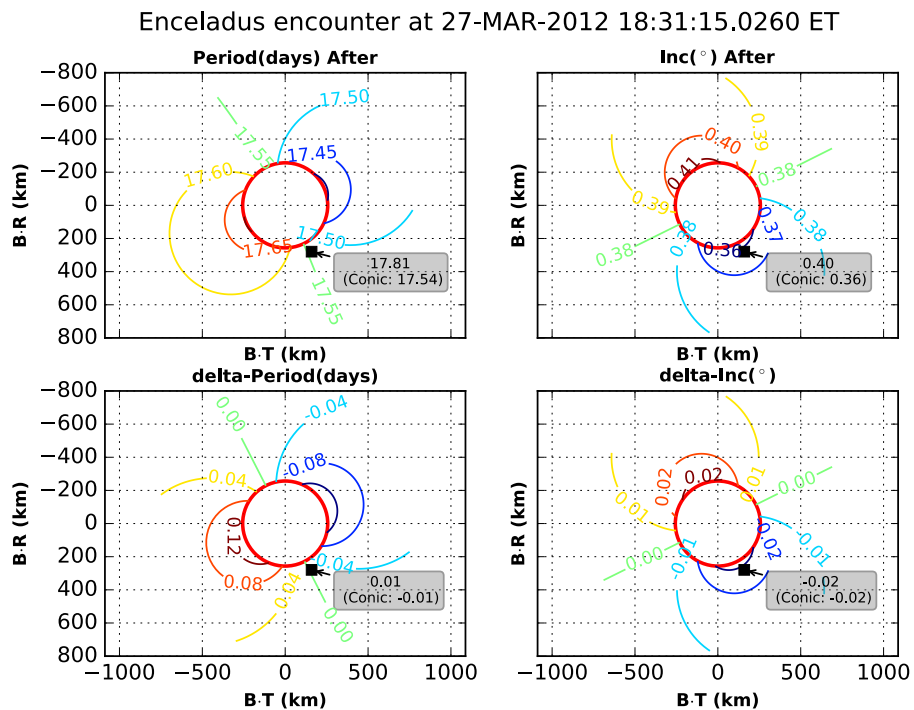


Figure A-36. Enceladus-17 (E17) Encounter Orbital Element Change Shown on the B-Plane.

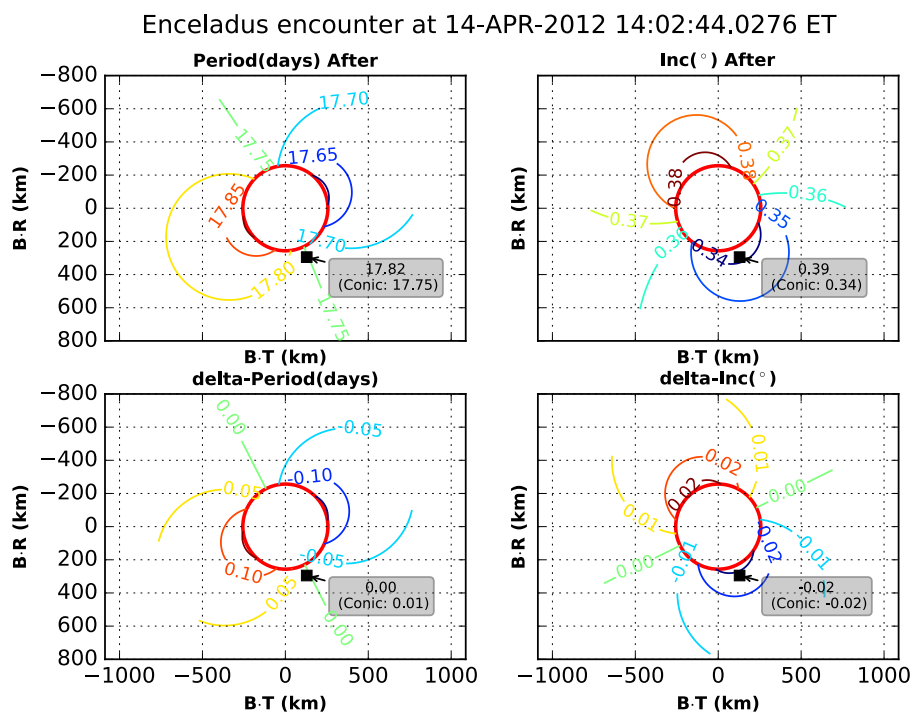


Figure A-37. Enceladus-18 (E18) Encounter Orbital Element Change Shown on the B-Plane.

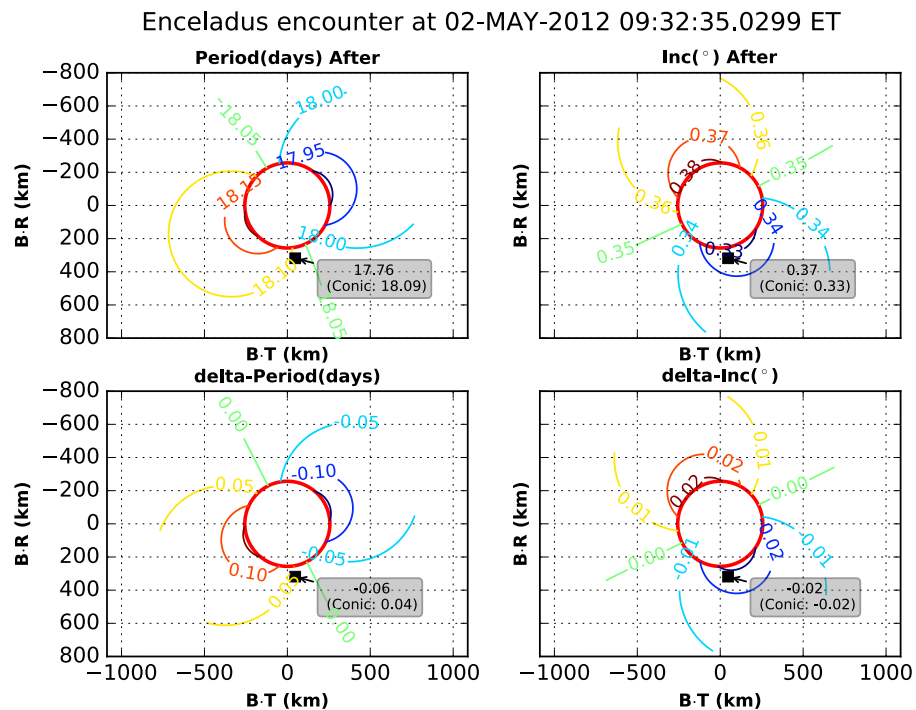


Figure A-38. Enceladus-19 (E19) Encounter Orbital Element Change Shown on the B-Plane.

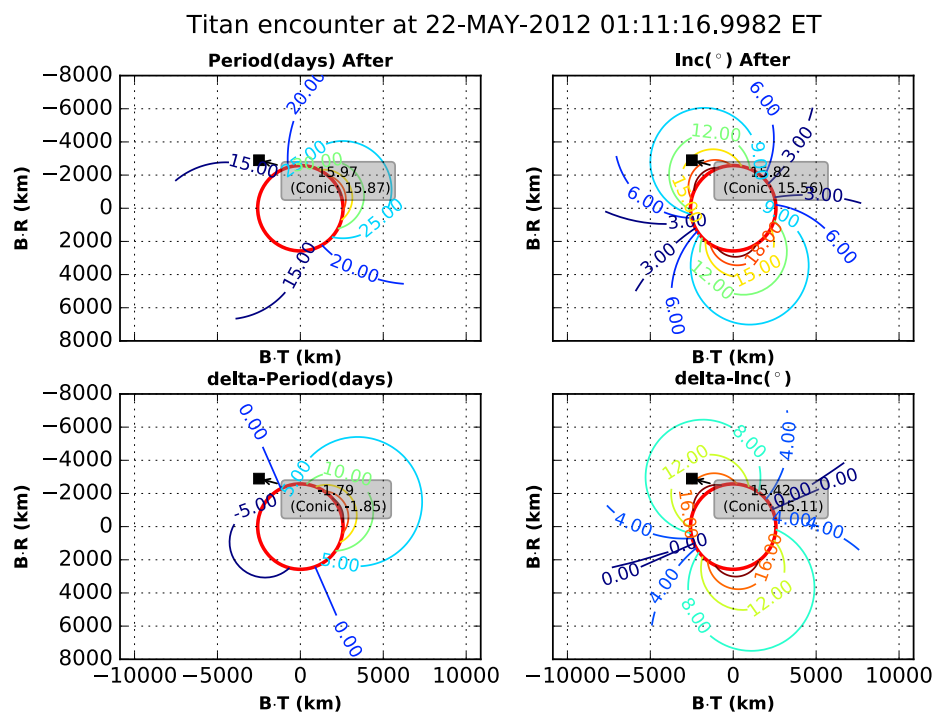


Figure A-39. Titan-83 (T83) Encounter Orbital Element Change Shown on the B-Plane.

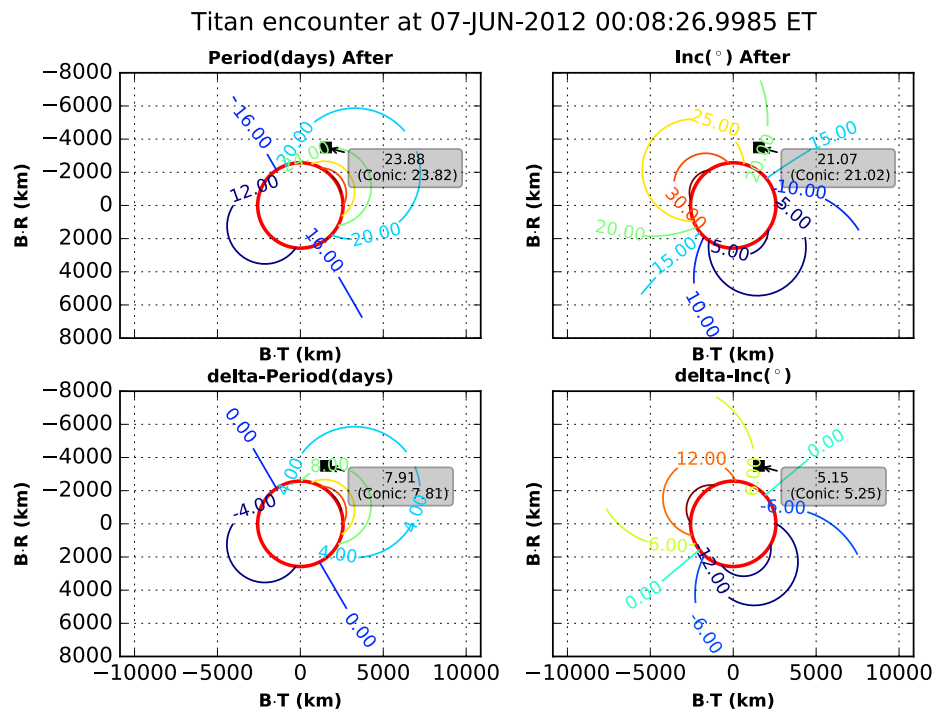


Figure A-40. Titan-84 (T84) Encounter Orbital Element Change Shown on the B-Plane.

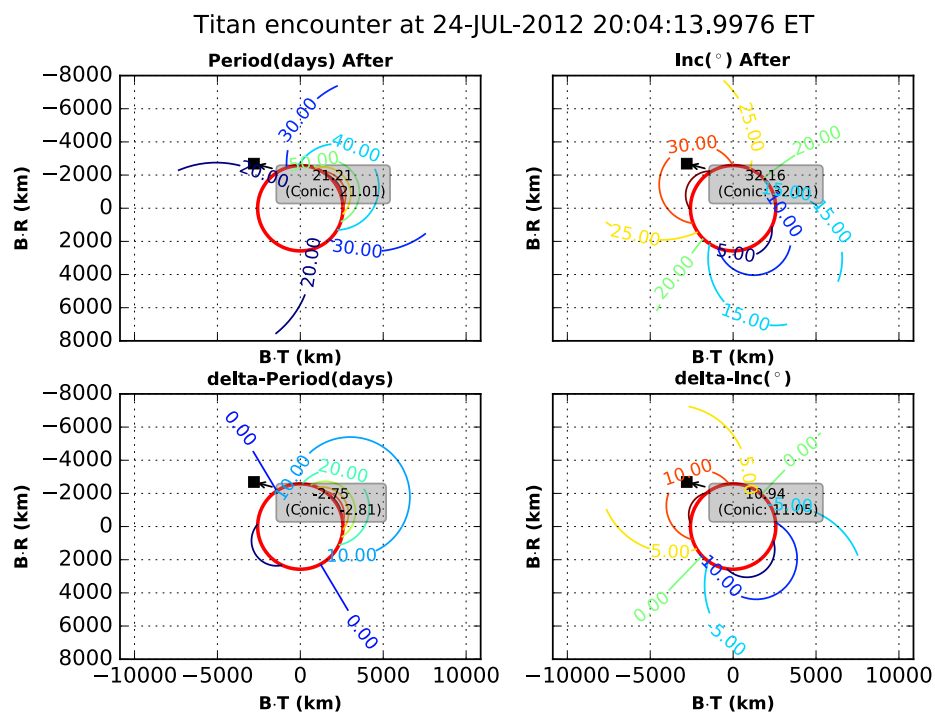


Figure A-41. Titan-85 (T85) Encounter Orbital Element Change Shown on the B-Plane.

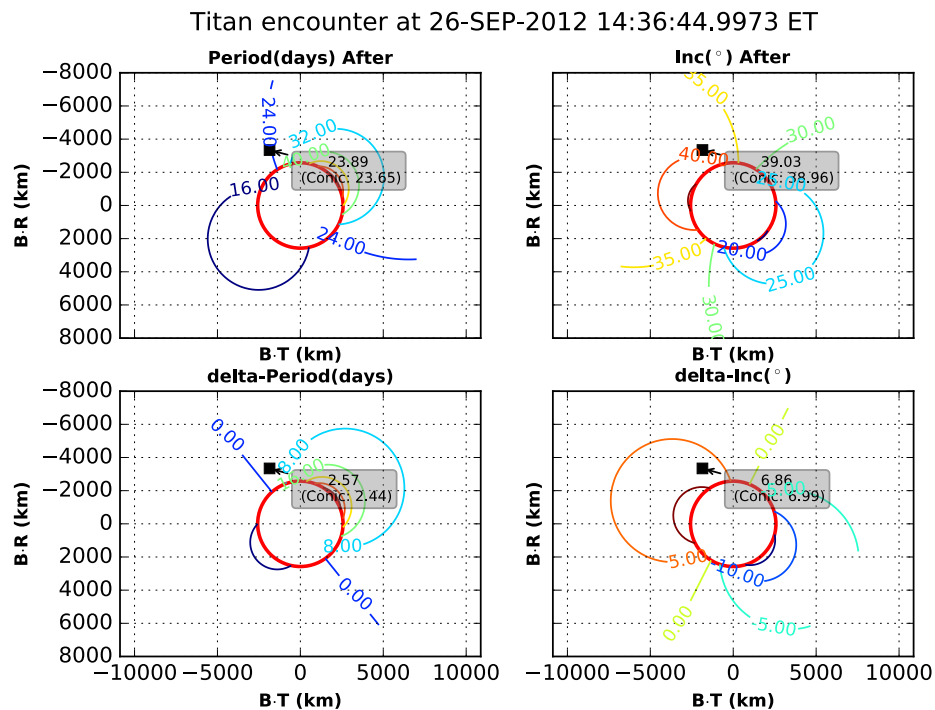


Figure A-42. Titan-86 (T86) Encounter Orbital Element Change Shown on the B-Plane.

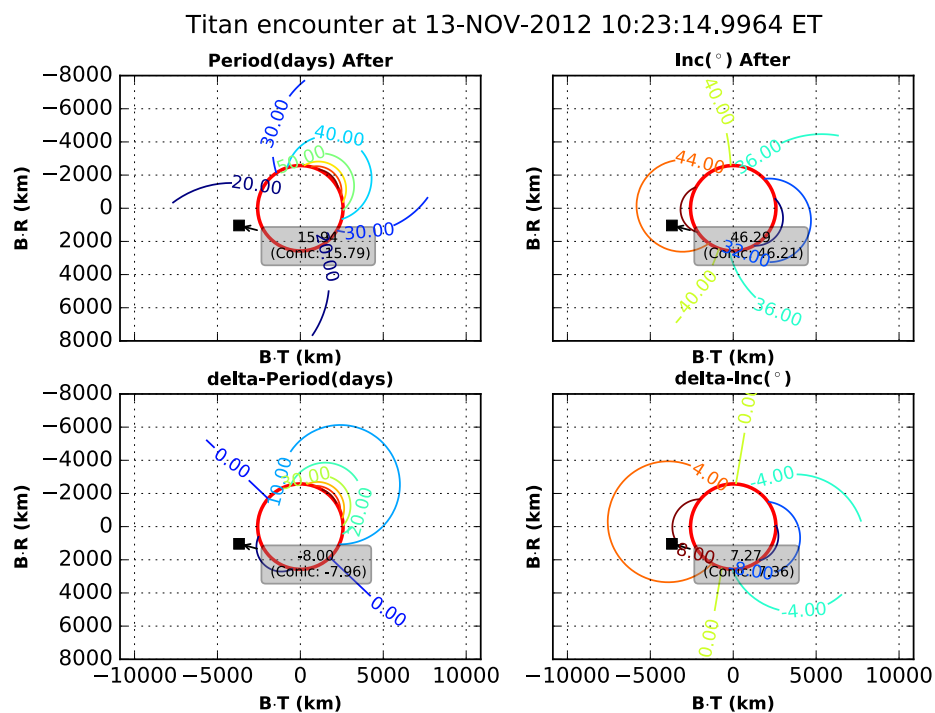


Figure A-43. Titan-87 (T87) Encounter Orbital Element Change Shown on the B-Plane.

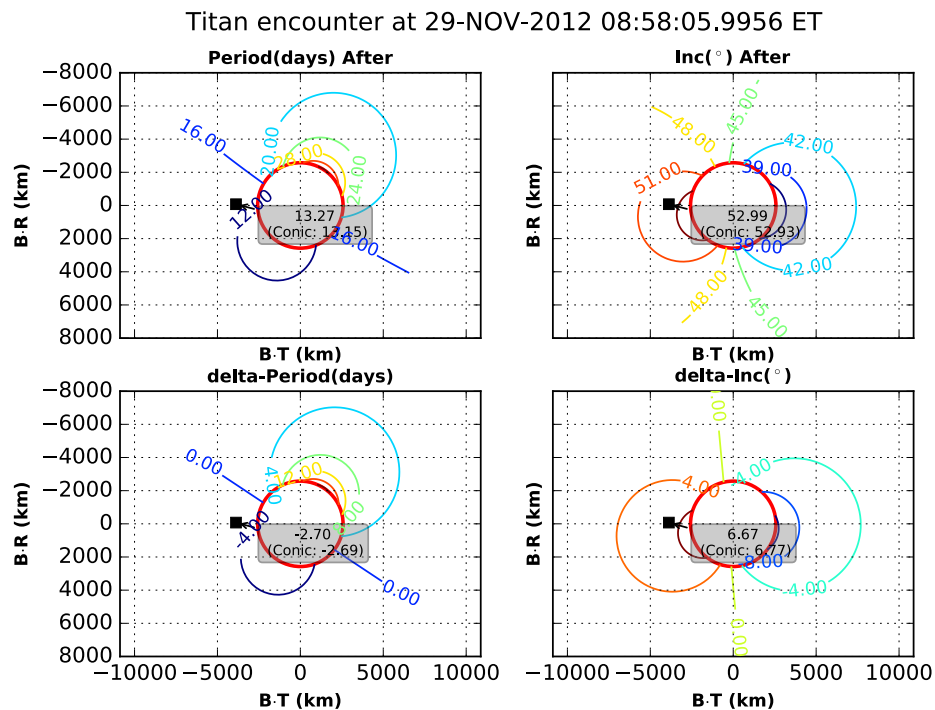


Figure A-44. Titan-88 (T88) Encounter Orbital Element Change Shown on the B-Plane.

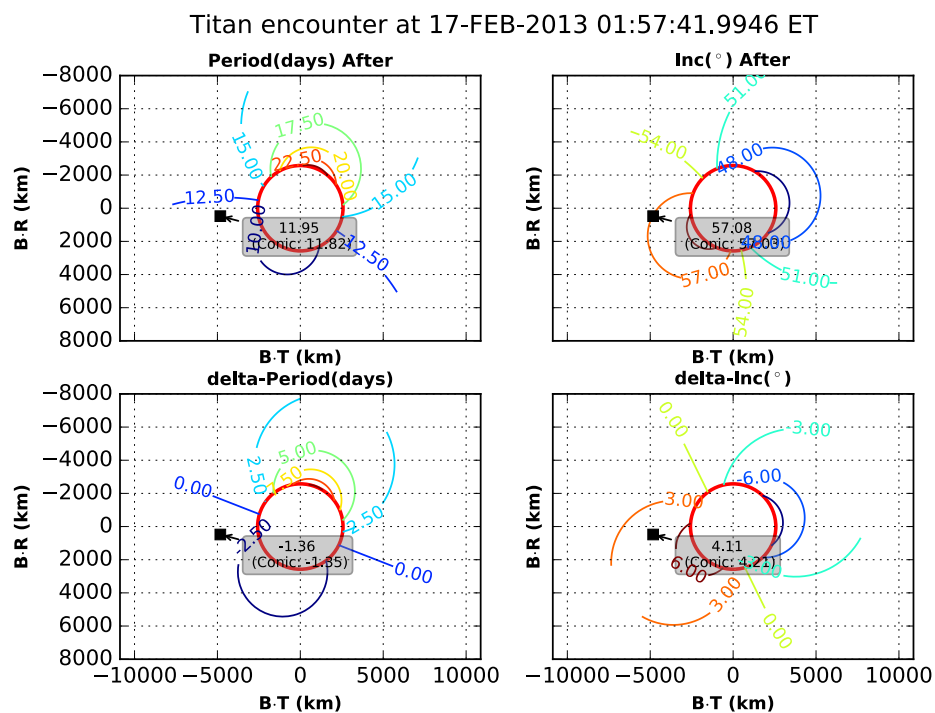


Figure A-45. Titan-89 (T89) Encounter Orbital Element Change Shown on the B-Plane.

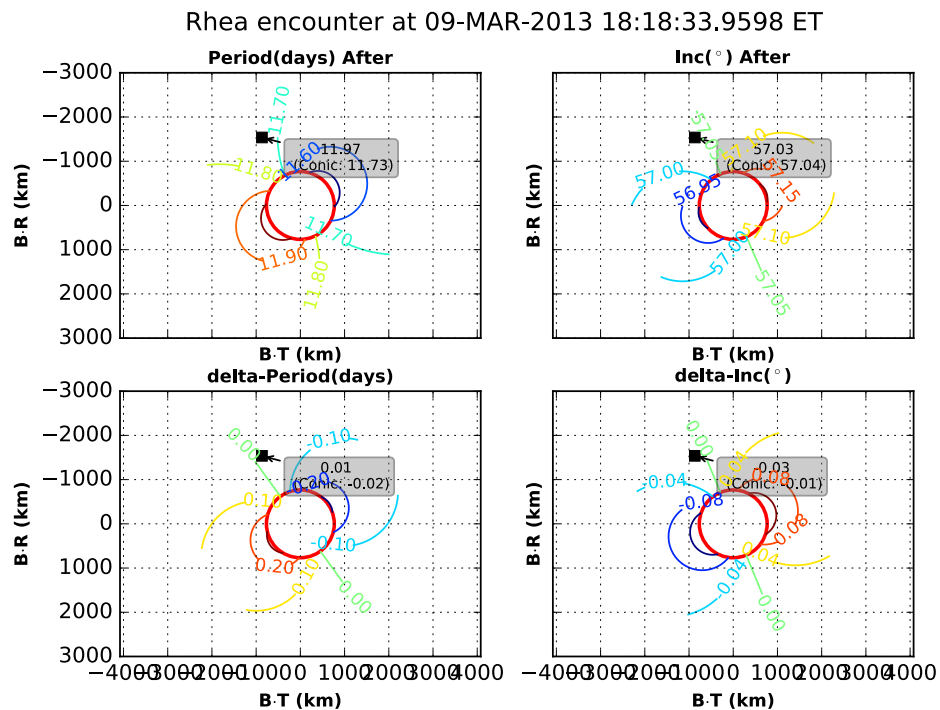


Figure A-46. Rhea-4 (R4) Encounter Orbital Element Change Shown on the B-Plane.

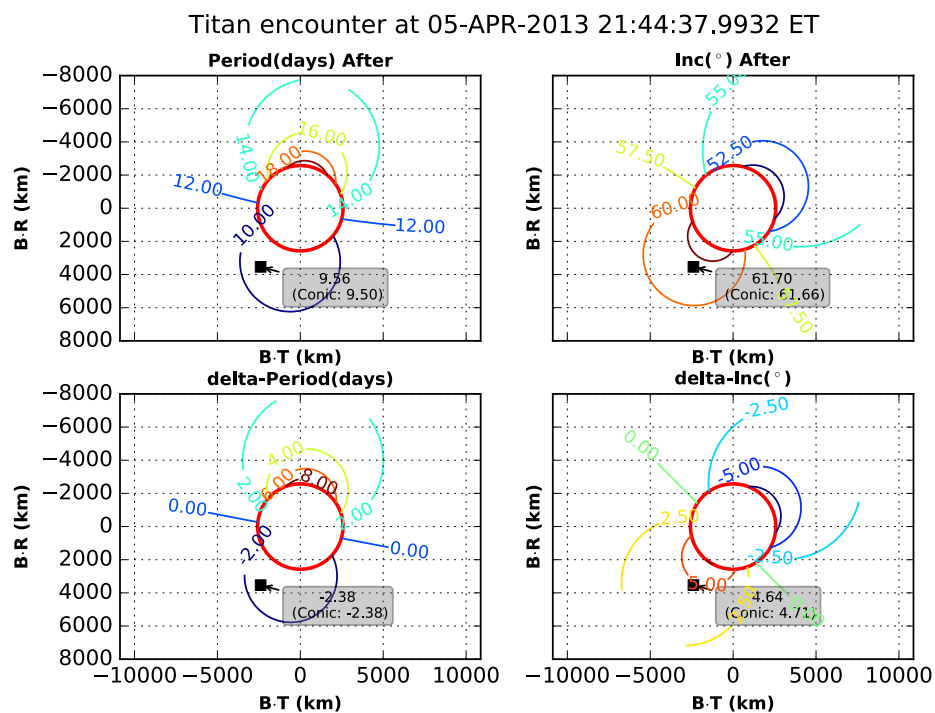


Figure A-47. Titan-90 (T90) Encounter Orbital Element Change Shown on the B-Plane.

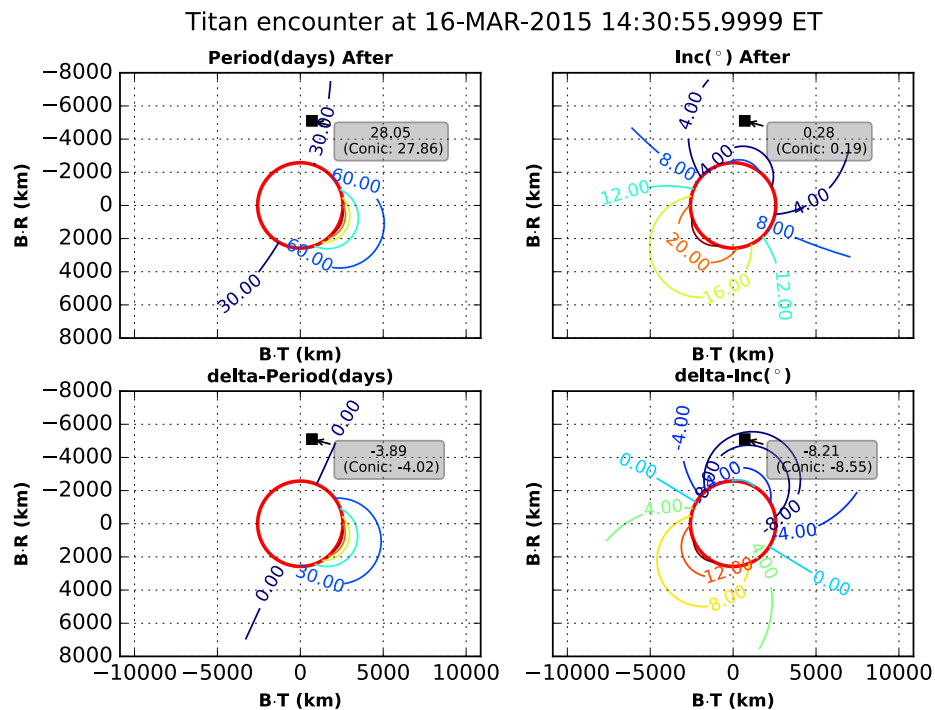


Figure A-48. Titan-110 (T110) Encounter Orbital Element Change Shown on the B-Plane.

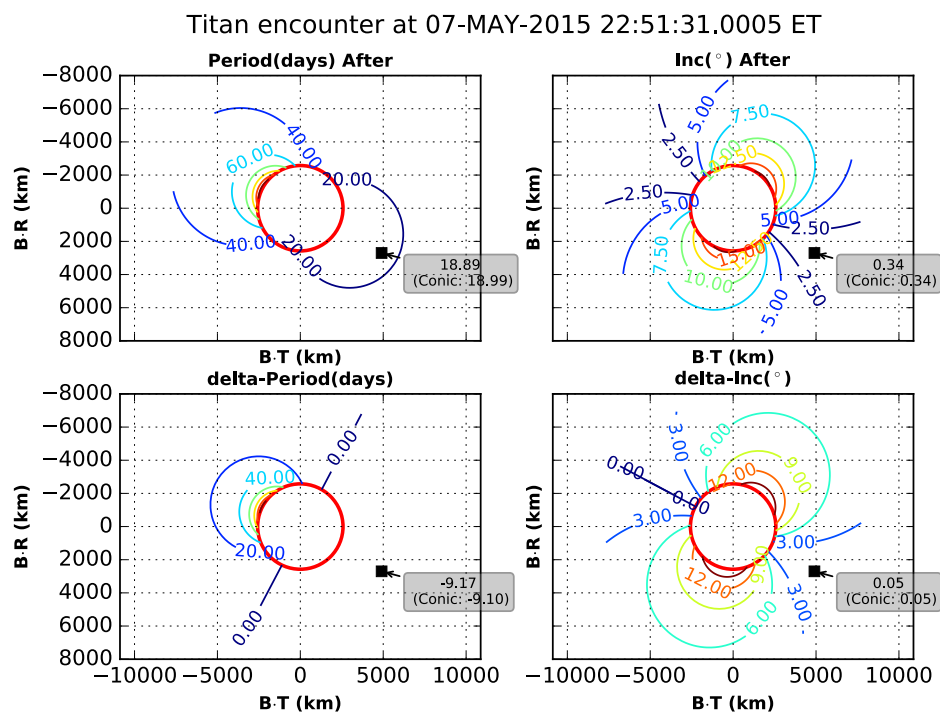


Figure A-49. Titan-111 (T111) Encounter Orbital Element Change Shown on the B-Plane.

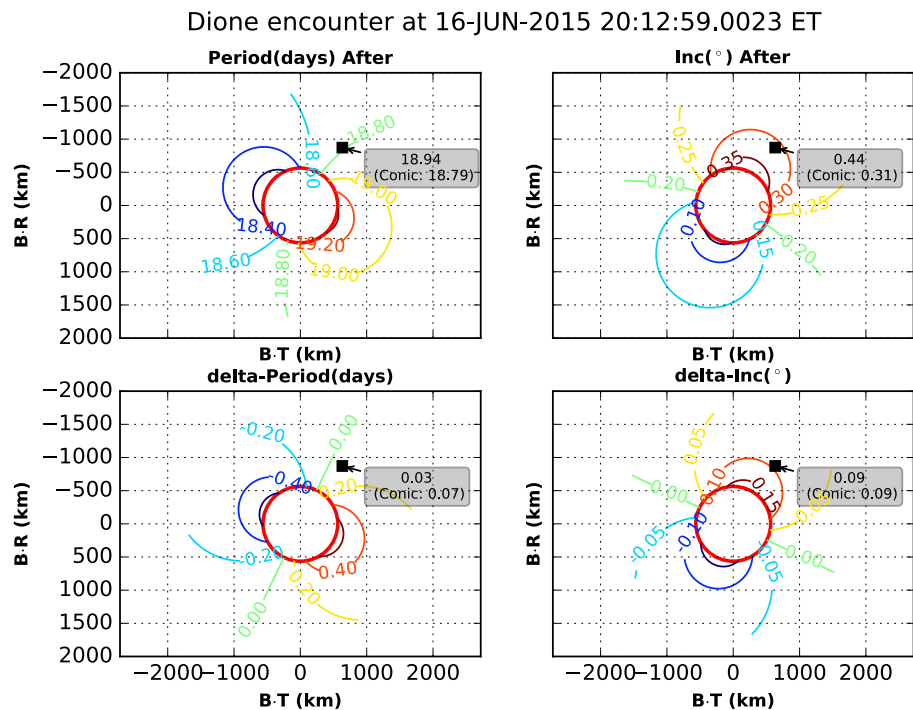


Figure A-50. Dione-4 (D4) Encounter Orbital Element Change Shown on the B-Plane.

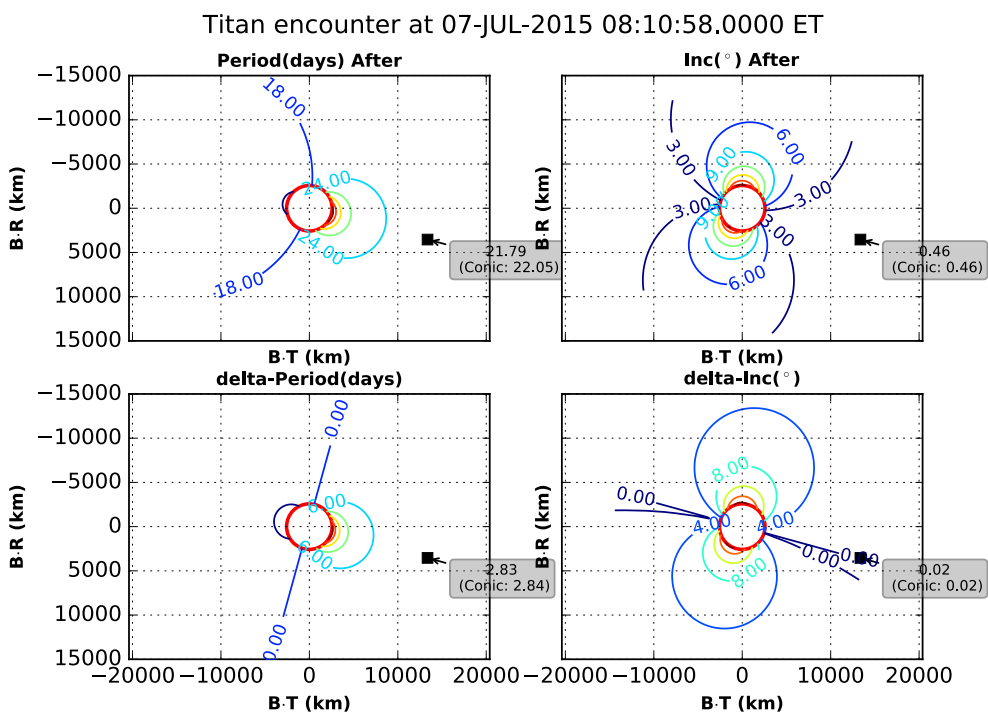


Figure A-51. Titan-112 (T112) Encounter Orbital Element Change Shown on the B-Plane.

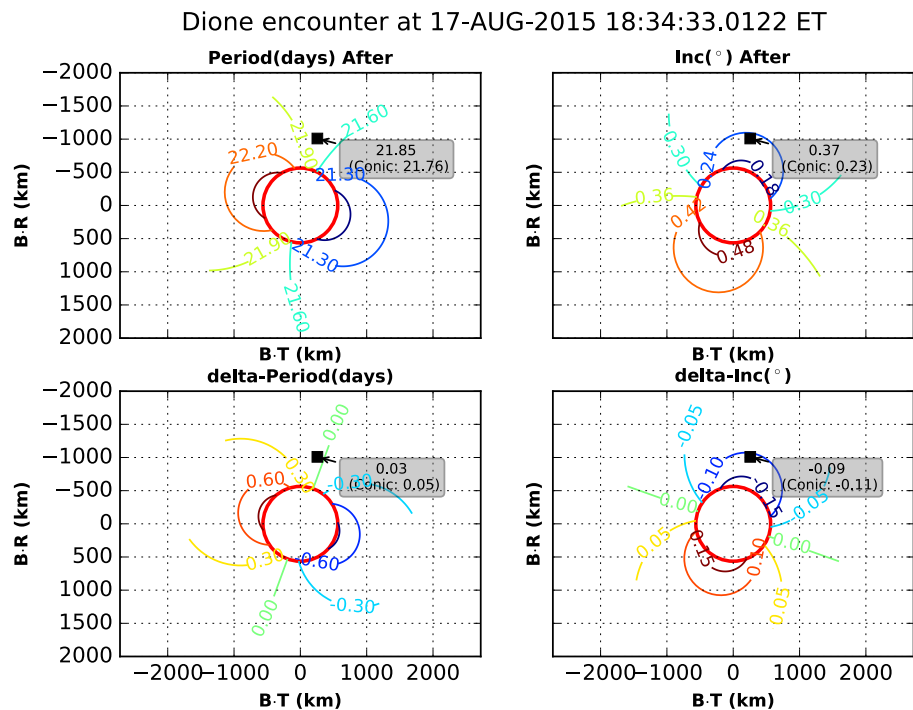


Figure A-52. Dione-5 (D5) Encounter Orbital Element Change Shown on the B-Plane.

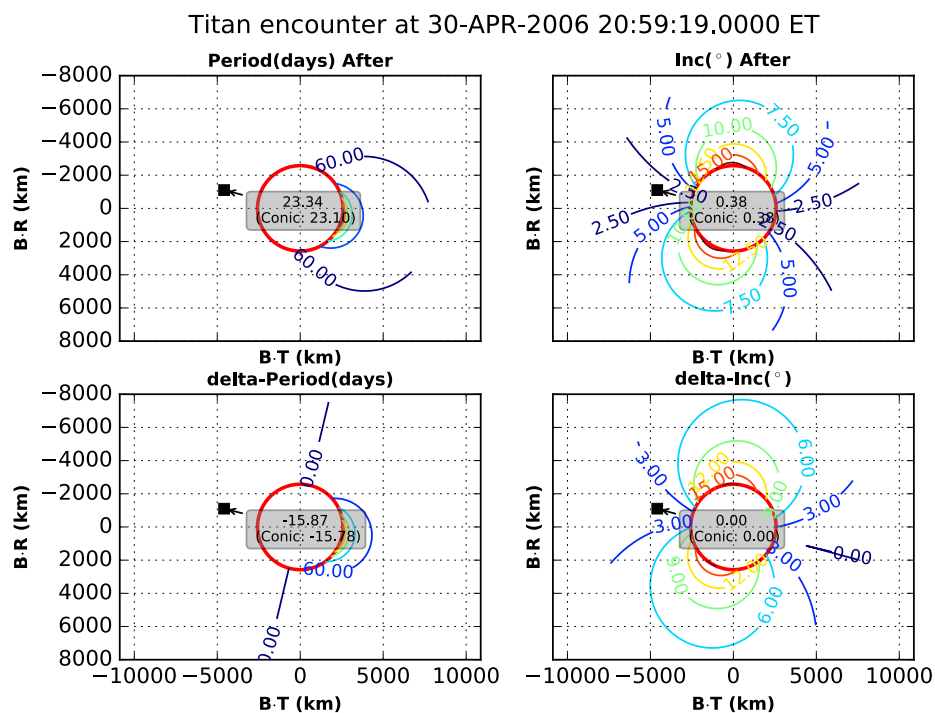


Figure A-53. Titan-113 (T113) Encounter Orbital Element Change Shown on the B-Plane.

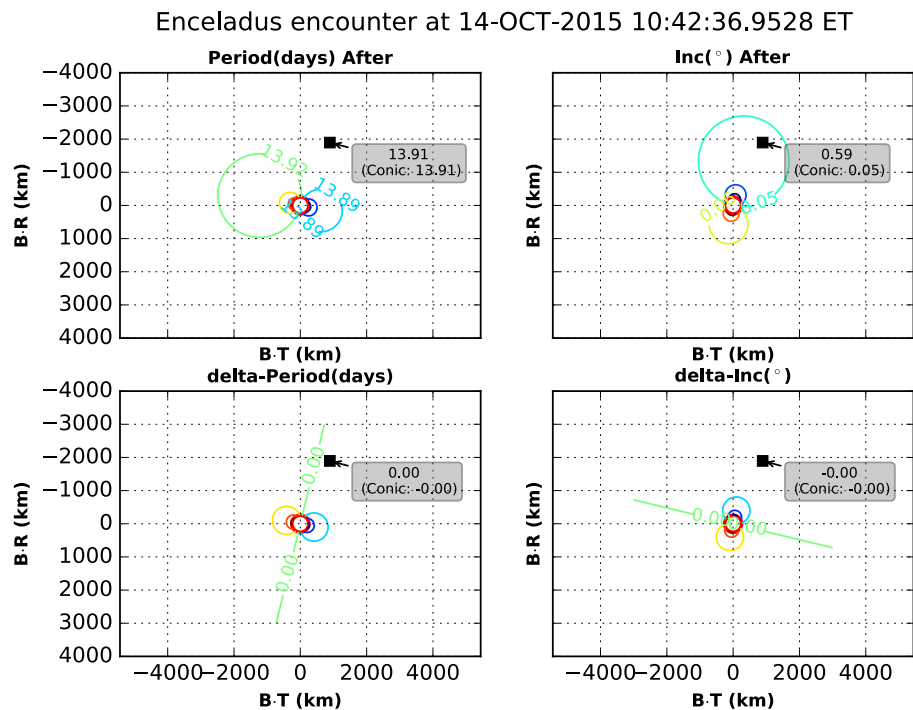


Figure A-54. Enceladus-20 (E20) Encounter Orbital Element Change Shown on the B-Plane.

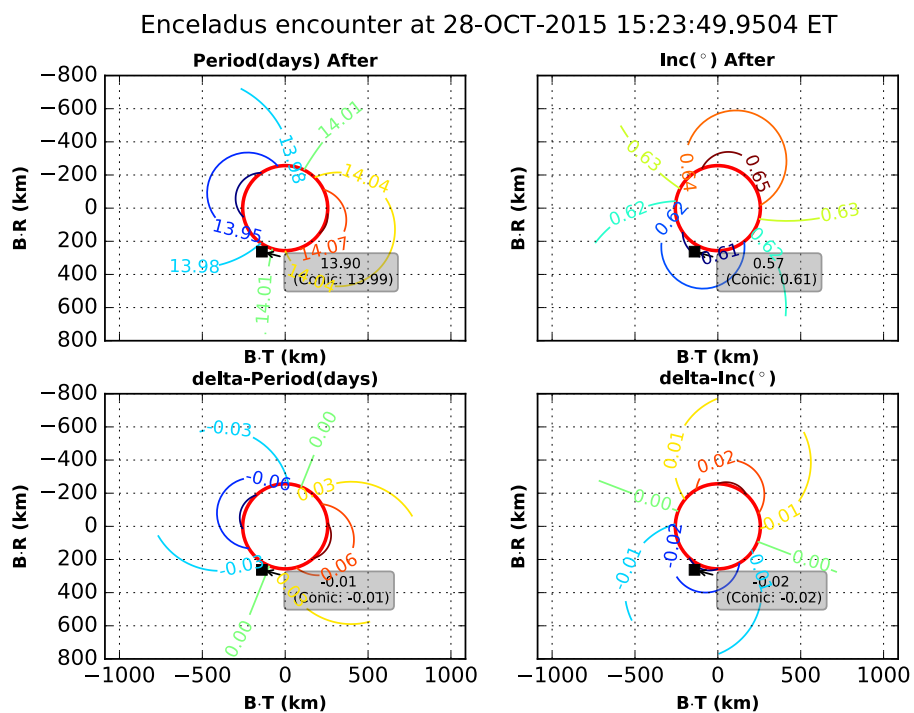


Figure A-55. Enceladus-21 (E21) Encounter Orbital Element Change Shown on the B-Plane.

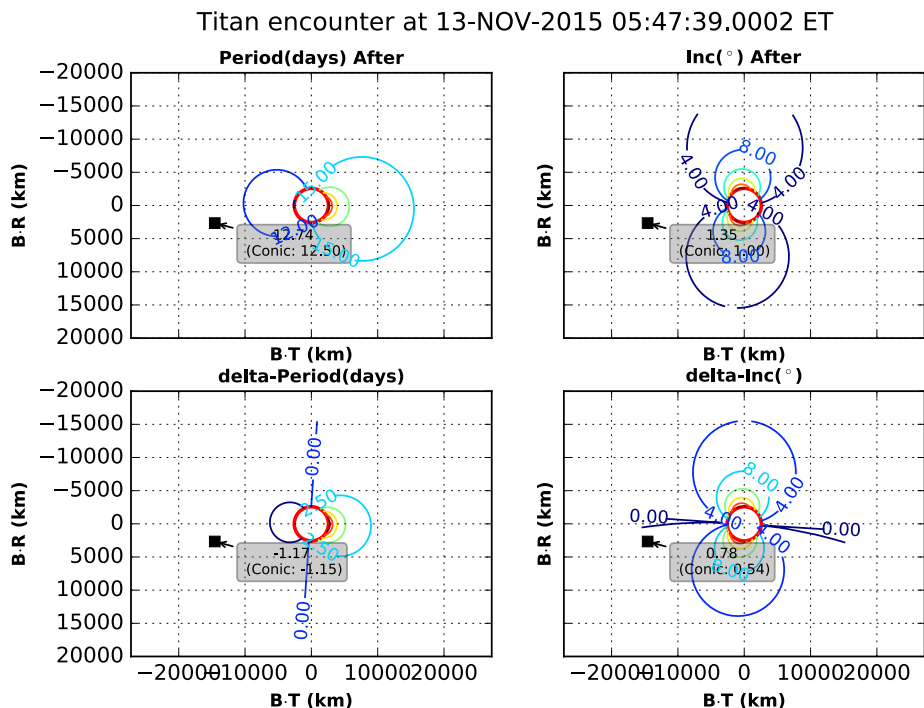


Figure A-56. Titan-114 (T114) Encounter Orbital Element Change Shown on the B-Plane.

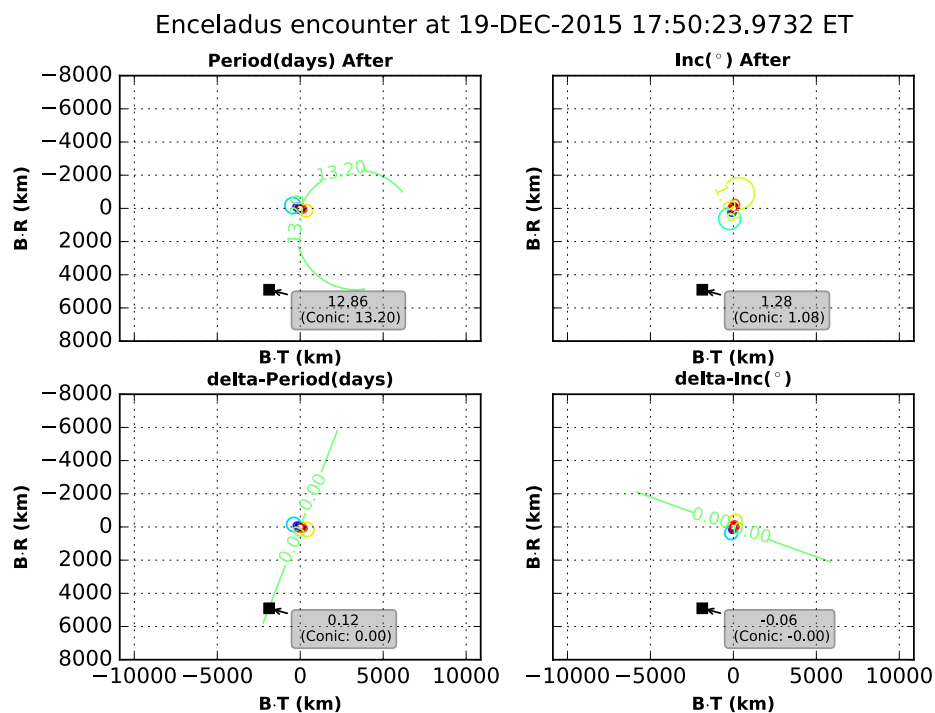


Figure A-57. Enceladus-22 (E22) Encounter Orbital Element Change Shown on the B-Plane.

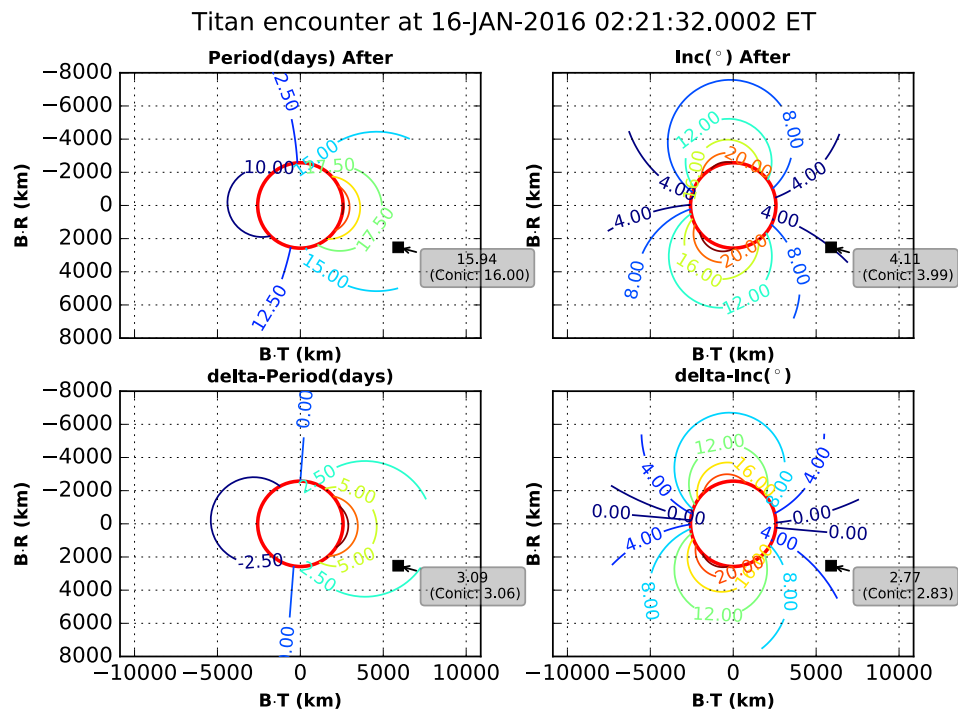


Figure A-58. Titan-115 (T115) Encounter Orbital Element Change Shown on the B-Plane.

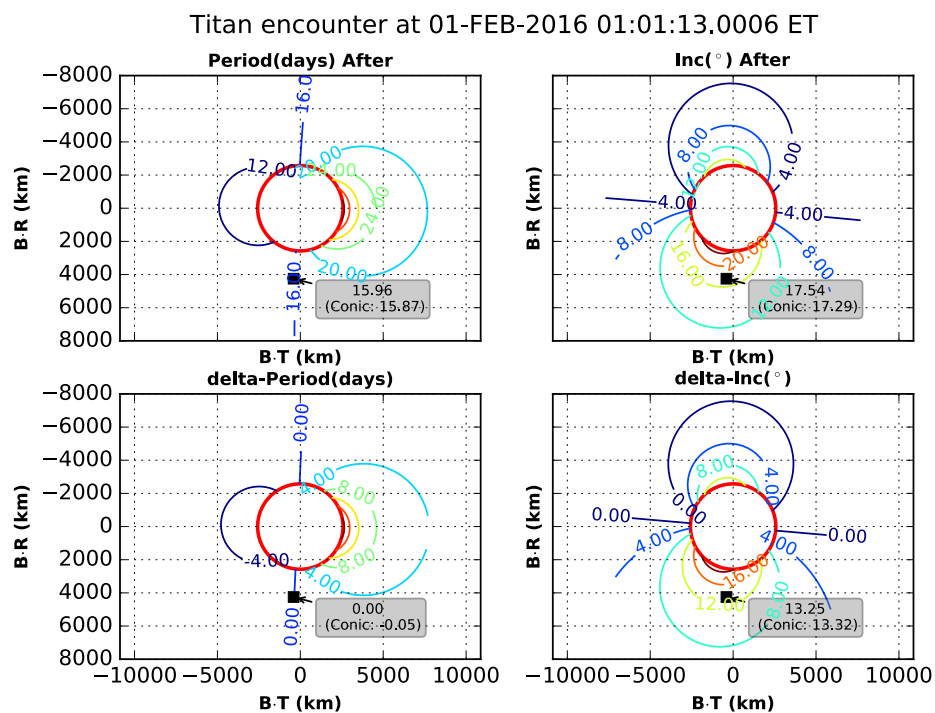


Figure A-59. Titan-116 (T116) Encounter Orbital Element Change Shown on the B-Plane.

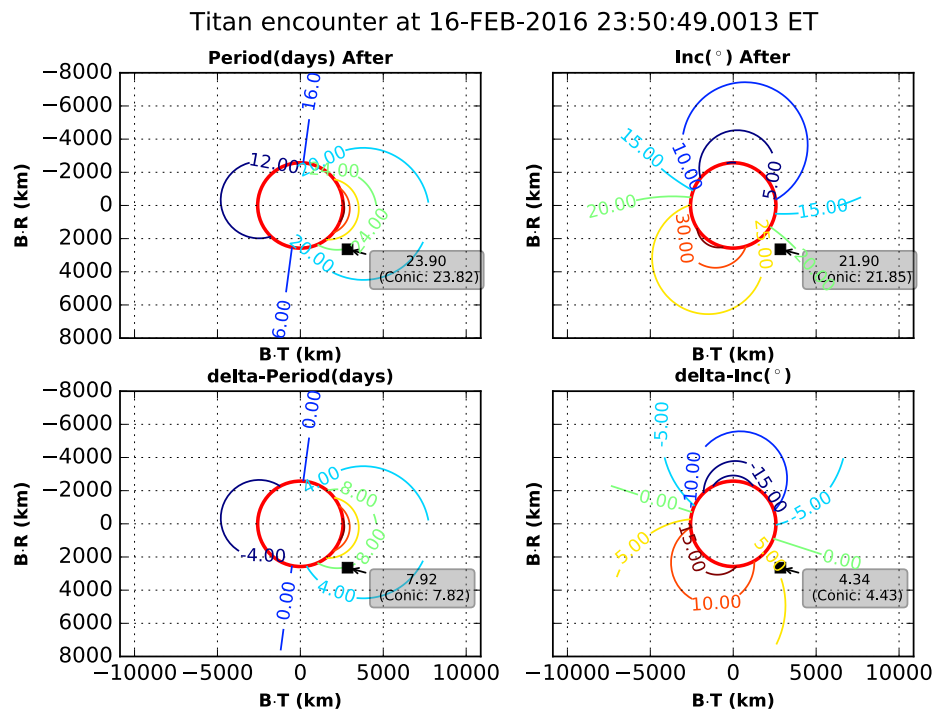


Figure A-60. Titan-117 (T117) Encounter Orbital Element Change Shown on the B-Plane.

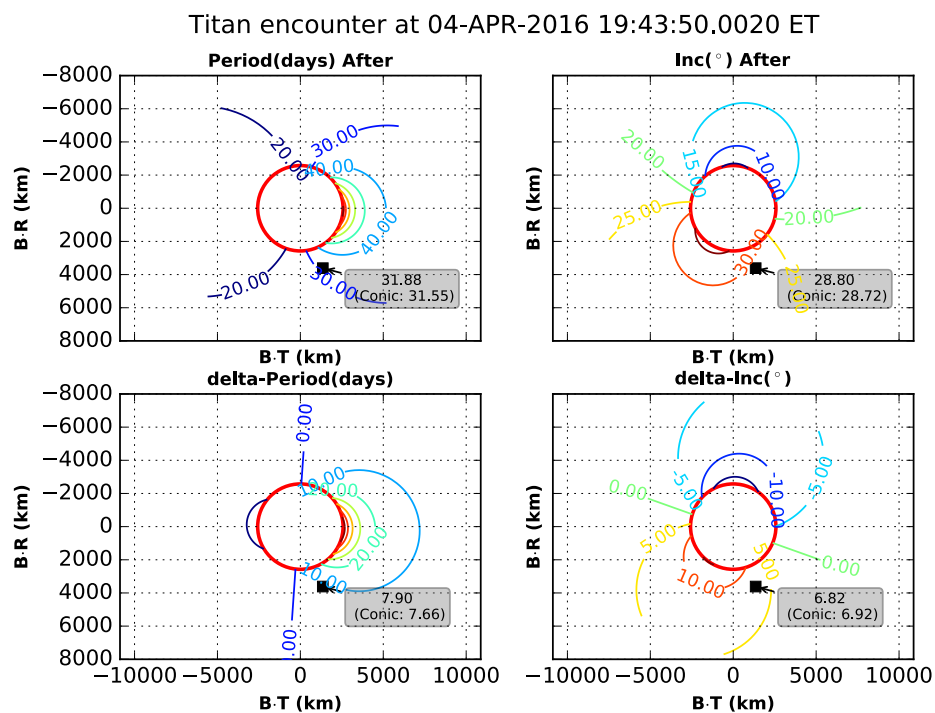


Figure A-61. Titan-118 (T118) Encounter Orbital Element Change Shown on the B-Plane.

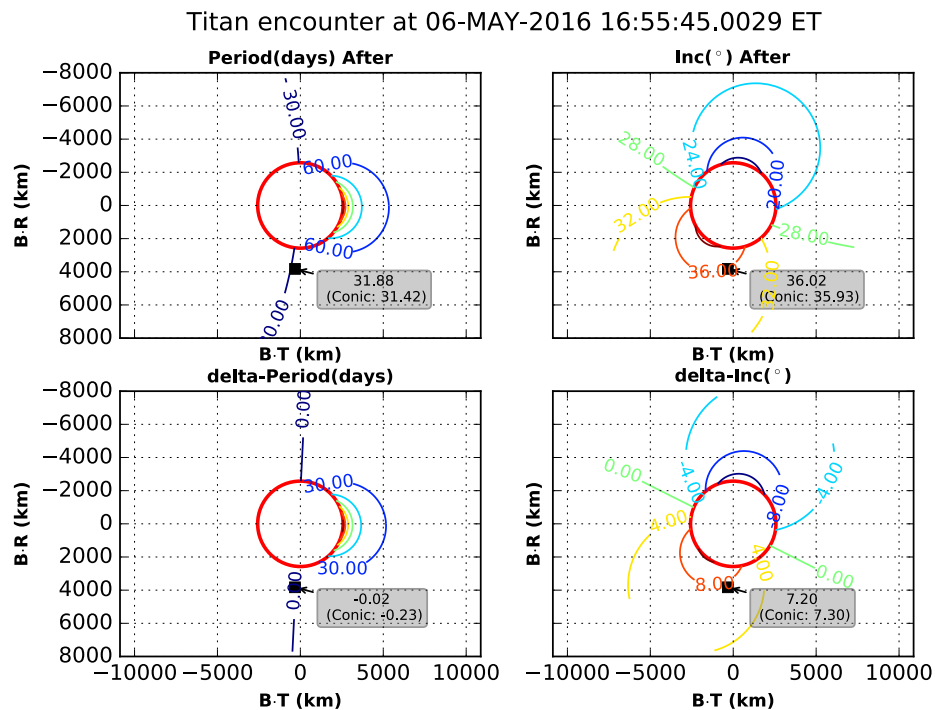


Figure A-62. Titan-119 (T119) Encounter Orbital Element Change Shown on the B-Plane.

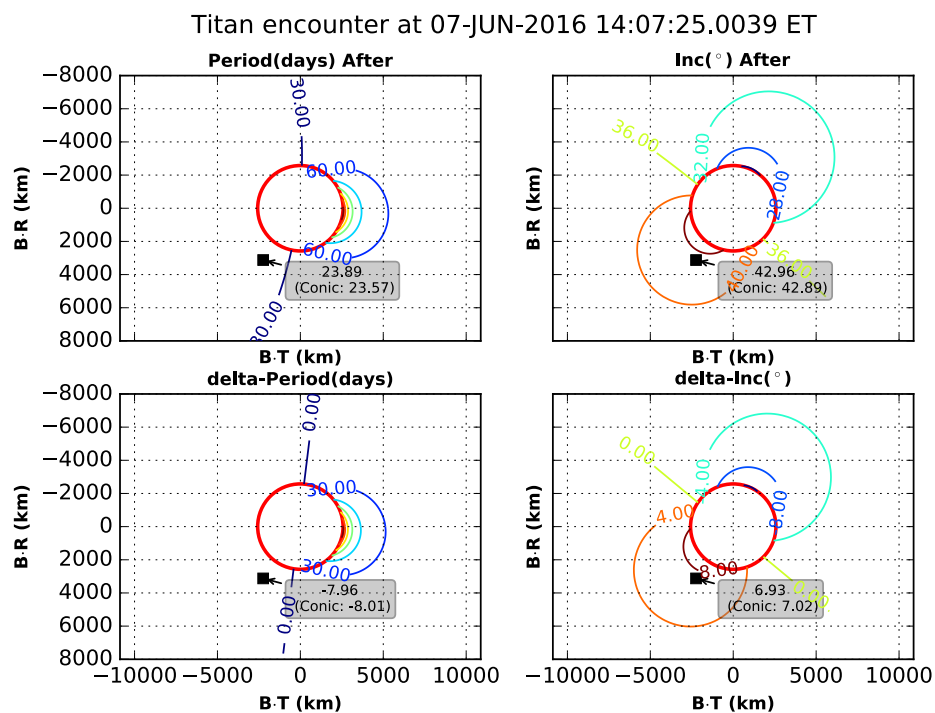


Figure A-63. Titan-120 (T120) Encounter Orbital Element Change Shown on the B-Plane.

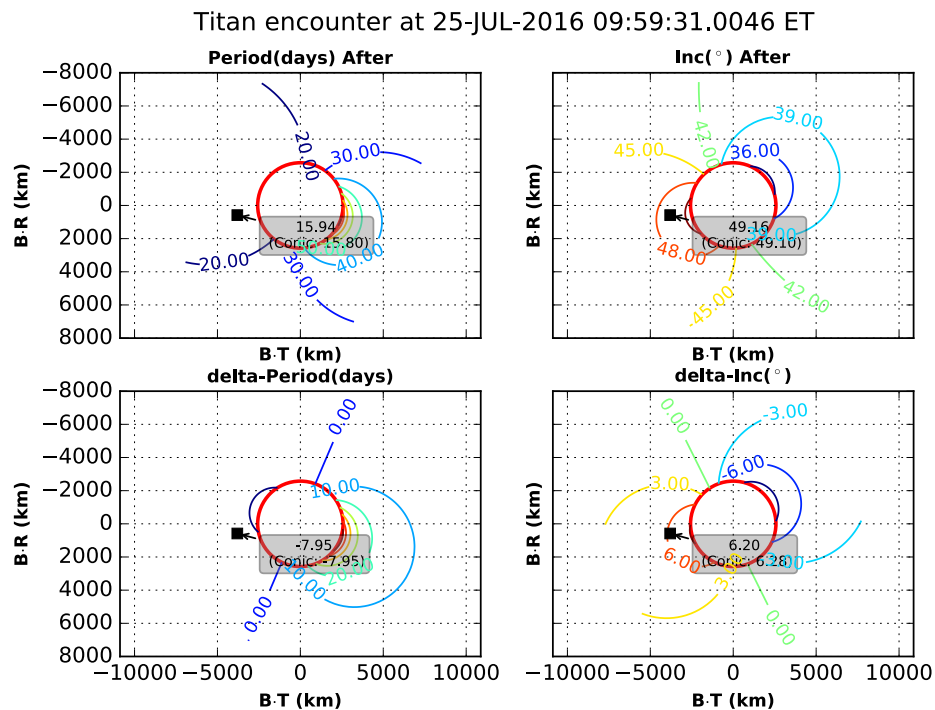


Figure A-64. Titan-121 (T121) Encounter Orbital Element Change Shown on the B-Plane.

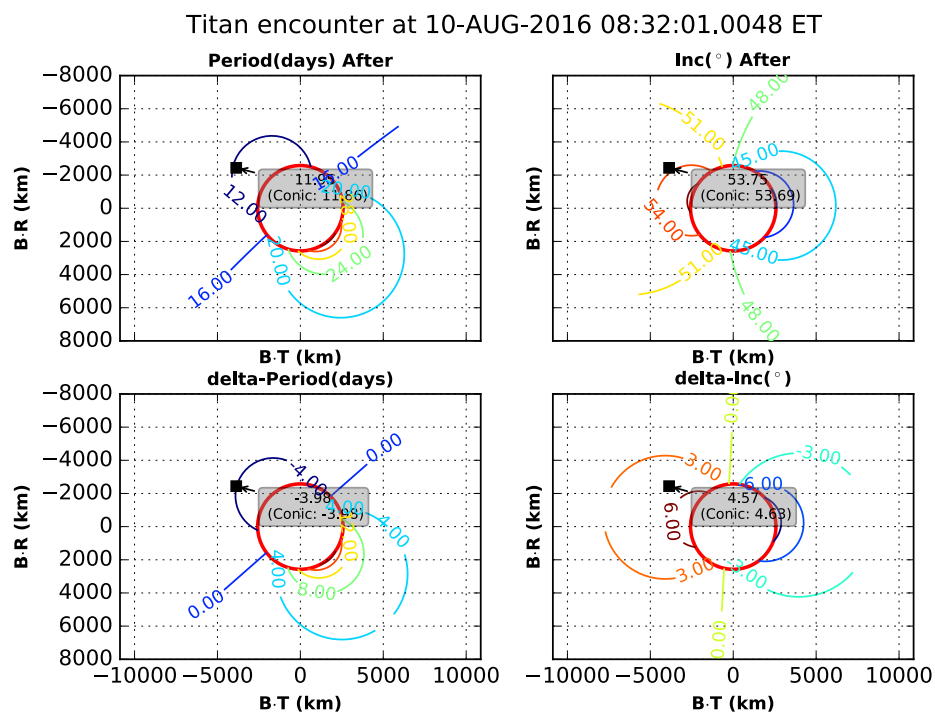


Figure A-65. Titan-122 (T122) Encounter Orbital Element Change Shown on the B-Plane.

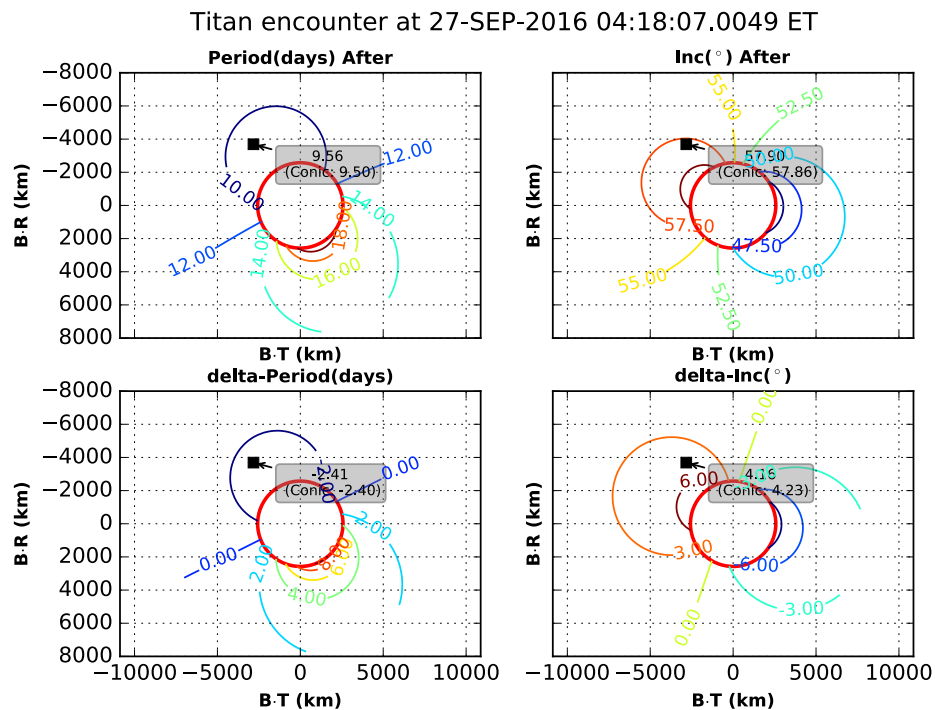


Figure A-66. Titan-123 (T123) Encounter Orbital Element Change Shown on the B-Plane.

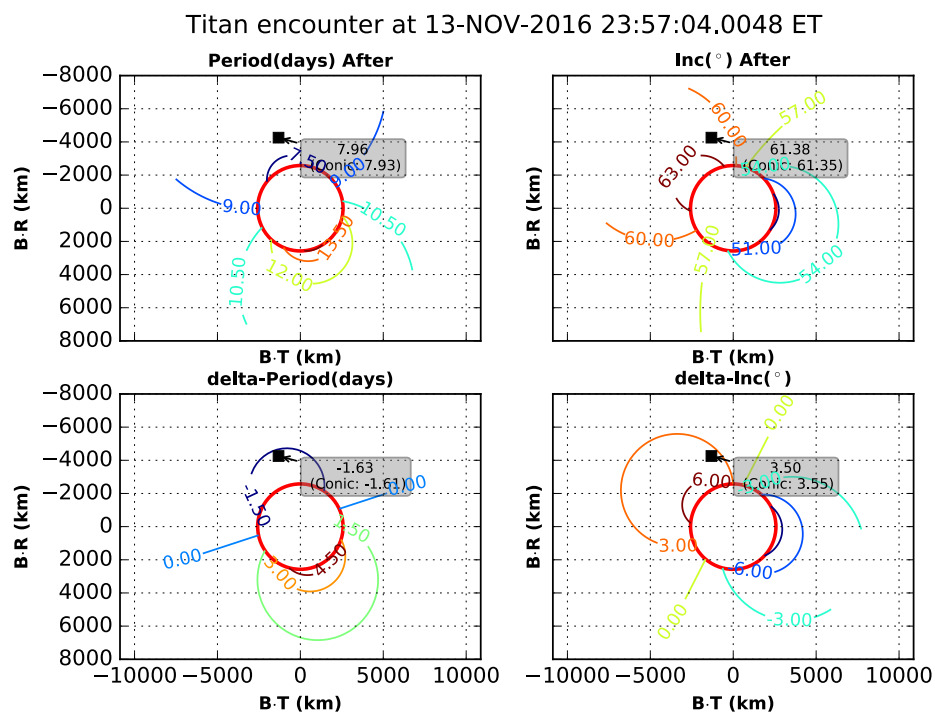


Figure A-67. Titan-124 (T124) Encounter Orbital Element Change Shown on the B-Plane.

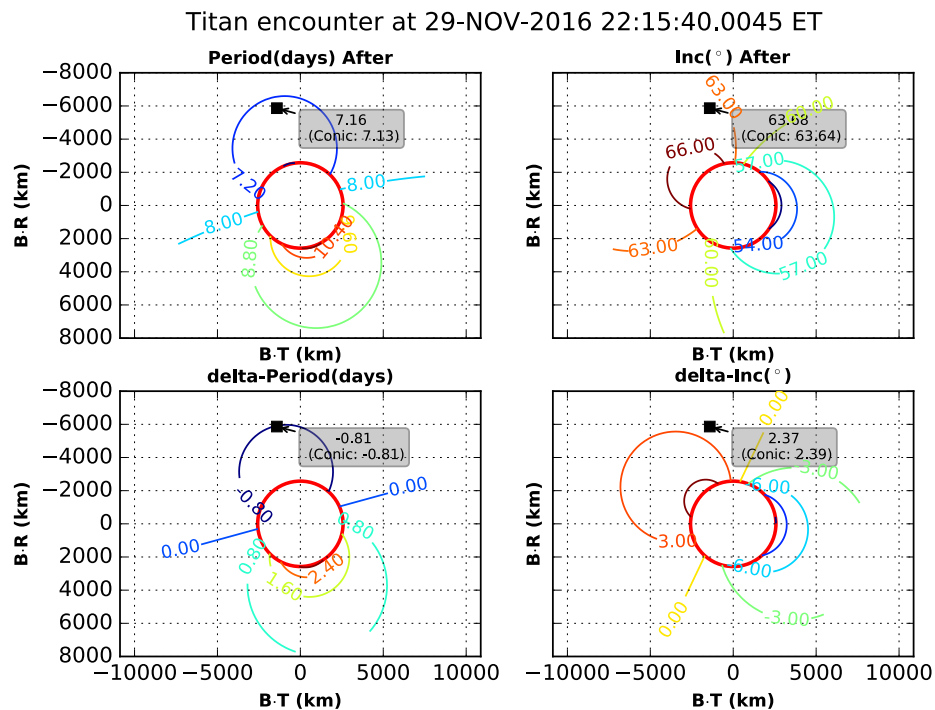


Figure A-68. Titan-125 (T125) Encounter Orbital Element Change Shown on the B-Plane.

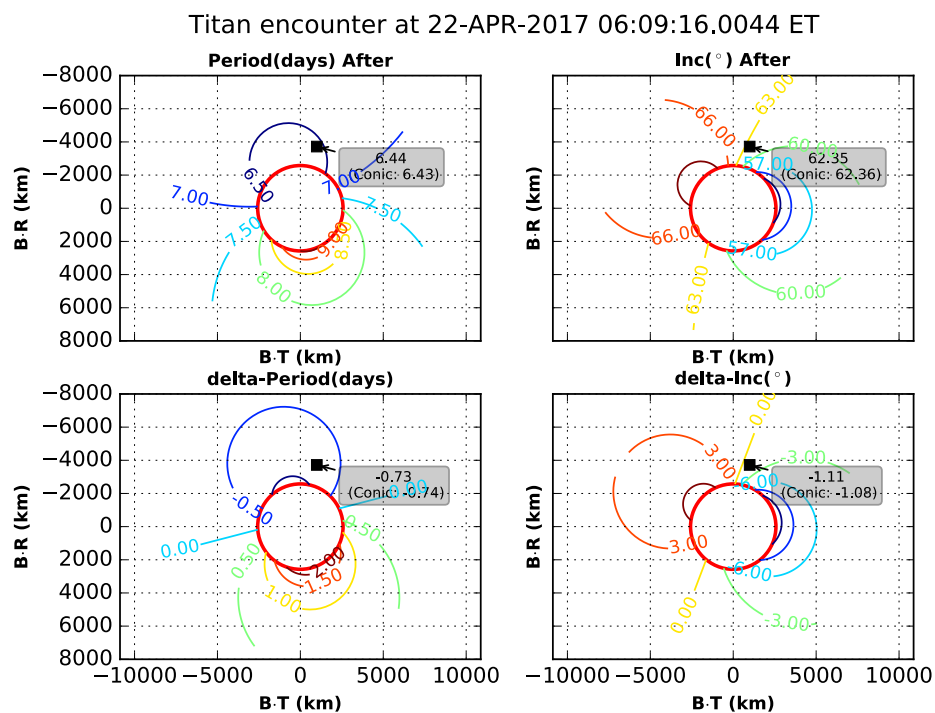


Figure A-69. Titan-126 (T126) Encounter Orbital Element Change Shown on the B-Plane.